UNIVERSITA' DEGLI STUDI DI PAVIA

Dottorato in Medicina Sperimentale

XXXIII Ciclo

Vascular Risk Factors and Glaucoma Optic Neuropathy

Dott.ssa Alice Verticchio Vercellin

Matricola n. 462291

Anno Accademico 2019-2020

“He sprinkled me in pixie dust and told me to believe.

Believe in him and believe in me.”

Table of Contents

I certify that my PhD involves an analysis of 5-year outcomes from the prospective observational clinical study: "The Indianapolis Glaucoma Progression Study" (IGPS) in which professor Alon Harris, MS, PhD, FARVO, serves as principal investigator. The IGPS study originated in 2008 at Indiana University School of Medicine and continues today at the Icahn School of Medicine with ongoing data analysis and modeling of risk factors in glaucoma.

Sincerely,

Alice Verticchio Vercellin

List of Abbreviations:

AGIS: Advanced Glaucoma Intervention Study
BMI: Body Mass Index
BP: Blood Pressure
C/D Ratio: Cup-to-Disc Ratio
CDI: Color Doppler Imaging
CI: Confidence Intervals
CRA: Central Retinal Artery
DBP: Diastolic Blood Pressure
DM: Diabetes Mellitus
DOPP: Diastolic Ocular Perfusion Pressure
EDV: End Diastolic Velocity
FD Doppler OCT: Fourier Domain Doppler Optical Coherence Tomography
HR: Hazard Ratio
HRT: Heidelberg Retinal Tomography
IGPS: Indianapolis Glaucoma Progression Study
IOP: Intraocular Pressure
MAP: Mean Arterial Pressure
MD: Mean Defect
MOPP: Mean Ocular Perfusion Pressure
NTG: Normal-Tension Glaucoma
NW: Normal Weight
NPCA: Nasal Posterior Ciliary Arteries
OA: Ophthalmic Artery
OAG: Primary open-angle glaucoma
OB: Obesity
OCT: Optical Coherence Tomography
ONH: Optic Nerve Head
OPP: Ocular Perfusion Pressure
OW: Overweight
PSD: Pattern Standard Deviation
PSV: Peak Systolic Velocity
RI: Resistivity Index
RNFL: Retinal Nerve Fiber Layer
SBP: Systolic Blood Pressure
SOPP: Systolic Ocular Perfusion Pressure
SPCA: Short Posterior Ciliary Arteries
TPCA: Temporal Posterior Ciliary Arteries

CHAPTER 1

Primary open-angle glaucoma

1. Definition:

Glaucoma is a leading cause of irreversible blindness worldwide (Quigley et al., 2006; Tham et al., 2014; WHO, 2020). There are several different subtypes of glaucoma that, while all having progressive degenerative properties, have different pathophysiologic mechanisms. Among these subtypes, primary open-angle glaucoma (OAG) is the most common form of glaucoma both in the United States and worldwide, defined by the American Academy of Ophthalmology (AAO) as a chronic, progressive ocular disease causing loss of optic nerve rim and retinal nerve fiber layer (RNFL) with associated visual fields defect (AAO Glaucoma Preferred Practice Pattern Panel, 2020). In 2020, it was estimated that 53 million people have OAG in the word, with a prevalence of 3.0% in the population aged 40 to 80 years (AAO Glaucoma Preferred Practice Pattern Panel, 2020).

Primary open-angle glaucoma is a form of glaucoma characterized by an open angle of the eye. The angle is the anatomic region of the eye where the cornea and the iris meet and is specifically significant as the site of aqueous humor outflow from the eye. Aqueous humor is secreted from the ciliary body, where it then travels through the anterior chamber to the drainage pathway through the trabecular meshwork (90% of aqueous drainage) and into the venous system via-Schlemm's canal, or through the uveoscleral drainage route (10% of aqueous drainage). OAG, therefore, is a form of glaucoma where the resistance to aqueous outflow is increased despite the angle being "open," and stands in contrast to closed-angle glaucoma where outflow resistance is increased as a result of the outflow tract being anatomically obstructed (Figure 1, Weinreb et al., 2014).

Figure 1. Anatomy of the angle of the eye.

Adapted from: Weinreb RN, Aung T, Medeiros FA. The pathophysiology and treatment of glaucoma: a review. *JAMA*. 2014;311(18):1901-1911.

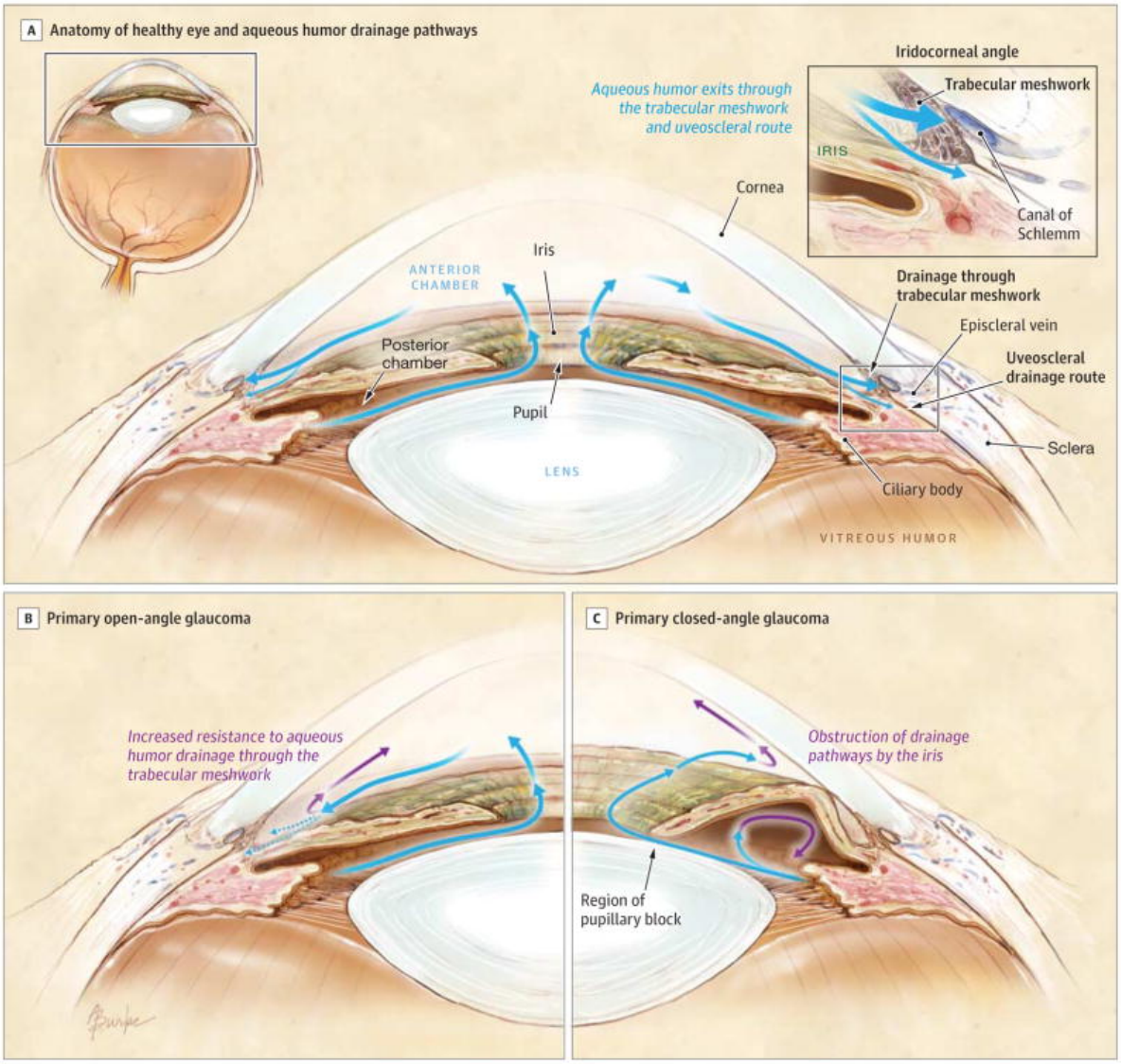

2. Epidemiology:

Primary open-angle glaucoma is responsible for close to three quarters of all glaucoma cases worldwide, and it is the most common form of glaucoma in populations of both European (ED) and African descent (AD) (Quigley et al., 2006; Glaucoma Preferred Practice Pattern Panel, 2020). Importantly, OAG disproportionately impacts people of AD compared to persons of ED. In fact, AD populations have nearly double the prevalence of OAG compared to ED

populations, have up to 5 times greater risk of disease, have a stronger vascular component to their disease, and are more likely to have severe disease resulting in total blindness (Youngblood et al., 2019; Harris et al., 2020). Meanwhile, Asian populations are also impacted by OAG, though the prevalence of primary angle-closure glaucoma in Asian populations is much higher than the prevalence of OAG in these populations (Zhang et al., 2019). In populations of Latin American descent, there seems to be a prevalence of OAG that is higher than ED populations, but lower than AD populations (Varma et al., 2004; Quigley et al., 2001). Finally, the epidemiology of OAG in Middle Eastern populations is less well-defined with wide variances based on country and population, and estimates have largely been based on European models (Eid et al., 2009; Quigley et al., 2006).

3. Risk factors:

3.1 Intraocular pressure (IOP):

Historically the key risk factor (RF) for OAG – and the only currently treatable one – has been elevated intraocular pressure (IOP). Elevated IOP occurs as a result of alterations to aqueous humor dynamics in the angle of the eye and the resulting pressure changes which then puts mechanical strain on the lamina cribrosa leading to glaucomatous damage of the optic nerve. Elevated IOP is the single most important, and the only modifiable, RF for OAG. Elevated IOP has been associated with both glaucoma onset and disease progression, as demonstrated by a wide variety of clinical literature including studies demonstrating the impact of IOP-reduction therapies on disease progression (Heijl et al., 2002; Weinreb et al., 2014). Generally, IOP measurements >21 mmHg are considered to be elevated, though IOP measurements and definitions of ocular hypertension vary by study (Weinreb et al., 2014). It is important to note, however, that glaucomatous damage can also occur in the setting of normal IOP. This form of

open-angle glaucoma is referred to as normal tension glaucoma (NTG), and 25-50% of OAG cases can be classified as NTG (Weinreb et al., 2014). It has been suggested that NTG may be the result of a similar mechanical stress mechanism on the optic nerve purported by low cerebrospinal fluid pressure (Ren et al., 2010; Wang et al., 2012). Additionally, several IOP-independent hypotheses have been suggested as proposed mechanisms for OAG, including the vascular theory of glaucoma which suggests that impaired blood flow to the retina and optic nerve head results in glaucomatous damage (Flammer, 1994; Harris et al., 2020).

3.2 Race:

Race is an important RF given the increased prevalence, incidence, and disease severity of OAG among certain genetic populations such as in AD populations when compared to ED populations. Race is also associated with disease progression, as AD patients generally have faster visual field loss and structural disease progression when compared to ED populations (Racette et al., 2003). Additionally, race may even be a predictor of elevated IOP, with studies demonstrating that African ancestry has been associated with ocular hypertension in LAD populations (Coleman et al., 2016). Data on other races and OAG are less established.

3.3 Age:

The incidence of OAG is noted to increase with age, with a prevalence <1% in individuals younger than 55 years increasing to nearly 4% in patients over the age of 80 years (Friedman et al., 2004). Additionally, increasing age is an important predictor of disease progression as older age is associated with faster visual field deterioration (Nouri-Mahdavi et al, 2004; Park et al., 2016). Possible explanations for the association between age and OAG include normal age-related changes in the viscoelasticity of the ocular vasculature and ocular tissues (Prada et al., 2016).

3.4 Family history and genetic factors:

Family history is a significant demographic RF for OAG. In 1994, data from the Baltimore Eye Survey demonstrated that there was a significant increase in the relative risk of OAG for individuals with an affected family member (Tielsch et al., 1994). More recently, large longitudinal studies have also shown that family history of OAG in first-degree relatives was significantly associated with increased risk of OAG in AD patients (O'Brien et al., 2019). The strong association between OAG, family history and, by extension, race and ethnicity suggests a possible genetic correlation for disease. OAG, however, is a multifactorial disease with a complex inheritance pattern, so genetic RF for disease are unclear and are still being studied (Zukerman et al., 2020). Importantly, population-based studies suggest that the OAG phenotype is associated with several genetic polymorphisms and environmental interactions. Further investigation is needed to determine if these factors are protective or associated with disease progression, or if they may represent potential novel therapeutic targets. For these reasons, currently routine genetic testing for glaucoma risk alleles is not recommended for patients with OAG (Glaucoma Preferred Practice Pattern Panel, 2020).

3.5 Other ocular and systemic risk factors:

Central corneal thickness (CCT) has been shown to be significantly associated with glaucoma severity as measured by both structural and functional parameters (Herndon et al., 2004). Interestingly, thinner CCT has also been associated with AD patients when compared to ED patients (Brandt et al., 2001). It is important to note, however, that while CCT may be an important RF for OAG, the role of CCT in the pathogenesis of OAG is still unclear (Jonas et al., 2005). It has been suggested that CCT and OAG may be linked through IOP, though the association between glaucoma risk and CCT is independent of IOP (Geisert, 2020).

Importantly, CCT is also a highly heritable ocular trait, as demonstrated by twin studies in ED populations, suggesting a possible genetic risk component to OAG through inherited OAG endophenotypes (Toh et al., 2005). Other important ocular risk factors to note include history of other ocular disease, myopia, and the presence of optic disc hemorrhage which may be indicative of vascular disease processes (Harris et al., 2020).

Systemically, there have been suggested associations between OAG and diabetes mellitus, cardiovascular disease, migraine hypertension, obstructive sleep apnea, and systemic vascular disease, though these associations may require further longitudinal study to yield conclusive results (Costa et al, 2013; Zhao et al., 2014; Zhao et al., 2015; Harris et al., 2020). Interestingly, there seems to be an association between glaucoma and family history of migraine, especially in female patients, which may help explain a female preponderance of disease (Gramer et al., 2015).

4. Presentation:

Primary open-angle glaucoma classically does not present until disease has advanced to the point of visual field loss, indicating a largely asymptomatic disease course. Patients with OAG who are not experiencing visual field loss are generally found via ophthalmic examination. As opposed to angle-closure glaucoma, which presents with erythema and pain in addition to visual field loss, OAG does not present with other symptoms as elevated IOP does not cause erythema, pain, or swelling. By the time OAG has progressed to the point of visual field loss, many patients experience reductions in quality of life related to difficulties performing instrumental activities of daily living as well as higher reports of motor vehicle collisions and falls (Haymes et al., 2007; Weinreb et al., 2014). As the disease progress leads to retinal ganglion cell loss and visual field deterioration, patients may report a classic pattern of visual

field loss progressing from the periphery eventually leaving only the center of the visual field, or “tunnel vision”.

5. Diagnosis:

Glaucoma is diagnosed by an ophthalmologist performing a comprehensive ophthalmic examination. The American Academy of Ophthalmology cites two forms of damage (structural and functional) in their definition of OAG (AAO Glaucoma Preferred Practice Pattern Panel, 2020):

1. Retinal nerve fiber layer (RNFL) or disc structural abnormalities (cupping, notching, thinning, RNFL defects, progressive change, etc.)
2. Visual field defects that are reliable and reproducible without an alterative explanation of cause

Given these challenges and loose definitions, comprehensive ophthalmic exam by a trained ophthalmologist remains the most important factor in timely and reliable OAG diagnosis.

IOP measurements are an important part of the ophthalmic exam, though IOP elevations are not sufficient alone to diagnose OAG. Traditionally, IOP measurements greater than 21 mmHg are indicative of ocular hypertension, though more than 90% of adults with IOP measurements greater than 21 mmHg do not have glaucomatous damage. Additionally, several population-based studies found that up to 50% of patients with OAG have IOP lower than 22 mmHg (Leske, 1983; Weinreb et al., 2014). The gold standard measurement for IOP is Goldmann applanation tonometry, which measures IOP by based on the force applied to the surface of the cornea. Importantly, Goldmann applanation tonometry is considered the gold standard of IOP measurement tools because it is the most accurate and reproducible test, though it is still subject to discrepancies between users as well as confounding measurements based on differences in CCT between patients (Brandt et al., 2001; Mihailovic et al., 2020). Other tools of measurement

include Schiotz tonometry, pneumotonometry, and air-puff tonometry, though these measurements are less reliable than applanation tonometry (Figure 2, Stevens et al., 2007).

Figure 2. Goldmann applanation tonometry.
Adapted from: Stevens S, Gilbert C, Astbury N. How to measure intraocular pressure: applanation tonometry. *Community Eye Health.* 2007 Dec;20(64):74-5.

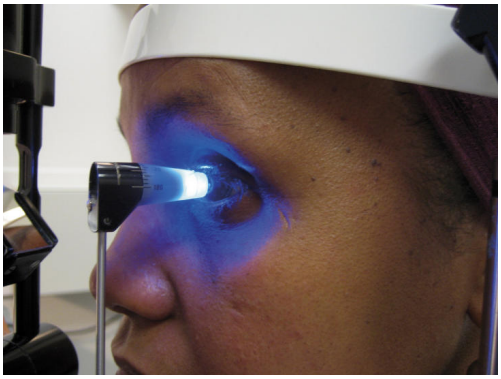

Given the association between CCT and OAG, measuring corneal thickness is also be an important part of the ophthalmic examination. Pachymetry is the measurement of CCT and is often performed using ultrasound. As mentioned earlier, CCT is most useful as a predictor of glaucoma progression, therefore pachymetry may be performed in patients with already diagnosed or with suspected OAG (Herndon et al., 2004). Importantly, all diagnostic tests for OAG suffer from insufficiencies. While optic nerve head cupping is the most reliable diagnostic assessment, there is no specific cutoff criteria that has been identified as being sufficiently sensitive and specific as a diagnostic tool (Harper and Reeves, 2000). Similarly, IOP measurements are most helpful for referral for further examination, though IOP measurement is often user-dependent and parameters for referral are not standardized. In fact, the unreliability of IOP as a diagnostic tool has also led to debate over the value of IOP as a screening tool for OAG (Moyer, 2013). It is important that all patients with elevated IOP have prompt referral to an ophthalmologist and have regular follow-up as necessary.

5.1 Structural evaluation:

The primary diagnostic tool for OAG is the fundus examination, which allows the ophthalmologist to evaluate glaucomatous structural damage. As OAG progresses, characteristic changes to the RNFL and optic nerve head become apparent on ophthalmic examination and are the most important part of diagnosing glaucoma (Figure 3, Weinreb et al., 2014). On a fundus examination, glaucomatous damage to the optic nerve classically presents as "cupping" – describing a hollow-appearing nerve head with an elevated cup-to-disc ratio (CDR). Additionally, fundus examination may reveal CDR asymmetries between the eyes, progressive changes to the shape and size of the cup, or alterations to the disc rim (Harper and Reeves, 2000).

Figure 1. Fundus exam findings and corresponding visual field defects.
Adapted from: Weinreb RN, Aung T, Medeiros FA. The pathophysiology and treatment of glaucoma: a review. *JAMA*. 2014;311(18):1901-1911.

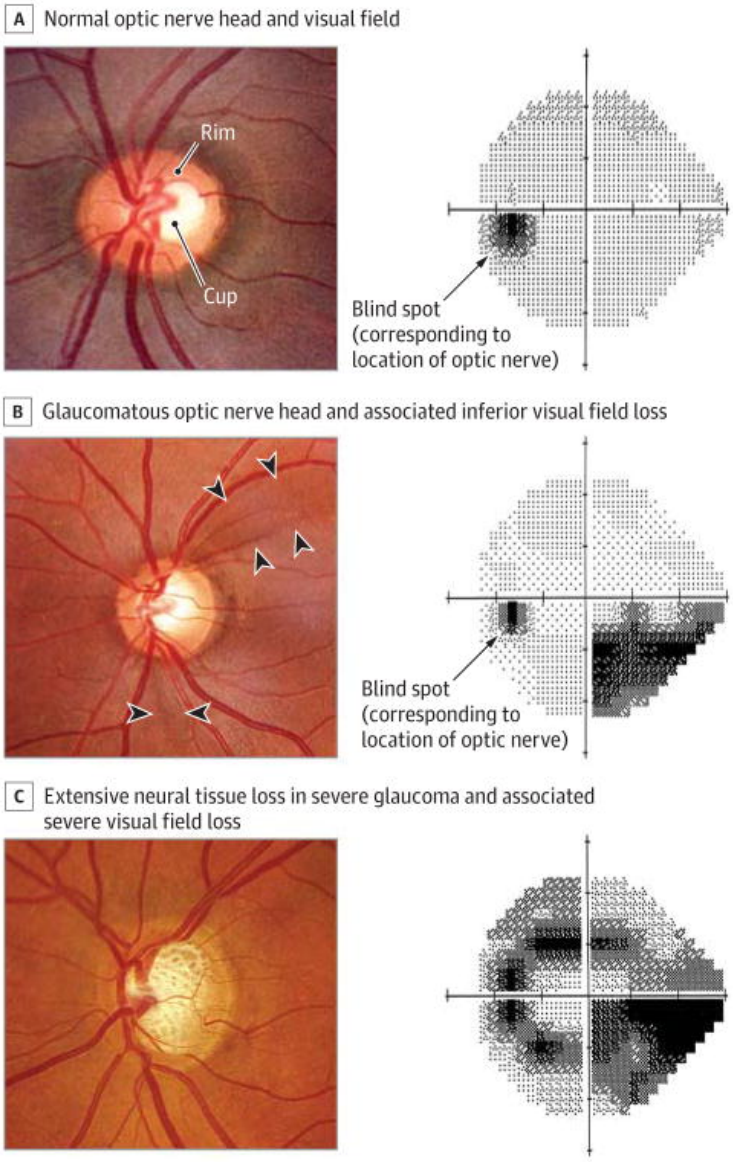

Newer technologies may also help with the diagnosis and monitoring of OAG by evaluating structural parameters. One important technology confocal scanning laser ophthalmoscopy (CSLO), which allows for imaging of the retina using a laser to scan the retina. CLSO is able to quantify retinal thickness and to create optic nerve head topographic maps. CSLO, however, is unable to capture images of the retina in full color. Alternatively, optical coherence tomography (OCT) utilizes reflected laser light to image the layers of the retina (Figure 4, Weinreb et al., 2014). For glaucoma, OCT is specifically relevant in its ability to measure the RNFL (Harris et al., 2020).

Figure 2. Optical coherence tomography findings in glaucoma patients.

Adapted from: Weinreb RN, Aung T, Medeiros FA. The pathophysiology and treatment of glaucoma: a review. *JAMA*. 2014;311(18):1901-1911.

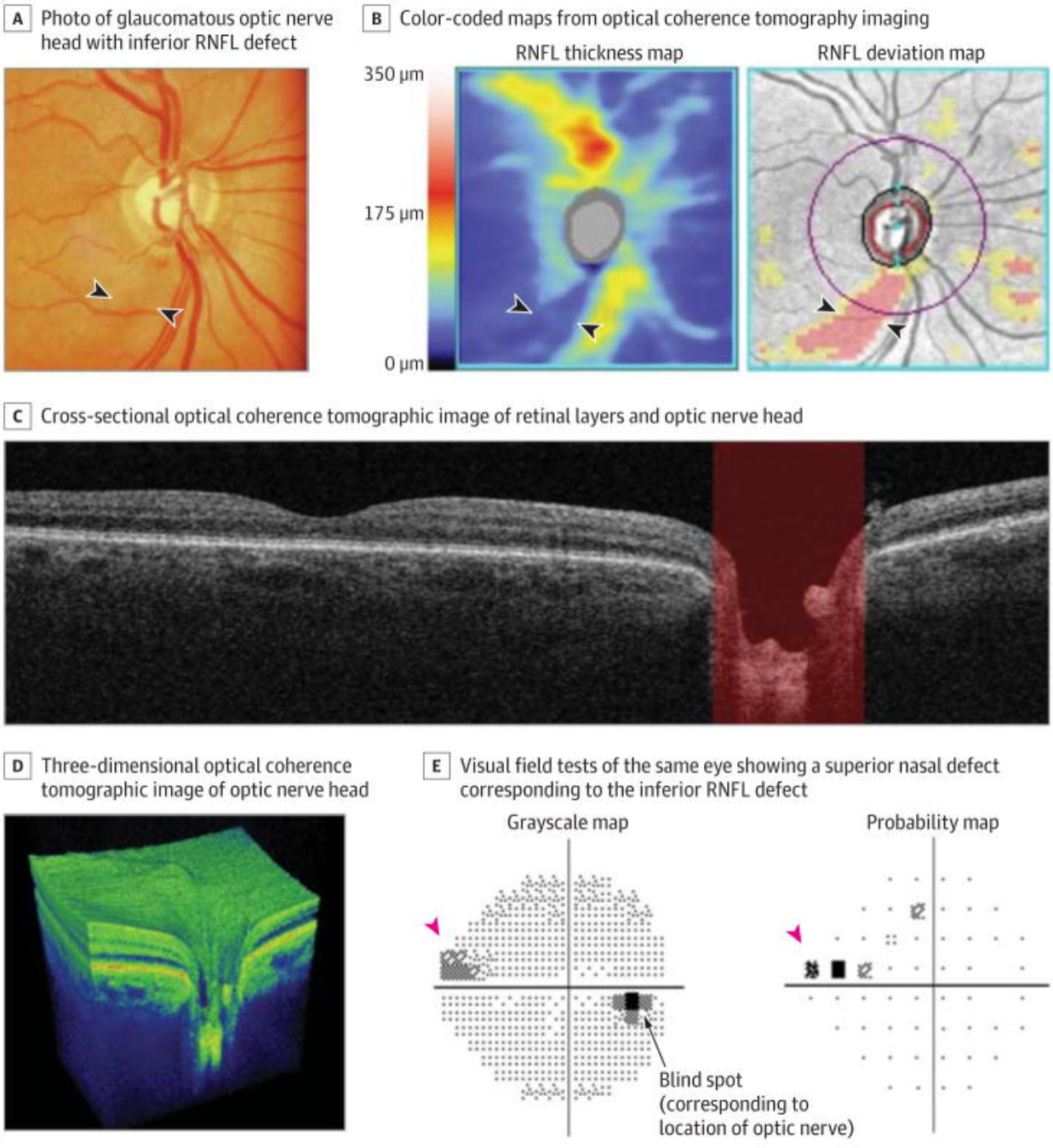

Similarly, Heidelberg retinal tomography (HRT) uses a laser to photograph the optic nerve head and the retina surrounding the nerve. This makes HRT particularly useful in measuring

and monitoring CDR as well as optic disc area, cup volume, and rim area (Figure 5, Heidelberg Engineering, 2015). All forms of laser technology provide detailed printouts for reading by experienced professionals. More recently, OCT technology has expanded to OCT angiography (OCTA), allowing for imaging of retinal vasculature and specific markers of ocular blood flow that may prove useful in diagnosing and monitoring glaucoma (Harris et al., 2020).

Figure 3. Example of a Heidelberg retinal tomography printout (Heidelberg Engineering, 2021).

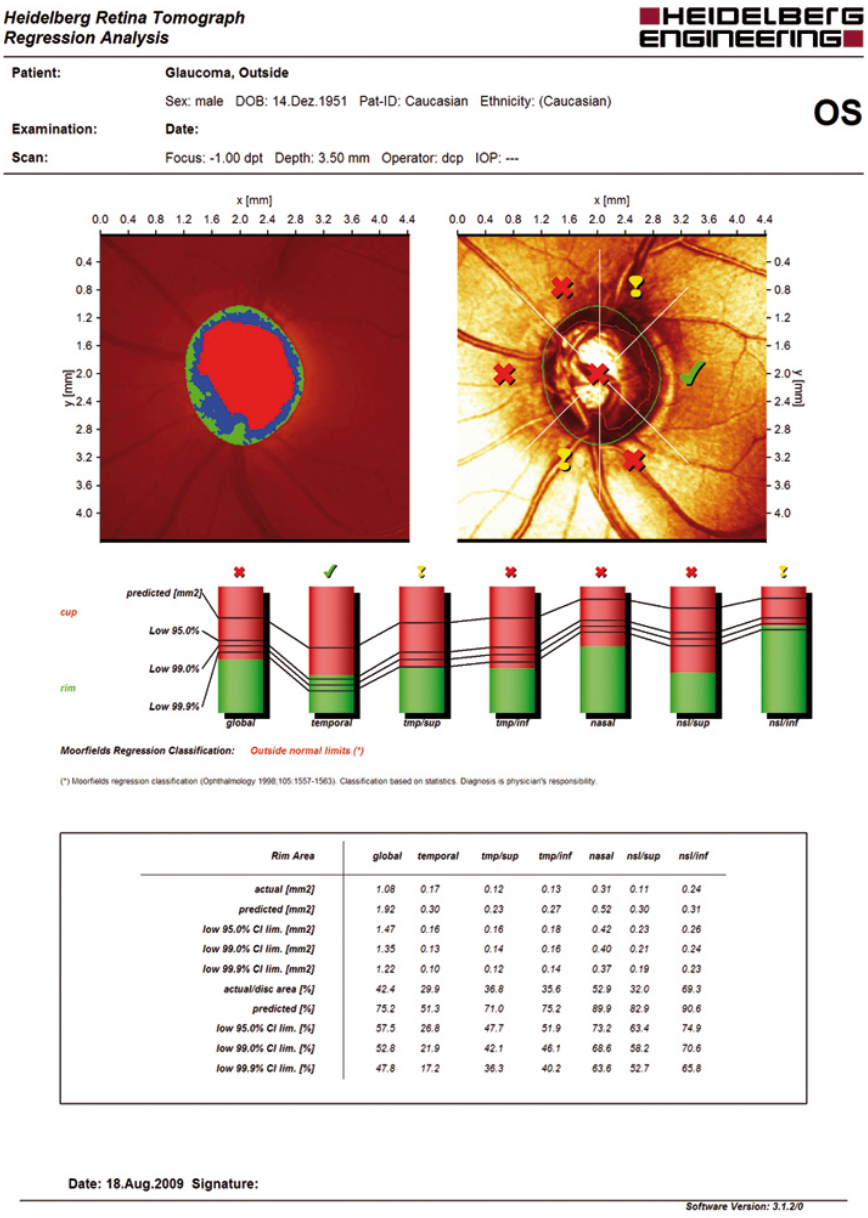

Heidelberg Retina Tomograph
Regression Analysis

HEIDELBERG ENGINEERING

Patient: Glaucoma, Outside
Sex: male DOB: 14.Dez.1951 Pat-ID: Caucasian Ethnicity: (Caucasian)
OS
Examination: **Date:**
Scan: Focus: -1.00 dpt Depth: 3.50 mm Operator: dcp IOP: ---

Moorfields Regression Classification: *Outside normal limits (*)*

(*) Moorfields regression classification (Ophthalmology 1998;105:1557-1563). Classification based on statistics. Diagnosis is physician's responsibility.

Rim Area	*global*	*temporal*	*tmp/sup*	*tmp/inf*	*nasal*	*nsl/sup*	*nsl/inf*
actual [mm2]	1.08	0.17	0.12	0.13	0.31	0.11	0.24
predicted [mm2]	1.92	0.30	0.23	0.27	0.52	0.30	0.31
low 95.0% CI lim. [mm2]	1.47	0.16	0.16	0.18	0.42	0.23	0.26
low 99.0% CI lim. [mm2]	1.35	0.13	0.14	0.16	0.40	0.21	0.24
low 99.9% CI lim. [mm2]	1.22	0.10	0.12	0.14	0.37	0.19	0.23
actual/disc area [%]	42.4	29.9	36.8	35.6	52.9	32.0	69.3
predicted [%]	75.2	51.3	71.0	75.2	89.9	82.9	90.6
low 95.0% CI lim. [%]	57.5	26.8	47.7	51.9	73.2	63.4	74.9
low 99.0% CI lim. [%]	52.8	21.9	42.1	46.1	68.6	58.2	70.6
low 99.9% CI lim. [%]	47.8	17.2	36.3	40.2	63.6	52.7	65.8

Date: 18.Aug.2009 Signature:

Software Version: 3.1.2/0

5.2 Functional evaluation:

Glaucoma is diagnosed and monitored based on functional parameters using visual field testing (Figure 6). Ideally, however, OAG should be diagnosed before the patient experiences severe visual function changes. Therefore, visual field testing is more reliable as an indicator of disease progression than as a specific diagnostic tool. Several types of visual field testing can be used for detecting and monitoring glaucoma, though it should be noted that confrontational

field testing is not a useful tool. Automated perimetry is a more reliable diagnostic and monitoring tool for OAG and has become the standard of care (Johnson and Baloh, 1991). Testing strategies should be tailored to the patient by varying the stimulus size and by using specific programs that evaluate the central threshold sensitivity at 24 degrees, 30 degrees, and 10 degrees. Careful manual combined kinetic (testing the patient using moving targets from nonseeing to seeing areas) and static (presenting fixed targets) threshold testing is an acceptable alternative when patients can not perform automated perimetry in a reliable manner (Kahook and Noecker, 2007). Repetition and confirmation of visual field examinations are recommended for unreliable results or tests that present show a new glaucomatous defect before changing glaucoma treatment. Also, in order to confirm visual field progression, it is important to repeat the same strategy that showed a new glaucomatous (Glaucoma Preferred Practice Pattern Panel, 2020). Importantly, though, reliable visual field testing requires cooperation of the patient, presenting challenges in certain patients who may not be able to participate in their care.

Figure 4. Example of Automated Perimetry printout.
Adapted from: Alencar LM, Medeiros FA. The role of standard automated perimetry and newer functional methods for glaucoma diagnosis and follow-up. *Indian J Ophthalmol*. 2001;59,Suppl S1:53-8.

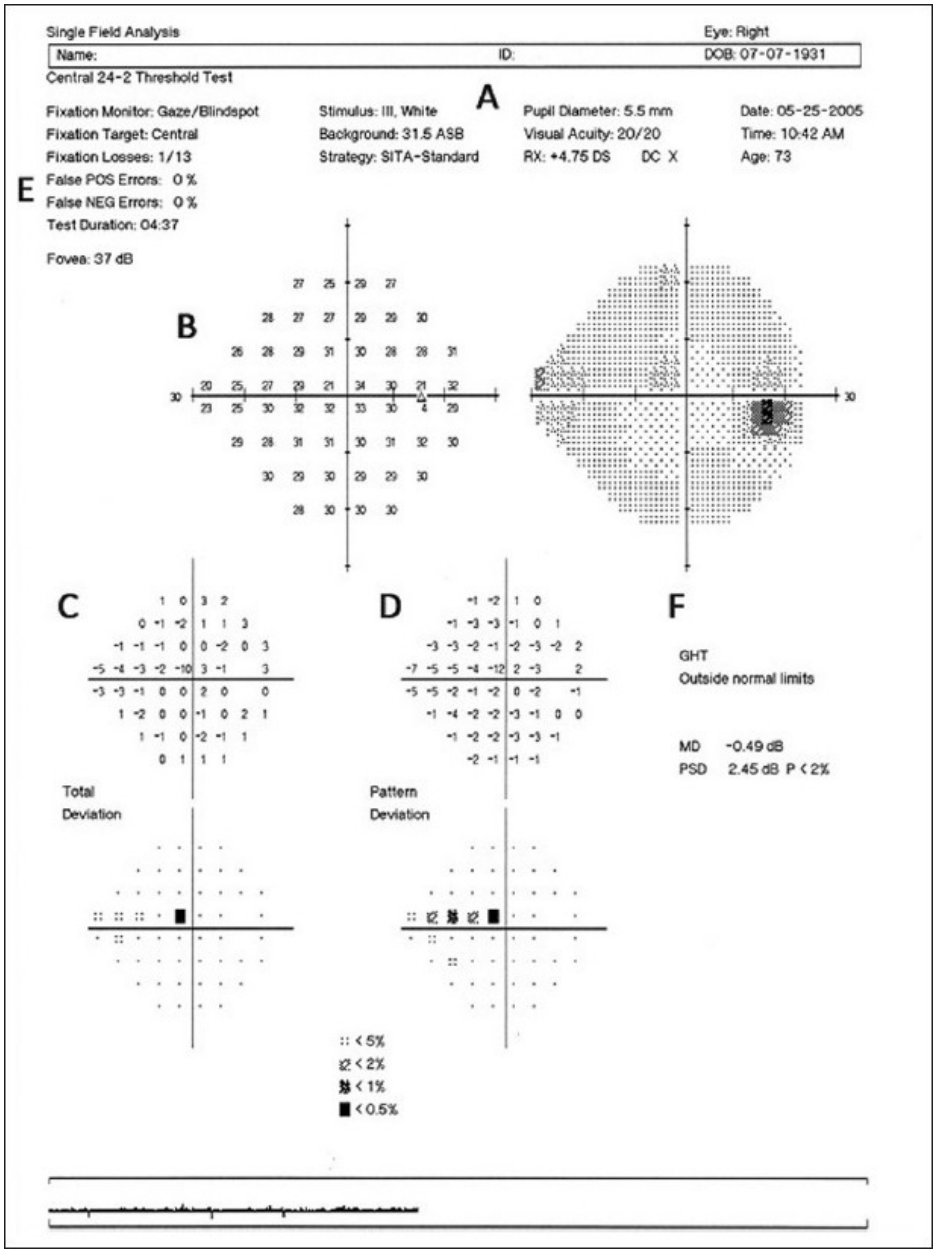

5.3 Structural and functional progression:

Importantly, both structural parameters and functional parameters are important to monitor regularly for the progression of disease. Structural progression can be measured using OCT, HRT, or CSLO. Meanwhile, functional progression is generally defined using standardized scores to quantify visual fields, such as the Advanced Glaucoma Intervention Study (AGIS) score and the Collaborative Initial Glaucoma Treatment Study (CIGTS) score, or analyzing global indices (such as the mean deviation, patter stand deviation, or visual field indeces (Kim

et al., 2004; Moore et al., 2017). Interestingly, functional progression was traditionally accepted as the result of structural damage. More recently, however, research has shown that functional and structural progression may occur both independent of each other and in a dependent manner (Schuman et al., 2020). Regardless, measurements of both structural and functional progression have limitations that require consideration by the managing ophthalmologist. Most important, though, is that each parameter may be significantly influenced by disease severity (Abe et al., 2016).

6. Treatment:

The main goals of OAG treatment are to control IOP in a target range and to prevent progressive visual field and optic nerve and RNFL damage in order to preserve visual function and quality of life (Glaucoma Preferred Practice Pattern Panel, 2020). Currently, the only therapy to slow the structural and functional progression of disease is lowering of IOP (Heijl et al., 2002; Kass et al., 2002). In fact, according to the AAO Preferred Practice Pattern, clinical management of glaucoma should include lowering IOP towards a specific, individualized target level (Glaucoma Preferred Practice Pattern Panel, 2020). Generally, the target IOP is between a 20-50% reduction, though this target should be regularly re-evaluated by the ophthalmologist managing disease (Weinreb et al., 2014).

There are a variety of methods to lower intraocular pressure, including pharmacologic and surgical management. Generally, prostaglandin analogues are the first-line pharmacologic therapy given their lower side effect profiles. Topical prostaglandin analogues are administered once nightly and reduce IOP by reducing aqueous humor outflow resistance through the uveoscleral drainage pathway (Weinreb et al., 2014). Other topical medications, such as alpha agonists, beta blockers, and carbonic anhydrase inhibitors are less efficacious and are generally used as second-line agents behind prostaglandin analogues or in conjunction with

prostaglandin analogues if monotherapy is not successful in lowering IOP sufficiently (Weinreb et al., 2014).

Alternatively, laser trabeculoplasty may be considered as a first-line therapy for patients who have severe disease or have difficulty with adhering to medication regimens (Weinreb et al., 2014). This therapy increases aqueous humor outflow through the trabecular meshwork leading to reductions in IOP. While laser trabeculoplasty can be performed in the office and is safe, there is a high failure rate that increases over time (Weinreb et al., 2014).

When patients have advanced disease and are not responding to first-line interventions, surgical therapy is indicated. Trabeculectomy, the most common procedure, creates an alternate filtration route for aqueous humor to drain from the eye to under the conjunctiva. There are a variety of complications associated with trabeculectomy that can lead to surgical failure, but the formation of excessive scar tissue is the most important surgical risk. As a result, anti-scarring agents are generally used in order to decrease scar formation and improve the chance of procedural success (Weinreb et al., 2014). Other complications associated with trabeculectomy include infection and hypotony. Additionally, the risk of cataract formation and required subsequent extraction is considerably higher in patients who undergo surgical treatment compared to medical therapy alone (Musch et al., 2006). Trabeculectomy may also be indicated as a first-line therapy for patients who present with severe disease at baseline. Meanwhile, alternatives to trabeculectomy include implantation of mechanical shunts and newer minimally invasive glaucoma surgeries which may carry less risk of complication but may also be less effective than trabeculectomy (Weinreb et al., 2014).

CHAPTER 2

PhD Research Project – Background and Significance

1. Vascular Risk Factors for Open-Angle Glaucoma:

Elevated IOP currently remains the major risk factor for OAG, however a high percentage of individuals with elevated IOP do not develop glaucoma (Hollows and Graham, 1996). In addition, many persons with OAG have relatively low IOP or continue to experience OAG progression despite medically reduced IOP. Other risk factors for OAG include age, myopia, ocular structure, race of the subject, and ocular blood flow abnormalities. Decreased central corneal thickness (CCT), higher vertical cup-to-disk ratios (CDR) of the optic disc, and increased pattern standard deviation (PSD) values on Humphrey automated perimeter at baseline (Coleman and Caprioli, 2009) have also been reported. Importantly, certain demographic groups, such as persons of African descent (AD) are at elevated risk for OAG, experiencing a significant disease disparity and impact on quality of life. Other patient characteristics including diabetes mellitus (DM), gender, and obesity have been correlated with variation in glaucoma development and differences in glaucoma progression. However, the mechanisms by which these factors contribute to OAG pathophysiology are still largely unknown. In fact, it remains unclear which of these factors are causes or consequences of the disease and whether combinations of different factors yield similar risk for OAG. The exact mechanisms behind differential OAG risk have yet to be fully defined, but may involve alterations to the ocular circulation and/or metabolism within the retina. Without significant advancement in the current understanding of the pathogenesis of glaucoma, the impact of this irreversible blindness on the quality of life worldwide will continue unabated.

The literature provides strong evidence to suggest ischemia to the optic nerve is likely responsible in part for glaucomatous damage in many individuals. Reduced ocular blood flow

has been demonstrated in multiple tissue beds of glaucoma patients and this ischemia may be secondary to elevated IOP, or of primary vascular origin (Butt et al., 1995; Rojanapongpun et al., 1993). Within ocular tissues blood flow deficiencies in the retina (Chung et al., 1999), choroid (Yin et al., 1997), and retrobulbar circulations have been reported in OAG patients (Butt et al., 1995; Galassi et al., 1998; Harris et al., 1994; Rojanapongpun et al., 1993). Reduced perfusion pressure, the difference between systemic blood pressure and IOP, has been linked in large population trials to both the prevalence and incidence of glaucoma (Bonomi et al., 2001; Leske et al., 2002; Quigley et al., 2001; Tieslch et al., 1995). Perfusion pressure can be reduced by either an increase in IOP or a reduction in blood pressure and data from the Thessaloniki eye study suggests treatment with antihypertensive medication is associated with increased cup-to-disc ratio and enlarged cup area of the optic nerve head (Topouzis et al., 2006). Further, the use of systemic diuretics was associated with the development of OAG (Miglior et al., 2007). In addition to localized ischemia, systemic vascular abnormalities have also been linked to OAG including arterial hypertension (Leighton et al., 1972), nocturnal hypotension (Hayreh et al., 1994), optic disc hemorrhage (Drance et al., 2001), migraine (Drance et al., 2001), and aging of the vasculature (Harris et al., 2000). These studies do not provide direct evidence to link reduced ocular blood flow with glaucomatous progression; however, they suggest a strong relationship between vascular health and ocular resiliency.

While the current literature contains much evidence linking OAG and vascular deficits, the data examining glaucoma progression and ocular blood flow is very limited in scope and execution. Only a handful of studies have examined ocular hemodynamic parameters in relation to clinical markers of glaucoma progression. The conclusions and applicability of these studies are limited by their small sample sizes, use of a single imaging technology, limited reporting of blood flow parameters, lack of controls, and limited follow up duration. For instance, progressive glaucoma has been associated with decreased blood flow velocities in the

retrobulbar vessels supplying the optic nerve head (ONH) (Galassi et al., 2003; Hesse et al., 1998; Satilmis et al., 2003; Schumann et al., 200; Xu et al., 1998; Yamazaki et al., 1998; Zeitz et al., 2006). However, all of these investigations utilized only color Doppler imaging of the retrobulbar blood vessels specifically. No study has comprehensively investigated retinal, choroidal, and ONH circulations in relation to structural and functional glaucomatous progression. The significance of steal phenomenon of retrobulbar blood flow by the choroidal and/or retinal tissues has also never been assessed. This "sharing" of perfusion likely hides significant reductions in overall perfusion when assessed with imaging protocols limited to only the retrobulbar circulation. Further, the retrobulbar blood flow investigations, while suggestive of a relationship between OAG and blood flow, do not have the statistical power or comprehensive methodology to establish a firm association between ocular ischemia and glaucoma progression (Galassi et al., 2003; Hesse et al., 1998; Satilmis et al., 2003; Schumann et al., 200; Xu et al., 1998; Yamazaki et al., 1998; Zeitz et al., 2006). The relationship between ocular hemodynamics and glaucoma progression in therefore still currently poorly understood and needs further investigation with an emphasis on assessing multiple tissue beds with multiple imaging modalities over a long period of time to observe vascular/OAG relationships.

2. Vascular Anatomy of the Eye:

The vascular anatomy of the eye is schematically represented in Figure 1.

Figure 1. Vascular anatomy of the eye.
Adapted from: Harris A, Jonescu C, Kagemann L, Ciulla T, Krieglstein GK. Atlas of Ocular Blood Flow. 2010; Philadelphia: Butterworth-Heinemann, Elsevier.

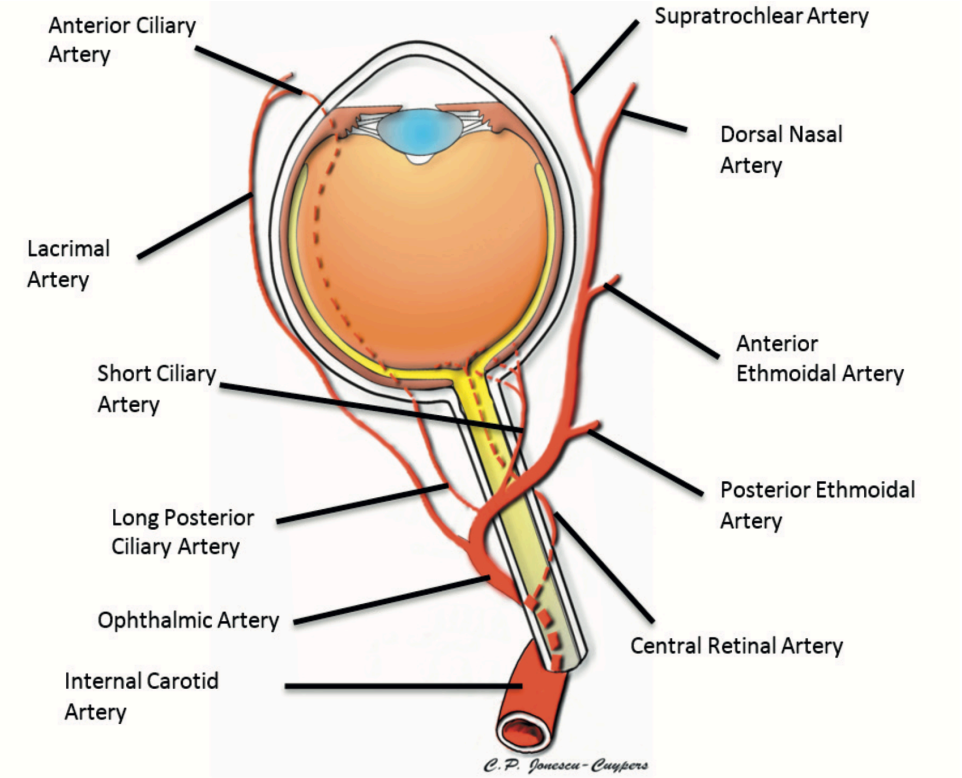

The optic nerve head is anatomically divided into the following four regions: superficial nerve fiber layer, pre-laminar region, lamina cribrosa region, and the retro-laminar region (Figure 2).

Figure 2. Anatomy and vascular supply of the optic nerve head.
Adapted from: Harris A, Jonescu C, Kagemann L, Ciulla T, Krieglstein GK. Atlas of Ocular Blood Flow. 2010; Philadelphia: Butterworth-Heinemann, Elsevier.

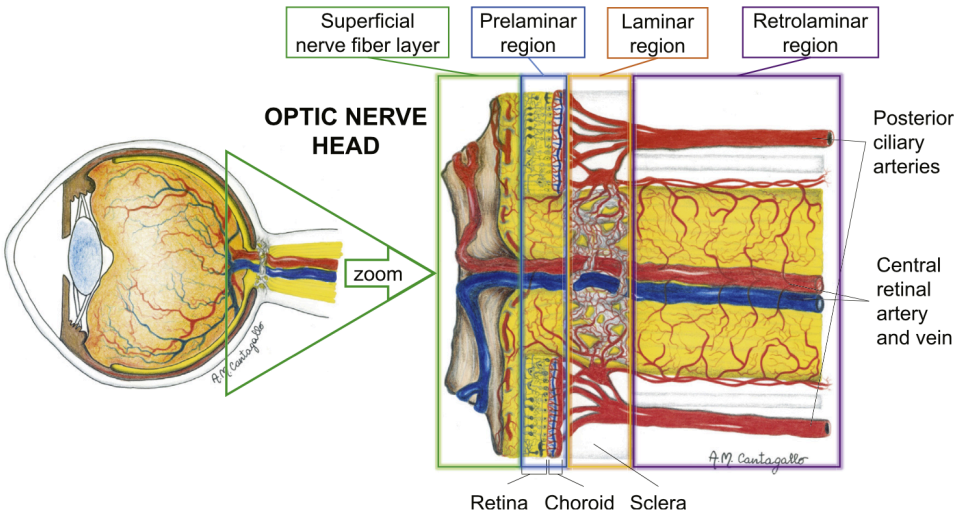

The first region is the superficial nerve fiber layer, which is the only one that is visible during the ophthalmologic examination of the fundus oculi. This region is continuous with the retinal nerve fiber layer and is vascularized by the recurrent retinal arterioles of the branches of the retinal arteries. These arterioles course towards the center of the optic nerve head from the peripapillary nerve fiber layer. The second region is the pre-laminar region, which receives its blood supply from the direct branches of the short posterior ciliary arteries (SPCAs), which branch off from the ophthalmic artery, and of the circle of Haller and Zinn. The latter is a ring of arterioles that is formed by branches of the SPCAs and is often within the perineural sclera. The lamina cribrosa is the third region, which is also perfused by the SPCAs and the circle of Haller and Zinn. The fourth region is the retro-laminar region which is supplied by both the pial system and the central retinal artery (CRA). The pial system is a network of capillaries within the pia mater that originates from the circle of Haller and Zinn, and extends outwards to perfuse the optic nerve axons. The venous drainage of the ONH is primarily via the central retinal vein, which drains into the cavernous sinus and flows into the internal jugular veins.

In summary, the main vascular supply of the ONH is represented by the SPCAs that are terminal arteries, resulting in watershed zones around the optic nerve. The precise positions of these zones vary amongst patients due to the variation of the vasculature. Therefore, the location of the watershed areas depends on the number and locations of the SPCAs that are supplying blood to the ONH. Consequently, if perfusion decreases in a particular SPCA, the portion of the ONH located in the respective watershed zone becomes susceptible to ischemia. It is important to highlight that the small vessel caliber and complex angioarchitecture of these arteries and arterioles have made the study of the vasculature of the optic nerve particularly difficult, thus prompting the search and development of imaging modalities to better characterize and understand the role of ONH perfusion in glaucoma pathogenesis.

3. PhD Research Project - Introduction Summary:

In summary, OAG is a multi-factorial high impact disease and a leading cause of irreversible blindness worldwide. The diagnosis and disease management of OAG is currently limited, with reduction of IOP being the only modifiable risk factor currently approved. Despite low or modified IOP, many patients continue to experience OAG disease onset and progression necessitating the need for identifying alternative risk factors. Among non-IOP risk factors, vascular deficits have been linked to OAG for many decades. Despite a wealth of pilot data showing strong associations to OAG, the exact nature of ocular vascular deficits in OAG remain unknown. Importantly, OAG is a disease that affects each individual differently, with strong variation in presentation of risk factors including age, gender, race, and comorbidities such as diabetes. Historically, there has been a lack of data available from a comprehensive assessment of OAG patients over time using multiple imaging platforms of different ocular tissue beds in a relevantly large patient sample.

My PhD has focused on analyzing how combinations of different risk factors, both demographic vascular biomarkers, are involved, possibly synergistically, in individual structural and functional glaucoma progression. My PhD involves analysis from a large, comprehensive, longitudinal dataset of OAG patients enrolled in the Indianapolis Glaucoma Progression study. The Indianapolis glaucoma progression study represented the first study in which multiple imaging modalities were used for a comprehensive ocular circulation assessment in a relatively large sample of OAG patients to determine its association with both structural and functional glaucomatous progression. This research has been accomplished using multiple measures of OAG structure and function alongside multiple hemodynamic imaging technologies and to adequately monitor OAG progression including biomarkers of retinal, choroidal and retrobulbar blood flow.

Overall, the objective of my PhD was to further the understanding of the relationships between ocular hemodynamics and glaucomatous optic neuropathy progression, based on patient-specific risk factors such as: race, diabetic status, gender, obesity, and age. The results of my investigation have the potential to enhance a clinician's ability to provide individualized therapeutic approaches based on ocular hemodynamic status and demographic characteristics, thus improving the quality of disease management.

4. Objective and specific aims:

The objective of my PhD project was to elucidate the relationships between ocular hemodynamics and glaucomatous optic neuropathy progression based on patient-specific risk factors. In details, the specific aims of my PhD thesis were:

1. ***To investigate the role of vascular risk factors in the functional and structural progression of the glaucomatous optic neuropathy***
2. ***To investigate the relationship between glaucoma progression, ocular hemodynamics, and race***
3. ***To investigate the relationship between glaucoma progression, ocular hemodynamics, and diabetes***
4. ***To investigate the relationship between glaucoma progression, ocular hemodynamics, and gender***
5. ***To investigate the relationship between glaucoma progression, ocular hemodynamics, and body mass index***
6. ***To investigate the relationship between glaucoma progression, ocular hemodynamics, and age***

CHAPTER 3

PhD Research Project – Material and Methods

1. Research design and methods:

My PhD research project utilizes data from 112 OAG patients, enrolled in the longitudinal and observational Indianapolis Glaucoma Progression study over a period of 5 years. The Indianapolis Glaucoma Progression Study was aimed to assess the role of vascular dysregulation in OAG patients at the Glaucoma Research and Diagnostic Center, Glick Eye Institute, Indiana University School of Medicine, Indianapolis, USA. All patients in this study have had multiple comprehensive assessments yearly for known clinical risk factors, multiple modalities for quantifying ocular blood flow and oxygenation of ocular tissues, and multiple methodologies for monitoring both structural and functional glaucoma progression.

This investigation was conducted at the Glaucoma Research and Diagnostic Center, Glick Eye Institute, in conjunction with the Department of Ophthalmology and Division of Biostatistics at the Indiana University School of Medicine, Indianapolis, Indiana, USA. All patients signed an informed consent prior to initiation of this study, which adhered to the tenets of the Declaration of Helsinki. The study protocol was approved by the Institutional Review Board committee at the Indiana University School of Medicine, Indianapolis, Indiana, USA. All participants were confirmed OAG patients (see criteria below) referred by the Indiana University Department of Ophthalmology at Indiana University and Wishard Hospital.

All the patients had to meet all of the following inclusion criteria to enter the study:

1. Age: 30 years or older.
2. Diagnosis: confirmed open-angle glaucoma in at least one eye:

a. glaucomatous visual field loss on Humphrey 24-2 or 10-2 perimetry

b. glaucomatous optic disc cupping

c. agreement between two baseline exams for reliability
3. Best corrected visual acuity at least 20/60 in at least one eye
4. Prior Humphrey visual fields demonstrate acceptable reliability standards

Patients were excluded for the following exclusion criteria:

1. Extensive Humphrey visual field damage consisting of either a mean deviation (MD) < -15 decibels or a clinically determined threat to fixation in both hemifields
2. Evidence of exfoliation or pigment dispersion
3. History of acute angle-closure or a narrow, occludable anterior chamber angle by gonioscopy
4. History of chronic or recurrent inflammatory eye diseases (e.g., scleritis, uveitis)
5. History or signs of intraocular trauma
6. Severe or potentially progressive retinal disease such as retinal degeneration, diabetic retinopathy, and retinal detachment
7. Any abnormality preventing reliable applanation tonometry
8. Current use of any ophthalmic or systemic steroid which may interfere with this investigation
9. Cataract surgery within the past year
10. Resting pulse < 50 beats per minute
11. Severe, unstable or uncontrolled cardiovascular, renal, or pulmonary disease

Recruited OAG patients participated over a 5-year observational follow-up period with two baseline measurements followed by evaluations of ocular blood flow and glaucoma progression every 6 months. The two baseline measurements served as confirmation of both glaucomatous status and measurement reliability. The study was purely observational; participation in this study did not affect treatment. All subjects in this study were on standard treatment for glaucoma, and all participating subjects received appropriate and individualized glaucoma care as directed by their treating ophthalmologist, with no consideration of their participation in this study. The natural history of glaucoma is that a significant portion of cases (up to 53% in EMGT) show progression even with standard treatment (Leske et al. 2003). The subjects that

showed functional and/or structural progression despite treatment received whatever treatment is necessary to stop or slow the progression of their glaucoma, as determined by their treating ophthalmologist. This group of patients served as the "progressing group" for the purposes of this study. Importantly, the aim of this study was to determine if measures other than intraocular pressure are associated with glaucoma progression. Thus, it depended on including some subjects who showed progression despite standard treatment to lower intraocular pressure. No subjects have been withdrawn from this study based on whether or not progression of disease has occurred.

At each visit, patients demographic and health information, visual function testing followed by blood flow and structure exams were performed in the same order at the same time of day for each patient (Table 1). Measurements were made at baseline and every 6 months over a 5-year period.

Table 1. Examinations and imaging techniques performed at each visit for the 5 years follow- up period.

Exams	Baseline X 2	0.5 year	1 year	1.5 year	2 year	2.5 year	3 year	3.5 year	4 year	4.5 year	5 year
Questionnaire/ History	√	√	√	√	√	√	√	√	√	√	√
Brachial artery blood pressure /Cardiac pulse	√	√	√	√	√	√	√	√	√	√	√
Height and weight	√	√	√	√	√	√	√	√	√	√	√
Autorefraction	√	√	√	√	√	√	√	√	√	√	√
Visual acuity and contrast sensitivity	√	√	√	√	√	√	√	√	√	√	√
Central Corneal Thickness	√										
Intraocular pressure	√	√	√	√	√	√	√	√	√	√	√
Ocular pulse amplitude	√	√	√	√	√	√	√	√	√	√	√
Fundus exam /Optic nerve exam	√	√	√	√	√	√	√	√	√	√	√
Color Doppler imaging (CDI)	√	√	√	√	√	√	√	√	√	√	√
Scanning laser Doppler flowmetry (HRF)	√	√	√	√	√	√	√	√	√	√	√
Visual Field Testing	√	√	√	√	√	√	√	√	√	√	√
Retinal Structure (Heidelberg Retinal	√	√	√	√	√	√	√	√	√	√	√

Tomograph, HRT 3)											
Retinal Structure (Optical Coherence Tomography)	√	√	√	√	√	√	√	√	√	√	√
Doppler Fourier-Domain OCT	Single time-point assessment during the follow- up period										

Measurements included in the following order:

- Questionnaire/history
- Brachial artery blood pressure and cardiac pulse
- Height and weight
- Autorefraction
- Visual acuity and contrast sensitivity
- Central corneal thickness
- Slit lamp examination:
    - measurement of the intraocular pressure (IOP)
    - measurement of the ocular pulse amplitude
    - fundus examination (optic nerve exam after pupil dilation)

Ocular blood flow was comprehensively determined using (Table 2):

- color Doppler imaging (CDI)
- confocal scanning laser Doppler flowmetry (HRF)
- Pascal dynamic contour tonometer
- calculated ocular perfusion pressures

Table 2. Summary of the multiple imaging approach to comprehensive ocular and systemic blood flow assessment.

Color Doppler imaging (CDI)	**Retrobulbar and optic nerve head blood flow** • OA PSV, EDV, RI • CRA PSV, EDV, RI • NPCA and TPCS PSV, EDV, RI
Scanning laser Doppler flowmetry (HRF)	**Retinal capillary blood flow** • Number of superior/inferior zero pixel blood flow • Superior/inferior mean blood flow
Fourier Domain Doppler OCT	**Retinal blood flow** • Total Blood Flow • Superior Hemisphere Blood Flow • Inferior Hemisphere Blood Flow

Choroidal blood flow	Pascal dynamic contour tonometer
Bulk ocular perfusion	Ocular perfusion pressures
Systemic blood flow	Blood pressure / heart rate

The use of multiple structure and visual field exams greatly enhanced the ability to identify and confirm glaucomatous progression (Sample et al., 2006). Structure exams included optic nerve and macula examination via (Table 3):

- Heidelberg Retinal Tomograph (HRT 3)
- Optical Coherence Tomography (OCT)

Visual field testing included:

- 24-2 standard automated perimetry (Swedish Interactive Threshold Algorithm, SITA)

All examinations were performed on one eye which that was randomly chosen. If only one eye qualified for inclusion in the study that eye was examined.

In addition, all the patients underwent at a single time-point during the follow- up assessment of the retinal blood flow with the RTVue Fourier Domain OCT equipped with Doppler functionality (Optovue, Inc., Freemont, CA, USA). The single time-point assessment was determined by the limited availability of the instrument for a short period of time at the Glaucoma Research and Diagnostic Center.

To limit reproducibility bias with imaging, a single experienced operator with over ten years of experience performed all measurements in the same order and at the same time of the day for each patient.

Table 3. Summary of the multiple imaging approach to comprehensive glaucomatous progression.

Functional progression	

Humphrey Visual Field Analyzer using the 24-2 SITA standard (white size III stimulus) algorithm	**Visual field testing** • mean deviation (MD) • pattern standard deviation (PSD) • Advanced Glaucoma Intervention Score (AGIS) visual field defect score
Structural progression	
Glaucoma specialist evaluation at the slit lamp	**Optic nerve exam** • Clinical evaluation of the Cup/Disk vertical ratio
Heidelberg Retinal Tomograph (HRT 3)	**Structure of the optic nerve head** • HRT 3 Cup Area • HRT 3 Rim Area • HRT 3 Cup Volume • HRT 3 Rim Volume • HRT 3 Cup/Disk Area Ratio • HRT 3 Linear Cup/Disk Ratio • HRT 3 Mean Cup Depth • HRT 3 Max Cup Depth • HRT 3 Cup Shape • HRT 3 Height Variation Contour **Structure of the peripapillary retinal nerve fiber layer (RNFL)** • HRT 3 Mean RNFL Thickness • HRT 3 RNFL Cross-Sectional Area
Zeiss Optical Coherence Tomography (OCT)	**Structure of optic nerve head** • Disk area • Cup area • Rim area • Cup/Disk vertical ratio • Cup/Disk horizontal ratio • Cup/Disk area ratio **Structure of the peripapillary retinal nerve fiber layer (RNFL)** • RNFL thickness average • RNFL thickness superior • RNFL thickness inferior • RNFL thickness nasal • RNFL thickness temporal **Structure of the macula** • macular thickness inner inferior • macular thickness outer nasal • macular thickness inner nasal • macular thickness outer temproal • macular thickness inner temporal • macula center • macular volume

2. Non Invasive Imaging Technologies:

Questionnaire/history

At baseline visit the participants gave basic health and demographic information. Any changes to the health or medication of subjects were recorded at subsequent follow up study visits. The questionnaire and history involved only health information relevant to the current project as listed: age (birth date), sex, race, smoking status (yes/no, years since cessation), hypertension status, diabetic status, ocular history (surgeries, disease, and trauma), glaucoma medications, systemic medications and years since glaucoma diagnosis. The questionnaire included a brief vision questionnaire based largely upon the National Eye Institute Visual Functioning Questionnaire – 25 (VFQ-25), a simple question list that the patients had to fill out (approximate duration: 5-10 minutes) aimed to assess the patients' functional ability and quality of life. The NEI-VFQ assessed other aspects of visual difficulties related to glaucoma which may not be apparent by visual acuity testing or contrast sensitivity.

Brachial artery blood pressure and cardiac pulse

Arterial blood pressure and cardiac pulse (heart rate) were measured with an automated ambulatory blood pressure monitor (CVS, Woonsocket, RI) after 5 minutes of rest in the seated position during the same time period that intraocular pressure was recorded for accurate calculation of ocular perfusion pressures. At each visit the measurement of systolic blood pressure (SBP) and diastolic blood pressure (DBP) were recorded, and the value of mean arterial pressure (MAP) was calculated by the equation MAP=DBP+1/3(SBP-DBP).

Height and weight

The body mass index (BMI) was obtained at each study visit by the formula BMI=weight (km)/height^2(m).

Auto refraction

Auto refraction testing was utilized at each study visit using a Cannon (Cannon, USA) autorefractor, GR-3100K. Autorefraction was carried out to establish optical correction for use in visual field examination.

Visual acuity and contrast sensitivity

Visual acuity (VA) and contrast sensitivity (CS) were assessed at each visit using Early Treatment Diabetic Retinopathy Study (ETRDS) vision chart and Vector vision analysis with the patient seated at rest. The contrast sensitivity testing involved reading an eye chart but instead of numbers and letters, as per the visual acuity testing, the patient identifies shades of grey lines using CSV-1000 charts (Vector Vision). Patented photocell circuitry automatically monitors and calibrates instrument testing light levels. CS determines the lowest contrast level which can be detected by a patient for a given size target. Normally a range of target sizes are used. In this way CS is unlike normal visual acuity as CS measures two variables, size and contrast, while acuity measures only size (approximate duration: 1 minute).

Central corneal thickness (CCT)

CCT was determined at the baseline visit by five consecutive measurements made with an ultrasonic corneal pachymeter averaged for each eye.

Intraocular pressure (IOP)

IOP was assessed with the patient sited at the slit lamp using the Goldmann applanation

tonometer. The Goldmann applanation tonometer represents the “gold” standard to measure the IOP. The method involves illumination of the biprism tonometer head with a blue light (obtained using a cobalt filter) used to flatten the anesthetized cornea, which has fluorescein in the tear film. The scaled knob on the side of the instrument is then turned until the inner border of the two hemi-circles of fluorescent tear meniscus, visualized through each prism, touch, thus indicating the value of the IOP in mmHg.

Ocular pulse amplitude

The ocular pulse amplitude was assessed at the slit lamp using the Pascal dynamic contour tonometer. The Pascal dynamic contour tonometer is a slit lamp mounted tonometer. A concave spherical tip is placed in contact with the central cornea. The radius of the tip surface will match the radius (within a very small margin of error) of the corneal segment it makes contact with. The IOP and ocular pulse data is acquired using a solid-state pressure sensor and therefore allows IOP measurements that are independent of corneal thickness without the need to put pressure directly on the cornea. Similar to the pulsatile ocular blood flow meter (pOBF), the Pascal dynamic contour tonometer additionally offers the possibility to acquire continuous ocular pulse measurements. A relationship has been derived between IOP and pulsatile blood flow in the eye (Silver et al., 1989). Measurements of IOP show a time variation that is associated with the pulsatile component of arterial pressure. Experimental results provide a means of transforming intraocular pressure changes into ocular volume changes (Silver et al., 1989). The eye is represented by a chamber with elastic walls, a pulsatile incoming flow of incompressible fluid (blood), and a steady outgoing flow of blood. Under these conditions, the rate of pulsatile blood flow through the eye, the majority representing choroidal blood flow, can be approximated from the instantaneous intraocular pressure measurements (Silver et al., 1989).

Fundus examination

The fundus exam was performed at the slit lamp after pupil dilation (optic nerve exam with evaluation of the cup to disc (c/d) ratio via indirect dilated ophthalmoscopy with a 90 diopters lens).

Ocular perfusion pressures (OPP)

OPP was calculated using the following equation: OPP = ((2/3 MAP) – IOP) where (MAP) is mean arterial pressure. Systolic ocular perfusion pressure (SOPP) was determined by subtracting IOP from systolic blood pressure and diastolic ocular perfusion pressure (DOPP) was determined by subtracting IOP from diastolic blood pressure.

Color Doppler imaging (CDI)

A Siemens Quantum 2000 CDI system (Siemens Quantum, Issaquah, WA) with a 7.5 MHz linear probe was utilized. This technique has been described in detail (Williamson et al., 1996). Samples of pulsed-Doppler signal from within a 0.2 x 0.2 mm sample area were analyzed to calculate blood velocities in the retrobulbar vasculature (Williamson et al., 1996). This technique has been shown to yield reproducible measurements of retrobulbar blood flow velocities (Harris et al., 1995; Quaranta et al., 1997; Williamson et al., 1996). CDI measurements were taken in the ophthalmic (OA), central retinal (CRA), and nasal (NPCA) and temporal (TPCA) posterior ciliary arteries. In each vessel, peak systolic velocity (PSV) and end diastolic velocity (EDV) were determined, and Pourcelot's resistive index was calculated (RI = (PSV-EDV)/PSV).

The parameters assessed by CDI considered in the study were:

- OA PSV, EDV, RI
- CRA PSV, EDV, RI
- NPCA and TPCS PSV, EDV, RI

Confocal scanning laser Doppler flowmetry (HRF)

Confocal scanning laser Doppler flowmetry (Heidelberg Retinal Flowmeter (HRF), Heidelberg Engineering, Heidelberg, Germany) was used to measure perfusion within peripapillary retinal capillary beds. This technique has been described in detail (Kagemann et al., 1998). Briefly, the HRF utilizes an infrared laser which scans the retina. The frequency and amplitude of Doppler shifts in the reflected light allow for determination of blood velocity and blood volume, respectively. This information is used to compute total blood flow and to create a physical map of flow values contained in the retina is created. The Glaucoma Research and Diagnostic center in Indianapolis has developed the "Harris" method of HRF analysis in which cumulative percentage landmarks are used to describe the "shape" of the flow distribution within the retina. This technique differs from other HRF software applications which have been shown to be less reliable (Jonescu-Cuypers et al., 2004; Yu et al., 2005). Notably, our analysis differentiated avascular tissue (measured as zero flow pixels) from perfused tissue, thereby describing the degree of vascularity of the fundus (Jonescu-Cuypers et al., 2004; Jonescu-Cuypers et al., 2004). The commercial HRF software assumes a normally distribution of flow values despite the fact that in reality these values are skewed and non-evenly distributed. The "Harris" pixel by pixel HRF analysis method overcomes issues related to the non-normal flow distribution as well as issues related to the cardiac cycle and smoothing of images (Jonescu-Cuypers et al., 2004; Yu et al., 2005).

The parameters assessed by HRF considered in the study were:

- Number of superior/inferior zero pixel blood flow: represent the % (shown as a decimal) avascular area of the total peripapillary retinal area measured with no detectable blood flow.
- Superior/inferior mean blood flow: represent the average recorded retinal capillary blood flow in the respective peripapillary superior and inferior retina (in arbitrary units).

Visual field testing

Visual fields were assessed by the Zeiss Humphrey Visual Field Analyzer (Carl Zeiss Meditec, Inc. 5160 Hacienda Drive, Dublin, CA 94568, USA) using the 24-2 SITA standard (white size III stimulus) algorithm. This instrument is considered the "Gold Standard" for visual field evaluation for glaucoma. All potential subjects underwent at least two tests with this instrument and most enrolled subjects will have even more experience. All subjects demonstrated the ability to perform the test reliably, as determined by the STATPAC software and the judgment of the three clinical investigators. Potential subjects were excluded if extensive damage is present (mean deviation < -15 decibels or a clinically determined threat to fixation in both hemi fields). Each subject was tested using the usual and standard procedures and experienced technicians. At the start of the test, the subject was asked to position his or her head in the head support and the instrument height is adjusted to maximize the subject's comfort. The appropriate refractive correction was placed in front of the eye being tested and the subject is given the standard instructions. The technician was present during the test to monitor for deviations in the testing procedure and to reinforce instructions. Visual field testing was performed at baseline and then every 6 months over 5 years.

Visual field progression is determined using the Humphrey Glaucoma Progression Analysis (GPA) software. This software has been validated for assessing progression in several studies including the Early Manifest Glaucoma Trial (Heijl et al., 2003). The software analyzes each point for decibel change and identifies any test point that has worsened by an amount that exceeds the variability expected in all but the most variable five percent ($p<0.05$) of glaucoma patients having similar visual field status. Thus the software determines if the change is larger than 95% of the variability seen at that exact test location in fields having a similar mean threshold deviation from normal values. Over multiple visual field examinations, the GPA software identifies points changing at the $p<0.05$ significance level in consecutive follow-up

exams. Points changing on 2 consecutive fields are considered possible progression while points changing on 3 consecutive fields are considered likely progression. As noted above, subjects are excluded if their mean deviation on their baseline or earlier visual field is < -15 dB. The Humphrey GPA software has not been well validated on these more advanced cases.

At the beginning of the study, it has been expected that, over the course of this 5-year study, approximately one-third of subjects will show glaucomatous visual field progression. This is based on results of the Early Manifest Glaucoma Trial, which used software similar to Humphrey GPA to assess progression. In that study, the percentage of normal tension glaucoma (IOP<21) patients that progressed on treatment by 5 years was just under 40% (Heijl et al., 2002). Treatment in the Early Manifest Glaucoma Trial consisted only of argon laser trabeculoplasty plus betaxolol. Our study did not impose these treatment limitations so we expected a lower rate of progression with more aggressive treatment.

Several different parameters have been used to measure extent of progression:

1. *The number of points that are considered "Likely Progression" compared to baseline by the GPA software.* Subjects with higher numbers of significantly progressed points are considered to have progressed more than subjects with only a few progressed points. Stable subjects will have few or no points that are considered "Likely Progression." The limitation of this method is that after a point is considered "Likely Progression," further decibel change is not taken into account. Thus this method indicates the breadth of points changing but not the depth.

2. *The slope of the mean deviation over serial visual field exams.* This slope is plotted on the GPA printout. A steeper slope indicates a more rapid progression compared to a flatter slope. A change in mean deviation indicates a global change and takes into account the depth of change of points. However, it is affected by media opacities, especially cataract progression.

3. *The slope of the Pattern Standard Deviation (PSD) over serial visual field exams.* This global index reflects the non-uniformity of the depth of glaucomatous visual field defects. A limited

number of focal defects that become deeper will result in a change in the PSD. As the visual field defects become more extensive and the overall field becomes more uniformly depressed, the magnitude of PSD may decrease. However, in this study, any potential subject with a MD < -15 dB is excluded, so we expected almost all progressing subjects to show a worsening or increasing PSD over the course of the study.

The parameters assessed by visual field testing considered in the study were:

- mean deviation (MD): global index that represents the average difference from normal expected value in the patients' particular age group. Typically, an MD of -2.00 or less could indicate glaucoma.
- pattern standard deviation (PSD): global index that provides information about localized loss. A high PSD indicates a nonuniform sensitivity loss (ie, not due to diffuse depression from cataract or vitreous hemorrhage).
- Advanced Glaucoma Intervention Score (AGIS) visual field defect score: visual field score based on the number and depth of clusters of adjacent depressed test sites in the upper and lower hemifields and in the nasal area of the total deviation printout of the threshold program single-field test STATPAC-2 analysis. The score ranges from 0 (no defect) to 20 (all test sites deeply depressed).

Optical coherence tomography (OCT)

Optical coherence tomography (Optical Coherence Tomograph (OCT), Stratus software V.4.0, Zeiss Meditec, Dublin, CA) was used to analyze the structure of the optic nerve head, of the peripapillary retinal nerve fiber layer (RNFL) and of the macula. The OCT provides real time cross sectional images and quantitative analysis of retinal features to optimize the monitoring of retinal nerve fiber layer changes. OCT is based on optical low-coherence reflectometry

which is a one dimensional ranging technique applied to investigations in fiber based waveguide devices. OCT are the two and three dimensional tomographic images created by transverse scanning of the target. An OCT image is created by combining one dimensional ranging scans which provide a map of the reflectivity of the structure. In OCT the internal structure is mapped by directing a beam of light onto the target and measuring the delay time of light reflected from microstructural features at different ranges.

The parameters assessed by OCT considered in the study were:

- Optic nerve head
    - Disk area
    - Cup area
    - Rim area
    - Cup/Disk vertical ratio
    - Cup/Disk horizontal ratio
    - Cup/Disk area ratio
- Retinal Nerve Fiber Layer (RNFL)
    - RNFL thickness average
    - RNFL thickness superior
    - RNFL thickness inferior
    - RNFL thickness nasal
    - RNFL thickness temporal
- Macula
    - macular thickness inner inferior
    - macular thickness outer nasal
    - macular thickness inner nasal
    - macular thickness outer temporal
    - macular thickness inner temporal
    - macula center
    - macular volume

Fourier Domain Doppler OCT

The RTVue Fourier Domain (FD) OCT equipped with Doppler functionality (Optovue, Inc., Freemont, CA, USA) was used for total retinal blood flow data collection. Five scans (DCSP Protocol) were taken on the selected eye at each session with the patient in a seated position in a darkened room. The DCSP scan was graded in Oregon Health & Science University, Portland, Oregon, under David Haung's direction. Importantly, the assessment of the retinal blood flow by Doppler FD OCT was realized at a single time-point during the follow- up due to the limited availability of the instrument for a short period of time.

The parameters assessed by Doppler FD OCT considered in the study were:

- Total Blood Flow
- Superior Hemisphere Blood Flow
- Inferior Hemisphere Blood Flow

Heidelberg Retinal Tomograph - III

The Heidelberg Retinal Tomograph-III (HRT 3, Heidelberg Engineering, Heidelberg, Germany) uses a special laser to take 3-dimensional photographs of the optic nerve and surrounding retina. This laser, which is not powerful enough to harm the eye, is first focused on the surface of the optic nerve to captures an image. Then, it is focused on the layer just below the surface to capture the next image. The HRT 3 continues to image subsequent layers until the desired depth is reached. Finally, the instrument uses the multiple 2-dimensional images to construct a 3-dimensional image of the entire optic nerve. The HRT 3 image can be used to compute the area of the optic disc, the volume of the cup, the area of the rim around the cup, and the depth of the optic nerve head. In details, based on the Ocular Hypertension Treatment Study (OHTS) (Zangwill et al., 2004; Zangwill et al., 2005) and the Thessaloniki Eye Study (Topouzis et al., 2006) the following structure variables were found to be among the significantly associated either with the development of glaucoma in persons with ocular hypertension or with blood pressure status in persons without glaucoma:

1. disc area – defined as the total area of the disc
2. cup area – defined as the total area of those parts within the disc margin located below the reference plane
3. rim area – defined as the total area within the disc margin minus the cup area
4. mean cup depth – defined as the mean depth of the cup
5. cup-to-disk area ratio – defined as the ratio of the cup area to the disc area (Zangwill et al., 1996).

These variables have been used in our study to determine how changes in ocular blood flow are related to changes in optic nerve structure. This was accomplished using these HRT 3 structure values in comparison to blood flow values including the retinal microcirculation, retrobulbar hemodynamics and ocular perfusion pressures. The computed HRT 3 parameters can detect optic nerve changes prior to visual field loss, may aid in earlier diagnosis of glaucoma, and can be used to monitor disease progression over time (DeLeon Ortega et al., 2007; Favers et al., 2007; Zangwill et al., 1996; Zangwill et al., 2004; Zangwill et al., 2005). The Topographic Change Analysis (TCA) software package in the HRT 3 compares variability between exams and provides a statistical indicator of change over time. The TCA provides change indicator and cluster analysis over time. Three exams are required to trigger progression analysis. Progression is defined as an area of change larger than 20 super-pixels that meets the following criteria: 1. Area shows statistically significant change based on comparing the amount of change with the image variability (statistical F test) and 2. the same area of change is consistent over 3 out of 4 of the last exams.

The parameters assessed by HRT 3 considered in the study were:

- Optic nerve head
    - HRT 3 Cup Area
    - HRT 3 Rim Area
    - HRT 3 Cup Volume
    - HRT 3 Rim Volume
    - HRT 3 Cup/Disk Area Ratio

- HRT 3 Linear Cup/Disk Ratio
- HRT 3 Mean Cup Depth
- HRT 3 Max Cup Depth
- HRT 3 Cup Shape
- HRT 3 Height Variation Contour

- Retinal Nerve Fiber Layer (RNFL)
  - HRT 3 Mean RNFL Thickness
  - HRT 3 RNFL Cross-Sectional Area

3. Definition of Glaucoma Progression:

Functional glaucoma progression assessed by visual field testing was defined as two consecutive visits with:

a) mean deviation (MD) decrease by at least 2 compared from baseline and/or

b) Advanced Glaucoma Index Study (AGIS) score increase by at least 2 from baseline

Structural glaucoma progression assessed by HRT 3 and OCT was defined as two consecutive visits with:

a) an RNFL thickness decrease ≥8%, and/or

b) horizontal or vertical cup/disc ratio increase by ≥0.2 from baseline

4. Statistical methods:

Mixed-model analysis of covariance (ANCOVA) was used to test for significance of changes from baseline to 5-year follow-up overall and then separately by race, diabetes status, gender, age (>= vs < 65), and BMI category (normal weight, overweight, obese). Two-sample t tests and $\chi 2$ tests were used to analyze differences in baseline data between patients who progressed and those who did not progress. The models were then extended to test for whether the changes were different by each of the 5 factors. Time to functional progression and time to structural progression were analyzed using Cox proportional hazards survival analysis. Factors were

analyzed as baseline measurements, as time-varying measurements, and as time-varying changes from baseline. Interactions were tested to determine if the effects of the factors on progression time differed by race, diabetes, gender, age category, or BMI category. Pearson correlation coefficients were calculated to evaluate linear associations. Correlations were adjusted for years of glaucoma, use of glaucoma or hypertension medications, age 65 or older, body mass index category, diabetic status, race, and sex. Correlations were compared between groups using Fisher z tests. P values <0.05 were considered statistically significant.

CHAPTER 4

PhD Research Project – Aim 1: To investigate the role of ocular and vascular risk factors in the functional and structural progression of the glaucomatous optic neuropathy

1. Introduction – Aim 1:

Primary open-angle glaucoma (OAG) is an optic neuropathy characterized by progressive death of the retinal ganglion cell and corresponding visual field loss. Elevated intraocular pressure (IOP) has been identified as a major risk factor, and only modifiable one, for OAG onset and progression. Currently, treatments focused on reducing the IOP by medical and surgical interventions represent the only option available for physicians to control and limit disease progression. However, it is well established that glaucoma progression is still observed in some patients, despite IOP reduction. Additionally, a high percentage of individuals do not develop glaucoma even with high level of IOP (Glaucoma Preferred Practice Pattern Panel, 2020; Hollows et al., 1996 Suzuki et al., 1999; Heijl et al. 2002; Leske et al., 2007). These findings suggest that glaucoma progression is multifactorial in origin and that underlying contributing factors – other than IOP – are possibly involved in the disease onset and progression (Fechtner et al., 1994; Sigal et al., 2009).

Importantly, the role of ocular blood flow in glaucoma has been widely investigated. Reduced ocular blood flow and ischaemia to the optic nerve have been shown to be contributing factors for the disease pathogenesis and progression (Harris et al., 1994; Chung et al. 1999). Vascular abnormalities, both in the systemic and ocular circulation, have been connected to OAG, such as systemic hypertension and hypotension (nocturnal), migraine, age-related changes of the vasculature, and hemorrhages of the optic nerve disc (Leighton et al. 1972; Hayreh et al. 1994; Harris et al., 2000; Drance et al., 2001). In addition, a decreased ocular pressure has been shown to be a risk factor for OAG prevalence, incidence and progression (Tielsch et al., 1995; Bonomi

et al., 2000; Leske et al., 2002; Topouzis et al., 2006; Bonomi et al., 2000; Moore et al., 2008). Primary open-angle glaucoma patients have also shown impaired hemodynamics in the retinal, choroidal and retrobulbar circulations, all associated with glaucomatous progression, both functional and structural (Flammer et al., 2002; Galassi et al., 2003; Martínez and Sánchez, 2005; Zeitz et al., 2006; Calvo et al. 2021; Jimenez-Aragon et al., 2013). However, the aforementioned studies present several limitations, such as small sample sizes, heterogeneity of inclusion criteria of the study subjects (many including glaucoma suspects and not with a confirmed diagnosis), use of different imaging techniques to evaluate the ocular blood flow and structural damage, and non-uniform definition and simultaneous assessment of structural and functional progression. Also, it important to highlight that the relationship between functional and structural progression itself is still not fully delineated, and a heavily researched topic in the ophthalmology research is currently represented by the development of prediction models for glaucoma progression.

In conclusion, the interaction between ocular blood flow and glaucoma functional and structural progression is still not fully elucidated, due to the limitations highlighted above. The Indianapolis Glaucoma Progression Study represented the first longitudinal and observational study in which a large sample of OAG patients was evaluated by multiple hemodynamic imaging technologies and multiple measures of structure and function to comprehensively assess the ocular and systemic circulation and to adequately monitor disease progression. The Aim 1 of my PhD analysis took advantage of the existing dataset of OAG patients enrolled in the Indianapolis Glaucoma Progression Study, in order to shed further light on the relationship between ocular and systemic hemodynamics and glaucoma progression. In details, the Aim 1 of my PhD project has been to specifically investigate the role of clinical and vascular risk factors in the functional and structural progression of the glaucomatous optic neuropathy.

2. Material and Methods - Aim 1:

The comprehensive discussion of the materials and methods is detailed in chapter 3. In brief, my PhD analysis took advantage of a large and comprehensive existing dataset of 112 OAG patients, enrolled in the longitudinal and observational Indianapolis Glaucoma Progression Study, in which a large sample of OAG patients was evaluated during 5 years by multiple hemodynamic imaging technologies and multiple measures of structure and function to comprehensively assess the ocular and systemic circulation and to adequately monitor disease progression.

In brief, a cohort of 112 patients with OAG were enrolled at baseline, and prospectively examined at baseline and every 6 months over a period of five years at the Glaucoma and Diagnostic Center at Indiana University School of Medicine, Indianapolis, Indiana. One qualified eye was randomly designated as the observational study eye in each subject. Measurements were made at baseline and every 6 months over a 5-year period.

To limit reproducibility bias with imaging, a single experienced operator with over ten years of experience performed all measurements in the same order and at the same time of the day for each patient. Functional disease progression was monitored by visual field testing and defined as two consecutive visits with an Advanced Glaucoma Intervention Study (AGIS) score increase ≥2 from baseline, and/ or MD decrease ≥2 from baseline. Structural disease progression was monitored with optical coherence tomography and Heidelberg retinal tomography and defined as two consecutive visits with RNFL thickness decrease ≥8% and/or horizontal or vertical cup/disk ratio increase ≥0.2 compared to baseline.

The statistical analysis involved mixed-model analysis of covariance (ANCOVA) to test for significance of changes from baseline to 5-year follow-up. Two-sample t tests and $\chi 2$ tests were used to analyze differences in baseline data between patients who progressed and those who did not progress. The models were then extended to test for whether the changes were different

overall. Time to functional progression and time to structural progression were analyzed using Cox proportional hazards survival analysis. Factors were analyzed as baseline measurements, as time-varying measurements, and as time-varying changes from baseline. Pearson correlation coefficients were calculated to evaluate linear associations. P values <0.05 were considered statistically significant.

3. Results – Aim 1

A cohort of 112 OAG patients were prospectively examined at baseline and every 6 months over a period of five years. Overall baseline characteristics of the population revealed a mean age 64.9 ± 11.0 years; female (n=68), male (n=44); African descent (n=29), European descent (n=83); and non-insulin-dependent diabetes mellitus (n=21), no diabetes mellitus (n = 91).

Table 1 shows the overall change in the study measurements (mean and 95% confidence interval, CI) from baseline to five years. After 5 years, 37 subjects (11 AD, 26 ED; 7 with DM, 30 without DM; 24 female; 13 male; 31 age >= 65yo, 6 age < 65yo; 16 NW, 11 OW, 10 OB) progressed functionally, and 76 (18 AD, 58 ED; 14 with DM, 62 without DM; 46 female, 30 male; 50 age >= 65yo, 26 age < 65yo; 31 NW, 25 OW, 20 OB) structurally.

Table 1. Change from baseline to five years in the study parameters in open-angle glaucoma patients. * p-value statistically significant < 0.05.

	All						
	Baseline		5 year		Change		
	N	Mean (95% CI)	N	Mean (95% CI)	Mean (95% CI)	p-value	
IOP	111	16.68 (15.52, 17.84)	75	15.28 (14.01, 16.54)	-1.41 (-2.36, -0.45)	0.0040	*
SBP	111	136.20 (131.41, 140.99)	77	129.78 (124.65, 134.91)	-6.42 (-10.68, -2.16)	0.0032	*
DBP	111	82.99 (80.15, 85.82)	77	77.74 (74.81, 80.66)	-5.25 (-7.92, -2.58)	0.0001	*
MAP	111	100.67 (97.46, 103.88)	77	95.03 (91.66, 98.40)	-5.64 (-8.60, -2.68)	0.0002	*
HR	111	71.34 (68.37, 74.31)	78	71.66 (68.28, 75.03)	0.31 (-2.18, 2.81)	0.8060	
Visual Acuity	111	0.09 (0.06, 0.12)	76	0.23 (0.18, 0.29)	0.14 (0.10, 0.19)	0.0000	*
OA PSV	112	23.03 (20.90, 25.37)	76	21.79 (19.42, 24.43)	-1.31 (-3.49, 0.69)	0.2054	
OA EDV	112	5.62 (5.10, 6.19)	76	3.93 (3.48, 4.44)	-2.41 (-3.26, -1.65)	0.0000	*
OA RI	112	0.755 (0.771, 0.738)	76	0.816 (0.832, 0.799)	0.081 (0.109, 0.056)	0.0000	*

CRA PSV	112	8.03 (7.53, 8.53)	76	7.44 (6.87, 8.02)	-0.59 (-1.05, -0.13)	0.0126	*
CRA EDV	112	2.26 (2.11, 2.42)	76	1.68 (1.55, 1.82)	-0.78 (-1.05, -0.53)	0.0000	*
CRA RI	112	0.702 (0.686, 0.717)	76	0.765 (0.747, 0.784)	0.064 (0.046, 0.081)	0.0000	*
NPCA PSV	111	7.44 (6.96, 7.92)	76	7.32 (6.73, 7.91)	-0.12 (-0.59, 0.36)	0.6309	
NPCA EDV	111	2.35 (2.21, 2.51)	76	1.83 (1.70, 1.98)	-0.67 (-0.91, -0.45)	0.0000	*
NPCA RI	111	0.668 (0.653, 0.682)	76	0.742 (0.725, 0.758)	0.074 (0.057, 0.091)	0.0000	*
TPCA PSV	112	7.76 (7.32, 8.21)	76	7.51 (7.00, 8.03)	-0.25 (-0.67, 0.17)	0.2376	
TPCA EDV	112	2.38 (2.24, 2.54)	76	1.82 (1.69, 1.96)	-0.75 (-0.99, -0.52)	0.0000	*
TPCA RI	112	0.686 (0.701, 0.671)	76	0.758 (0.771, 0.743)	0.092 (0.118, 0.068)	0.0000	*
Superior Zero Pixels	112	0.200 (0.189, 0.213)	30	0.225 (0.202, 0.251)	0.022 (0.002, 0.040)	0.0334	*
Inferior Zero Pixels	111	0.185 (0.174, 0.197)	30	0.205 (0.186, 0.225)	0.018 (0.001, 0.033)	0.0418	*
Inferior Mean Flow	111	417.94 (386.46, 451.98)	30	397.46 (348.18, 453.71)	-21.53 (-78.59, 28.97)	0.4193	
Superior Mean Flow	112	415.92 (390.01, 443.56)	30	394.91 (345.51, 451.39)	-22.13 (-82.58, 31.00)	0.4314	
MD	112	-3.38 (-4.43, -2.34)	78	-4.88 (-6.18, -3.57)	-1.49 (-2.35, -0.63)	0.0007	*
PSD	112	4.00 (3.03, 4.97)	78	4.85 (3.80, 5.89)	0.85 (0.41, 1.29)	0.0002	*
AGIS score	112	1.41 (0.86, 2.12)	77	2.14 (1.37, 3.16)	0.56 (0.28, 0.81)	0.0002	*
Disk area	112	2.272 (2.141, 2.403)	73	2.618 (2.469, 2.766)	0.346 (0.249, 0.442)	0.0000	*
Cup area	112	1.184 (1.016, 1.352)	73	1.513 (1.324, 1.703)	0.329 (0.234, 0.425)	0.0000	*
Rim area	112	1.080 (0.950, 1.211)	73	1.104 (0.963, 1.246)	0.024 (-0.071, 0.119)	0.6199	
cup/disk area ratio	112	0.514 (0.455, 0.574)	73	0.572 (0.509, 0.634)	0.058 (0.026, 0.090)	0.0005	*
cup/disk horiz ratio	112	0.70 (0.65, 0.74)	73	0.76 (0.71, 0.80)	0.06 (0.03, 0.08)	0.0000	*
cup/disk vert ratio	112	0.684 (0.639, 0.730)	73	0.716 (0.666, 0.767)	0.032 (0.005, 0.059)	0.0182	*
RNFL thickness superior	112	89.08 (82.24, 95.92)	71	82.85 (75.58, 90.13)	-6.23 (-10.80, -1.66)	0.0076	*
RNFL thickness inferior	112	91.32 (83.09, 99.55)	71	87.41 (78.10, 96.73)	-3.91 (-9.24, 1.42)	0.1502	
RNFL thickness nasal	112	63.15 (58.44, 67.86)	71	65.93 (60.15, 71.71)	2.78 (-1.58, 7.14)	0.2110	
RNFL thickness temporal	112	54.93 (50.02, 59.84)	71	54.44 (49.07, 59.81)	-0.49 (-3.90, 2.92)	0.7789	
RNFL average	112	74.91 (70.11, 79.70)	71	72.82 (67.59, 78.05)	-2.09 (-5.10, 0.92)	0.1740	
macular thickness outer superior	112	221.60 (216.02, 227.18)	75	214.71 (208.94, 220.49)	-6.88 (-9.56, -4.20)	0.0000	*
macular thickness inner superior	112	262.57 (256.48, 268.65)	75	251.68 (245.13, 258.23)	-10.89 (-13.98, -7.79)	0.0000	*
macular thickness outer inferior	112	208.45 (203.12, 213.78)	75	202.43 (196.81, 208.06)	-6.02 (-8.58, -3.46)	0.0000	*
macular thickness inner inferior	112	256.55 (250.47, 262.63)	75	247.73 (241.00, 254.46)	-8.82 (-12.18, -5.46)	0.0000	*
macular thickness outer nasal	112	235.05 (229.65, 240.45)	75	230.33 (224.57, 236.10)	-4.72 (-7.27, -2.16)	0.0003	*
macular thickness inner nasal	112	262.02 (256.12, 267.91)	75	251.75 (245.29, 258.20)	-10.27 (-13.85, -6.69)	0.0000	*
macular thickness	112	204.78 (200.04, 209.51)	75	196.35 (191.17, 201.53)	-8.42 (-11.56, -5.28)	0.0000	*

outer temporal							
macular thickness inner temporal	112	247.58 (241.56, 253.60)	75	238.97 (232.24, 245.69)	-8.61 (-13.08, -4.15)	0.0002	*
Macula center	112	201.44 (193.51, 209.37)	75	201.45 (191.66, 211.24)	0.01 (-6.87, 6.90)	0.9971	
macular volume	112	6.40 (6.27, 6.53)	75	6.20 (6.06, 6.33)	-0.21 (-0.26, -0.15)	0.0000	*
HRT3 Cup Area	111	0.870 (0.735, 1.015)	77	0.908 (0.768, 1.059)	0.037 (-0.001, 0.075)	0.0574	
HRT3 Rim Area	111	1.268 (1.159, 1.377)	77	1.227 (1.115, 1.339)	-0.041 (-0.083, 0.002)	0.0600	
HRT3 Cup Volume	111	0.296 (0.224, 0.368)	77	0.319 (0.246, 0.392)	0.023 (0.003, 0.042)	0.0215	*
HRT3 Rim Volume	111	0.295 (0.246, 0.344)	77	0.292 (0.242, 0.341)	-0.003 (-0.022, 0.015)	0.7186	
HRT3 Cup/Disk Area Ratio	111	0.410 (0.359, 0.461)	77	0.429 (0.377, 0.482)	0.019 (0.000, 0.038)	0.0463	*
HRT3 Linear Cup/Disk Ratio	111	0.619 (0.573, 0.665)	77	0.632 (0.584, 0.679)	0.013 (-0.003, 0.029)	0.1019	
HRT3 Mean Cup Depth	111	0.300 (0.266, 0.334)	77	0.309 (0.275, 0.343)	0.009 (0.001, 0.018)	0.0356	*
HRT3 Max Cup Depth	111	0.724 (0.659, 0.790)	77	0.730 (0.665, 0.795)	0.006 (-0.015, 0.027)	0.5806	
HRT3 Cup Shape	111	-0.128 (-0.149, -0.108)	77	-0.115 (-0.137, -0.092)	0.014 (0.004, 0.024)	0.0081	*
HRT3 Height Variation Contour	111	0.330 (0.297, 0.366)	77	0.353 (0.316, 0.396)	0.022 (0.004, 0.040)	0.0196	*
HRT3 Mean RNFL Thickness	111	0.196 (0.172, 0.219)	77	0.185 (0.159, 0.210)	-0.011 (-0.025, 0.003)	0.1231	
HRT3 RNFL Cross-Sectional Area	111	1.025 (0.901, 1.148)	77	0.973 (0.839, 1.108)	-0.051 (-0.125, 0.022)	0.1692	

In the overall group of OAG patients the IOP decreased significantly from 16.68 at baseline to 15.28 at five years, with a statistically significant mean change of -1.41 (95% CI: -2.36, -0.45; p=0.0040), Table 1 and Figure 1. The functional parameters assessed by visual field testing significantly changed from baseline to five years: mean deviation decreased significantly from -3.38 to -4.88, with a statistically significant mean change of -1.49 (95% CI: -2.35, -0.63; p=0.0007); pattern standard deviation significantly increased from 4.0 to 4.85, change of 0.85 (95% CI: 0.41, 1.29; p=0.0002); Advanced Glaucoma Intervention Study score increased from 1.41 to 2.14, change of 0.56 (0.28, 0.81; p=0.0002), Table 1 and Figure 1.

Figure 1. Intraocular pressure (IOP) and visual field parameters (mean deviation, pattern standard deviation, and Advance Glaucoma Intervention Score) (mean +/- standard error) in open-angle glaucoma patients at baseline (BL) and 5 years (5 yr).

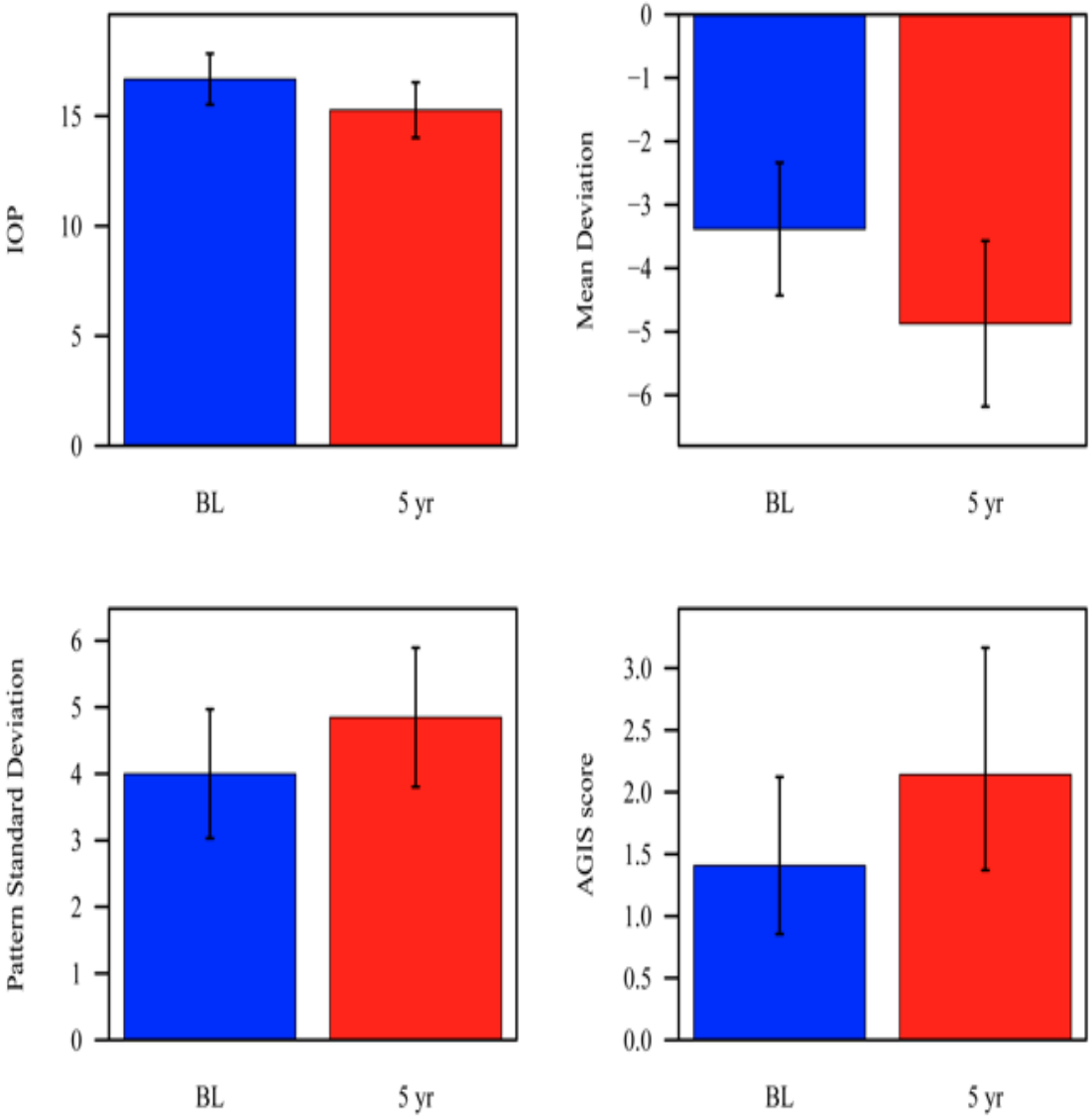

Lower baseline MD (p=0.0055) and higher AGIS score (p=0.0196) were associated with shorter time to structural progression after 5 years, Figure 2.

Figure 2. Survival function for time to structural progression for open-angle glaucoma patients for baseline functional parameters (mean deviation, MD, and advanced glaucoma intervention study (AGIS) score). Lines represent survival curves for lowest and highest observed measurements. Lower baseline MD and higher AGIS score were associated with shorter time to structural progression.

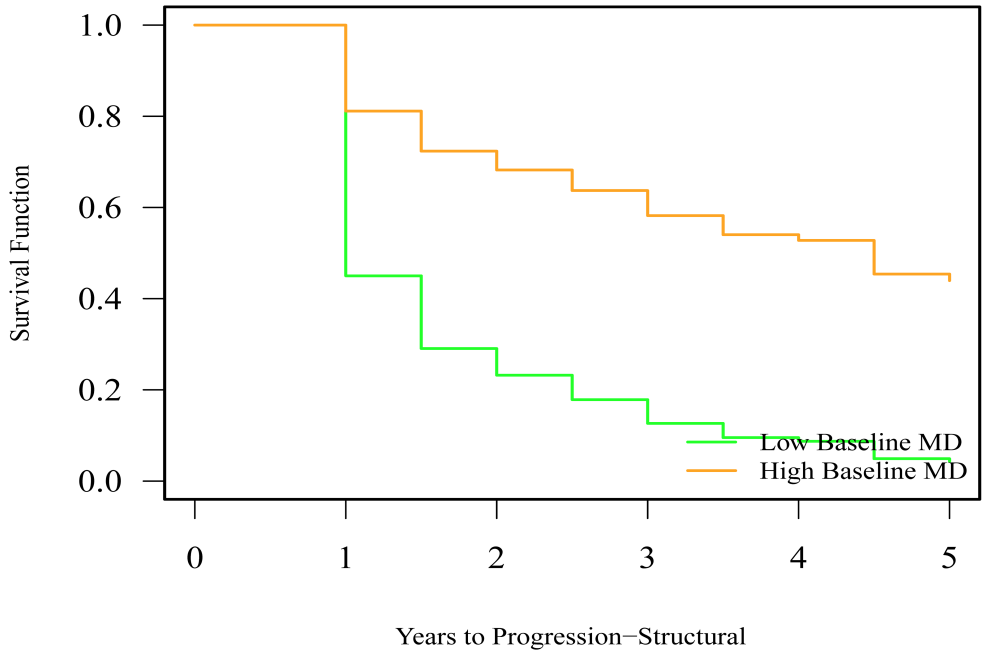

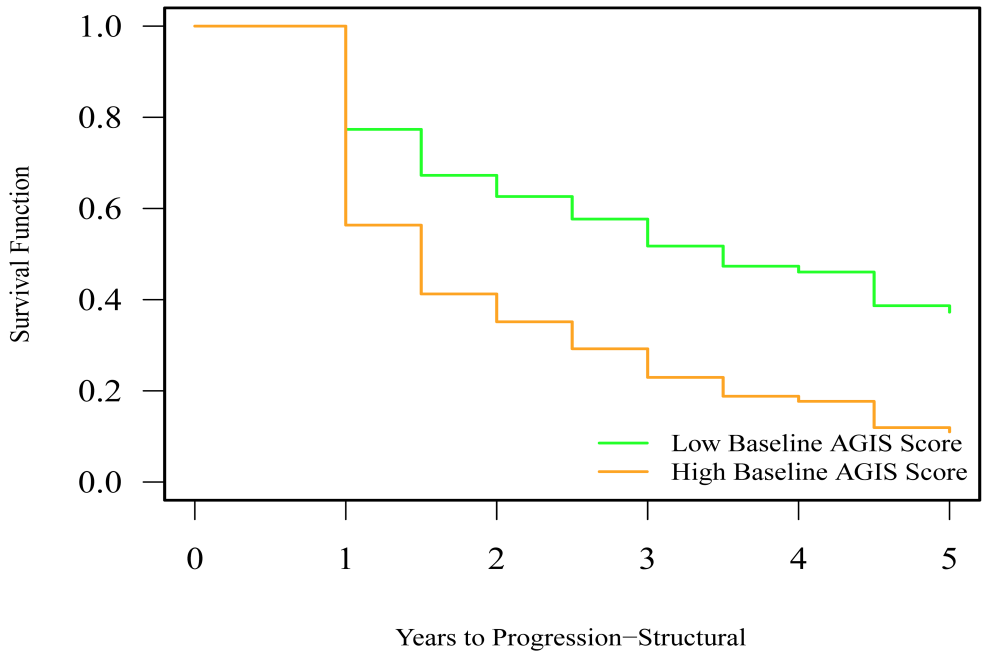

The optic nerve head and RNFL parameters assessed by Heidelberg tomograph 3 changed as follows from baseline to 5 years: cup area increased from 0.870 to 0.908, with a mean change of 0.037 (95% CI: -0.001, 0.075; p=0.0574); rim area decreased from 1.268 to 1.227, with a mean change of -0.041, 95% CI: -0.083, 0.002; p=0.0600); cup volume increased significantly from 0.296 to 0.319, with a statistically significant mean change of 0.023 (95% CI: 0.003, 0.042; p=0.0215); rim volume decreased from 0.295 to 0.292, with a mean change of -0.003,

(95% CI: -0.022, 0.015; p=0.7186); cup/disc area ratio significantly increased from 0.410 to 0.429, with a statistically significant mean change of 0.019 (95% CI: 0.000, 0.038; p=0.0463); linear cup/disk increased from 0.619 to 0.632, with a mean change of 0.013 (95% CI: -0.003, 0.029; p=0.1019); mean cup depth significantly increased from 0.300 to 0.309, with a statistically significant change of 0.009 (95% CI: 0.001, 0.018; p=0.0356); cup shape significantly changed from -0.128 to -0.115, with a statistically significant change of 0.014 (95% CI: 0.004, 0.024; p=0.0081); height variation contour significantly increased from 0.330 to 0.353, with a statistical significant change of 0.022 (95% CI: 0.004; p=0.0196); mean RNFL thickness decreased from 0.196 to 0.185, with a mean change of -0.011 (95% CI: -0.025, 0.003; p=0.1231); RNFL cross-sectional area decreased from 1.025 to 0.973, with a mean change of -0.051, 95% CI: -0.125, 0.022; p=0.162), Table 1, Figure 3.

Figure 3. Optic nerve head parameters assessed by Heidelberg retinal tomograph 3 (mean +/- standard error) in open-angle glaucoma patients at baseline (BL) and 5 years (5 yr).

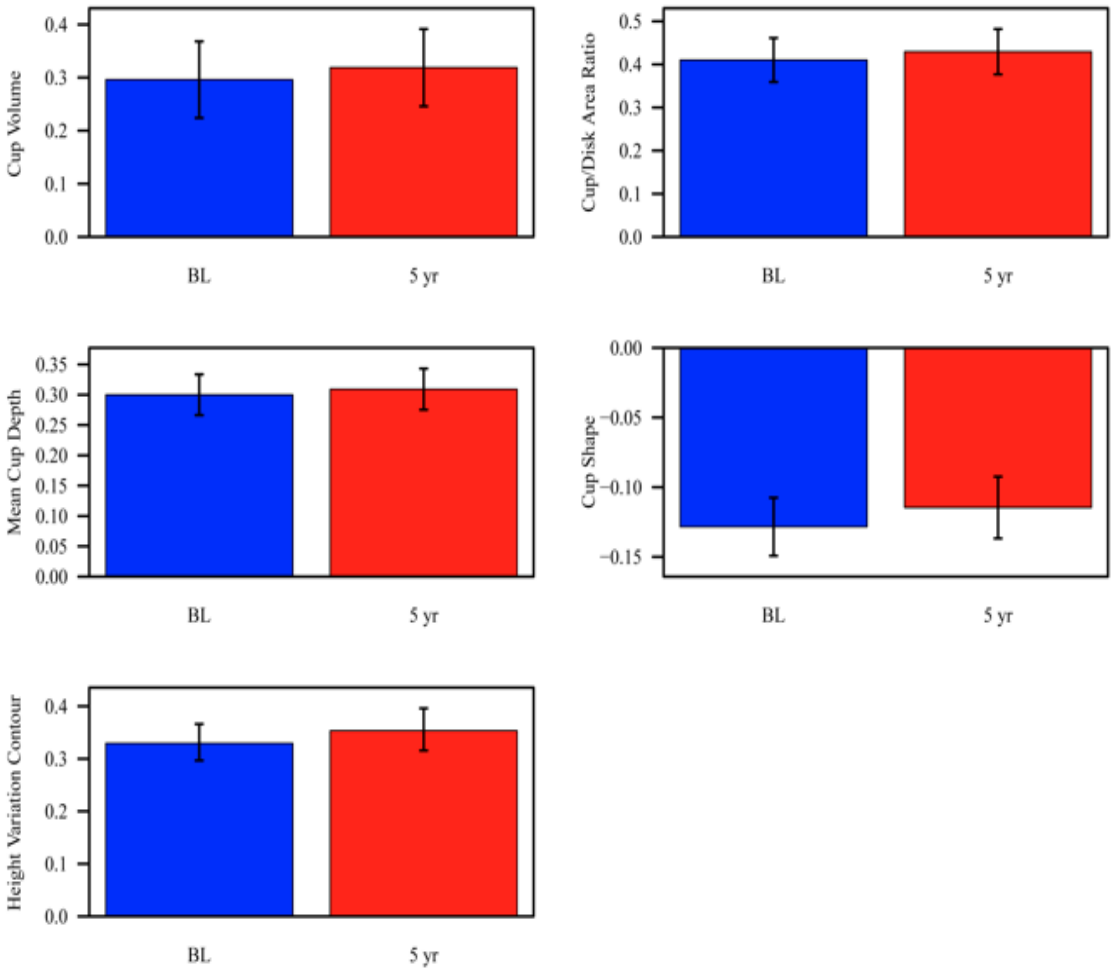

Similarly, the structural parameters of the optic nerve head and peripapillary RNFL measured by optical coherence tomography (OCT) changed as follows from baseline to 5 years: disc area significantly increased from 2.272 to 2.618, with a statistically significant mean change of 0.346 (95% CI: 0.249, 0.442; p<0.0001); cup area significantly increased from 1.18 to 1.51, with a statistically significant mean change of 0.329 (95% CI: 0.234, 0.425; p<0.0001); cup/disk area ratio significantly increased from 0.514 to 0.572, with a statistically significant mean change of 0.058 (95% CI: 0.026, 0.090; p=0.0005) ; RNFL average thickness decreased from 74.91 to 72.82, with a mean change of -2.1 (95% CI: -5.10, 0.92; p=0.1740); RNFL temporal thickness decreased from 54.93 to 54.44, with a mean change of -0.49 (95% CI: -

3.90, 2.92; p= 0.7789), Table 1, Figure 4. Macular thickness and volume parameters measured by OCT decreased all significantly over 5 years (macular thickness outer superior: from 221.60 to 214.71, statistically significant mean change of -6.88, 95% CI: -9.56, -4.20, p<0.0001; inner superior: from 262.57 to 251.68, statistically significant mean change of -10.89, 95% CI: -13.98, -7.79, p<0.0001; outer inferior: from 208.45 to 202.43, statistically significant mean change of -6.02, 95% CI: -8.58, -3.46, p<0.0001; inner inferior: from 256.55 to 247.73, statistically significant mean change of -8.82, 95% CI: -12.18, -5.46, p<0.0001; outer nasal: from 235.05 to 230.33, statistically significant mean change of -4.72, 95% CI: -7.27, -2.16, p=0.0003; inner nasal: from 262.02 to 251.75, statistically significant mean change of -10.27, 95% CI: -13.85, -6.69, p<0.0001; outer temporal: from 204.78 to 196.35, statistically significant mean change of -8.42, 95% CI: -11.56, -5.28, p<0.0001; inner temporal: from 247.58 to 238.97, statistically significant mean change of -8.61, 95% CI: -13.08, -4.15, p=0.0002; macular volume: from 6.40 to 6.20, statistically significant mean change of -0.21, 95% CI: -0.26, -0.15, p<0.0001), Table 1, Figure 4.

Figure 4. Optic nerve head parameters assessed by optical coherence tomography (mean +/- standard error) in open-angle glaucoma patients at baseline (BL) and 5 years (5 yr).

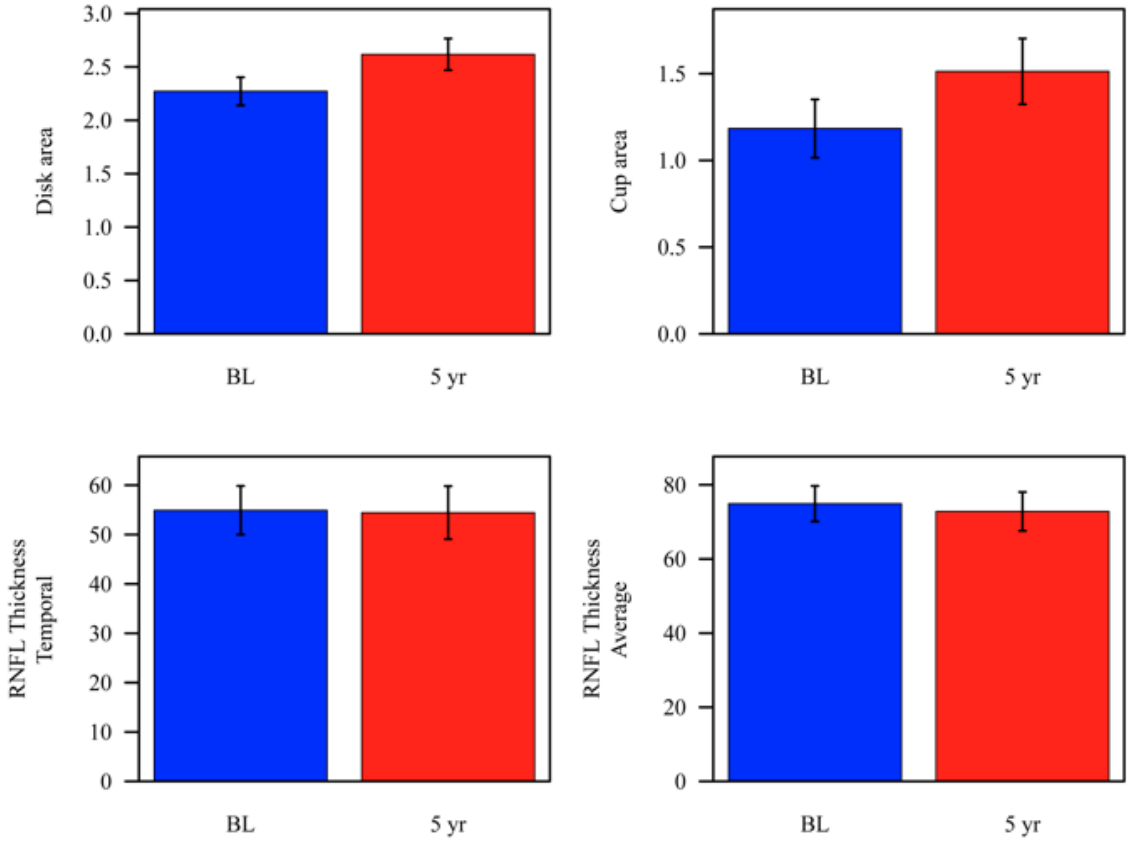

In OAG patients over a 5-year period of time, the retinal capillary blood flow parameters assessed by Heidelberg retinal flowmeter changed as follows: the number of superior zero pixels significantly increased from 0.200 (95% CI: 0.189, 0.213) at baseline to 0.225 (95% CI: 0.202, 0.251) at 5 years with a statistically significant mean change of 0.022 (95% CI: 0.002, 0.040; p=0.0334); the number of inferior zero pixels significantly increased from 0.185 (95% CI: 0.174, 0.197) at baseline to 0.205 (95% CI: 0.186, 0.225) at 5 years with a statistically significant mean change of 0.018 (95% CI: 0.001, 0.033; p=0.0418), Table 1 and Figure 5. Neither inferior (baseline: 417.94, 95% CI: 386.46, 451.98; 5 years: 397.46, 95% CI: 348.18, 453.71, p=0.4193) nor superior (baseline: 415.92, 95% CI: 390.01, 443.56; 5 years: 394.91, 95% CI: 345.51, 451.39, p=0.4314) mean flow changed significantly, Table 1.

Figure 5. Retinal capillary blood flow parameters assessed by Heidelberg retinal flowmeter (mean with 95% confidence interval) in open-angle glaucoma patients at baseline (BL) and 5 years (5 yr).

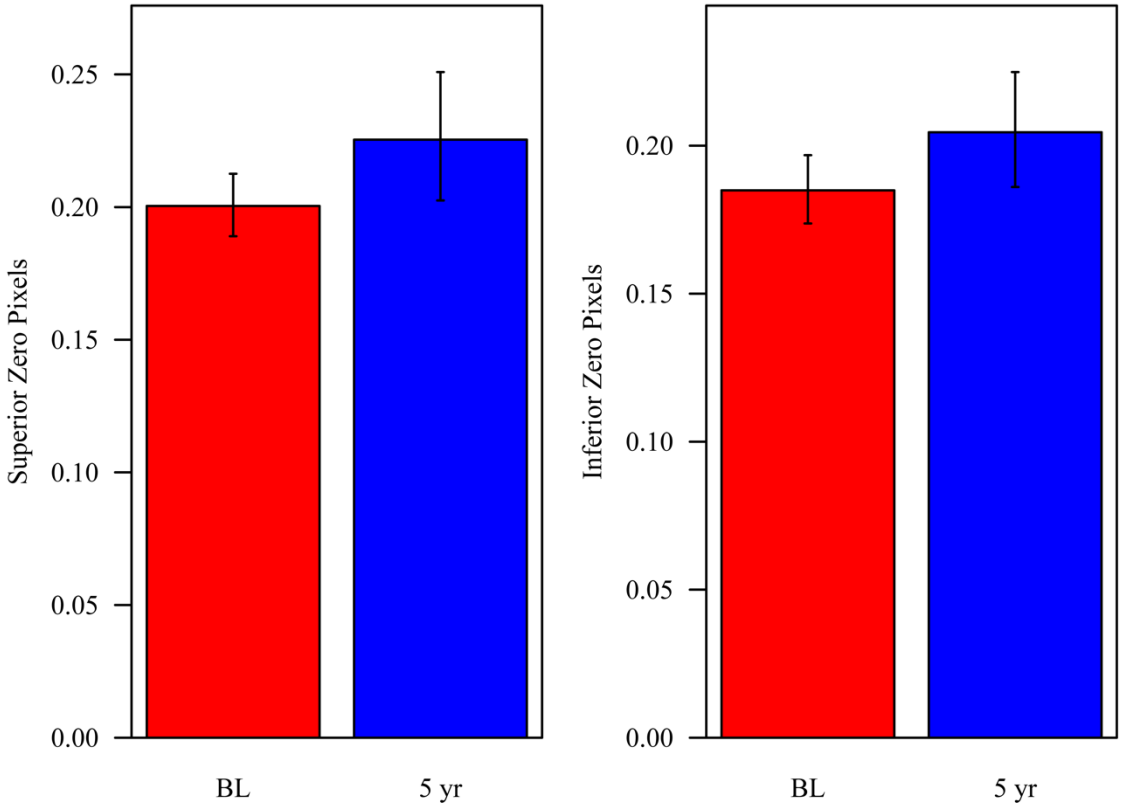

Higher number of superior zero pixels (p=0.0009) was significantly associated with shorter time to structural progression, Figure 6.

Figure 6. Survival function for time to structural progression for open-angle glaucoma patients for retinal capillary blood flow parameters (superior zero pixels) assessed by Heidelberg retinal flowmeter. Lines represent survival curves for lowest and highest observed superior zero pixels. Higher number of superior zero pixels was associated with shorter time to structural progression.

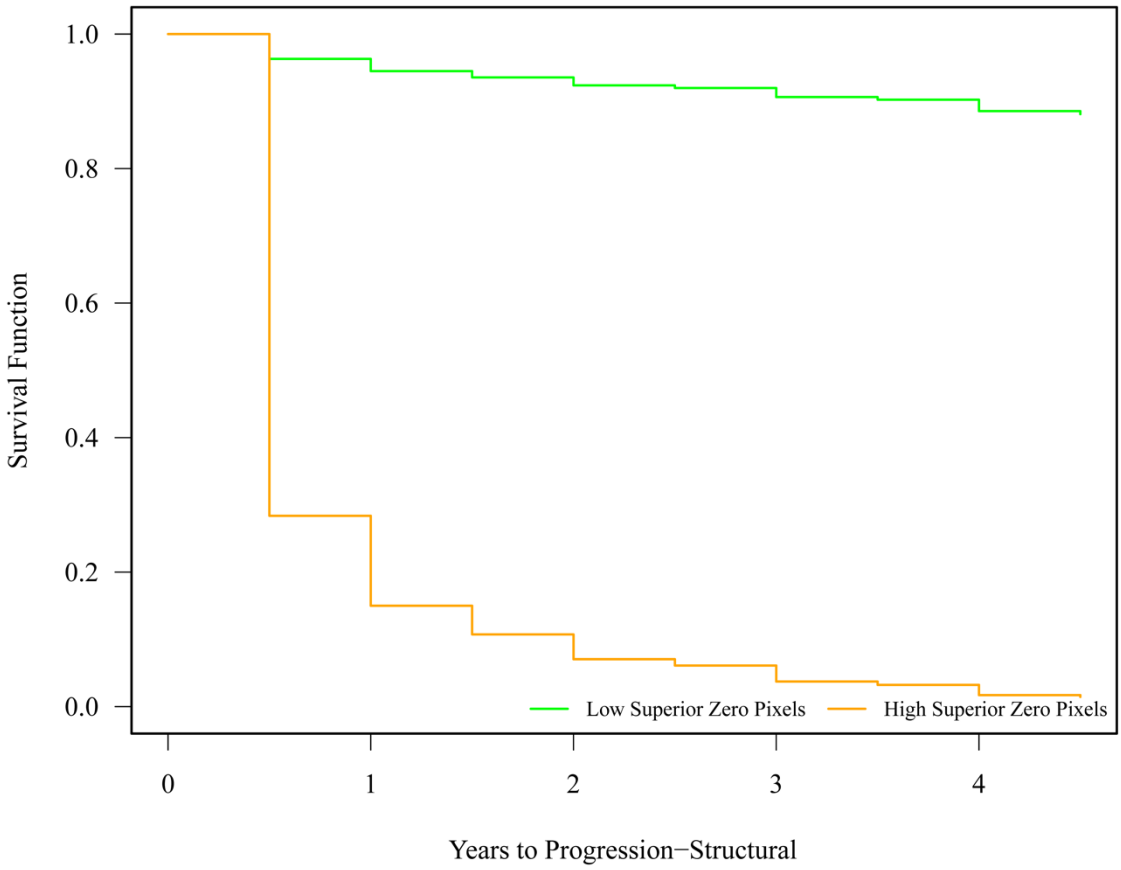

In the overall group of OAG patients the retrobulbar blood flow parameters measured by color Doppler imaging changed as follows from baseline to 5 years: OA Peak Systolic Velocity (PSV) decreased from 23.03 (95% CI: 20.90, 25.37) at baseline to 21.79 (95% CI: 19.42, 24.43) at 5 years, with a mean change of -1.31 (95% CI: -3.49, 0.69; p= 0.2054), OA End Diastolic Velocity (EDV) significantly decreased from 5.62 (95% CI: 5.10, 6.19) at baseline to 3.93 (3.48, 4.44) at 5 years, with a statistically significant mean change of -2.41 (95% CI: -3.26, -1.65; p<0.0001). CRA PSV (baseline: 8.03, 95% CI: 7.53, 8.53; 5 years: 7.44, 95% CI: 6.87, 8.02) and EDV (baseline: 2.26, 95% CI: 2.11, 2.42; 5 years: 1.68, 95% CI: 1.55, 1.82) significantly decreased with statistically significant mean changes of -0.59 (95% CI: -1.05, -0.13; p=0.0126) and -0.78 (95% CI: -1.05, -0.53; p<0.0001), respectively, Table 1 and Figure 9. NPCA EDV (baseline: 2.35, 95% CI: 2.21, 2.51; 5 years: 1.83, 95% CI: 1.70, 1.98) and TPCA EDV (baseline: 2.38, 95% CI: 2.24, 2.54; 5 years: 1.82, 95% CI: 1.69, 1.96) significantly

decreased with statistically significant mean changes of -0.67 (-0.91, -0.45; p<0.0001) and -0.75 (-0.99, -0.52; p<0.0001), respectively, while neither NPCA PSV (baseline: 7.44, 95% CI: 6.96, 7.92; 5 years: 7.32, 95% CI: 6.73, 7.91) nor TPCA PSV (baseline: 7.76, 95% CI: 7.32, 8.21; 5 years: 7.51, 95% CI: 7.00, 8.03) changed significantly (NPCA PSV p=0.6309; TPCA PSV p= 0.2376), Table 1 and Figure 7. Resistivity indices (RI) in all retrobulbar vessels significantly increased over five years: OA RI from 0.755 (95% CI: 0.771, 0.738) to 0.816 (95% CI: 0.832, 0.799) with a statistically significant mean change of 0.081 (95% CI: 0.109, 0.056, p<0.0001); CRA RI from 0.702 (95% CI: 0.686, 0.717) to 0.765 (95% CI: 0.747, 0.784), with a statistically significant mean change of 0.064 (0.046, 0.081; p<0.0001); NPCA RI from 0.668 (95% CI: 0.653, 0.682) to 0.742 (95% CI: 0.725, 0.758), with a statistically significant mean change of 0.074 (95% CI: 0.057, 0.091; p<0.0001); TPCA RI from 0.686 (95% CI: 0.701, 0.671) to 0.758 (95% CI: 0.771, 0.743) with a statistically significant mean change of 0.092 (95% CI: 0.118, 0.068; p<0.0001), Table 1 and Figure 7.

Figure 7. Retrobulbar blood flow parameters assessed by color Doppler imaging (mean with 95% confidence interval) in open-angle glaucoma patients at baseline (BL) and 5 years (5 yr). CRA: central retinal artery; EDV: end diastolic velocity; NPCA: nasal posterior ciliary artery; OA: ophthalmic artery; PSV: peak systolic velocity; RI: resistivity index; TPCA: temporal posterior ciliary artery.

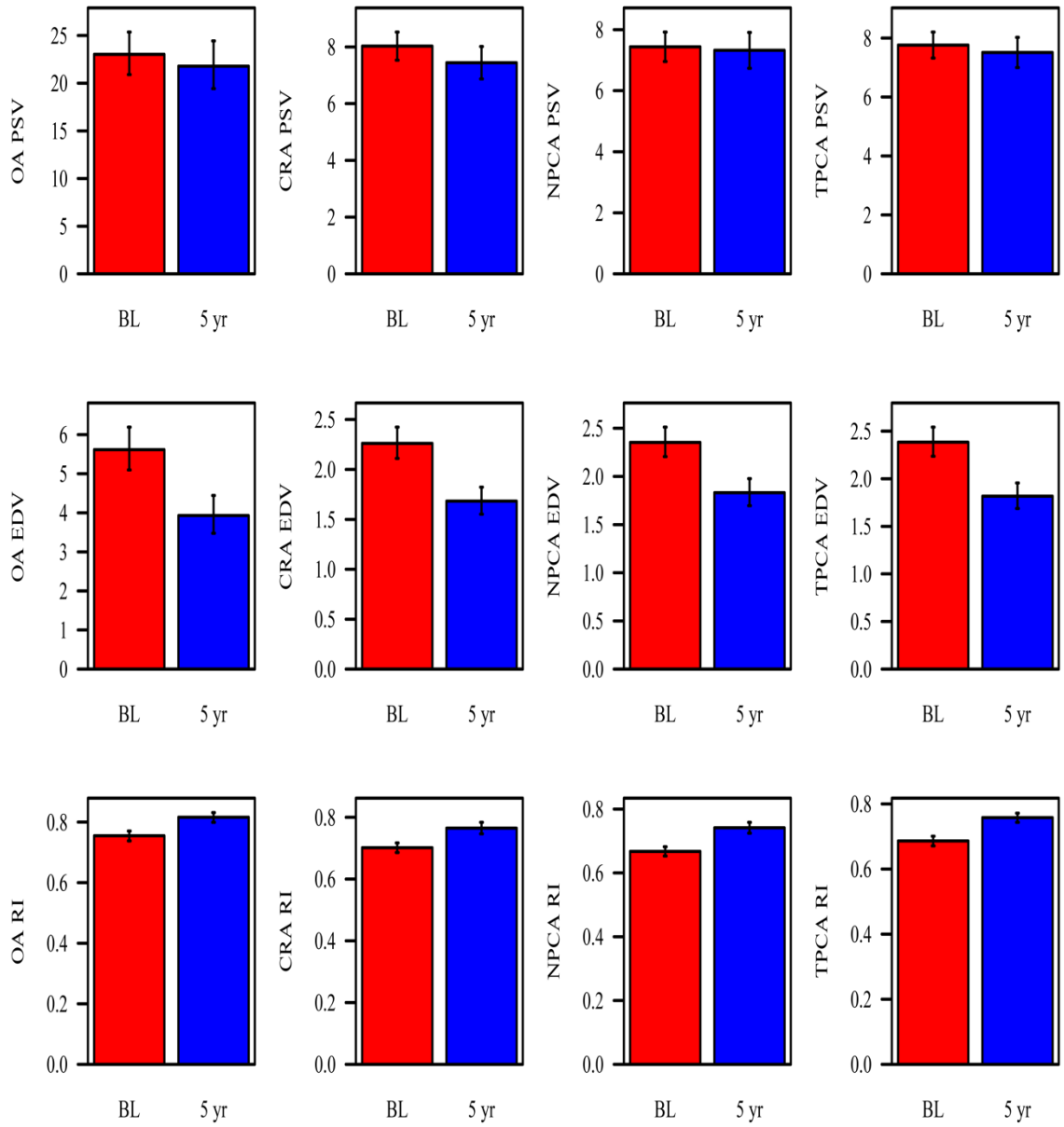

Lower baseline OA PSV and OA EDV were associated with shorter time to functional (OA PSV, p=0.038; OA EDV p=0.0080) and structural (OA PSV, p=0.0464; OA EDV p=0.0213) progression, Figure 8.

Figure 8. Survival function for time to functional (top) and structural progression for open-angle glaucoma patients for baseline retrobulbar blood flow parameters assessed by color Doppler imaging. Lines represent survival curves for lowest and highest

observed ophthalmic artery (OA) peak systolic velocity (PSV) and end diastolic velocity (EDV). Lower baseline OA PSV and EDV were associated with shorter time to functional and structural progression.

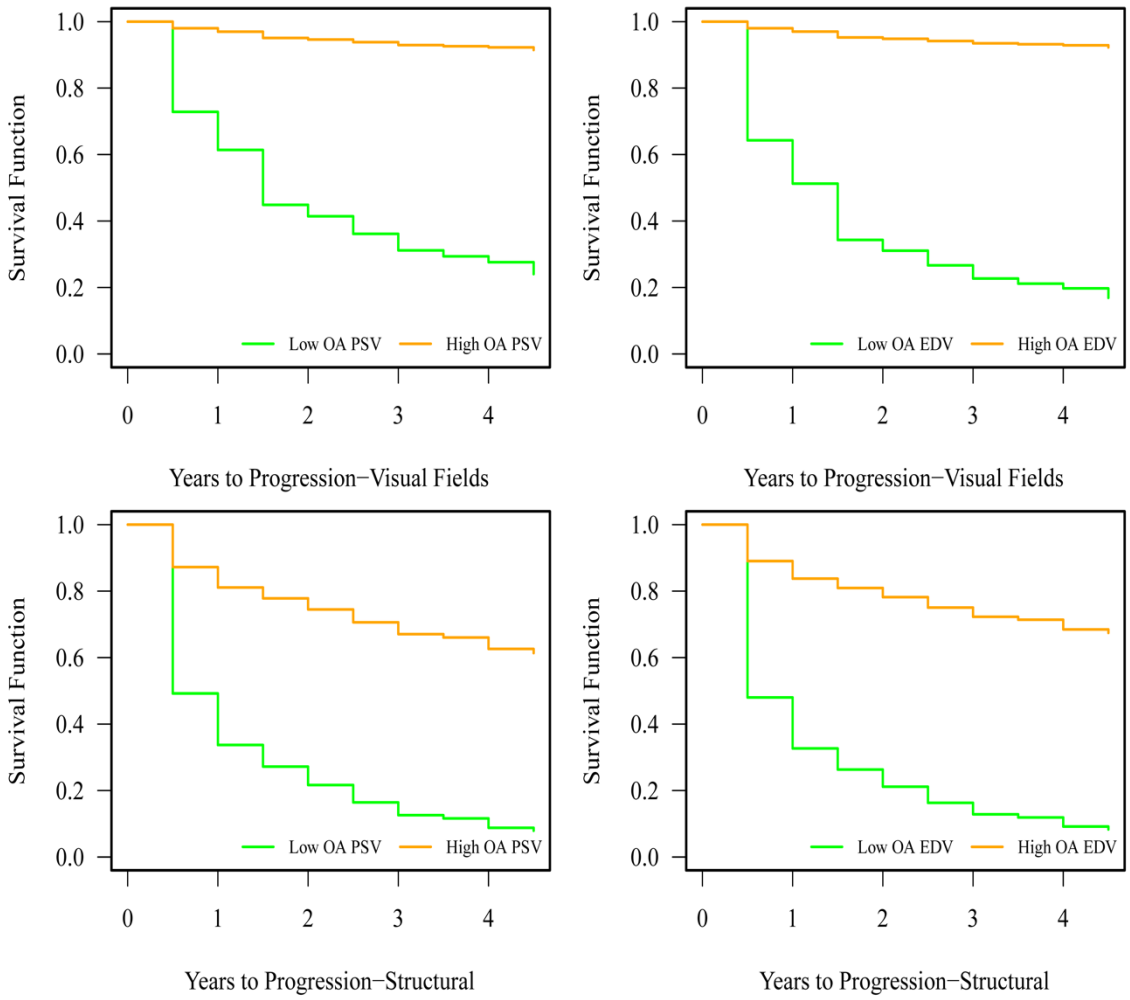

A complete summary of the other significant results related to the Aim 1 of my PhD thesis is shown in Table 2 to 5.

Table 2 shows the significant changes of the studied parameters between baseline and 5 years in the overall population of open-angle glaucoma patients.

Table 2. Significant changes of the studied parameters between baseline and 5 years in the overall population of open-angle glaucoma patients.

Changes from Baseline to 5 years
IOP decreased

SBP decreased
DBP decreased
MAP decreased
Visual Acuity increased
OA EDV decreased
OA RI increased
CRA PSV decreased
CRA EDV decreased
CRA RI increased
NPCA EDVdecreased
NPCA RI increased
TPCA EDV decreased
TPCA RI increased
Superior Zero Pixels increased
Inferior Zero Pixels increased
MD decreased
PSD increased
AGIS score increased
Disk area increased
Cup area increased
cup/disk area ratio increased
cup/disk horizontal ratio increased
cup/disk vertical ratio increased
RNFL thickness superior decreased
macular thickness outer superior decreased
macular thickness inner superior decreased
macular thickness outer inferior decreased
macular thickness inner inferior decreased
macular thickness outer nasal decreased
macular thickness inner nasal decreased
macular thickness outer temporal decreased
macular thickness inner temporal decreased
macular volume decreased
HRT3 Cup volume increased
HRT3 Cup/Disk Area Ratio increased
HRT3 Mean Cup Depth increased
HRT3 Cup Shape increased
HRT3 Height Variation Contour increased

Table 3 shows the associations between baseline parameters and shorter time to functional and structural disease progression in the overall population of open-angle glaucoma patients.

Table 3. Associations of baseline data with shorter time to functional and structural disease progression in the overall population of open-angle glaucoma patients.

Baseline predictors of shorter time to progression in the overall population
FUNCTIONAL PROGRESSION
lower OA PSV
lower OA EDV
lower (more negative) MD
higher PSD
higher AGIS score
higher Disk area
lower RNFL thickness temporal
lower macular thickness outer superior
higher HRT3 Cup Area
lower HRT3 Rim Volume
higher HRT3 Cup/Disk Area Ratio
higher HRT3 Linear Cup/Disk Ratio
higher HRT3 Cup Shape
lower HRT3 Height Variation Contour
lower HRT3 Mean RNFL Thickness
lower HRT3 RNFL Cross-Sectional Area
higher Age
Cardiovascular Disease
Age >= 65
STRUCTURAL PROGRESSION
lower OA PSV
higher AGIS score
lower BMI

Table 4 shows the other associations between parameters (multiple observations over time) and shorter time to functional and structural disease progression in the overall population of open-angle glaucoma patients.

Table 4. Associations of parameters (multiple observations over time) with shorter time to functional and structural disease progression in the overall population of open-angle glaucoma patients.

Predictors (multiple observations over time) of shorter time to progression in the overall population
FUNCTIONAL PROGRESSION
lower OA PSV

lower OA EDV
higher PSD
higher Disk area
higher Cup area
higher cup/disk area ratio
higher cup/disk horizontal ratio
higher cup/disk vert ratio
lower RNFL thickness temporal
lower RNFL average
lower HRT3 Rim Area
lower HRT3 Rim Volume
lower HRT3 Mean RNFL Thickness
lower HRT3 RNFL Cross-Sectional Area
STRUCTURAL PROGRESSION
higher Superior Zero Pixels
higher Inferior Mean Flow
higher PSD

Table 5 shows the other associations between change from baseline measurements (multiple observations over time) and shorter time to functional and structural disease progression in the overall population of open-angle glaucoma patients.

Table 5. Associations of parameters (change from baseline measurements, multiple observations over time) with shorter time to functional and structural disease progression in the overall population of open-angle glaucoma patients.

Predictors (change from baseline measurements, multiple observations over time) of shorter time to progression in the overall population
FUNCTIONAL PROGRESSION
more increase in cup/disk area ratio
more increase in cup/disk vert ratio
HRT3 Cup Volume
HRT3 Cup/Disk Area Ratio
STRUCTURAL PROGRESSION
N/A

4. Discussion – Aim 1:

The Aim 1 of my PhD project was to evaluate the relationship between ocular and vascular risk factors and glaucoma functional and structural progression.

In this cohort of OAG patients evaluated over a 5-year period, despite a decrease in the mean IOP, glaucomatous functional and structural progression assessed by multiple imaging modalities occurred (Table 1). These findings confirm those from previous studies, that showed that many patients undergo disease progression despite their IOP being well- controlled (Heijl et al., 2002). In fact, in our study although IOP decreased significantly from baseline to five years, the functional parameters assessed by visual field testing deteriorated over the same period of time (significant increase in the mean deviation, decrease in the pattern standard deviation, and increase in the AGIS score), Table 1 and Figure 1. Parallel to the visual field deterioration, structural damage was detected in the optic nerve head (ONH), retinal nerve fiber layer (RNFL) and macula assessed by HRT3 (Table 1-2, Figure 3) and OCT (Table 1-2, Figure 3). In details, from baseline to 5 years HRT3 detected morphological damage at the level of the optic nerve head (significant increase in the HRT3 cup volume, HRT3 cup/disk Area Ratio, HRT3 mean Cup depth increased, HRT3 Cup Shape, HRT3 Height Variation Contour), Table 1-2, Figure 3. Similarly, OCT assessed typical glaucomatous deterioration at the level of the ONH parameters (increase in the disk area, cup area, cup/disk area ratio, cup/disk horizontal ratio, cup/disk vertical ratio), RNFL and macula (decrease in the RNFL thickness superior, macular thickness outer and inner superior, macular thickness outer and inner inferior, macular thickness outer and inner nasal, macular thickness outer and inner temporal, and in the macular volume), Table 1-2, Figure 4. Taken together, these findings indicate that other factors, besides IOP, influence both structural and functional glaucoma disease progression.

Importantly, in our analysis we found that ocular blood flow parameters, assessed by multiple imaging modalities, were predictive of structural and functional progression, thus confirming results from previous studies that highlighted the association between reduced ocular

hemodynamics and glaucomatous progression (Flammer et al., 2002; Galassi et al., 2003; Martínez and Sánchez, 2005; Zeitz et al., 2006; Calvo et al. 2021; Jimenez-Aragon et al., 2013). Specifically, we found that from baseline to five years, the percentage of avascular area in the inferior and superior retina (corresponding to the amount of area with absent capillary blood flow detected as number of zero pixels) assessed by confocal scanning laser Doppler significantly, increased (Table 1, Figure 5). Also, our data showed that a lower capillary blood flow (as higher number of superior zero pixels) was predictive of structural progression after five years (Figure 6), thus suggesting the association between impaired retinal capillary blood flow and glaucomatous structural damage. Our results parallel previous findings on the correlation between reduced retinal blood flow and structural glaucomatous changes (Logan et al., 2004, Resch et al., 2011, Tobe et al., 2015). These finding support the hypothesis that reductions in retinal blood flow can predict structural progression in glaucoma, though it is not known whether reduced retinal blood flow is contributory to the disease process or represents a marker of pathogenesis.

In respect to the retrobulbar blood flow parameters assessed by color Doppler imaging, our analysis showed how the velocities in the ophthalmic artery (OA), central retinal artery (CRA) and nasal (NPCA) and temporal posterior ciliary arteries (TPCA) decreased over time, and their resistivity indices increased (Table 1, Figure 7). Importantly, lower baseline OA PSV and OA EDV were found to be predictive factors of structural and functional progression after five years (Figure 8). There results confirmed findings of previous studies investigating the relationship between retrobulbar blood flow and glaucoma progression, both functional (Galassi et al., 2003; Martínez and Sánchez, 2005), and structural (Calvo et al., 2012; Jimenez-Aragon et al., 2013). Similar to our results, Galassi et al. showed that lower OA EDV and higher OA RI were predictive of functional progression over a 7-year period in OAG patients (Galassi et al. 2003). Also, findings from a 3-year study from Martinez et al. suggested that the

OA and NPCA RI could represent reliable predictors of functional disease progression (Martínez and Sánchez, 2005). Results from Jimenez-Aragon et al. also found that subjects who progressed structurally had significantly different EDV and RI of the OA and CRA, compared to subjects who did not progressed (Jimenez-Aragon et al., 2013). Finally, in a study from Calvo et al. glaucoma suspects who converted to glaucoma based on the Moorfields Regression Analysis showed reduced OA EDV and mean velocity and increased OA RI compared to suspects who did not convert (Calvo et al., 2012). These results support the notion that reduction in the retrobulbar blood flow may represent a contributing factor to the glaucomatous structural and functional progression that we observed in our study population. Finally, in our cohort of subjects we also investigated the relationship between structural and functional parameters as predictors of disease progression. Our results highlighted the complexity of the relationship between structure and function in glaucoma. In fact, our findings support on one hand the notion that baseline functional parameters are predictor of structural progression (lower baseline MD and higher AGIS score were associated with structural progression after 5 years, Figure 2). On the other end, our results showed also that baseline structural parameters assessed via both HRT 3 and OCT were predictive of functional disease progression. This data confirms the well-established notion that a significant amount of retinal ganglion cell loss can occur before standard tests may detect a functional loss (Garway-Heath et al., 2000 (a and b); Hood et al. 2007). Also, our findings are in agreement with previous investigations that showed how structural parameters were predictive of functional progression over time (Gordon et al., 2002; Lalezary et al., 2006; Sehi and Iverson, 2013). Importantly, current evidence highlights that intervention for glaucoma patients may be warranted at the pre-perimetric stage, defined as glaucomatous structural disease without evidence of any perimetric visual field compromise (Zangwill et al., 2001). Thus, these findings may prove to be useful for the development of prediction models utilizing baseline structural parameters in

newly-diagnosed OAG patients to determine whether or not a patient is likely to progress, the rate at which they may progress, and if they require earlier interventions at the time of diagnosis.

In conclusion, in our study we found that over a 5-year period in 112 OAG patients, even though IOP decreased over time, functional and structural progression continued, thus highlighting the importance of risk factors different compared to IOP in the disease progression. Importantly, our results showed how baseline retrobulbar and retinal capillary blood flow parameters were predictive of both glaucoma structural and functional progression, supporting the notion that vascular alterations may be important contributors in the pathophysiology of the disease. Our findings also support the existing data related to the complexity of the structure-function relationship in glaucoma, and showed how both structural and functional parameters at baseline may be useful indicators of disease progression. Finally, there is urgent need for the development of tools and models able to include baseline ocular and systemic vascular parameters along with structural and functional measurement in subjects suspect or with a new diagnosis of glaucoma in order to predict the individualized likelihood of disease progression and improve the quality of patient's care.

CHAPTER 5

PhD Research Project – Aim 2: To investigate the relationship between glaucoma progression, ocular hemodynamics, and *race*

1. Introduction – Aim 2:

Primary open angle glaucoma (OAG) represents a leading cause of blindness worldwide, especially in persons from African descent (AD) (Tham et al., 2014). It is a multifactorial disease characterized by a progressive death of retinal ganglion cells and loss of visual fields. Disease management is currently limited to IOP-lowering medications and surgical interventions, however many treated patients experience disease progression, and subjects with elevated IOP do not always develop disease (Glaucoma Preferred Practice Pattern Panel, 2020; Heijl et al. 2002). Importantly, other factors have been shown to be involved in OAG onset and progression including compromised vascular health (Harris et al. 2008). In fact, ocular and systemic vascular abnormalities involving perfusion, metabolism, and blood flow, along with optic disc hemorrhages, migraine, systemic hypertension and nocturnal hypotension have also been associated with OAG (Flammer et al., 1994, Harris et al. 2020; Weinreb and Harris, 2009; Harris et a. 2020). However, it is still a matter of debate the extent to which mechanical damage induced by IOP on one hand and vascular damage on the other hand occur in glaucoma, either separate or in combination.

Although glaucoma is a disease that universally affects all humans, significant OAG disease disparities exist within certain population groups, especially in persons of AD (Racette et al. 2003; Huck et al., 2014). Several investigations have shown that people of AD are disproportionately affected by OAG compared to those of European descent (ED). Moreover, OAG represents the leading cause of blindness in the AD population, where it occurs at a younger age, with greater severity and more rapid progression compared to the ED population

(Wilensky et al., 1978; Martin et al., 1985; Wilson et al., 1987; Sommer et al., 1991; Tielsch et al., 1991; Hyman et al., 2001; Racette et al., 2003; Congdon et al., 2004; Racette et al., 2010; Friedman et al. 2004). OAG affects up to six times more people of AD than those of ED (Congdon et al 2004; Friedman et al., 2004), and data from the Ocular Hypertensive Treatment study highlighted how African American race represents a baseline factor that predicted increased risk of disease onset (Gordon et al., 2002).

AD and ED OAG patients have also shown to differ significantly in several ocular structural and functional parameters related to glaucoma. Compared to the ED population, OAG patients of AD showed thinner corneas (Racette et al., 2003, Racette et al., 2005; Haseltine et al., 2012), larger optic disc area (Girkin et al., 2010), cup to disc ratio (Beck et al., 1985; Martin et al., 1985; Chi et al. 1989; Higginbotham et al., 2004) and deeper maximum cup depth (Beck et al. 1985; Mikelberg et al., 1995; Girkin et al., 2003; Racette et al., 2003; Girkin et al., 2005), all risk factors for OAG. Also, OAG persons of AD present worse global indices (mean deviation and pattern standard deviation) for standard automated perimetry fields (Racette et al. 2010). Populations of AD tend to have a higher prevalence of systemic vascular complications, including cardiovascular disease (CVD), diabetes mellitus (DM) and associated RF such as sedentary lifestyle and smoking with resulting organ damage that occurs earlier and is largely more severe than in other ethnicities (Ferdinand, 2008; Harris et. al. 2020).

Despite studies demonstrating the differences in the onset and progression of OAG between persons of AD and ED, the mechanisms underlying this disparity have yet been elucidated. Importantly, the possible connection between systemic and localized vascular pathology and glaucoma onset and progression may be a contributory mechanism to the observed disease disparity in persons of AD. The Indianapolis Glaucoma Progression Study represented the first longitudinal and observational study in which a large sample of OAG patients of both AD and ED was evaluated by multiple hemodynamic imaging technologies and multiple measures of

structure and function to comprehensively assess the ocular and systemic circulation and to adequately monitor disease progression. The Aim 2 of my PhD analysis took advantage of the dataset of OAG patients of AD and ED in order to shed further light on the relationship between ocular and systemic hemodynamics and glaucoma progression in persons of different races. In details, the Aim 2 of my PhD project has been to specifically investigate the relationship between glaucoma progression, ocular hemodynamics, and *race.*

2. Material and Methods - Aim 2:

The comprehensive discussion of the materials and methods for the IGPS study are detailed in chapter 3. In brief, a cohort of 112 patients (29 of AD, 83 of ED) with OAG were enrolled at baseline, and prospectively examined at baseline and every 6 months over a period of five years at the Glaucoma and Diagnostic Center at Indiana University School of Medicine, Indianapolis, Indiana. The data were categorized into groups depending on race (AD or ED) based on self-reported status. Reporting of races other than AD or ED were excluded from this analysis. One qualified eye was randomly designated as the observational study eye in each subject. Measurements were made at baseline and every 6 months over a 5-year period.

To limit reproducibility bias with imaging, a single experienced operator with over ten years of experience performed all measurements in the same order and at the same time of the day for each patient. Functional disease progression was monitored by visual field testing and defined as two consecutive visits with an Advanced Glaucoma Intervention Study (AGIS) score increase ≥2 from baseline, and/ or MD decrease ≥2 from baseline. Structural disease progression was monitored with optical coherence tomography and Heidelberg retinal tomography and defined as two consecutive visits with RNFL thickness decrease ≥8% and/or horizontal or vertical cup/disk ratio increase ≥0.2 compared to baseline.

The statistical analysis involved mixed-model analysis of covariance (ANCOVA) to test for significance of changes from baseline to 5-year follow-up separately by race (AD or ED). Two-sample t tests and $\chi 2$ tests were used to analyze differences in baseline data between patients who progressed and those who did not progress. The models were then extended to test for whether the changes were different by race (AD or ED). Time to functional progression and time to structural progression were analyzed using Cox proportional hazards survival analysis. Factors were analyzed as baseline measurements, as time-varying measurements, and as time-varying changes from baseline. Interactions were tested to determine if the effects of the factors on progression time differed by race (AD or ED). Pearson correlation coefficients were calculated to evaluate linear associations. Correlations were adjusted for years of glaucoma, use of glaucoma or hypertension medications, age 65 or older, body mass index category, diabetes status, and gender. Correlations were compared between groups using Fisher z tests. P values <0.05 were considered statistically significant.

3. Results – Aim 2:

A cohort of 112 OAG patients (29 of AD, 83 of ED) were prospectively examined at baseline and every 6 months over a period of five years. After 5 years, 37 subjects (11 AD, 26 ED) progressed functionally, and 76 (18 AD, 58 ED) structurally.

Table 1 and 2 show the change in the study measurements (mean and 95% confidence interval, CI) from baseline to five years in patients of AD and ED, respectively. Table 3 summarizes all the significant results related to the changes between parameters from baseline to 5 years and to the associations between measurements and shorter time to functional and structural progression based on race.

Table 1. Change from baseline to five years in the study parameters in open-angle glaucoma patients of European descent (ED). * p-value statistically significant < 0.05.

	European descent (ED)							African descent versus European descent	
	Baseline		5 years		Change			Change	
	N	Mean (95% CI)	N	Mean (95% CI)	Mean (95% CI)	p-value		p-value	
IOP	82	16.24 (15.03, 17.45)	55	14.73 (13.41, 16.05)	-1.51 (-2.59, -0.43)	0.0063	*	0.8377	
SBP	82	136.84 (131.63, 142.06)	57	129.72 (124.16, 135.28)	-7.12 (-12.03, -2.21)	0.0046	*	0.7139	
DBP	82	82.45 (79.37, 85.54)	57	77.03 (73.84, 80.22)	-5.42 (-8.54, -2.31)	0.0007	*	0.8446	
MAP	82	100.49 (97.01, 103.98)	57	94.51 (90.84, 98.18)	-5.98 (-9.42, -2.55)	0.0007	*	0.7582	
HR	82	71.13 (67.97, 74.28)	58	70.81 (67.12, 74.50)	-0.32 (-3.25, 2.61)	0.8315		0.3794	
Visual Acuity	82	0.09 (0.05, 0.12)	58	0.20 (0.15, 0.26)	0.11 (0.07, 0.16)	0.0000	*	0.0388	*
OA PSV	83	24.09 (21.84, 26.56)	57	23.09 (20.51, 26.00)	-1.04 (-3.57, 1.26)	0.3887		0.5577	
OA EDV	83	5.90 (5.35, 6.50)	57	4.09 (3.60, 4.64)	-2.61 (-3.63, -1.71)	0.0000	*	0.8311	
OA RI	83	0.755 (0.772, 0.737)	57	0.821 (0.838, 0.803)	0.091 (0.125, 0.059)	0.0000	*	0.2528	
CRA PSV	83	8.04 (7.50, 8.57)	57	7.46 (6.81, 8.10)	-0.58 (-1.14, -0.02)	0.0413	*	0.9395	
CRA EDV	83	2.28 (2.11, 2.46)	57	1.68 (1.53, 1.84)	-0.81 (-1.14, -0.52)	0.0000	*	0.7401	
CRA RI	83	0.697 (0.681, 0.714)	57	0.763 (0.742, 0.784)	0.066 (0.045, 0.087)	0.0000	*	0.6569	
NPCA PSV	82	7.52 (7.01, 8.02)	57	7.25 (6.63, 7.87)	-0.27 (-0.80, 0.26)	0.3197		0.2379	
NPCA EDV	82	2.40 (2.24, 2.58)	57	1.79 (1.65, 1.94)	-0.83 (-1.12, -0.56)	0.0000	*	0.0430	*
NPCA RI	82	0.661 (0.645, 0.677)	57	0.742 (0.723, 0.762)	0.081 (0.061, 0.102)	0.0000	*	0.1368	
TPCA PSV	83	7.74 (7.28, 8.20)	57	7.50 (6.96, 8.05)	-0.24 (-0.72, 0.24)	0.3217		0.9074	
TPCA EDV	83	2.38 (2.22, 2.55)	57	1.83 (1.69, 1.99)	-0.71 (-0.99, -0.46)	0.0000	*	0.5885	
TPCA RI	83	0.684 (0.701, 0.668)	57	0.754 (0.769, 0.737)	0.088 (0.118, 0.061)	0.0000	*	0.4845	
Superior Zero Pixels	83	0.201 (0.189, 0.214)	23	0.232 (0.207, 0.261)	0.027 (0.005, 0.047)	0.0174	*	0.3447	
Inferior Zero Pixels	83	0.186 (0.174, 0.199)	23	0.195 (0.175, 0.216)	0.008 (-0.012, 0.027)	0.4121		0.0436	*
Inferior Mean Flow	83	385.68 (355.32, 418.63)	23	373.78 (321.69, 434.30)	-12.28 (-73.21, 40.57)	0.6659		0.5884	
Superior Mean Flow	83	393.84 (367.61, 421.95)	23	362.02 (312.01, 420.05)	-34.62 (-102.07, 23.65)	0.2582		0.3511	
MD	83	-2.73 (-3.72, -1.73)	58	-3.88 (-5.06, -2.70)	-1.15 (-1.92, -0.39)	0.0032	*	0.3087	
PSD	83	3.69 (2.80, 4.57)	58	4.10 (3.18, 5.03)	0.42 (0.08, 0.75)	0.0162	*	0.0359	*
AGIS score	83	1.08 (0.62, 1.67)	58	1.60 (0.99, 2.40)	0.42 (0.17, 0.63)	0.0019	*	0.3846	
Disk area	83	2.179 (2.048, 2.310)	57	2.479 (2.328, 2.630)	0.300 (0.193, 0.407)	0.0000	*	0.0696	
Cup area	83	1.146 (0.987, 1.305)	57	1.421 (1.236, 1.607)	0.275 (0.171, 0.379)	0.0000	*	0.0327	*
Rim area	83	1.026 (0.901, 1.151)	57	1.055 (0.914, 1.197)	0.029 (-0.081, 0.139)	0.6027		0.8562	
cup/disk area ratio	83	0.517 (0.460, 0.574)	57	0.566 (0.505, 0.626)	0.049 (0.013, 0.084)	0.0069	*	0.3204	
cup/disk horizontal ratio	83	0.70 (0.66, 0.75)	57	0.75 (0.71, 0.80)	0.05 (0.02, 0.08)	0.0003	*	0.2426	
cup/disk vert ratio	83	0.689 (0.645, 0.732)	57	0.717 (0.668, 0.766)	0.028 (-0.002, 0.058)	0.0635		0.5845	
RNFL thickness superior	83	85.32 (78.59, 92.04)	55	80.67 (73.66, 87.68)	-4.65 (-9.45, 0.16)	0.0583		0.1418	
RNFL thickness inferior	83	90.69 (83.12, 98.27)	55	88.89 (80.06, 97.72)	-1.81 (-7.43, 3.82)	0.5288		0.1531	
RNFL thickness nasal	83	61.52 (56.81, 66.23)	55	64.26 (58.45, 70.06)	2.74 (-1.90, 7.38)	0.2470		0.9975	
RNFL thickness temporal	83	58.21 (53.15, 63.27)	55	58.78 (53.07, 64.49)	0.57 (-3.48, 4.62)	0.7821		0.2569	

RNFL average	83	74.33 (69.84, 78.82)	55	73.41 (68.53, 78.29)	-0.92 (-4.01, 2.16)	0.5575		0.1489	
macular thickness outer superior	83	222.26 (216.84, 227.68)	58	216.00 (210.31, 221.69)	-6.26 (-9.35, -3.17)	0.0001	*	0.3463	
macular thickness inner superior	83	261.20 (255.27, 267.13)	58	250.67 (244.47, 256.87)	-10.53 (-13.48, -7.59)	0.0000	*	0.8390	
macular thickness outer inferior	83	209.07 (203.78, 214.36)	58	203.88 (198.16, 209.59)	-5.19 (-8.17, -2.21)	0.0007	*	0.2027	
macular thickness inner inferior	83	258.65 (252.65, 264.66)	58	251.12 (244.45, 257.80)	-7.53 (-11.02, -4.04)	0.0000	*	0.2795	
macular thickness outer nasal	83	236.48 (231.35, 241.62)	58	233.02 (227.37, 238.66)	-3.47 (-6.39, -0.54)	0.0203	*	0.0295	*
macular thickness inner nasal	83	264.08 (258.26, 269.90)	58	253.39 (247.00, 259.77)	-10.69 (-14.47, -6.91)	0.0000	*	0.5672	
macular thickness outer temporal	83	204.53 (199.97, 209.09)	58	194.73 (189.72, 199.75)	-9.80 (-13.25, -6.34)	0.0000	*	0.0642	
macular thickness inner temporal	83	249.61 (243.60, 255.63)	58	240.55 (234.33, 246.77)	-9.06 (-13.29, -4.83)	0.0000	*	0.5377	
Macula center	83	210.06 (202.08, 218.04)	58	206.48 (197.70, 215.25)	-3.58 (-9.40, 2.23)	0.2266		0.1358	
macular volume	83	6.43 (6.30, 6.56)	58	6.23 (6.10, 6.36)	-0.20 (-0.26, -0.13)	0.0000	*	0.6716	
HRT3 Cup Area	82	0.822 (0.694, 0.960)	59	0.854 (0.721, 0.996)	0.031 (-0.008, 0.069)	0.1146		0.7988	
HRT3 Rim Area	82	1.205 (1.100, 1.311)	59	1.173 (1.064, 1.282)	-0.032 (-0.079, 0.015)	0.1811		0.5579	
HRT3 Cup Volume	82	0.246 (0.178, 0.314)	59	0.272 (0.203, 0.341)	0.026 (0.005, 0.048)	0.0164	*	0.5491	
HRT3 Rim Volume	82	0.259 (0.214, 0.305)	59	0.261 (0.215, 0.307)	0.002 (-0.019, 0.022)	0.8684		0.4539	
HRT3 Cup/Disk Area Ratio	82	0.407 (0.356, 0.458)	59	0.423 (0.371, 0.475)	0.016 (-0.004, 0.037)	0.1177		0.6626	
HRT3 Linear Cup/Disk Ratio	82	0.613 (0.567, 0.659)	59	0.624 (0.577, 0.671)	0.011 (-0.006, 0.028)	0.1899		0.7548	
HRT3 Mean Cup Depth	82	0.266 (0.235, 0.298)	59	0.277 (0.245, 0.309)	0.010 (0.001, 0.020)	0.0283	*	0.6430	
HRT3 Max Cup Depth	82	0.658 (0.595, 0.720)	59	0.667 (0.605, 0.729)	0.009 (-0.015, 0.033)	0.4517		0.6353	
HRT3 Cup Shape	82	-0.130 (-0.151, -0.109)	59	-0.115 (-0.138, -0.093)	0.015 (0.003, 0.027)	0.0130	*	0.7120	
HRT3 Height Variation Contour	82	0.318 (0.288, 0.352)	59	0.338 (0.303, 0.377)	0.019 (-0.002, 0.037)	0.0705		0.4473	
HRT3 Mean RNFL Thickness	82	0.178 (0.155, 0.200)	59	0.169 (0.144, 0.194)	-0.009 (-0.024, 0.006)	0.2548		0.7886	
HRT3 RNFL Cross-Sectional Area	82	0.908 (0.788, 1.028)	59	0.865 (0.734, 0.996)	-0.043 (-0.123, 0.037)	0.2917		0.8853	

Table 2. Change from baseline to five years in patients in the study parameters in patients of African descent (AD). * p-value statistically significant < 0.05.

	African Descent			**African descent versus European descent**
	Baseline	**5 years**	**Change**	**Change**

	N	Mean (95% CI)	N	Mean (95% CI)	Mean (95% CI)	p-value		p-value	
IOP	29	17.33 (15.57, 19.09)	20	16.06 (13.90, 18.22)	-1.27 (-3.28, 0.73)	0.2118		0.8377	
SBP	29	136.95 (130.06, 143.85)	20	131.69 (123.43, 139.94)	-5.27 (-13.96, 3.43)	0.2348		0.7139	
DBP	29	83.82 (79.33, 88.32)	20	79.00 (74.25, 83.75)	-4.82 (-10.02, 0.37)	0.0687		0.8446	
MAP	29	101.42 (96.47,106.36)	20	96.48 (91.08, 101.88)	-4.94 (-10.70, 0.82)	0.0929		0.7582	
HR	29	71.22 (67.35, 75.09)	20	73.33 (68.51, 78.15)	2.11 (-2.50, 6.72)	0.3697		0.3794	
Visual Acuity	29	0.09 (0.04, 0.14)	18	0.32 (0.22, 0.42)	0.23 (0.13, 0.33)	0.0000	*	0.0388	*
OA PSV	29	22.20 (19.01, 25.94)	19	20.06 (16.33, 24.64)	-2.37 (-7.09, 1.59)	0.2567		0.5577	
OA EDV	29	5.34 (4.52, 6.31)	19	3.80 (2.98, 4.84)	-2.16 (-3.98, -0.70)	0.0022	*	0.8311	
OA RI	29	0.760 (0.785, 0.732)	19	0.806 (0.833, 0.774)	0.056 (0.104, 0.015)	0.0064	*	0.2528	
CRA PSV	29	7.99 (7.31, 8.66)	19	7.37 (6.58, 8.16)	-0.62 (-1.44, 0.20)	0.1393		0.9395	
CRA EDV	29	2.20 (1.95, 2.49)	19	1.68 (1.46, 1.92)	-0.69 (-1.19, -0.27)	0.0008	*	0.7401	
CRA RI	29	0.708 (0.684, 0.733)	19	0.765 (0.734, 0.796)	0.057 (0.023, 0.090)	0.0010	*	0.6569	
NPCA PSV	29	7.40 (6.67, 8.13)	19	7.79 (6.76, 8.82)	0.39 (-0.57, 1.35)	0.4287		0.2379	
NPCA EDV	29	2.24 (2.02, 2.49)	19	2.00 (1.74, 2.30)	-0.27 (-0.69, 0.09)	0.1494		0.0430	*
NPCA RI	29	0.685 (0.661, 0.709)	19	0.737 (0.708, 0.766)	0.052 (0.020, 0.085)	0.0018	*	0.1368	
TPCA PSV	29	7.66 (6.96, 8.36)	19	7.36 (6.45, 8.27)	-0.30 (-1.15, 0.56)	0.4931		0.9074	
TPCA EDV	29	2.30 (2.07, 2.57)	19	1.70 (1.49, 1.93)	-0.82 (-1.29, -0.42)	0.0000	*	0.5885	
TPCA RI	29	0.691 (0.716, 0.664)	19	0.770 (0.793, 0.745)	0.106 (0.158, 0.061)	0.0000	*	0.4845	
Superior Zero Pixels	29	0.196 (0.177, 0.217)	7	0.202 (0.163, 0.249)	0.005 (-0.041, 0.042)	0.8148		0.3447	
Inferior Zero Pixels	28	0.175 (0.157, 0.195)	7	0.231 (0.192, 0.278)	0.042 (0.013, 0.066)	0.0059	*	0.0436	*
Inferior Mean Flow	28	470.58 (417.00, 531.03)	7	417.02 (310.49, 560.10)	-60.44 (-240.77, 74.18)	0.4173		0.5884	
Superior Mean Flow	29	437.14 (394.10, 484.88)	7	468.27 (351.44, 623.94)	29.06 (-106.93, 131.07)	0.6387		0.3511	
MD	29	-3.93 (-5.76, -2.10)	20	-6.42 (-9.41, -3.42)	-2.49 (-4.95, -0.03)	0.0475	*	0.3087	
PSD	29	4.15 (2.47, 5.83)	20	5.98 (3.89, 8.07)	1.83 (0.55, 3.12)	0.0053	*	0.0359	*
AGIS score	29	1.64 (0.73, 3.03)	19	2.91 (1.31, 5.64)	0.86 (0.09, 1.40)	0.0318	*	0.3846	
Disk area	29	2.350 (2.146, 2.555)	16	2.858 (2.602, 3.114)	0.508 (0.308, 0.708)	0.0000	*	0.0696	
Cup area	29	1.217 (0.939, 1.495)	16	1.730 (1.397, 2.063)	0.514 (0.319, 0.709)	0.0000	*	0.0327	*
Rim area	29	1.115 (0.885, 1.344)	16	1.124 (0.867, 1.381)	0.009 (-0.177, 0.196)	0.9211		0.8562	
cup/disk area ratio	29	0.513 (0.416, 0.611)	16	0.600 (0.492, 0.707)	0.086 (0.020, 0.153)	0.0112	*	0.3204	
cup/disk horiz ratio	29	0.69 (0.61, 0.76)	16	0.77 (0.69, 0.86)	0.08 (0.04, 0.13)	0.0008	*	0.2426	
cup/disk vert ratio	29	0.685 (0.611, 0.760)	16	0.731 (0.643, 0.819)	0.046 (-0.010, 0.101)	0.1093		0.5845	
RNFL thickness superior	29	93.63 (82.25, 105.00)	16	80.78 (67.54, 94.01)	-12.85 (-22.80, -2.91)	0.0114	*	0.1418	
RNFL thickness inferior	29	91.85 (77.38, 106.33)	16	80.10 (61.75, 98.45)	-11.75 (-24.28, 0.77)	0.0658		0.1531	
RNFL thickness nasal	29	64.63 (56.82, 72.45)	16	67.39 (55.39, 79.39)	2.76 (-7.74, 13.25)	0.6060		0.9975	
RNFL thickness temporal	29	51.26 (43.93, 58.60)	16	47.38 (38.90, 55.85)	-3.89 (-10.52, 2.75)	0.2505		0.2569	
RNFL average	29	75.66 (67.29, 84.03)	16	69.19 (59.10, 79.28)	-6.47 (-13.39, 0.45)	0.0670		0.1489	
macular thickness outer superior	29	222.17 (213.19, 231.16)	17	213.12 (203.69, 222.54)	-9.06 (-14.10, -4.01)	0.0005	*	0.3463	
macular thickness	29	263.22 (253.32, 273.11)	17	253.69 (240.59, 266.79)	-9.53 (-18.88, -0.17)	0.0460	*	0.8390	

inner superior									
macular thickness outer inferior	29	208.25 (200.38, 216.12)	17	199.52 (190.99, 208.05)	-8.73 (-13.37, -4.08)	0.0002	*	0.2027	
macular thickness inner inferior	29	254.82 (245.71, 263.92)	17	242.35 (230.37, 254.32)	-12.47 (-20.81, -4.13)	0.0034	*	0.2795	
macular thickness outer nasal	29	234.65 (225.80, 243.50)	17	225.42 (215.92, 234.92)	-9.23 (-13.63, -4.83)	0.0000	*	0.0295	*
macular thickness inner nasal	29	259.82 (250.51, 269.12)	17	251.85 (239.91, 263.78)	-7.97 (-16.61, 0.67)	0.0706		0.5672	
macular thickness outer temporal	29	205.51 (197.35, 213.67)	17	202.43 (193.12, 211.75)	-3.08 (-9.40, 3.25)	0.3397		0.0642	
macular thickness inner temporal	29	244.82 (234.93, 254.72)	17	240.40 (224.28, 256.53)	-4.42 (-18.67, 9.83)	0.5429		0.5377	
Macula center	29	192.58 (180.53, 204.62)	17	208.65 (181.66, 235.63)	16.07 (-9.17, 41.31)	0.2117		0.1358	
macular volume	29	6.39 (6.18, 6.61)	17	6.17 (5.93, 6.40)	-0.23 (-0.35, -0.10)	0.0004	*	0.6716	
HRT3 Cup Area	29	0.912 (0.713, 1.134)	18	0.960 (0.739, 1.209)	0.047 (-0.058, 0.146)	0.3731		0.7988	
HRT3 Rim Area	29	1.333 (1.163, 1.503)	18	1.270 (1.086, 1.454)	-0.063 (-0.157, 0.031)	0.1866		0.5579	
HRT3 Cup Volume	29	0.346 (0.229, 0.463)	18	0.358 (0.237, 0.478)	0.012 (-0.032, 0.055)	0.6033		0.5491	
HRT3 Rim Volume	29	0.325 (0.240, 0.410)	18	0.309 (0.220, 0.399)	-0.016 (-0.058, 0.026)	0.4590		0.4539	
HRT3 Cup/Disk Area Ratio	29	0.410 (0.337, 0.483)	18	0.437 (0.355, 0.518)	0.027 (-0.017, 0.071)	0.2325		0.6626	
HRT3 Linear Cup/Disk Ratio	29	0.621 (0.557, 0.685)	18	0.639 (0.567, 0.710)	0.018 (-0.020, 0.056)	0.3582		0.7548	
HRT3 Mean Cup Depth	29	0.336 (0.280, 0.393)	18	0.342 (0.284, 0.400)	0.006 (-0.013, 0.024)	0.5442		0.6430	
HRT3 Max Cup Depth	29	0.797 (0.691, 0.903)	18	0.794 (0.687, 0.902)	-0.002 (-0.045, 0.040)	0.9083		0.6353	
HRT3 Cup Shape	29	-0.126 (-0.156, -0.096)	18	-0.116 (-0.150, -0.081)	0.010 (-0.010, 0.031)	0.3223		0.7120	
HRT3 Height Variation Contour	29	0.338 (0.283, 0.405)	18	0.380 (0.308, 0.469)	0.037 (-0.005, 0.074)	0.0833		0.4473	
HRT3 Mean RNFL Thickness	29	0.213 (0.173, 0.253)	18	0.199 (0.149, 0.248)	-0.014 (-0.049, 0.021)	0.4236		0.7886	
HRT3 RNFL Cross-Sectional Area	29	1.136 (0.928, 1.343)	18	1.078 (0.816, 1.340)	-0.058 (-0.245, 0.129)	0.5445		0.8853	

From baseline to 5 years, the visual field parameters (MD, PSD, AGIS score) deteriorated significantly in both persons of ED and AD, but the change in PSD was more significant in AD, with a statistically significant difference between the two groups (p=0.0359; Table 1 and 2). With respect to structural parameters assessed by OCT, changes indicative of glaucomatous structural progression (increase in the cup area, decrease in the macular thickness outer nasal)

were more prominent in the AD population compared to ED, with statistical significant differences between groups (cup area, p=0.0327; macular thickness outer nasal, p=0.0295; Table 1 and 2).

In OAG patients of AD, the percentage of avascular area in the inferior retina (number of inferior zero pixels) assessed by Heidelberg retinal flowmetry significantly increased from 0.175 (95% CI: 0.157, 0.195) at baseline to 0.231 (0.195, 0.278) at 5 years with a statistically significant mean change of 0.042 (95% CI: 0.013, 0.066; p=0.0059). In patients of ED, the percentage of avascular area in the inferior retina (number of inferior zero pixels) increased from 0.186 (95% CI: 0.174, 0.199) at baseline to 0.195 (95% CI: 0.175, 0.216) at 5 years with a non statistically significant change of 0.008 (95% CI: -0.012, 0.027; p=0.4121), resulting in a significant difference between groups of open-angle glaucoma patients of AD and ED for the change from baseline (p=0.0436), Table 1 and 2, Figure 1. The change in percentage of avascular area from baseline to 5 years in the superior retina (number of superior zero pixels) did not differ significantly between race-based groups (p=0.3447), Table 1.

Figure 1. Retinal capillary blood flow parameters (inferior zero pixels) assessed by Heidelberg retinal flowmetry in open-angle glaucoma patients of African (AD) and European (ED) descent at baseline and 5 years. Larger increase from baseline to 5 years were found for open-angle glaucoma patients of AD than ED.

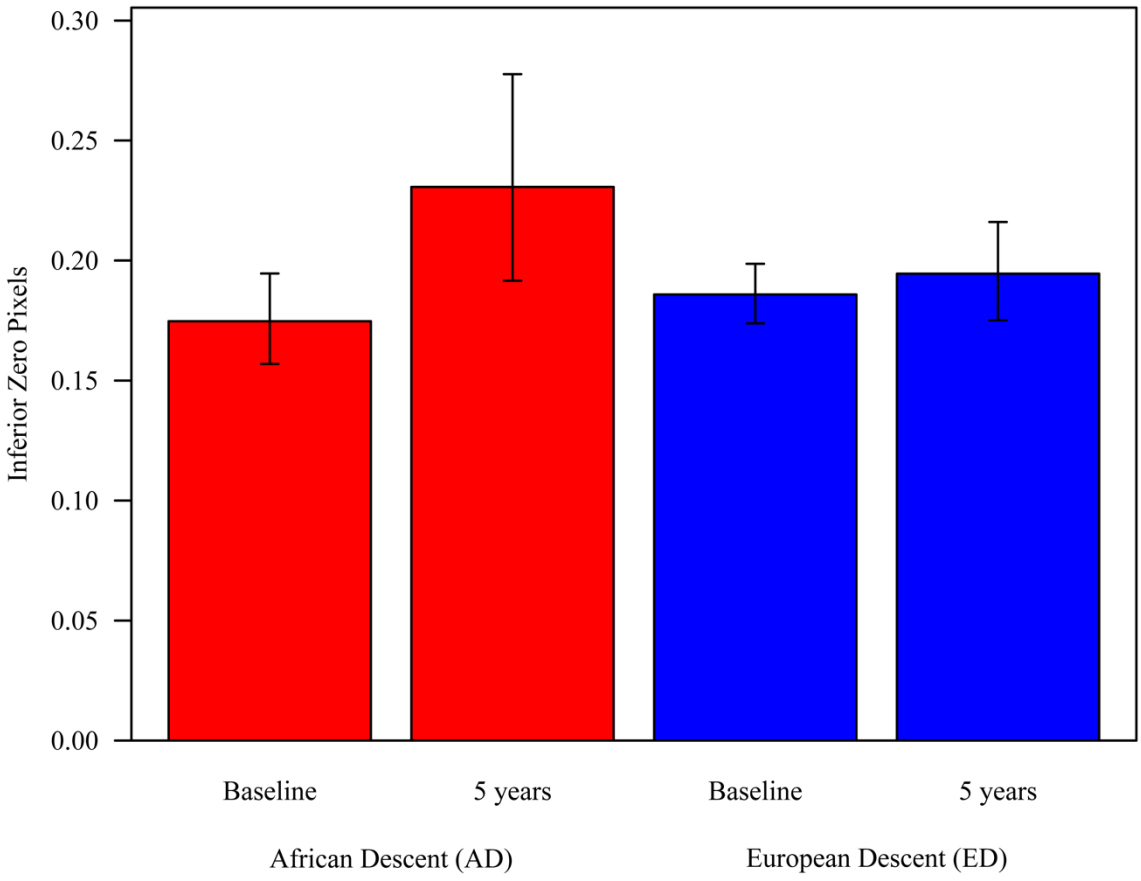

For the retrobulbar blood flow parameters, the NPCA EDV decreased significantly in OAG patients of ED from 2.40 to 1.79, with a statistically significant mean change of -0.83 (95% CI: -1.12, -0.56; $p<0.0001$), but did not decrease significantly in OAG patients of AD ($p=0.1494$), leading to a statistically significant difference between the two groups ($p=0.0430$). There was no significant difference in the changes in OA, CRA, NPCA and TPCA Peak Systolic Velocities, OA, CRA, TPCA End Diastolic Velocities, or OA, CRA, NPCA and TPCA Resistivity Indices between OAG of AD and ED ($p>0.05$), Table 1 and Figure 2.

Figure 2. Retrobulbar blood flow parameters assessed by color Doppler imaging in open-angle glaucoma patients of African (AD) and European (ED) descent at baseline and 5 years.

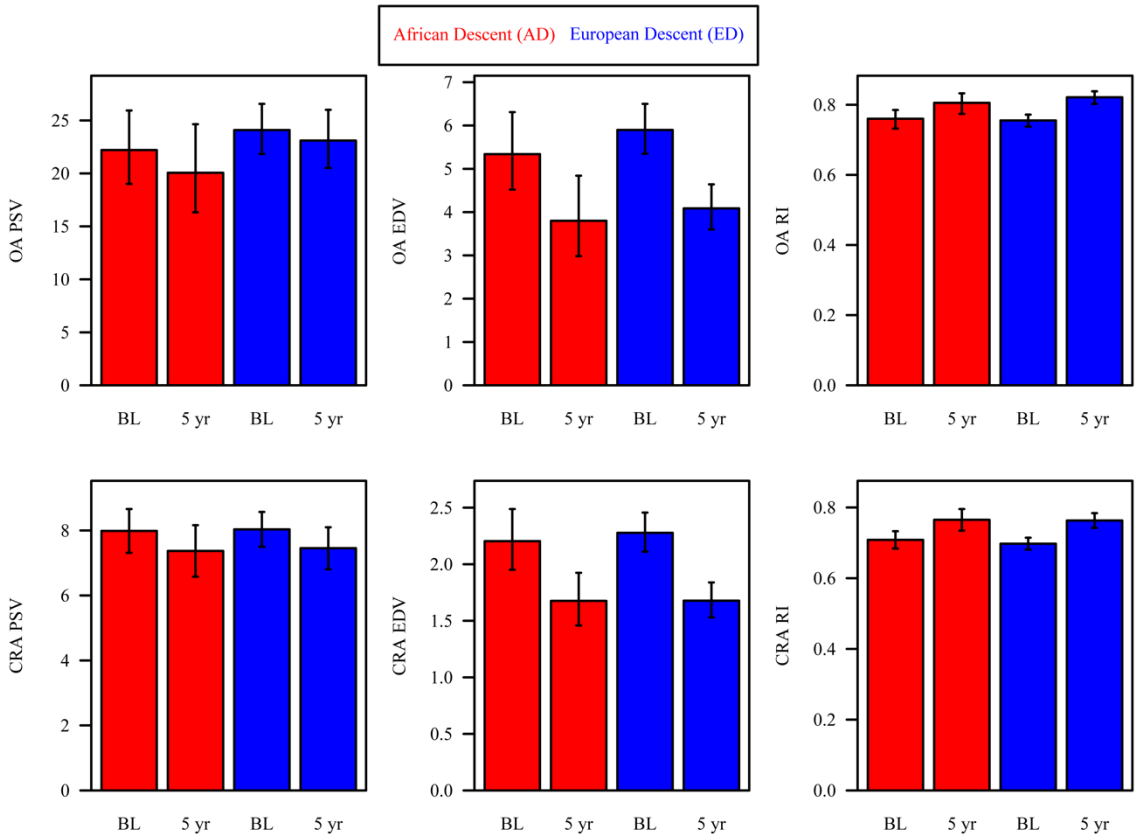

In OAG patients of AD, a higher baseline OPA was predictive of shorter time to structural progression (p=0.017), but not in patients of ED (p=0.7763), leading to a statistically significant difference between groups (p=0.113). In OAG patients of ED, lower baseline SBP (p=0.0332), SPP (p=0.0472) and RNFL thickness inferior (p=0.0472) were associated with shorter time to structural progression, but not in patients of AD, leading to a statistically significant difference between groups (SBP p=0.0217; SPP p=0.0306; RNFL thickness inferior (p=0.0379).

The mean arterial area was measured by Fourier Domain Doppler optical coherence tomography (FD Doppler OCT) in 122 open-angle glaucoma patients (35 AD, 87 ED) during a single study visit. The mean arterial area (mm^2) was 0.0316 (standard error, SE: 0.0010) and 0.0300 (SE: 0.0008) in patients of AD and ED, respectively. In OAG patients of AD, arterial area (mm^2) was positively correlated with OCT rim area (r=0.47, p=0.004), OCT superior

RNFL thickness (r=0.39, p=0.021), OCT temporal RNFL thickness (r=0.40, p=0.017), OCT average RNFL thickness (r=0.38, p=0.025), and negatively correlated with OCT cup/disc area ratio (r=-0.38, p=0.025) and OCT cup/disc vertical ratio (r=-0.44, p=0.008). In ED patients, correlations were weak and non-significant (r=-0.17 to 0.07; all p>0.05), leading to a significant difference between groups (rim area: p=0.027; superior RNFL thickness: p=0.009; temporal RNFL thickness: p=0.004, average RNFL thickness: p=0.018; cup/disc area ratio: p=0.045; cup/disc vertical ratio: p=0.010), Figure 3 and 4.

Figure 3. Arterial Area assessed by Fourier Domain Doppler optical coherence tomography versus average RNFL Thickness assessed by optical coherence tomography by race in open-angle glaucoma patients.

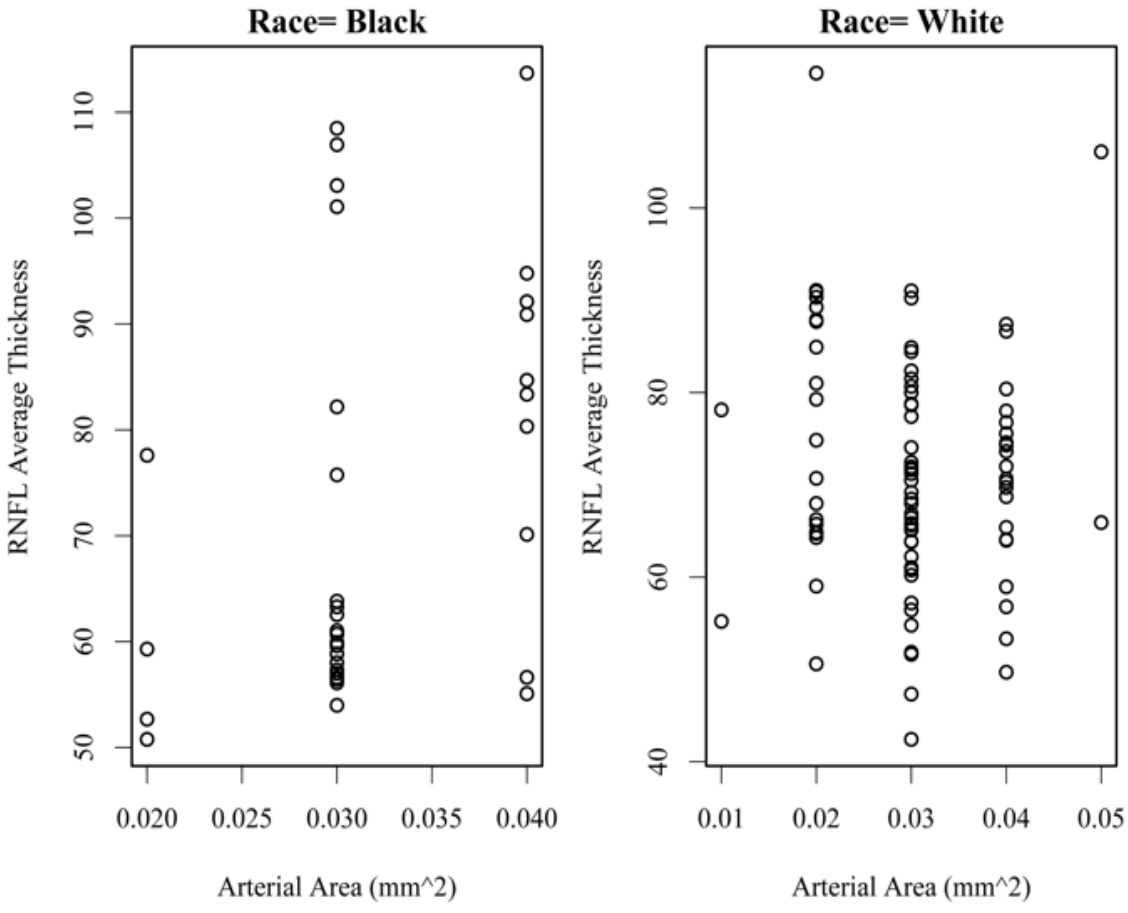

Figure 4. Arterial Area assessed by Fourier Domain Doppler optical coherence tomography versus Cup/Disc Area Ratio assessed by optical coherence tomography by race in open-angle glaucoma patients.

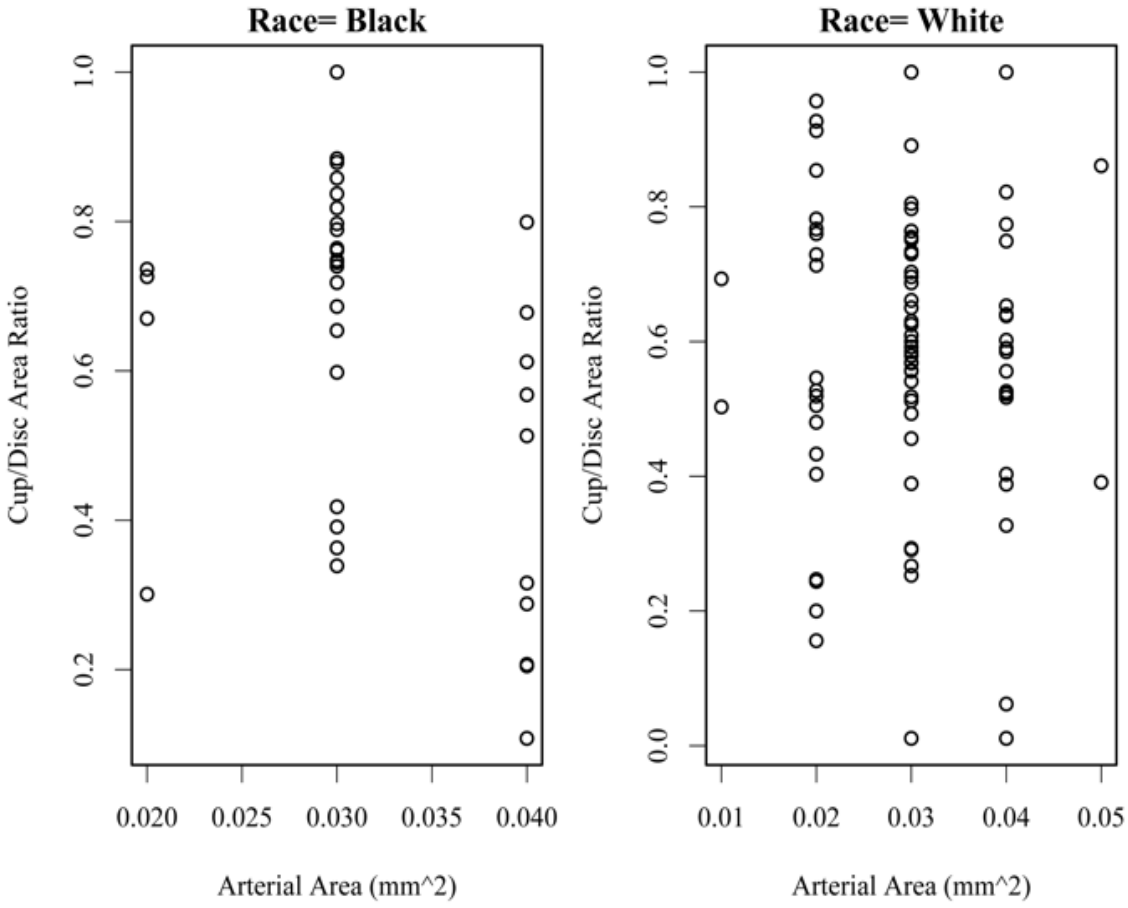

The summary of the other significant results of the Aim 2 of my PhD project are shown in Table 3.

Table 3. Summary of the significant changes over time and predictors of diseases progression from baseline to 5 years in open-angle glaucoma patients based on race (ED: European descent; AD: African descent).

Changes from Baseline to 5 years based on race (AD versus ED)
Visual Acuity increased more in AD than ED
NPCA EDV decreased in ED but did not decrease significantly in AD
Inferior Zero Pixels increased in AD but not in ED
PSD increased, but increased more in AD than ED

Cup area increased more in AD than ED
macular thickness outer nasal decreased more in AD than ED

Baseline predictors of shorter time to progression based on race (AD versus ED)
FUNCTIONAL PROGRESSION
N/A
STRUCTURAL PROGRESSION
higher OPA, for AD
lower SBP, for ED
lower SPP, for ED
lower RNFL thickness inferior, for ED
Predictors (multiple observations over time) of shorter time to progression based on race (AD versus ED)
FUNCTIONAL PROGRESSION
N/A
STRUCTURAL PROGRESSION
higher OPA, for AD
Predictors (change from baseline measurements, multiple observations over time) of shorter time to progression based on race (AD versus ED)
FUNCTIONAL PROGRESSION
less increase in BMI, for blacks
STRUCTURAL PROGRESSION
N/A

4. Discussion – Aim 2:

Aim 2 was to investigate the relationship between glaucoma progression, ocular hemodynamics, and *race*.

Structural and functional deterioration was observed in several measurements in both ED and AD OAG patients; however, we identified several statistically significant differences in the changes from baseline to five years between OAG of AD and ED in both functional and structural parameters. The visual field global index pattern standard deviation, indicative of the focal visual damage typically induced by glaucoma, increased over time both in persons of ED and AD, but the change was more significant in AD, with a statistically significant difference between the two groups (Table 1 and 2). With respect to structural parameters assessed by

OCT, changes characteristics of structural progression (increase in in the cup area, decrease in the macular thickness outer nasal) were more prominent in the AD population (Table 1 and 2). These results agree with previous studies that highlighted how OAG patients of AD progress more severely compared to ED (Huck et al., 2014). Importantly, there was no difference at baseline and over the 5 years period between patients of African and European descent with respect to IOP and its changes over time, thereby indicating that the observed differences between study groups were likely not related to IOP differences, the major risk factor for glaucoma onset and progression. This result adds to the previous studies that reported no overall differences in mean IOP levels between persons of AD and ED (Sample et al., 2009; Siesky et al., 2013), thus supporting the potential role of ocular vascular differences between patients of AD and ED as to explain glaucoma disease disparity.

Interestingly, in our cohort of OAG patients, the amount of area with no retinal capillary blood flow assessed by Heidelberg retinal flowmetry increased over a 5-year period in patients of AD, but not in patients of ED (Table 1, Figure 2). These findings agree with previous analyses performed after 4 years, that showed also a strong correlation between the retinal capillary dropout and macular thinning in patients of AD (Siesky et al. 2016). This finding is particularly important in the field OAG since the macular inner retinal layer thickness may be used as parameter to monitor glaucoma progression (Hwang et al., 2014). Importantly, in our analyses we also found that hemodynamics parameters assessed by Fourier domain Doppler OCT were correlated to structural parameters of the optic nerve head and peripapillary retinal nerve fiber layer, while these correlations were weak and non-significant in OAG of ED (Figure 3 and 4). These results parallel previous findings that showed a strong correlation between retinal blood flow parameters and optic nerve head morphology in patients of AD (Kanakamedala et al., 2014). Taken together, these data support the strong probability that alterations to the ocular hemodynamics may be more significant in OAG patient of AD compared to ED, thus

explaining non-IOP related relative risk factors in this specific population.

It is important to highlight that while significant changes based on race were found retinal capillary blood flow parameters, no significant changes were found in the retrobulbar blood flow parameters assessed by color Doppler imaging between AD and ED OAG patients for the OA< CRA, TPCA and NPCA, except for NPCA EDV (Table 1, Figure 2), thus suggesting that the retinal capillary blood flow may play a more significant role compared to the retrobulbar vascular bed in the disease progression of patients of African disease.

Finally, our results showed that in OAG patients of ED, lower baseline systolic blood pressure (SBP) and perfusion pressure (SPP) were associated with shorter time to structural progression, supporting the findings from previous studies that showed how lower SBP and SPP were predictors of OAG progression (Leske et al., 2007). Importantly, it must be highlighted that the known higher incidence of arterial hypertension in the AD populations (Huck et al., 2014), may make more difficult to derive conclusions regarding the predictive role of parameters such as blood pressure and perfusion pressure based on race.

In it important to highlight that Aim 2 of my PhD project has a major limitation in that only people of AD and ED were included in the study. It is known that across other populations groups, average prevalence rates of OAG are greater in Asian and Latin American descent (LAD) than ED but less than AD, while in Middle Eastern (ME) populations the prevalence is estimated to be similar to that of Asian populations with relatively limited data available. Further studies are needed including not only OAG patients of AD and ED, but also Asians, LAD and ME, in order to further the understanding of the role of race and ocular hemodynamics in glaucoma progression.

In conclusion, in our study we found that over 5-year period the visual and structural parameters indicative of disease progression deteriorated more in patients of AD compared to their ED counterparts, while the level of IOP did not changed significantly in patients of different race,

thus highlighting how patients of AD are at a greater risk for OAG progression at similar IOP levels. Importantly, our data also highlighted how avascular area increased more significantly over time in patients of AD, and significant correlation between structural parameters indicative of disease progression and ocular hemodynamics were found in patients of AD compared to ED. Taken together, these results support the notion of a possible vascular contributory mechanism of glaucoma progression over time, specifically in patients of AD. The results from the Aim 2 of my PhD highlight the importance of race as a contributing factor of disease progression. Indeed, clinicians should be encouraged to take into account the race of their glaucoma patients in their clinical management and therapeutic decisions.

CHAPTER 6

PhD Research Project – Aim 3: To investigate the relationship between glaucoma progression, ocular hemodynamics, and *diabetes status*

1. Introduction – Aim 3:

Open-angle glaucoma (OAG) and diabetes mellitus (DM) represent leading causes of impaired vision worldwide (Leske, 2007; Cheung et al., 2010). OAG represents a multifactorial optic neuropathy characterized by progressive death of the retinal ganglion cell and corresponding visual field loss (Leske, 2007). The major risk factor for the development and progression of OAG is represented by an elevated intraocular pressure (IOP); however, a high percentage of subjects with high level of IOP do not develop glaucoma, and many patients experience progression of the disease despite IOP in the normal range (Hollows and Graham 1966; Suzuki et al., 1999; Heijl et al., 2002: Leske et al., 2007). Significantly, vascular contributions to OAG pathogenesis and progression have been shown in many studies (Harris et al., 2020).

Several large scale clinical trials have evaluated the relationship between DM and OAG, and the results show that DM represents a controversial risk factor for glaucomatous optic neuropathy. In fact, some studies reported an increased risk of OAG in diabetics (Klein et al., 1994; Mitchell et al., 1997; Dielemans et al., 1996; Hennis et al., 2003; Bonovas et al., 2004; Chopra et al., 2008; Newman-Casey et al., 2011), while other large clinical trials have failed to find meaningful association between diabetes and glaucoma (Tielsch et al., 1995; de Voogd et al., 2006; Miglior et al., 2007; Gordon et al., 2008; Tan et al., 2009; Xu et al., 2009). In 2002, the Ocular Hypertension Treatment Study found evidence that diabetes may be a protective factor against the onset of glaucoma (Gordon et al., 2002); however, such effect was not confirmed in other studies (Coleman and Miglior, 2008). The contrasting results from the aforementioned studies highlight how the association the pathophysiology underlying the

relationship between DM and OAG remains poorly understood.

Importantly, vascular complications characterize both OAG and DM. In fact, both OAG and diabetic patients have been shown to present dysfunctional vascular regulation (Moore et al., 2008; Triggle and Ding, 2010). In details, deficiencies in the retinal, choroidal, and retrobulbar circulations have been shown in glaucomatous patients as contributors to the disease pathogenesis and progression (Galassi et al., 2003; Gugleta et al., 2003; Satilmis et al., 2003; Martinez et al., 2005; Feke and Pasquale. 2008; Harris et al., 2008). This dysfunctional vascular regulation may lead to an ischemic damage of the optic nerve head and apoptosis of the retinal ganglion cells, thus contributing to glaucomatous neuronal damage (Hayreh et al, 1970; Harris et al, 2008). Similarly, diabetic patients have been shown to exhibit vascular regulation dysfunction (Triggle and Ding, 2010), especially in retrobulbar and retinal circulations (Dimitrova et al., 2003; Ludovico et al., 2003), thus leading to the characteristic manifestations of diabetic patients, such as retinopathy and neuropathy (Chopra et al., 2008; Creager et al. 2003). As vascular abnormalities are associated with both diseases and these deficits may predispose patients toward a comorbid state, further evaluation to determine whether OAG patients with diabetes are more prone to glaucomatous progression is essential.

Due to the potential role of vascular abnormalities as a risk factor for both OAG and diabetes, and to the high epidemiologic impact of these two diseases, understanding the role of DM in the progression of OAG and elucidation of translatable risk factors is essential to improve vision preservation in diabetic glaucoma patients. Diabetes is an increasingly common malady that affects may organ systems, yet its influence on glaucoma pathology is not well understood. Identification of specific clinical and hemodynamic influences and/or synergies of risk factors involving diabetes as a comorbidity of glaucoma has therefore the potential to bring instantly translatable improvements to glaucoma screening and disease management. The Indianapolis Glaucoma Progression Study represented the first longitudinal and observational study in

which a large sample of OAG patients with and without DM was evaluated by multiple hemodynamic imaging technologies and multiple measures of structure and function to comprehensively assess the ocular and systemic circulation and to adequately monitor disease progression. The Aim 3 of my PhD analysis took advantage of the dataset of OAG patients with and without DM in order to shed further light on the relationship between ocular and systemic hemodynamics and glaucoma progression and diabetes. The aim 3 of my PhD project was to investigate the relationship between glaucoma progression, ocular hemodynamics, and *diabetes status.*

2. Material and Methods - Aim 3:

The comprehensive discussion of the materials and methods is detailed in chapter 3. In brief, a cohort of 112 patients (21 with DM, 91 without DM) with OAG were enrolled at baseline, and prospectively examined at baseline and every 6 months over a period of five years at the Glaucoma and Diagnostic Center at Indiana University School of Medicine, Indianapolis, Indiana. The data were categorized into groups depending on diabetic status (DM or no DM) based on self-reported status. OAG patients with self-reported diabetic status during the eligibility visit had to present a confirmed diagnosis of DM by their primary care physicians, and their retinas have been evaluated by a retina specialist, in order to be recruited in the study (in order to exclude the presence of diabetic retinopathy, exclusion criteria of the study). One qualified eye was randomly designated as the observational study eye in each subject. Measurements were made at baseline and every 6 months over a 5-year period.

To limit reproducibility bias with imaging, a single experienced operator with over ten years of experience performed all measurements in the same order and at the same time of the day for each patient. Functional disease progression was monitored by visual field testing and defined as two consecutive visits with an Advanced Glaucoma Intervention Study (AGIS)

score increase ≥2 from baseline, and/ or MD decrease ≥2 from baseline. Structural disease progression was monitored with optical coherence tomography and Heidelberg retinal tomography and defined as two consecutive visits with RNFL thickness decrease ≥8% and/or horizontal or vertical cup/disk ratio increase ≥0.2 compared to baseline.

The statistical analysis involved mixed-model analysis of covariance (ANCOVA) to test for significance of changes from baseline to 5-year follow-up separately by diabetes status (DM or no DM). Two-sample t tests and $\chi 2$ tests were used to analyze differences in baseline data between patients who progressed and those who did not progress. The models were then extended to test for whether the changes were different by diabetes status (DM or no DM). Time to functional progression and time to structural progression were analyzed using Cox proportional hazards survival analysis. Factors were analyzed as baseline measurements, as time-varying measurements, and as time-varying changes from baseline. Interactions were tested to determine if the effects of the factors on progression time differed by diabetes status (DM or no DM). Pearson correlation coefficients were calculated to evaluate linear associations. Correlations were adjusted for years of glaucoma, use of glaucoma or hypertension medications, age 65 or older, body mass index category, race, and gender. Correlations were compared between groups using Fisher z tests. P values <0.05 were considered statistically significant.

3. Results – Aim 3:

A cohort of 112 OAG patients (21 with DM, 91 without DM) were prospectively examined at baseline and every 6 months over a period of five years. After 5 years, 37 subjects (7 with DM, 30 without DM) progressed functionally, and 76 (14 with DM, 62 without DM) structurally.

Table 1 and 2 show the change in the study measurements (mean and 95% confidence interval, CI) from baseline to five years in patients with and without DM, respectively. Table 3

summarizes all the significant results related to the changes between parameters from baseline to 5 years and to the associations between measurements and shorter time to functional and structural progression based on diabetic status.

Table 1. Change from baseline to five years in the study parameters in open-angle glaucoma patients with diabetes (DM). * p-value statistically significant < 0.05.

	Diabetes							DM vs No DM	
	Baseline		5 years		Change			Change	
	N	Mean (95% CI)	N	Mean (95% CI)	Mean (95% CI)	p-value		p-value	
IOP	21	17.45 (15.56, 19.34)	12	14.09 (11.79, 16.39)	-3.36 (-5.59, -1.13)	0.0032	*	0.0522	
SBP	21	138.68 (128.42, 148.94)	14	129.27 (117.43, 141.11)	-9.41 (-19.73, 0.92)	0.0741		0.5472	
DBP	21	82.00 (76.48, 87.51)	14	75.18 (69.41, 80.94)	-6.82 (-12.75, -0.90)	0.0241	*	0.5661	
MAP	21	100.82 (94.36, 107.27)	14	93.14 (86.26, 100.03)	-7.67 (-14.26, -1.08)	0.0226	*	0.5134	
HR	21	73.30 (66.86, 79.75)	14	76.97 (68.91, 85.03)	3.67 (-2.67, 10.01)	0.2563		0.2440	
Visual Acuity	21	0.14 (0.08, 0.21)	14	0.25 (0.15, 0.35)	0.11 (0.01, 0.20)	0.0231	*	0.3816	
OA PSV	21	21.72 (17.61, 26.78)	14	22.02 (16.56, 29.27)	0.30 (-5.37, 4.77)	0.9088		0.4936	
OA EDV	21	5.40 (4.54, 6.43)	14	3.24 (2.51, 4.18)	-3.60 (-6.02, -1.69)	0.0000	*	0.1485	
OA RI	21	0.746 (0.777, 0.711)	14	0.854 (0.880, 0.823)	0.188 (0.280, 0.111)	0.0000	*	0.0017	*
CRA PSV	21	7.75 (6.85, 8.65)	14	7.38 (6.30, 8.46)	-0.37 (-1.36, 0.63)	0.4672		0.6441	
CRA EDV	21	2.37 (2.07, 2.72)	14	1.60 (1.37, 1.88)	-1.14 (-1.85, -0.55)	0.0000	*	0.2419	
CRA RI	21	0.681 (0.653, 0.708)	14	0.780 (0.744, 0.817)	0.100 (0.059, 0.140)	0.0000	*	0.0482	*
NPCA PSV	21	7.71 (6.89, 8.53)	14	7.37 (6.15, 8.58)	-0.35 (-1.49, 0.80)	0.5533		0.6362	
NPCA EDV	21	2.41 (2.14, 2.71)	14	1.64 (1.42, 1.89)	-1.13 (-1.75, -0.61)	0.0000	*	0.0762	
NPCA RI	21	0.669 (0.642, 0.697)	14	0.765 (0.730, 0.801)	0.096 (0.055, 0.136)	0.0000	*	0.2368	
TPCA PSV	21	7.72 (6.83, 8.62)	14	7.68 (6.41, 8.96)	-0.04 (-1.20, 1.13)	0.9474		0.6878	
TPCA EDV	21	2.38 (2.10, 2.71)	14	1.73 (1.47, 2.04)	-0.89 (-1.52, -0.37)	0.0004	*	0.5537	
TPCA RI	21	0.684 (0.713, 0.651)	14	0.774 (0.804, 0.739)	0.126 (0.200, 0.062)	0.0000	*	0.2508	
Superior Zero Pixels	21	0.200 (0.179, 0.224)	6	0.216 (0.168, 0.278)	0.015 (-0.041, 0.058)	0.5652		0.6928	
Inferior Zero Pixels	21	0.186 (0.167, 0.208)	6	0.193 (0.152, 0.244)	0.006 (-0.047, 0.047)	0.7993		0.5669	
Inferior Mean Flow	21	429.06 (375.61, 490.11)	6	406.10 (310.51, 531.11)	-24.26 (-163.19, 82.09)	0.6864		0.9711	
Superior Mean Flow	21	397.59 (354.88, 445.43)	6	397.40 (303.10, 521.04)	-0.18 (-125.51, 95.12)	0.9974		0.6812	
MD	21	-3.26 (-4.84, -1.69)	14	-3.36 (-5.23, -1.50)	-0.10 (-1.36, 1.16)	0.8758		0.0324	*
PSD	21	3.99 (2.73, 5.24)	14	4.53 (3.15, 5.91)	0.54 (-0.17, 1.25)	0.1359		0.4003	
AGIS score	21	1.49 (0.65, 2.76)	14	1.62 (0.69, 3.05)	0.12 (-0.54, 0.63)	0.6930		0.0669	
Disk area	21	2.339 (2.099, 2.579)	13	2.657 (2.374, 2.941)	0.318 (0.109, 0.527)	0.0029	*	0.7705	
Cup area	21	1.064 (0.766, 1.362)	13	1.330 (0.985, 1.675)	0.266 (0.075, 0.457)	0.0064	*	0.4664	
Rim area	21	1.269 (1.039, 1.500)	13	1.324 (1.072, 1.577)	0.055 (-0.139, 0.248)	0.5772		0.7490	
cup/disk area ratio	21	0.466 (0.365, 0.568)	13	0.495 (0.390, 0.600)	0.029 (-0.033, 0.091)	0.3576		0.3296	
cup/disk horizontal ratio	21	0.64 (0.56, 0.72)	13	0.69 (0.61, 0.78)	0.05 (0.00, 0.10)	0.0365	*	0.6396	

cup/disk vert ratio	21	0.632 (0.553, 0.712)	13	0.670 (0.583, 0.757)	0.037 (-0.013, 0.088)	0.1455		0.8824	
RNFL thickness superior	21	89.15 (77.01, 101.30)	10	95.16 (81.30, 109.01)	6.00 (-4.82, 16.83)	0.2766		0.0146	*
RNFL thickness inferior	21	95.82 (81.85, 109.79)	10	84.15 (67.20, 101.10)	-11.67 (-23.36, 0.02)	0.0504		0.1636	
RNFL thickness nasal	21	66.20 (57.84, 74.55)	10	64.71 (54.17, 75.24)	-1.49 (-10.32, 7.34)	0.7405		0.3104	
RNFL thickness temporal	21	54.76 (46.55, 62.97)	10	59.16 (49.44, 68.87)	4.40 (-3.39, 12.18)	0.2680		0.1799	
RNFL average	21	77.08 (68.65, 85.51)	10	75.97 (66.66, 85.29)	-1.11 (-7.35, 5.13)	0.7279		0.7397	
macular thickness outer superior	21	222.51 (213.22, 231.81)	13	212.47 (202.78, 222.17)	-10.04 (-15.54, -4.54)	0.0004	*	0.2034	
macular thickness inner superior	21	261.67 (251.61, 271.72)	13	245.50 (234.15, 256.84)	-16.17 (-22.82, -9.52)	0.0000	*	0.0836	
macular thickness outer inferior	21	208.23 (197.46, 219.01)	13	201.25 (190.39, 212.12)	-6.98 (-11.28, -2.67)	0.0015	*	0.6931	
macular thickness inner inferior	21	259.04 (247.01, 271.07)	13	248.10 (234.69, 261.50)	-10.94 (-17.85, -4.04)	0.0019	*	0.5256	
macular thickness outer nasal	21	234.12 (225.12, 243.13)	13	226.84 (216.03, 237.65)	-7.28 (-14.06, -0.51)	0.0352	*	0.4063	
macular thickness inner nasal	21	260.04 (248.30, 271.77)	13	245.15 (230.60, 259.71)	-14.89 (-24.90, -4.87)	0.0036	*	0.3242	
macular thickness outer temporal	21	204.17 (195.62, 212.73)	13	195.23 (186.27, 204.19)	-8.94 (-14.77, -3.11)	0.0027	*	0.8150	
macular thickness inner temporal	21	246.85 (235.02, 258.68)	13	236.57 (223.72, 249.42)	-10.28 (-19.18, -1.38)	0.0237	*	0.6741	
Macula center	21	202.61 (189.23, 215.98)	13	196.54 (182.38, 210.71)	-6.06 (-15.66, 3.53)	0.2150		0.2423	
macular volume	21	6.39 (6.15, 6.64)	13	6.14 (5.89, 6.38)	-0.26 (-0.36, -0.15)	0.0000	*	0.2951	
HRT3 Cup Area	20	0.860 (0.625, 1.130)	14	0.904 (0.660, 1.185)	0.043 (-0.034, 0.117)	0.2705		0.8723	
HRT3 Rim Area	20	1.297 (1.106, 1.488)	14	1.263 (1.065, 1.460)	-0.034 (-0.123, 0.055)	0.4544		0.8582	
HRT3 Cup Volume	20	0.286 (0.154, 0.418)	14	0.306 (0.172, 0.440)	0.020 (-0.023, 0.062)	0.3687		0.8750	
HRT3 Rim Volume	20	0.313 (0.233, 0.393)	14	0.306 (0.227, 0.385)	-0.007 (-0.042, 0.028)	0.7005		0.8338	
HRT3 Cup/Disk Area Ratio	20	0.404 (0.311, 0.497)	14	0.420 (0.325, 0.516)	0.017 (-0.021, 0.054)	0.3826		0.8782	
HRT3 Linear Cup/Disk Ratio	20	0.611 (0.529, 0.692)	14	0.628 (0.544, 0.712)	0.018 (-0.013, 0.048)	0.2554		0.7669	
HRT3 Mean Cup Depth	20	0.290 (0.232, 0.348)	14	0.309 (0.248, 0.370)	0.018 (-0.008, 0.045)	0.1662		0.4477	
HRT3 Max Cup Depth	20	0.707 (0.601, 0.813)	14	0.894 (0.537, 1.251)	0.187 (-0.156, 0.531)	0.2848		0.2814	
HRT3 Cup Shape	20	-0.134 (-0.170, -0.098)	14	-0.128 (-0.169, -0.086)	0.006 (-0.019, 0.032)	0.6173		0.5505	
HRT3 Height Variation Contour	20	0.336 (0.288, 0.390)	14	0.362 (0.309, 0.423)	0.024 (-0.008, 0.053)	0.1304		0.9158	
HRT3 Mean RNFL Thickness	20	0.200 (0.165, 0.235)	14	0.188 (0.149, 0.227)	-0.012 (-0.038, 0.014)	0.3728		0.9584	
HRT3 RNFL Cross-Sectional Area	20	1.049 (0.869, 1.228)	14	0.999 (0.804, 1.193)	-0.050 (-0.183, 0.083)	0.4604		0.9723	

Table 2. Change from baseline to five years in the study parameters in open-angle glaucoma patients without diabetes (DM). * p-value statistically significant < 0.05.

	No Diabetes							DM vs No DM	
	Baseline		5 year		Change			Change	
	N	Mean (95% CI)	N	Mean (95% CI)	Mean (95% CI)	p-value		p-value	
IOP	90	16.46 (15.36, 17.57)	63	15.53 (14.31, 16.74)	-0.94 (-1.97, 0.10)	0.0771		0.0522	
SBP	90	133.65 (129.21, 138.10)	63	127.72 (122.81, 132.64)	-5.93 (-10.68, -1.18)	0.0145	*	0.5472	
DBP	90	83.70 (80.91, 86.49)	63	78.81 (75.89, 81.74)	-4.89 (-7.88, -1.90)	0.0014	*	0.5661	
MAP	90	100.31 (97.21, 103.41)	63	95.09 (91.79, 98.39)	-5.22 (-8.52, -1.93)	0.0019	*	0.5134	
HR	90	70.20 (67.60, 72.80)	64	69.80 (66.73, 72.87)	-0.40 (-3.05, 2.25)	0.7685		0.2440	
Visual Acuity	90	0.04 (0.01, 0.07)	62	0.19 (0.14, 0.25)	0.15 (0.10, 0.20)	0.0000	*	0.3816	
OA PSV	91	24.44 (22.45, 26.59)	62	22.69 (20.42, 25.22)	-1.88 (-4.42, 0.44)	0.1162		0.4936	
OA EDV	91	5.98 (5.46, 6.55)	62	4.35 (3.85, 4.91)	-2.24 (-3.19, -1.39)	0.0000	*	0.1485	
OA RI	91	0.755 (0.770, 0.738)	62	0.803 (0.819, 0.785)	0.060 (0.087, 0.035)	0.0000	*	0.0017	*
CRA PSV	91	8.43 (7.96, 8.90)	62	7.80 (7.23, 8.36)	-0.63 (-1.15, -0.12)	0.0163	*	0.6441	
CRA EDV	91	2.30 (2.14, 2.46)	62	1.76 (1.61, 1.91)	-0.71 (-1.01, -0.43)	0.0000	*	0.2419	
CRA RI	91	0.710 (0.694, 0.725)	62	0.764 (0.746, 0.783)	0.055 (0.035, 0.074)	0.0000	*	0.0482	*
NPCA PSV	90	7.46 (7.00, 7.91)	62	7.41 (6.83, 8.00)	-0.04 (-0.57, 0.48)	0.8712		0.6362	
NPCA EDV	90	2.41 (2.26, 2.57)	62	1.93 (1.78, 2.10)	-0.59 (-0.86, -0.35)	0.0000	*	0.0762	
NPCA RI	90	0.660 (0.645, 0.675)	62	0.729 (0.711, 0.746)	0.069 (0.050, 0.088)	0.0000	*	0.2368	
TPCA PSV	91	7.88 (7.47, 8.28)	62	7.58 (7.12, 8.05)	-0.29 (-0.72, 0.14)	0.1838		0.6878	
TPCA EDV	91	2.46 (2.31, 2.62)	62	1.90 (1.76, 2.05)	-0.73 (-1.00, -0.48)	0.0000	*	0.5537	
TPCA RI	91	0.681 (0.696, 0.666)	62	0.749 (0.763, 0.734)	0.085 (0.112, 0.060)	0.0000	*	0.2508	
Superior Zero Pixels	91	0.196 (0.184, 0.208)	24	0.224 (0.200, 0.251)	0.025 (0.004, 0.044)	0.0238	*	0.6928	
Inferior Zero Pixels	90	0.186 (0.174, 0.198)	24	0.208 (0.188, 0.231)	0.020 (0.001, 0.037)	0.0411	*	0.5669	
Inferior Mean Flow	90	410.94 (380.94, 443.29)	24	391.13 (338.19, 452.35)	-20.81 (-86.15, 35.93)	0.4913		0.9711	
Superior Mean Flow	91	422.70 (397.03, 450.03)	24	395.76 (340.25, 460.31)	-28.78 (-102.02, 34.24)	0.3900		0.6812	
MD	91	-3.36 (-4.31, -2.41)	64	-5.22 (-6.56, -3.88)	-1.86 (-2.89, -0.84)	0.0004	*	0.0324	*
PSD	91	4.13 (3.25, 5.01)	64	5.05 (4.05, 6.04)	0.92 (0.40, 1.44)	0.0005	*	0.4003	
AGIS score	91	1.27 (0.79, 1.87)	63	2.13 (1.39, 3.09)	0.62 (0.33, 0.87)	0.0001	*	0.0669	
Disk area	91	2.264 (2.147, 2.382)	60	2.618 (2.476, 2.759)	0.353 (0.245, 0.461)	0.0000	*	0.7705	
Cup area	91	1.275 (1.129, 1.421)	60	1.623 (1.442, 1.804)	0.348 (0.234, 0.463)	0.0000	*	0.4664	
Rim area	91	0.982 (0.863, 1.101)	60	1.001 (0.866, 1.137)	0.019 (-0.087, 0.125)	0.7228		0.7490	
cup/disk area ratio	91	0.550 (0.496, 0.603)	60	0.614 (0.555, 0.674)	0.065 (0.027, 0.103)	0.0008	*	0.3296	
cup/disk horizontal ratio	91	0.73 (0.69, 0.77)	60	0.79 (0.74, 0.84)	0.06 (0.03, 0.09)	0.0000	*	0.6396	
cup/disk vert ratio	91	0.716 (0.675, 0.756)	60	0.749 (0.700, 0.797)	0.033 (0.001, 0.065)	0.0442	*	0.8824	
RNFL thickness superior	91	86.84 (80.61, 93.08)	61	78.07 (71.38, 84.76)	-8.78 (-13.69, -3.86)	0.0005	*	0.0146	*
RNFL thickness inferior	91	88.15 (80.79, 95.50)	61	85.79 (76.93, 94.65)	-2.36 (-8.36, 3.64)	0.4400		0.1636	
RNFL thickness nasal	91	60.74 (56.41, 65.07)	61	64.49 (58.61, 70.36)	3.75 (-1.27, 8.77)	0.1431		0.3104	

RNFL thickness temporal	91	55.14 (50.63, 59.64)	61	53.64 (48.56, 58.72)	-1.50 (-5.25, 2.26)	0.4337		0.1799	
RNFL average	91	72.80 (68.52, 77.08)	61	70.49 (65.59, 75.40)	-2.31 (-5.72, 1.10)	0.1844		0.7397	
macular thickness outer superior	91	222.72 (217.71, 227.73)	62	216.72 (211.40, 222.04)	-6.00 (-9.00, -2.99)	0.0001	*	0.2034	
macular thickness inner superior	91	264.77 (259.34, 270.19)	62	255.20 (249.11, 261.29)	-9.57 (-13.06, -6.09)	0.0000	*	0.0836	
macular thickness outer inferior	91	208.73 (204.21, 213.26)	62	202.81 (197.79, 207.83)	-5.93 (-8.96, -2.89)	0.0001	*	0.6931	
macular thickness inner inferior	91	255.91 (250.77, 261.04)	62	247.50 (241.40, 253.61)	-8.40 (-12.22, -4.59)	0.0000	*	0.5256	
macular thickness outer nasal	91	235.74 (230.96, 240.53)	62	231.55 (226.28, 236.81)	-4.20 (-6.97, -1.43)	0.0030	*	0.4063	
macular thickness inner nasal	91	265.41 (260.33, 270.50)	62	255.85 (250.24, 261.46)	-9.57 (-13.11, -6.02)	0.0000	*	0.3242	
macular thickness outer temporal	91	205.84 (201.56, 210.12)	62	197.71 (192.78, 202.64)	-8.13 (-11.72, -4.54)	0.0000	*	0.8150	
macular thickness inner temporal	91	250.18 (244.84, 255.52)	62	242.10 (235.68, 248.51)	-8.09 (-13.25, -2.92)	0.0022	*	0.6741	
Macula center	91	201.98 (194.70, 209.26)	62	203.51 (193.22, 213.81)	1.53 (-6.94, 10.00)	0.7226		0.2423	
macular volume	91	6.43 (6.31, 6.54)	62	6.24 (6.12, 6.36)	-0.19 (-0.26, -0.13)	0.0000	*	0.2951	
HRT3 Cup Area	91	0.888 (0.772, 1.012)	63	0.925 (0.803, 1.056)	0.036 (-0.009, 0.080)	0.1115		0.8723	
HRT3 Rim Area	91	1.239 (1.145, 1.333)	63	1.196 (1.097, 1.295)	-0.043 (-0.092, 0.005)	0.0800		0.8582	
HRT3 Cup Volume	91	0.297 (0.236, 0.359)	63	0.321 (0.259, 0.383)	0.023 (0.002, 0.045)	0.0335	*	0.8750	
HRT3 Rim Volume	91	0.280 (0.237, 0.323)	63	0.277 (0.233, 0.321)	-0.002 (-0.024, 0.019)	0.8233		0.8338	
HRT3 Cup/Disk Area Ratio	91	0.419 (0.376, 0.463)	63	0.439 (0.393, 0.485)	0.020 (-0.002, 0.042)	0.0719		0.8782	
HRT3 Linear Cup/Disk Ratio	91	0.629 (0.589, 0.668)	63	0.641 (0.599, 0.683)	0.012 (-0.006, 0.030)	0.1907		0.7669	
HRT3 Mean Cup Depth	91	0.302 (0.273, 0.331)	63	0.310 (0.281, 0.339)	0.008 (-0.001, 0.017)	0.0915		0.4477	
HRT3 Max Cup Depth	91	0.726 (0.668, 0.783)	63	0.724 (0.667, 0.781)	-0.002 (-0.022, 0.019)	0.8780		0.2814	
HRT3 Cup Shape	91	-0.124 (-0.142, -0.105)	63	-0.109 (-0.129, -0.089)	0.015 (0.004, 0.026)	0.0091	*	0.5505	
HRT3 Height Variation Contour	91	0.326 (0.296, 0.359)	63	0.349 (0.313, 0.390)	0.022 (0.000, 0.042)	0.0529		0.9158	
HRT3 Mean RNFL Thickness	91	0.196 (0.175, 0.218)	63	0.185 (0.161, 0.210)	-0.011 (-0.027, 0.005)	0.1810		0.9584	
HRT3 RNFL Cross-Sectional Area	91	1.026 (0.913, 1.138)	63	0.973 (0.843, 1.102)	-0.053 (-0.138, 0.033)	0.2259		0.9723	

From baseline to 5 years, in OAG patients with DM, the intra-ocular pressure and systemic blood pressures changed as follows: IOP decreased from 17.45 to 14.09, with a significant mean change of -3.36 (95%CI: -5.59, -1.13; p=0.0032); systolic blood pressure (BP) decreased from 138.68 to 129.27, with a mean change of -9.41 (95% CI: -19.73, 0.92, p=0.0741), Table 1 and Figure 1. Diastolic BP decreased from 82.00 to 75.18, with a statistically significant mean change of -6.82 (95% CI: -12.75, -0.90, p=0.0241), Table 1. In OAG patients without DM IOP decreased from 16.46 to 15.53, with a mean change of -0.94 (95%CI: -1.97, 0.10; p=0.0771); SBP decreased from 133.65 to 127.72, with a statistically significant mean change of -5.93 (95%CI: -10.68, -1.18, p=0.0145), Table 1 and Figure 1. Diastolic BP decreased from 83.70 to 78.81, with a statistically significant mean change of -4.89 (95% CI: -7.88, -1.90 p=0.0014), Table 1. No statistically significant difference was found in the change the ocular and systemic parameters from baseline to 5 years between OAG patients with and without diabetes (all p values>0.05, Table 1).

Figure 1. Systolic blood pressure (SBP) and systolic perfusion pressure (SPP) (mean with 95% confidence interval) in open-angle glaucoma patients with diabetes (DM) and without diabetes (No DM) at baseline (BL) and 5 years (5 yr).

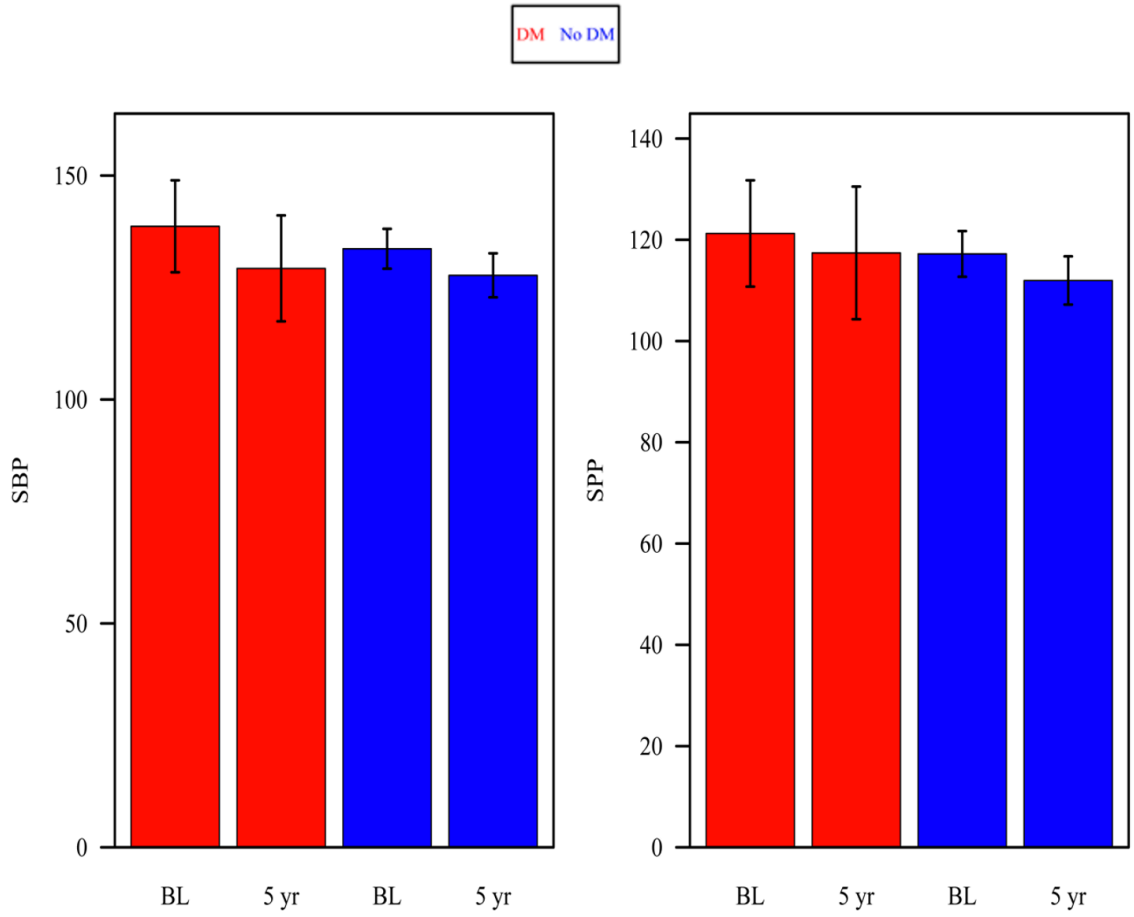

Changes in SBP (p=0.0169) and SPP (p=0.0291) were significantly associated with shorter time to functional progression in patients with DM, but not in patients without DM (SBP, p=0.0169; SPP, p=0.0291), leading to a significant difference between groups (SBP, p<0.001; SPP, p=0.0183), Figure 2.

Figure 2. Survival function for time to functional progression for open-angle glaucoma patients with and without diabetes for changes from baseline to 5 years for changes in systolic blood pressure (SBP) and systolic perfusion pressure (SPP). Lines represent survival curves for lowest and highest observed measurements. For open-angle glaucoma patients with diabetes, increases in SBP and SPP were associated with shorter time to functional progression.

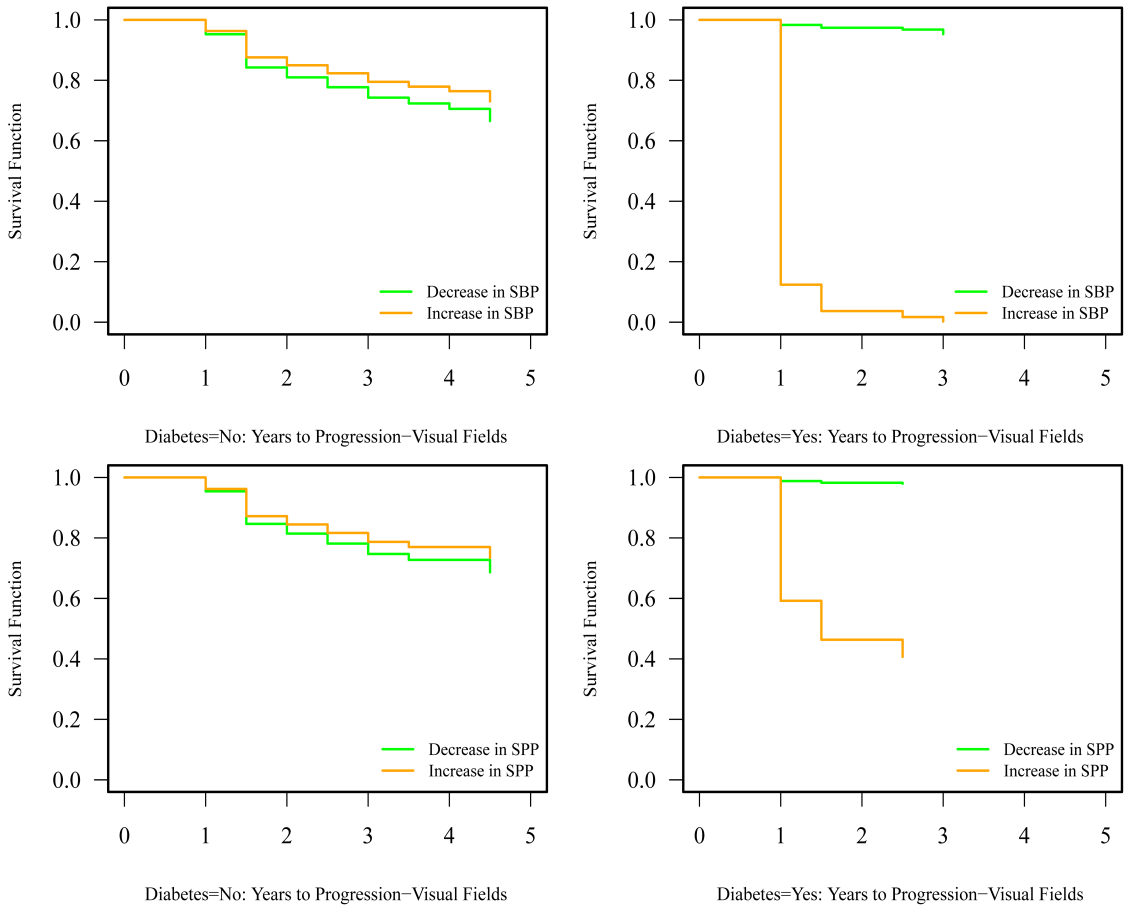

From baseline to 5 years, in OAG patients with DM, the optic nerve head parameters measured by Heidelberg retinal tomograph 3 changed as follows: cup area increased from 0.860 to 0.904, mean change of 0.043 (95%CI: -0.034, 0.117; p=0.2705); rim area decreased from 1.297 to 1.263, mean change of -0.034 (95%CI: -0.123, 0.055; p=0.4544); cup volume increased from 0.286 to 0.306, mean change of 0.020 (95%CI: -0.023, 0.062; p=0.3687); rim volume decreased from 0.313 to 0.306, mean change of -0.007 (95%CI: -0.042, 0.028; p=0.7005); cup/disc area ratio increased from 0.404 to 0.420, mean change of 0.017 (95%CI: -0.021, 0.054; p=0.3826); linear cup/disc ratio increased from 0.611 to 0.628, mean change of 0.018 (95%CI: -0.013, 0.048; p=0.2554); mean cup depth increased from 0.290 to 0.309, mean change of 0.018 (95%CI: -0.008, 0.045; p=0.1662); max cup depth increased from 0.707 to 0.894, mean change of 0.187 (95%CI: -0.156, 0.531; p=0.2848); cup shape changed from -0.134 to -0.128, mean change of 0.006 (95%CI: -0.019, 0.032; p=0.6173), Figure 3. In patients without DM, cup area

increased from 0.888 to 0.925, mean change of 0.036 (95%CI: -0.009, 0.080; p=0.1115); rim area decreased from 1.239 to 1.196, mean change of -0.043 (95%CI: -0.092, 0.005; p=0.0800); cup volume increased from 0.297 to 0.321, with a statistically significant mean change of 0.023 (95%CI: 0.002, 0.045; p=0.0335); rim volume decreased from 0.280 to 0.277, mean change of -0.002 (95%CI: -0.024, 0.019); p=0.8233); cup/disc ratio increased from 0.419 to 0.439, mean change of 0.020 (95%CI: -0.002, 0.042; p=0.0719); linear cup/disc ratio increased from 0.629 to 0.641, mean change of 0.012 (95%CI: -0.006, 0.030; p=0.1907); mean cup depth increased from 0.302 to 0.310, mean change of 0.008 (95%CI: -0.001, 0.017; p=0.0915); max cup depth decreased from 0.726 to 0.724, mean change of -0.002 (95%CI: -0.022, 0.019; p=0.2814); cup shape changed from -0.124 to -0.109, with a statistically significant mean change of 0.015 (95%CI: 0.004, 0.026; p=0.0091), Figure 3. No statistically significant difference was found in the change of the HRT 3 optic nerve head parameters from baseline to 5 years between OAG patients with and without diabetes (all p values>0.05, Table 1).

Figure 3. Optic nerve head parameters assessed by Heidelberg retinal tomograph 3 (mean with 95% confidence interval) in open-angle glaucoma patients with and without at baseline (BL) and 5 years (5 yr).

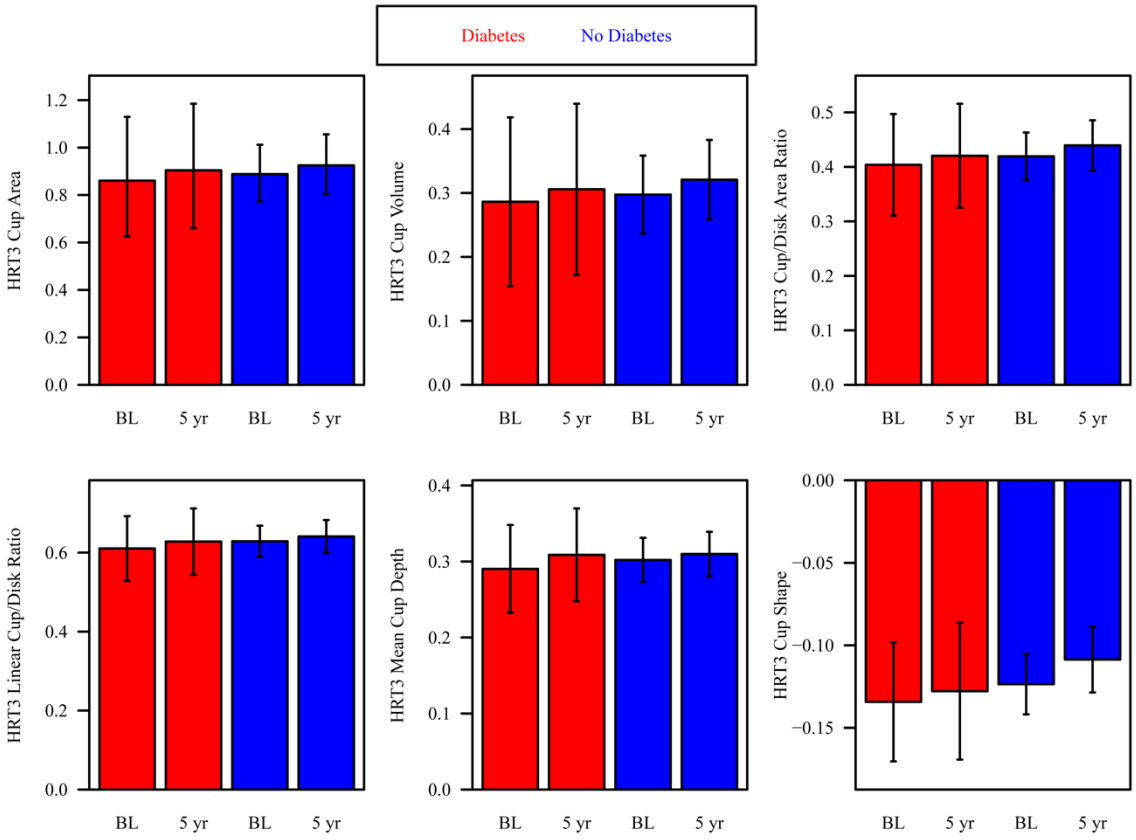

Higher cup area (p=0.0028), cup volume (0.0033), cup/disc area ratio (p= 0.0085), and mean cup depth (p= 0.0045) were significantly associated with shorter time to functional progression in patients with DM, but not in patients without DM (cup area, p=0.0952; cup volume, 0.5309; cup/disc area ratio, p=0.0505; mean cup depth, p=0.4649), leading to a significant difference between groups (cup area, p= 0.0213; cup volume, 0.0108; cup/disc area ratio, p=0.0419; mean cup depth, p=0.0013), Figure 4.

Figure 4. Survival function for time to functional progression for open-angle glaucoma patients with and without diabetes (DM) for optic nerve head parameters assessed by Heidelberg Retinal Tomograph 3. Lines represent survival curves for lowest and highest observed optic nerve head measurements. In open-angle glaucoma patients with DM, higher cup area, cup volume, cup/disc area ratio, and mean cup depth were associated with shorter time to functional progression, compared to patients without DM.

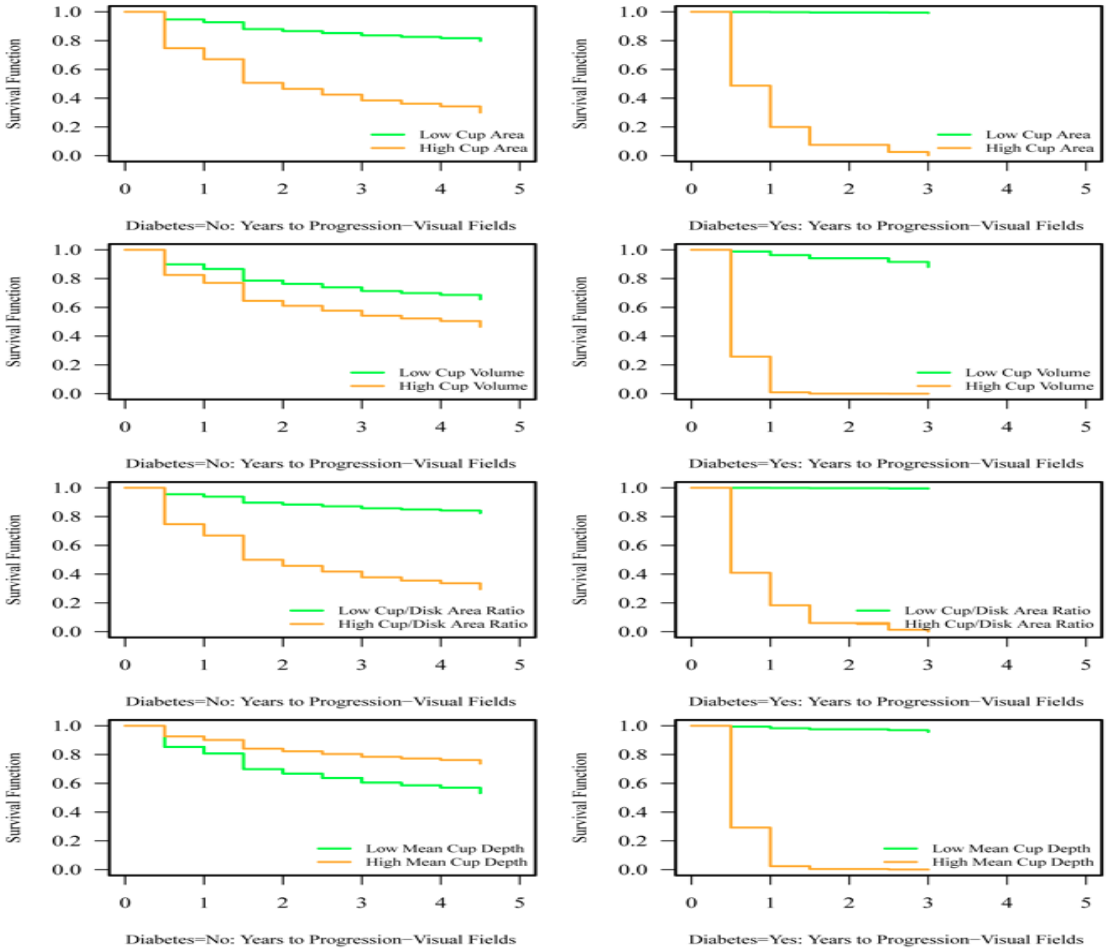

From baseline to 5 years, in OAG patients with DM, the retinal capillary blood flow parameters measured by Heidelberg retinal flowmeter (HRF) changed as follows: the number of superior zero pixels increased from 0.200 to 0.216, mean change of 0.015 (95%CI: -0.041, 0.058; p=0.5652; the number of inferior zero pixels increased from 0.186 to 0.193, mean change of 0.006 (95%CI: -0.047, 0.047; p=0.7993), Figure 5. The superior mean flow decreased from 397.59 to 397.40, mean change of -0.18 (95%CI: -125.51, 95.12; p=0.9974); the inferior mean flow decreased from 429.06 to 406.10, mean change of -24.26 (95%CI: -163.19, 82.09; p=0.6864). In OAG patients without DM, the number of superior zero pixels increased from 0.196 to 0.224, with a statistically significant mean change of 0.025 (95%CI: 0.004, 0.044; p=0.0238; the number of inferior zero pixels increased from 0.186 to 0.208, with a statistically

significant mean change mean change of 0.020 (95%CI: 0.001, 0.037; p=0.0411), Figure 5. The superior mean flow decreased from 422.70 to 395.76, mean change of -28.78 (95%CI: 102.02, 34.24; p=0.3900); the inferior mean flow decreased from 410.94 to 391.13, mean change of -20.81(95%CI: -86.15, 35.93; p=0.4913). No statistically significant difference was found in the change of the retinal capillary blood flow parameters from baseline to 5 years between OAG patients with and without diabetes (all p-values>0.05, Table 1).

Figure 5. Retinal capillary blood flow parameters (superior and inferior zero pixels) assessed by Heidelberg retinal flowmeter (mean with 95% confidence interval) in open-angle glaucoma patients with and without at baseline (BL) and 5 years (5 yr).

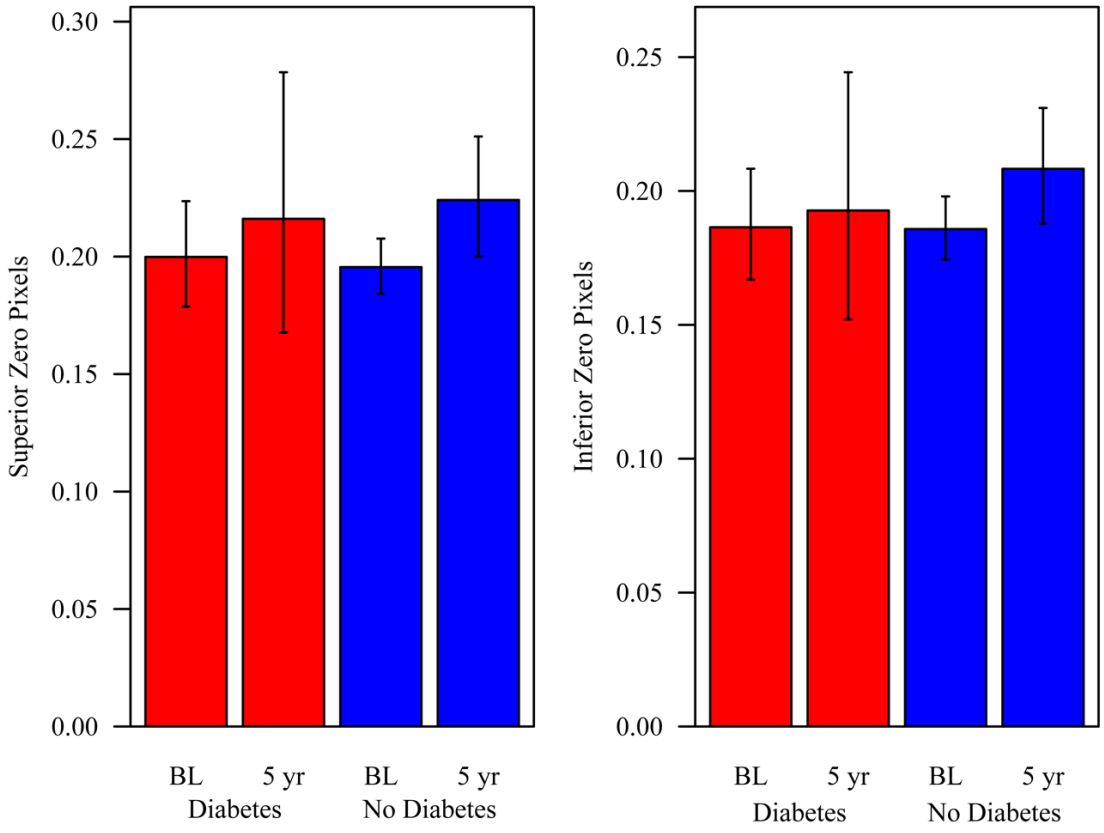

Higher number of superior zero pixels at baseline was significantly associated with shorter time to structural progression in patients with DM (p=0.0297) but not in patients without DM (p=0.5924), leading to a significant difference between groups (p=0.0352), Figure 6.

Figure 6. Survival function for time to structural progression for open-angle glaucoma patients with diabetes and without diabetes for baseline capillary blood flow parameters (superior zero pixels) assessed by Heidelberg retinal flowmeter. Lines represent survival curves for lowest and highest observed superior zero pixels. In open-angle glaucoma patients with diabetes, higher number of baseline superior zero pixels was associated with shorter time to functional progression, compared to patients without diabetes.

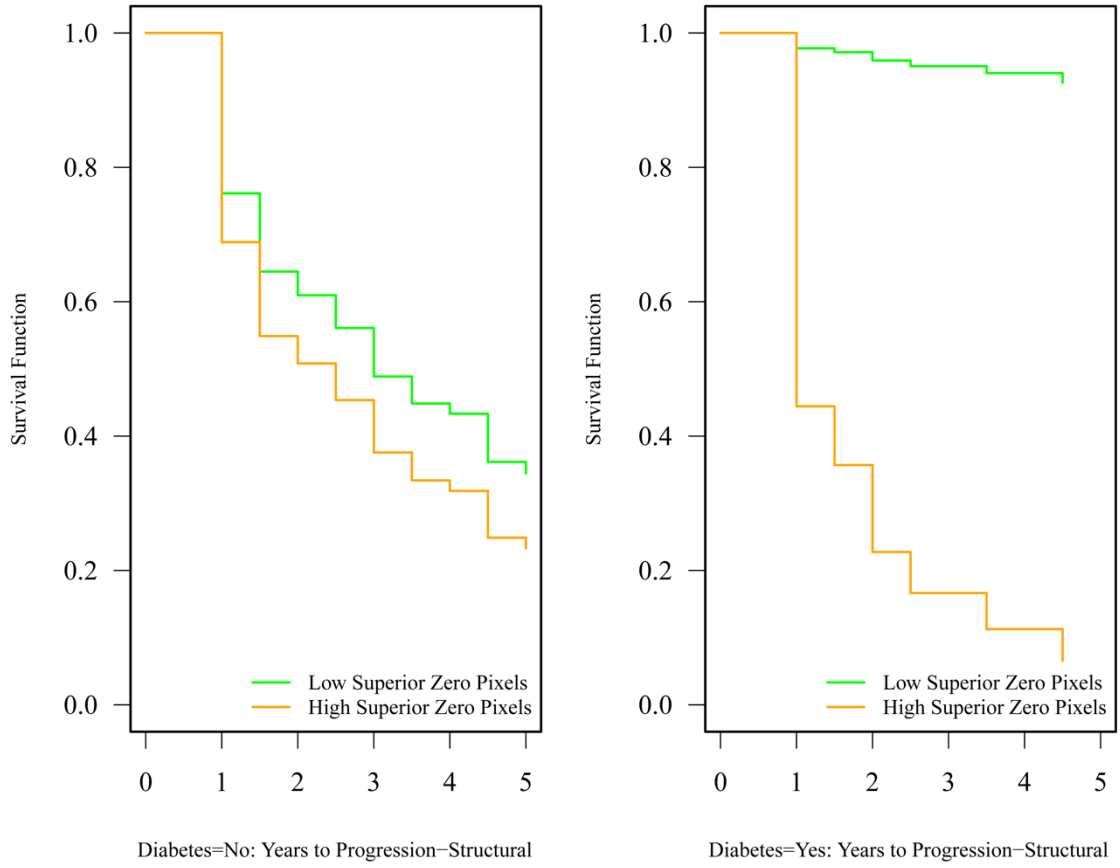

From baseline to 5 years, in OAG patients with DM, the retrobulbar blood flow parameters measured by color Doppler imaging changed as follows: OA PSV increased from 21.72 to 22.02, mean change of 0.30 (95%CI: -5.37, 4.77; p=0.9088); OA EDV decreased from 5.40 to 3.24, with a statistically significant mean change of -3.60 (95%CI: -6.02, -1.69; p<0.001); OA RI increased from 0.746 to 0.854, with a statistically significant mean change of 0.188 (95%CI: 0.280, 0.111; p<0.001); CRA PSV decreased from 7.75 to 7.38, mean change of -0.37 (95%CI:

-1.36, 0.63; p=0.4672); CRA EDV decreased from 2.37 to 1.60, with a statistically significant mean change of mean change of -1.14 (95%CI: -1.85, -0.55; p<0.001); CRA RI increased from 0.681 to 0.780, with a statistically significant mean change of 0.100 (95%CI: 0.059, 0.140; p<0.001); NPCA PSV decreased from 7.71 to 7.37, mean change of -0.35 (95%CI: -1.49, 0.80; p=0.5533); NPCA EDV decreased from 2.41 to 1.64, with a statistically significant mean change of -1.13 (95%CI: -1.75, -0.61; p<0.001); NPCA RI increased from 0.669 to 0.765, with a statistically significant mean change of 0.096 (95%CI: 0.055, 0.136; p<0.001); TPCA PSV decreased from 7.72 to 7.68, mean change of -0.04 (95%CI: -1.20, 1.13; p=0.9474); TPCA EDV decreased from 2.38 to 1.73, with a statistically significant mean change of -0.89 (95%CI: -1.52, -0.37; p<0.001); TPCA RI increased from 0.684 to 0.774, with a statistically significant mean change of 0.126 (95%CI: 0.200, 0.062; p<0.001), Figure 7. In OAG patients without DM, OA PSV decreased from 24.44 to 22.69, mean change of -1.88 (95%CI: -4.42, 0.44; p=0.1162); OA EDV decreased from baseline 5.98 to 4.35 at five years, with a statistically significant mean change of -2.24 (95% CI -3.19, -1.39; p<0.001); OA RI increased from 0.755 to 0.803, with a statistically significant mean change of 0.060 (95%CI: (0.087, 0.035); p<0.001); CRA PSV decreased from 8.43 to 7.80, with a statistically significant mean change of -0.63 (95%CI: -1.15, -0.12; p=0.0163); CRA EDV decreased from 2.30 to 1.76, with a statistically significant mean change of -0.71 (95%CI: -1.01, -0.43; p<0.001); CRA RI increased from 0.710 to 0.764, with a statistically significant mean change of 0.055 (95%CI: 0.035, 0.074; p<0.001); NPCA PSV decreased from 7.46 to 7.41, mean change of 0.04 (-0.57, 0.48; p=0.8712); NPCA EDV decreased from 2.41 to 1.93, mean change of -0.59 (-0.86, -0.35; p<0.001); NPCA RI increased from 0.660 to 0.729, with a statistically significant mean change of 0.069 (95%CI: 0.050, 0.088; p<0.001); TPCA PSV decreased from 7.88 to 7.58, mean change of -0.29 (95%CI: 0.72, 0.14; p=0.1838); TPCA EDV decreased from 2.46 to 1.90, with a statistically significant mean

change of -0.73 (95%CI: -1.00, -0.48; p<0.001); TPCA RI increased from 0.681 to 0.749, with a statistically significant mean change of 0.085 (95%CI: 0.112, 0.060; p<0.001), Figure 7.

A statistically significant difference was found in the change of the following CDI parameters from baseline to 5 years between OAG patients with and without diabetes for OA RI (p=0.0017), and CRA RI (p=0.0482), Table 1. For all the other parameters the change from baseline to 5 years was not statistically significantly different between OAG patients with and without diabetes (all p-values>0.05), Table 1.

Figure 7. Retrobulbar blood flow parameters assessed by color Doppler imaging (mean with 95% confidence interval) in open-angle glaucoma patients with diabetes (DM) and without diabetes (No DM) at baseline (BL) and 5 years (5 yr). EDV: end diastolic velocity; NPCA: nasal posterior ciliary artery; OA: ophthalmic artery; PSV: peak systolic velocity.

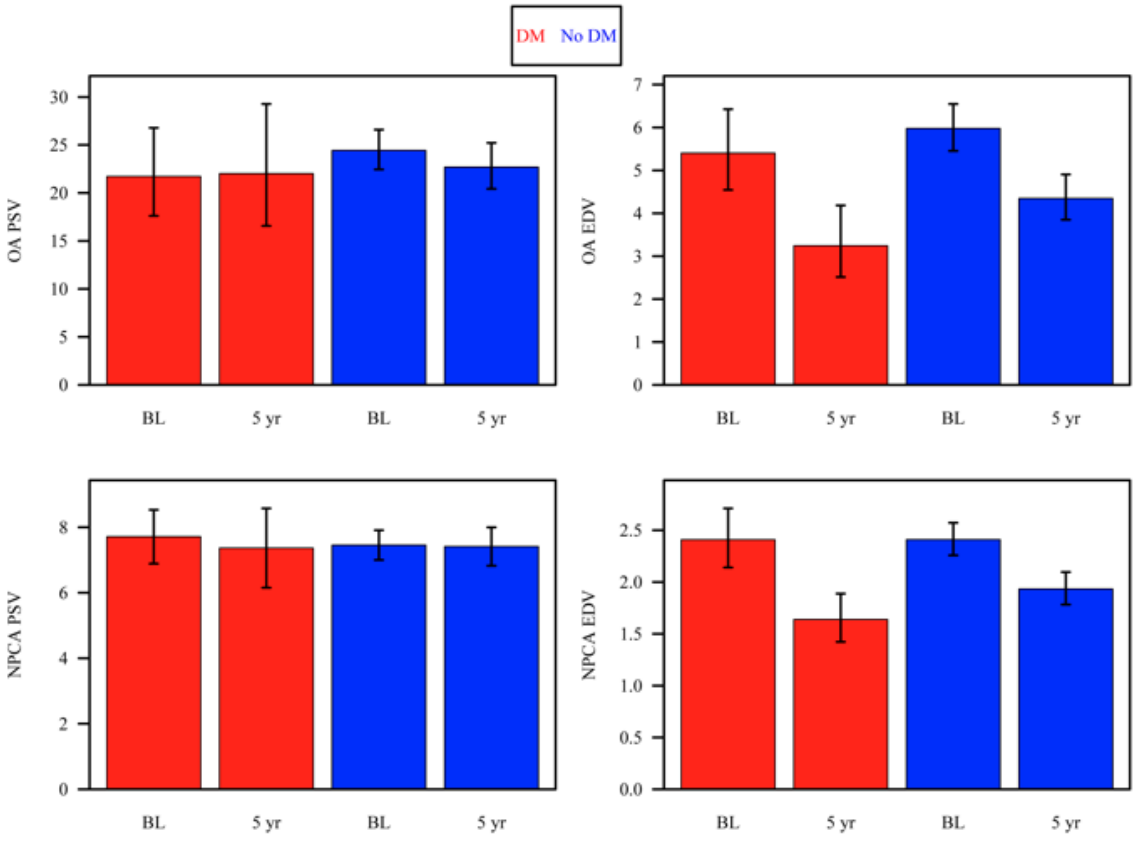

A smaller decrease in NPCA PSV was significantly associated with shorter time to functional progression in patients with DM (p=0.0211), but not in patients without DM (p= 0.2188), leading to a significant difference between groups (p=0.0021), Figure 8. A larger decrease in OA EDV (p=0.0281) and NPCA EDV (p=0.0490) were associated with shorter time to functional progression in patients without DM, but not in patients with DM (OA EDV, p=0.1212; NPCA EDV p=0.1279), leading to a significant difference between groups (OA EDV, p=0.0288; NPCA EDV, p=0.0248), Figure 8.

Figure 8. Survival function for time to functional progression for open-angle glaucoma patients with and without diabetes for changes from baseline to 5 years in retrobulbar blood flow parameters assessed by color Doppler imaging. Lines represent survival curves for lowest and highest observed changes. For open-angle glaucoma patients with diabetes a smaller decrease in NPCA PSV was associated with shorter time to functional progression. For open-angle glaucoma patients without diabetes a larger decrease in OA EDV and NPCA EDV was associated with shorter time to functional progression. EDV: end diastolic velocity; NPCA: nasal posterior ciliary artery; OA: ophthalmic artery; PSV: peak systolic velocity.

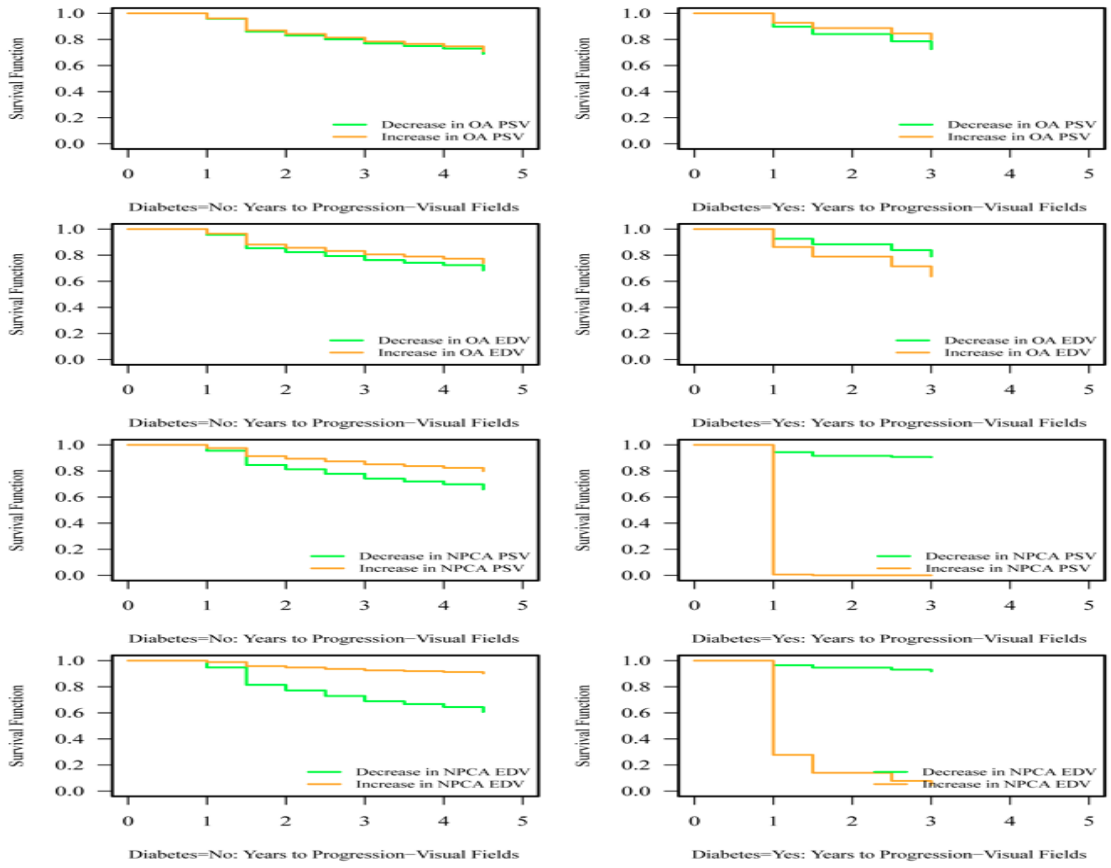

The volumetric ocular blood flow parameters were assessed by Fourier Domain Doppler optical coherence tomography (FD Doppler OCT) in 110 open-angle glaucoma patients (19 with DM; 91 without DM) during a single study visit. The total blood flow (microliters/min) was (in mean and standard error, SE) 32.32 (standard error, SE: 1.38) and 33.57 (SE: 0.88) in patients with and without DM, respectively; the superior hemisphere blood flow was 16.45 (SE: 1.38) and 17.68 (SE: 0.58) in patients with and without DM, respectively; the inferior hemisphere blood flow was 15.87 (SE: 2.16) and 15.89 (SE: 0.50) in patients with and without DM, respectively. In OAG patients with DM, superior hemisphere blood flow was positively correlated with diastolic BP (DBP) (r=0.53, p= 0.0189), mean arterial pressure (MAP) (r=0.50, p=0.0267), OPP (r=0.45, p=0.0542), diastolic perfusion pressure (DPP) (r=0.49, p=0.0319) and mean perfusion pressure (MPP) (r=0.47, p=0.0409). In OAG patients without DM, these correlations were weak and non-significant (DBP, r=-0.02; MAP, r=-0.02; OPP, r=-0.12; DPP, r=-0.10; MPP, r=-0.09, all p>0.05), leading to a significant difference between groups (DBP,

p=0.0221; MAP: p=0.0308; OPP: p=0.0246; DPP: p=0.0176; MPP: p=0.0241), Figure 9 and 10.

Figure 9. Volumetric ocular blood flow (superior hemisphere blood flow) assessed by Fourier Domain Doppler optical coherence tomography versus diastolic blood pressure (DBP) by diabetes status in open-angle glaucoma patients.

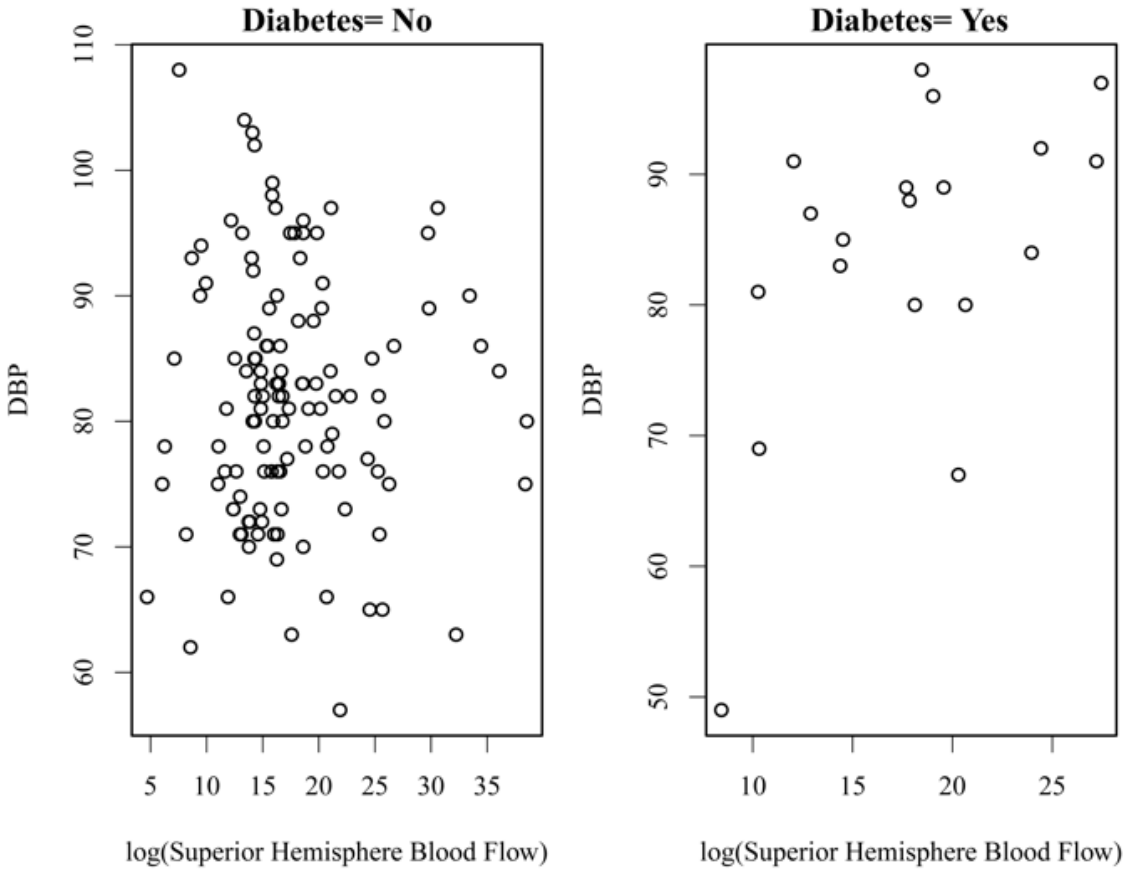

Figure 10. Volumetric ocular blood flow (superior hemisphere blood flow) assessed by Fourier Domain Doppler optical coherence tomography versus diastolic perfusion pressure (DPP) by diabetes status in open-angle glaucoma patients.

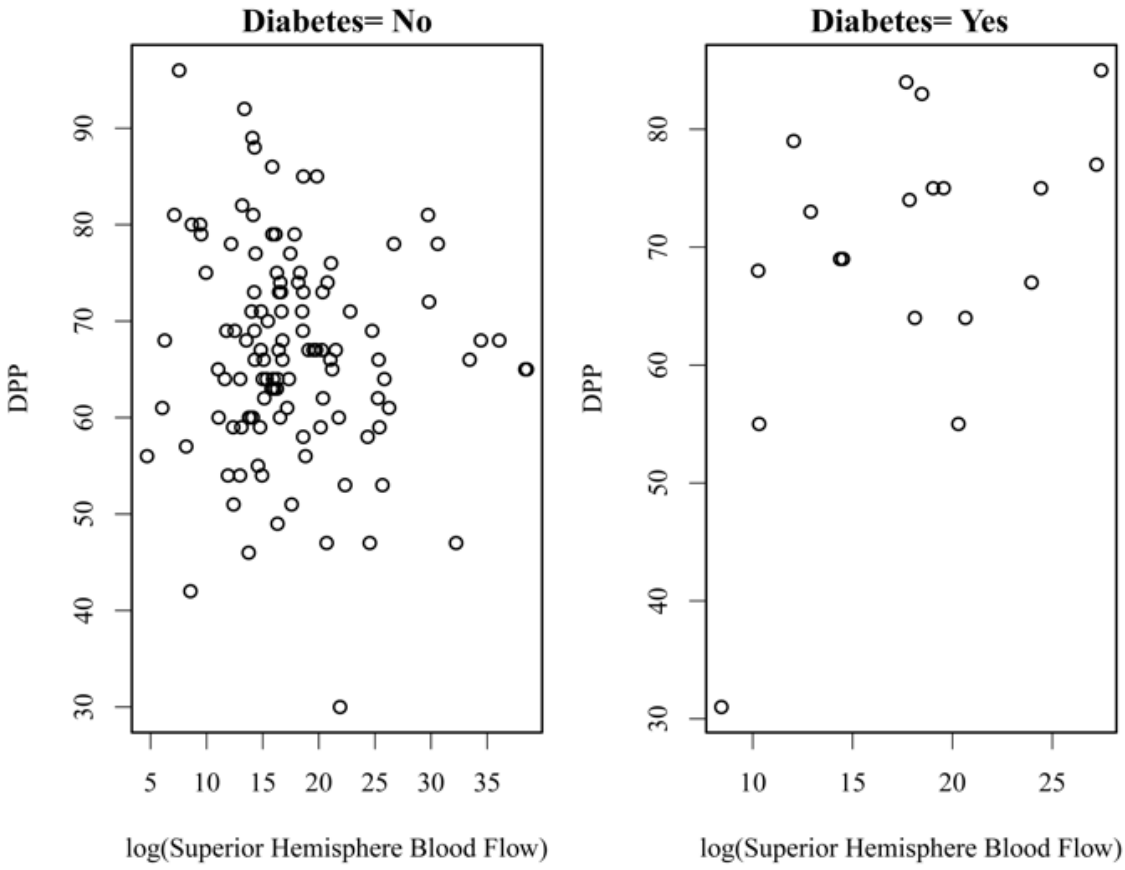

The summary of the other significant results of the Aim 3 of my PhD project is shown in Table 3.

Table 3. Summary of the significant changes over time and predictors of diseases progression from baseline to 5 years in open- angle glaucoma patients based on diabetic status.

Changes from Baseline to 5 years
OA RI increased more for diabetics than non-diabetics
CRA RI increased more for diabetics
MD decreased in non-diabetics but did not change in diabetics
RNFL thickness superior decreased in non-diabetics but did not change in diabetics
Baseline predictors of shorter time to progression
FUNCTIONAL PROGRESSION
higher Cup area, for diabetic
higher HRT3 Cup Volume, for diabetic
higher HRT3 Mean Cup Depth, for diabetic

STRUCTURAL PROGRESSION
higher Superior Zero Pixels, for diabetic
lower macular thickness inner superior, for diabetic
Predictors (multiple observations over time) of shorter time to progression
FUNCTIONAL PROGRESSION
lower HR, for diabetic
higher cup/disk horizontal ratio, especially, for diabetic
higher cup/disk vert ratio, especially, for diabetic
higher HRT3 Cup Area, especially, for diabetic
higher HRT3 Cup Volume, for diabetic
higher HRT3 Cup/Disk Area Ratio, especially, for diabetic
higher HRT3 Linear Cup/Disk Ratio, especially, for diabetic
higher HRT3 Mean Cup Depth, for diabetic
higher HRT3 Cup Shape, especially, for diabetic
STRUCTURAL PROGRESSION
lower BMI, for non-diabetic
Predictors (change from baseline measurements, multiple observations over time) of shorter time to progression in the overall population
FUNCTIONAL PROGRESSION
less decrease in OA EDV, for diabetic
less decrease/more increase in NPCA PSV, for diabetics
less decrease in NPCA EDV, for diabetics
less decrease in macular thickness outer inferior, for diabetics
less decrease in macular thickness outer nasal, for diabetics
STRUCTURAL PROGRESSION
more increase in Superior Zero Pixels, for non-diabetics

4. Discussion – Aim 3:

The Aim 3 of my PhD project was to investigate the relationship between glaucoma progression, ocular hemodynamics, and *diabetic status*.

In our study population, IOP, the major risk factor for OAG onset and progression, was found to be in the normal range and to not differ significantly at baseline and over the 5 years period between patients with and without DM (Table 1 and 2). In the literature, contrasting results have been shown regarding the relationship between DM and elevated IOP. In fact, although some studies have found an association between diabetes and elevated IOP, others have failed to find such an interaction (Gerber et al. 2015). These results highlight the fact that other than

IOP, additional contributing factors to glaucoma may play a significant role in the relationship between OAG and DM, and in our study, we investigated ocular and systemic vascular risk factors by assessing the retinal, retrobulbar and systemic circulation with multiple imaging techniques.

In our study, we evaluated the retinal capillary blood flow in OAG patients with and without DM using the Heidelberg retinal flowmeter (Table 1 and 2, Figure 5). We found that a higher amount of retinal avascular area at baseline was predictive of glaucomatous structural progression in patients with DM but not in patients without DM (Figure 5 and 6). These results are in agreement with previous studies that highlighted the correlation between changes in structural parameters are correlated with changes in retinal blood flow in glaucomatous patients with diabetes. Lee et al. found that changes in optic disc parameters have a much stronger correlation to retinal capillary change in patients with diabetes (Lee et al. 2014). Similarly, Shoshani et al. found significant correlations between avascular areas in the superior and inferior retina and average RNFL thickness in OAG patients with diabetes compared to those without (Shoshani et al., 2012). Taken together, these findings suggest that OAG diabetic patients may be more sensitive to retinal blood flow abnormalities, thus supporting the results from previous studies that highlighted the presence of altered retinal blood flow in patients with diabetes. For example, Burgansky-Eliash et al. found that retinal arterial and venous flow velocities were initially increased in diabetic patients who did not show signs of retinopathy, suggesting that irregularities in vessel function exist in diabetic eyes before structural changes occur (Burgansky-Eliash et al., 2012). Interestingly, along with the structural disease progression to non-proliferative retinopathy, the blood flow velocity subsequently decreased below normal levels (Burgansky-Eliash et al., 2010). Similarly, in a study from Bursell et al., retinal blood flow was shown to be significantly decreased in patients with diabetes compared to those without (Bursell et al., 1996). Finally, in the Optical Coherence Tomography (OCT)

Study, patients with glaucoma and treated proliferative diabetic retinopathy presented significantly decreased retinal blood flow assessed by Doppler OCT compared with normal patients (Wang et al. 2011). Taken together, these findings suggest that diabetic may be more sensitive to retinal blood flow abnormalities, thus supporting the results from previous studies that highlighted the presence of altered retinal blood flow in patients with diabetes.

The retrobulbar circulation was assessed in our study using CDI, and significant differences were shown in the changes over time between OAG patients with and without DM (Table 1 and 2, Figure 7). Also, we found that a smaller decrease in NPCA PSV led to a shorter time to functional progression in OAG patients with DM, while a larger decrease in EDV of the OA and NPCA led to a shorter time to functional progression in non-diabetic OAG patients (Figure 7 and 8). These results are in agreement with previous finding that showed how the presence of DM has been shown to have an effect on the retrobulbar hemodynamics. Goebel et al. showed a strong correlation between proliferative diabetic retinopathy and impaired retrobulbar flow (Goebel et al., 1995). Additionally, under hyperoxic conditions, healthy subjects showed a reduction in the retrobulbar blood flow, while no change was detected in patients with DM (Evans et al., 1997). These studies indicate that diabetic patients with display altered hemodynamics in the major vessels of the eye, thus suggesting that retrobulbar blood flow have varied implications on the progression on glaucoma based on the diabetic status of the OAG patient.

Systemic blood pressures and ocular perfusion pressures and their correlation with volumetric blood flow assessed by Doppler OCT in OAG patients with and without DM were also investigated in our study (Table 1 and 2). Changes in SBP and SPP were associated with a shorter time to functional progression in OAG patients with DM (Figure 1 and 2), and a strong correlation was found between volumetric blood flow and DBP and OPP compared to non-diabetic OAG patients (Figure 9 and10). Such results may be explained by the presence of

ocular perfusion abnormalities that can be induced in diabetic patients via atherosclerosis of the vessels upstream from the disc, arteriolosclerosis, or vasospasm, as shown in previous studies (Bonomi et al., 2000; Chait et al., 2009). Also, endothelial dysfunction characterized diabetic patients (Schalkwijk and Stehouwer, 2005), thus possibly amplifying the lack of local autoregulation withing retinal tissue in OAG patients with DM. Results from our and previous findings therefore suggest that via several pathophysiological mechanisms induced by diabetes, OAG patients with DM may be more susceptible to changes in systemic blood pressure and ocular perfusion pressure, and this vulnerability may increase their risk for glaucomatous progression compared to OAG patients without DM.

It is important to acknowledge that only subjects with non-insulin dependent DM and with mild non-proliferative diabetic retinopathy or no non-proliferative diabetic retinopathy at all were included, thus limiting our results to this group of patients. Also, our study did not include blood glucose levels and haemoglobin A1c measurements. Further studies are therefore needed in glaucomatous patients with more advanced stages of diabetic retinopathy in order to further the understanding of the effect of glycemic levels on the ocular blood flow biomarkers.

In summary, our findings highlight how OAG patients with DM present different susceptibility to vascular risk factors compared to patients without DM. In our study in OAG patients evaluated over a 5-year period vascular risk factors influenced disease progression differently based on the presence of diabetes. Ophthalmologists should be encouraged to take into account the presence of DM as modifying risk factor in the disease progression of their glaucomatous patients.

CHAPTER 7

PhD Research Project – Aim 4: To investigate the relationship between glaucoma progression, ocular hemodynamics, and *gender*

1. Introduction – Aim 4:

The relationship between gender and open-angle glaucoma (OAG) is not fully understood. OAG represents a multifactorial optic neuropathy characterized by progressive retinal ganglion cell death and visual field loss. An elevated intraocular pressure (IOP) has been shown to be the major risk factor for the disease onset and progression, and it is currently the only modifiable one. However, high IOP does not always lead to glaucoma, and disease progression occur even for normal levels of IOP, and impaired ocular hemodynamic in the retinal, retrobulbar, and choroidal circulations have been shown to be involved in the pathogenesis and progression of the disease (Harris et al, 2020). The pathogenesis of the disease is still not fully understood, and it has been suggested that gender may play a role in OAG risk and pathogenesis.

Importantly, contrasting data have been published regarding the prevalence and incidence of OAG among male and female. In fact, while women have been shown to be disproportionately affected by OAG compared to male in some studies (Higgenbotham, 2004; Quigley and Broman, 2006), others analyses, including a meta-analysis evaluating the global prevalence of glaucoma through the year 2040, male were more likely to develop OAG than female (Tham et al. 2014; Zetterberg, 2016). Mukesh et al., in a 5-year incidence study on 3,271 participants found higher OAG incidence rates in men compared to women in the 5th, 6th, and 7th decades, whereas by the 8th decade they were similar (Mukesh et al., 2002). Multiple other studies, such as the Baltimore Eye Survey, Beaver Dam Eye Study, and Blue Mountains Eye Study have shown no difference in OAG prevalence and incidence between male and female (Tielsch et

al., 1991; Klein et al., 1992; Mitchell et al., 1996; Wensor et al. 1998; Varma et al. 2004). Physiologic ocular structural differences have been shown existing between men and women, such as in the axial length and corneal curvature, that may contribute to the disease differently in the two sexes (Mark, 2005). The hormonal status has also been suggested as another possible explanation for the gender differences in the pathogenesis of glaucoma, with studies showing a protective effect of estrogens on the onset and progression of the disease (Phillps and Gore Hulsman et al., 2001; de Voogd et al., 2008; Phillps and Gore 1985). In addition, variable effects of sex hormones have been reported on risk factors for glaucoma, such as IOP and ocular blood flow (Altintas et al., 2004; Siesky et al. 2008).

The aforementioned results highlight how conflicting data are present in the literature regarding both the epidemiology of OAG between the sexes, and the pathophysiologic mechanism behind these differences currently are not clearly delineated. Importantly, the relationship between glaucoma progression, sex hormones and ocular blood flow is not fully understood. Taking advantage of data collected in the Indianapolis Glaucoma Progression Study, which used multiple hemodynamic imaging technologies and measures of structure and function to comprehensively assess the ocular and systemic circulation and to adequately monitor disease progression, the aim 4 of my PhD project was to investigate the relationship between glaucoma progression, ocular hemodynamics, and *gender.*

2. Material and Methods - Aim 4:

The comprehensive discussion of the materials and methods is detailed in chapter 3.

In brief, a cohort of 112 OAG patients (68 female, 44 male) were enrolled at baseline, and prospectively examined at baseline and every 6 months over a period of five years at the Glaucoma and Diagnostic Center at Indiana University School of Medicine, Indianapolis, Indiana. The data were categorized into groups depending on gender (female or male) based

on self-reported biologic gender. One qualified eye was randomly designated as the observational study eye in each subject. Measurements were made at baseline and every 6 months over a 5-year period.

To limit reproducibility bias with imaging, a single experienced operator with over ten years of experience performed all measurements in the same order and at the same time of the day for each patient.

Functional disease progression was monitored by visual field testing and defined as two consecutive visits with an Advanced Glaucoma Intervention Study (AGIS) score increase ≥2 from baseline, and/ or MD decrease ≥2 from baseline. Structural disease progression was monitored with optical coherence tomography and Heidelberg retinal tomography and defined as two consecutive visits with RNFL thickness decrease ≥8% and/or horizontal or vertical cup/disk ratio increase ≥0.2 compared to baseline.

The statistical analysis involved mixed-model analysis of covariance (ANCOVA) to test for significance of changes from baseline to 5-year follow-up separately by gender (female or male). Two-sample t tests and $\chi 2$ tests were used to analyze differences in baseline data between patients who progressed and those who did not progress. The models were then extended to test for whether the changes were different by gender (female or male). Time to functional progression and time to structural progression were analyzed using Cox proportional hazards survival analysis. Factors were analyzed as baseline measurements, as time-varying measurements, and as time-varying changes from baseline. Interactions were tested to determine if the effects of the factors on progression time differed by gender (female or male). Pearson correlation coefficients were calculated to evaluate linear associations. Correlations were adjusted for years of glaucoma, use of glaucoma or hypertension medications, age 65 or older, body mass index category, race, and diabetes status. Correlations were compared between groups using Fisher z tests. P values <0.05 were considered statistically significant.

3. Results – Aim 4:

A cohort of 112 OAG patients (68 female, 44 male) were prospectively examined at baseline and every 6 months over a period of five years. After 5 years, 37 subjects (24 female; 13 male) progressed functionally, and 76 (46 female, 30 male) structurally. Table 1 and 2 show the change in the study measurements (mean and 95% confidence interval, CI) from baseline to five years in female and male OAG patients, respectively. Table 3 summarizes all the significant results related to the changes between parameters from baseline to 5 years and to the associations between measurements and shorter time to functional and structural progression based on gender.

Table 1. Change from baseline to five years in the study parameters in female open-angle glaucoma patients. * p-value statistically significant < 0.05.

	Female							Female vs Male	
	Baseline		5 year		Change			Change	
	N	Mean (95% CI)	N	Mean (95% CI)	Mean (95% CI)	p-value		p-value	
IOP	68	16.67 (15.32, 18.03)	45	14.92 (13.44, 16.39)	-1.76 (-2.98, -0.53)	0.0051	*	0.4152	
SBP	68	135.13 (129.39, 140.86)	46	128.58 (122.42, 134.74)	-6.55 (-12.13, -0.98)	0.0213	*	0.9382	
DBP	68	83.75 (80.45, 87.05)	46	77.32 (73.94, 80.70)	-6.43 (-9.89, -2.98)	0.0003	*	0.2920	
MAP	68	100.89 (97.10, 104.68)	46	94.42 (90.43, 98.41)	-6.47 (-10.34, -2.61)	0.0010	*	0.5091	
HR	68	74.11 (70.59, 77.63)	46	73.93 (69.93, 77.92)	-0.18 (-3.30, 2.94)	0.9097		0.6089	
Visual Acuity	68	0.12 (0.08, 0.16)	44	0.23 (0.17, 0.29)	0.11 (0.05, 0.16)	0.0001	*	0.1230	
OA PSV	68	23.38 (20.97, 26.08)	45	20.99 (18.41, 23.95)	-2.66 (-5.67, 0.03)	0.0530		0.1671	
OA EDV	68	5.49 (4.94, 6.10)	45	3.49 (3.06, 3.99)	-3.15 (-4.27, -2.15)	0.0000	*	0.0241	*
OA RI	68	0.763 (0.781, 0.743)	45	0.829 (0.847, 0.809)	0.092 (0.130, 0.058)	0.0000	*	0.2381	
CRA PSV	68	8.44 (7.87, 9.01)	45	7.48 (6.86, 8.10)	-0.96 (-1.51, -0.40)	0.0008	*	0.0784	
CRA EDV	68	2.24 (2.06, 2.43)	45	1.73 (1.57, 1.90)	-0.66 (-1.00, -0.36)	0.0000	*	0.2914	
CRA RI	68	0.715 (0.696, 0.733)	45	0.763 (0.741, 0.785)	0.048 (0.025, 0.071)	0.0000	*	0.0496	*
NPCA PSV	68	8.01 (7.44, 8.58)	45	7.77 (7.02, 8.53)	-0.24 (-0.90, 0.43)	0.4856		0.6219	
NPCA EDV	68	2.44 (2.26, 2.64)	45	1.94 (1.76, 2.13)	-0.64 (-0.96, -0.35)	0.0000	*	0.5321	
NPCA RI	68	0.678 (0.661, 0.696)	45	0.742 (0.724, 0.761)	0.064 (0.043, 0.085)	0.0000	*	0.2475	
TPCA PSV	68	7.90 (7.41, 8.38)	45	7.89 (7.33, 8.45)	-0.01 (-0.52, 0.51)	0.9790		0.1555	
TPCA EDV	68	2.36 (2.19, 2.55)	45	1.89 (1.74, 2.06)	-0.58 (-0.87, -0.32)	0.0000	*	0.0970	
TPCA RI	68	0.694 (0.712, 0.675)	45	0.759 (0.775, 0.741)	0.082 (0.114, 0.052)	0.0000	*	0.4113	
Superior Zero Pixels	68	0.202 (0.188, 0.217)	14	0.221 (0.190, 0.257)	0.018 (-0.013, 0.044)	0.2446		0.6673	
Inferior Zero Pixels	68	0.180 (0.167, 0.194)	14	0.213 (0.186, 0.245)	0.028 (0.004, 0.048)	0.0217	*	0.1691	

Inferior Mean Flow	68	405.44 (369.89, 444.41)	14	355.13 (293.52, 429.68)	-57.43 (-152.46, 21.40)	0.1640		0.2734	
Superior Mean Flow	68	392.52 (363.79, 423.51)	14	361.61 (297.54, 439.48)	-33.54 (-125.29, 41.95)	0.4093		0.7933	
MD	68	-3.72 (-4.90, -2.53)	45	-5.38 (-7.10, -3.66)	-1.66 (-3.00, -0.32)	0.0151	*	0.7924	
PSD	68	4.38 (3.25, 5.51)	45	5.12 (3.91, 6.33)	0.74 (0.22, 1.26)	0.0051	*	0.7068	
AGIS score	68	1.51 (0.87, 2.38)	44	2.14 (1.27, 3.36)	0.50 (0.09, 0.85)	0.0192	*	0.5390	
Disk area	68	2.247 (2.113, 2.381)	42	2.608 (2.445, 2.771)	0.361 (0.230, 0.492)	0.0000	*	0.8004	
Cup area	68	1.159 (0.982, 1.335)	42	1.490 (1.278, 1.701)	0.331 (0.200, 0.462)	0.0000	*	0.9447	
Rim area	68	1.073 (0.919, 1.228)	42	1.122 (0.954, 1.290)	0.048 (-0.072, 0.169)	0.4294		0.6012	
cup/disk area ratio	68	0.521 (0.455, 0.588)	42	0.561 (0.492, 0.630)	0.039 (0.000, 0.079)	0.0525		0.3125	
cup/disk horizontal ratio	68	0.70 (0.65, 0.75)	42	0.74 (0.68, 0.79)	0.04 (0.01, 0.07)	0.0111	*	0.1507	
cup/disk vert ratio	68	0.692 (0.641, 0.743)	42	0.710 (0.655, 0.766)	0.019 (-0.014, 0.051)	0.2578		0.3844	
RNFL thickness superior	68	92.57 (84.55, 100.60)	41	86.77 (78.27, 95.27)	-5.81 (-11.59, -0.03)	0.0490	*	0.8421	
RNFL thickness inferior	68	92.33 (82.90, 101.75)	41	88.72 (77.32, 100.11)	-3.61 (-11.20, 3.98)	0.3507		0.8390	
RNFL thickness nasal	68	63.87 (58.36, 69.39)	41	67.90 (60.48, 75.32)	4.03 (-2.19, 10.25)	0.2041		0.4921	
RNFL thickness temporal	68	56.59 (51.06, 62.12)	41	57.94 (51.89, 64.00)	1.35 (-2.93, 5.64)	0.5356		0.2581	
RNFL average	68	76.74 (71.21, 82.28)	41	75.42 (69.18, 81.66)	-1.32 (-5.38, 2.74)	0.5227		0.5743	
macular thickness outer superior	68	223.01 (216.78, 229.24)	44	217.59 (211.21, 223.97)	-5.42 (-8.77, -2.07)	0.0016	*	0.2354	
macular thickness inner superior	68	261.84 (254.94, 268.75)	44	253.24 (245.52, 260.97)	-8.60 (-13.08, -4.12)	0.0002	*	0.1297	
macular thickness outer inferior	68	210.23 (204.27, 216.18)	44	203.60 (196.96, 210.24)	-6.63 (-10.49, -2.77)	0.0008	*	0.5779	
macular thickness inner inferior	68	255.69 (249.04, 262.34)	44	248.23 (240.21, 256.25)	-7.46 (-12.55, -2.38)	0.0041	*	0.3771	
macular thickness outer nasal	68	238.05 (231.86, 244.24)	44	232.64 (225.96, 239.32)	-5.41 (-8.80, -2.02)	0.0018	*	0.5346	
macular thickness inner nasal	68	260.10 (253.36, 266.85)	44	251.39 (243.70, 259.07)	-8.72 (-13.81, -3.63)	0.0008	*	0.3242	
macular thickness outer temporal	68	201.78 (196.35, 207.21)	44	197.35 (191.50, 203.20)	-4.43 (-8.30, -0.56)	0.0247	*	0.0034	*
macular thickness inner temporal	68	243.86 (236.72, 251.00)	44	239.33 (230.66, 247.99)	-4.53 (-11.27, 2.20)	0.1866		0.0568	
Macula center	68	197.58 (188.62, 206.54)	44	203.96 (190.96, 216.96)	6.38 (-4.45, 17.21)	0.2478		0.0432	*
macular volume	68	6.39 (6.24, 6.54)	44	6.23 (6.07, 6.38)	-0.17 (-0.24, -0.09)	0.0000	*	0.1379	
HRT3 Cup Area	68	0.880 (0.743, 1.029)	44	0.917 (0.774, 1.071)	0.036 (-0.014, 0.084)	0.1613		0.8726	
HRT3 Rim Area	68	1.316 (1.190, 1.443)	44	1.264 (1.134, 1.395)	-0.052 (-0.106, 0.002)	0.0598		0.5987	
HRT3 Cup Volume	68	0.268 (0.195, 0.340)	44	0.298 (0.224, 0.372)	0.030 (0.004, 0.056)	0.0233	*	0.4098	
HRT3 Rim Volume	68	0.310 (0.254, 0.367)	44	0.301 (0.245, 0.358)	-0.009 (-0.033, 0.015)	0.4549		0.5072	
HRT3 Cup/Disk Area Ratio	68	0.408 (0.353, 0.463)	44	0.429 (0.372, 0.486)	0.021 (-0.003, 0.045)	0.0822		0.8173	

HRT3 Linear Cup/Disk Ratio	68	0.619 (0.570, 0.669)	44	0.632 (0.581, 0.683)	0.013 (-0.007, 0.033)	0.2154		0.9318	
HRT3 Mean Cup Depth	68	0.281 (0.246, 0.316)	44	0.291 (0.257, 0.326)	0.010 (0.000, 0.021)	0.0572		0.7943	
HRT3 Max Cup Depth	68	0.701 (0.633, 0.769)	44	0.699 (0.632, 0.767)	-0.002 (-0.029, 0.026)	0.8946		0.3875	
HRT3 Cup Shape	68	-0.135 (-0.158, -0.112)	44	-0.120 (-0.145, -0.095)	0.015 (0.001, 0.029)	0.0376	*	0.8748	
HRT3 Height Variation Contour	68	0.337 (0.298, 0.381)	44	0.359 (0.314, 0.411)	0.021 (-0.005, 0.045)	0.1078		0.7619	
HRT3 Mean RNFL Thickness	68	0.195 (0.169, 0.222)	44	0.174 (0.144, 0.204)	-0.022 (-0.040, -0.003)	0.0247	*	0.0942	
HRT3 RNFL Cross-Sectional Area	68	1.036 (0.894, 1.178)	44	0.935 (0.776, 1.093)	-0.102 (-0.201, -0.003)	0.0440	*	0.1240	

Table 2. Change from baseline to five years in the study parameters in male open-angle glaucoma patients. * p-value statistically significant < 0.05.

	Male							**Female vs Male**	
	Baseline		**5 year**		**Change**			**Change**	
	N	Mean (95% CI)	N	Mean (95% CI)	Mean (95% CI)	p-value		p-value	
IOP	43	16.69 (15.12, 18.26)	30	15.74 (13.94, 17.54)	-0.94 (-2.48, 0.59)	0.2270		0.4152	
SBP	43	135.87 (129.53, 142.20)	31	129.66 (122.55, 136.77)	-6.21 (-12.92, 0.50)	0.0697		0.9382	
DBP	43	82.09 (78.02, 86.16)	31	78.55 (74.23, 82.87)	-3.54 (-7.70, 0.62)	0.0951		0.2920	
MAP	43	99.98 (95.52, 104.44)	31	95.52 (90.71, 100.32)	-4.46 (-9.05, 0.12)	0.0566		0.5091	
HR	43	68.54 (64.92, 72.16)	32	69.67 (65.09, 74.24)	1.13 (-2.83, 5.09)	0.5763		0.6089	
Visual Acuity	43	0.06 (0.01, 0.10)	32	0.24 (0.15, 0.32)	0.18 (0.11, 0.25)	0.0000	*	0.1230	
OA PSV	44	22.68 (19.85, 25.91)	31	22.99 (19.46, 27.15)	0.30 (-2.91, 3.11)	0.8439		0.1671	
OA EDV	44	5.70 (4.97, 6.55)	31	4.56 (3.79, 5.49)	-1.43 (-2.65, -0.38)	0.0059	*	0.0241	*
OA RI	44	0.747 (0.769, 0.722)	31	0.799 (0.822, 0.773)	0.066 (0.106, 0.030)	0.0002	*	0.2381	
CRA PSV	44	7.86 (7.17, 8.55)	31	7.72 (6.89, 8.56)	-0.13 (-0.87, 0.60)	0.7233		0.0784	
CRA EDV	44	2.34 (2.12, 2.59)	31	1.65 (1.47, 1.86)	-0.98 (-1.45, -0.57)	0.0000	*	0.2914	
CRA RI	44	0.689 (0.667, 0.711)	31	0.773 (0.746, 0.800)	0.084 (0.057, 0.111)	0.0000	*	0.0496	*
NPCA PSV	43	6.85 (6.21, 7.50)	31	6.85 (6.08, 7.62)	0.00 (-0.66, 0.66)	0.9966		0.6219	
NPCA EDV	43	2.30 (2.10, 2.53)	31	1.74 (1.55, 1.95)	-0.75 (-1.13, -0.41)	0.0000	*	0.5321	
NPCA RI	43	0.653 (0.633, 0.674)	31	0.739 (0.713, 0.765)	0.085 (0.056, 0.114)	0.0000	*	0.2475	
TPCA PSV	44	7.84 (7.21, 8.47)	31	7.21 (6.40, 8.01)	-0.63 (-1.32, 0.06)	0.0749		0.1555	
TPCA EDV	44	2.48 (2.26, 2.72)	31	1.75 (1.56, 1.96)	-1.04 (-1.49, -0.64)	0.0000	*	0.0970	
TPCA RI	44	0.678 (0.699, 0.656)	31	0.759 (0.779, 0.737)	0.108 (0.152, 0.068)	0.0000	*	0.4113	
Superior Zero Pixels	44	0.198 (0.182, 0.215)	16	0.228 (0.197, 0.263)	0.026 (-0.002, 0.050)	0.0677		0.6673	
Inferior Zero Pixels	43	0.192 (0.175, 0.209)	16	0.198 (0.175, 0.224)	0.006 (-0.021, 0.029)	0.6514		0.1691	
Inferior Mean Flow	43	431.11 (386.68, 480.63)	16	433.44 (364.90, 514.85)	2.32 (-72.97, 66.36)	0.9478		0.2734	
Superior Mean Flow	44	439.58 (402.16, 480.48)	16	419.30 (351.39, 500.33)	-21.26 (-108.25, 51.92)	0.5919		0.7933	
MD	44	-2.99 (-4.33, -1.65)	33	-4.43 (-6.04, -2.81)	-1.43 (-2.46, -0.41)	0.0063	*	0.7924	
PSD	44	3.56 (2.40, 4.72)	33	4.47 (3.12, 5.82)	0.91 (0.17, 1.65)	0.0159	*	0.7068	
AGIS score	44	1.29 (0.63, 2.22)	33	2.14 (1.15, 3.58)	0.62 (0.22, 0.94)	0.0042	*	0.5390	

Disk area	44	2.327 (2.133, 2.520)	31	2.663 (2.444, 2.882)	0.336 (0.195, 0.477)	0.0000	*	0.8004	
Cup area	44	1.204 (0.965, 1.443)	31	1.542 (1.269, 1.814)	0.338 (0.199, 0.476)	0.0000	*	0.9447	
Rim area	44	1.103 (0.945, 1.260)	31	1.099 (0.908, 1.289)	-0.004 (-0.159, 0.152)	0.9632		0.6012	
cup/disk area ratio	44	0.502 (0.421, 0.584)	31	0.577 (0.486, 0.668)	0.075 (0.019, 0.131)	0.0090	*	0.3125	
cup/disk horizontal ratio	44	0.69 (0.63, 0.76)	31	0.77 (0.70, 0.85)	0.08 (0.03, 0.13)	0.0008	*	0.1507	
cup/disk vert ratio	44	0.676 (0.615, 0.737)	31	0.719 (0.646, 0.792)	0.043 (-0.003, 0.090)	0.0666		0.3844	
RNFL thickness superior	44	86.76 (78.15, 95.38)	30	80.03 (70.40, 89.65)	-6.73 (-13.88, 0.42)	0.0649		0.8421	
RNFL thickness inferior	44	89.47 (78.81, 100.14)	30	84.79 (72.73, 96.86)	-4.68 (-11.77, 2.40)	0.1950		0.8390	
RNFL thickness nasal	44	62.61 (56.58, 68.64)	30	63.66 (56.27, 71.05)	1.05 (-4.78, 6.89)	0.7235		0.4921	
RNFL thickness temporal	44	53.21 (46.44, 59.98)	30	50.55 (42.74, 58.35)	-2.66 (-8.20, 2.87)	0.3452		0.2581	
RNFL average	44	73.20 (67.09, 79.31)	30	70.15 (63.27, 77.03)	-3.05 (-7.56, 1.46)	0.1845		0.5743	
macular thickness outer superior	44	219.94 (212.39, 227.50)	31	211.33 (203.37, 219.30)	-8.61 (-12.74, -4.47)	0.0000	*	0.2354	
macular thickness inner superior	44	262.14 (254.24, 270.03)	31	248.85 (240.31, 257.38)	-13.29 (-17.46, -9.12)	0.0000	*	0.1297	
macular thickness outer inferior	44	206.62 (199.52, 213.72)	31	201.42 (194.03, 208.81)	-5.20 (-8.49, -1.92)	0.0019	*	0.5779	
macular thickness inner inferior	44	257.58 (249.39, 265.77)	31	247.23 (238.36, 256.10)	-10.35 (-14.31, -6.38)	0.0000	*	0.3771	
macular thickness outer nasal	44	231.70 (224.92, 238.48)	31	227.89 (220.39, 235.39)	-3.81 (-7.61, -0.02)	0.0489	*	0.5346	
macular thickness inner nasal	44	263.11 (255.37, 270.85)	31	250.94 (242.56, 259.33)	-12.16 (-16.84, -7.49)	0.0000	*	0.3242	
macular thickness outer temporal	44	207.31 (201.21, 213.41)	31	193.97 (187.10, 200.84)	-13.34 (-17.93, -8.75)	0.0000	*	0.0034	*
macular thickness inner temporal	44	249.91 (242.36, 257.45)	31	236.97 (229.03, 244.91)	-12.94 (-18.45, -7.42)	0.0000	*	0.0568	
Macula center	44	205.36 (194.70, 216.03)	31	197.88 (185.73, 210.02)	-7.49 (-15.56, 0.59)	0.0691		0.0432	*
macular volume	44	6.38 (6.22, 6.55)	31	6.13 (5.96, 6.31)	-0.25 (-0.33, -0.17)	0.0000	*	0.1379	
HRT3 Cup Area	43	0.869 (0.676, 1.084)	33	0.912 (0.710, 1.137)	0.042 (-0.019, 0.100)	0.1743		0.8726	
HRT3 Rim Area	43	1.214 (1.089, 1.338)	33	1.184 (1.052, 1.317)	-0.029 (-0.095, 0.037)	0.3854		0.5987	
HRT3 Cup Volume	43	0.333 (0.227, 0.438)	33	0.347 (0.240, 0.453)	0.014 (-0.014, 0.043)	0.3303		0.4098	
HRT3 Rim Volume	43	0.279 (0.220, 0.337)	33	0.282 (0.222, 0.343)	0.004 (-0.026, 0.034)	0.8048		0.5072	
HRT3 Cup/Disk Area Ratio	43	0.412 (0.342, 0.483)	33	0.429 (0.355, 0.503)	0.017 (-0.013, 0.047)	0.2761		0.8173	
HRT3 Linear Cup/Disk Ratio	43	0.618 (0.554, 0.682)	33	0.632 (0.565, 0.699)	0.014 (-0.011, 0.039)	0.2745		0.9318	
HRT3 Mean Cup Depth	43	0.319 (0.271, 0.368)	33	0.327 (0.278, 0.377)	0.008 (-0.006, 0.022)	0.2586		0.7943	
HRT3 Max Cup Depth	43	0.744 (0.651, 0.837)	33	0.760 (0.667, 0.854)	0.017 (-0.015, 0.048)	0.3103		0.3875	
HRT3 Cup Shape	43	-0.121 (-0.149, -0.093)	33	-0.108 (-0.138, -0.077)	0.013 (-0.002, 0.028)	0.0844		0.8748	
HRT3 Height Variation Contour	43	0.328 (0.289, 0.374)	33	0.356 (0.308, 0.412)	0.026 (-0.002, 0.051)	0.0660		0.7619	

HRT3 Mean RNFL Thickness	43	0.196 (0.165, 0.227)	33	0.198 (0.164, 0.232)	0.002 (-0.018, 0.022)	0.8473		0.0942	
HRT3 RNFL Cross-Sectional Area	43	1.014 (0.856, 1.172)	33	1.025 (0.850, 1.200)	0.011 (-0.094, 0.116)	0.8409		0.1240	

In male and female OAG patients over 5 years, intraocular pressure, blood pressure and perfusion pressure all decreased. In female OAG patients, IOP significantly decreased from 16.67 at baseline to 14.92 at 5 years with a statistically significant mean change of -1.76 (95% CI: -2.98, -0.53; p=0.051), SBP significantly decreased from 135.13 at baseline to 128.58 at 5 years with a statistically significant mean change of -6.55 (95% CI: -12.13; p=0.213), DBP significantly decreased from 83.75 at baseline to 77.32 at 5 years with a statistically significant mean change of -6.43 (95% CI: -9.89, -2.98; p=0.0003), MAP significantly decreased from 100.89 at baseline to 94.42 at 5 years with a statistically significant mean change of -6.47 (95% CI: -10.34, -2.61), Table 1 and Figure 1. In male OAG patients, the parameters decreased from baseline to 5 years, but non significantly (IOP from 16.69 to 15.74, mean change of -0.94, 95% CI: -2.48, 0.59, p=0.2270; SBP from 135.87 to 129.66, mean change of -6.21, 95% CI: -12.92, 0.50, p=0.069; DBP from 82.09 to 78.55, mean change of -3.54, 95% CI: -7.70, 0.62, p=0.0951; MAP from 99.98 to 95.52, mean change of -4.46, 95% CI: -9.05, 0.12, p=0.0566), Table 1 and Figure 1.

Figure 1. Intraocular pressure (IOP), systolic blood pressure (SBP) and ocular perfusion pressure (OPP) (mean with 95% confidence interval) in open-angle glaucoma patients by gender at baseline (BL) and 5 years (5 yr).

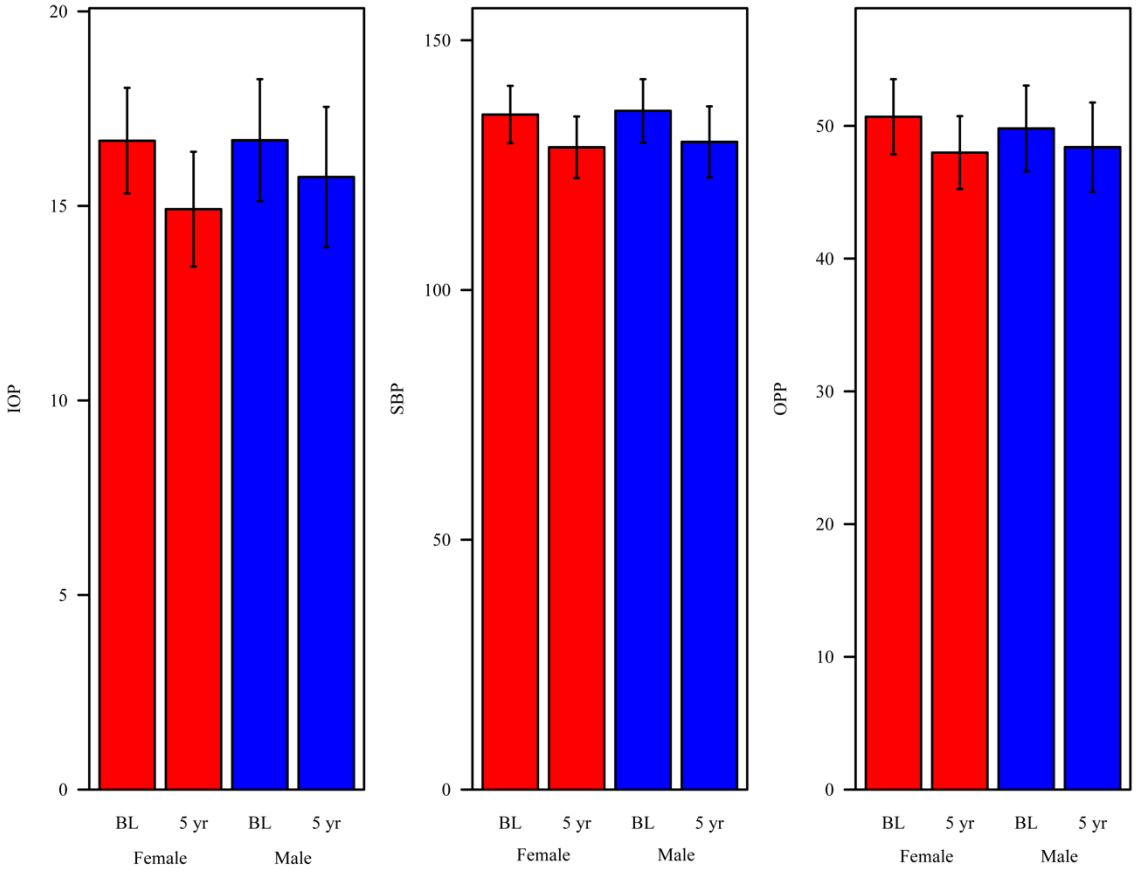

Higher SBP, MAP, SPP, DPP, OPP and MPP were associated with shorter time to functional progression in males (SBP, p=0.0028; MAP, p=0.0111; SPP, p=0.0009; DPP, p=0.0048; OPP= p=0.0048; and MPP, p=0.0009) but not in females (p-value from 0.1460 to 0.9637), leading to a significant gender difference SBP, p=0.0230; MAP, p=0.0156; SPP, p=0.0060; DPP, p=0.0066; OPP= p=0.0061; and MPP, p=0.0035), Figure 2.

Figure 2. Survival function for time to functional progression for open-angle glaucoma patients for intraocular pressure (IOP), systolic blood pressure (SBP) and ocular perfusion pressure (OPP) by gender. Lines represent survival curves for lowest and highest observed IOP, SBP, and OPP. Higher SBP and OPP were associated with shorter time to progression in males.

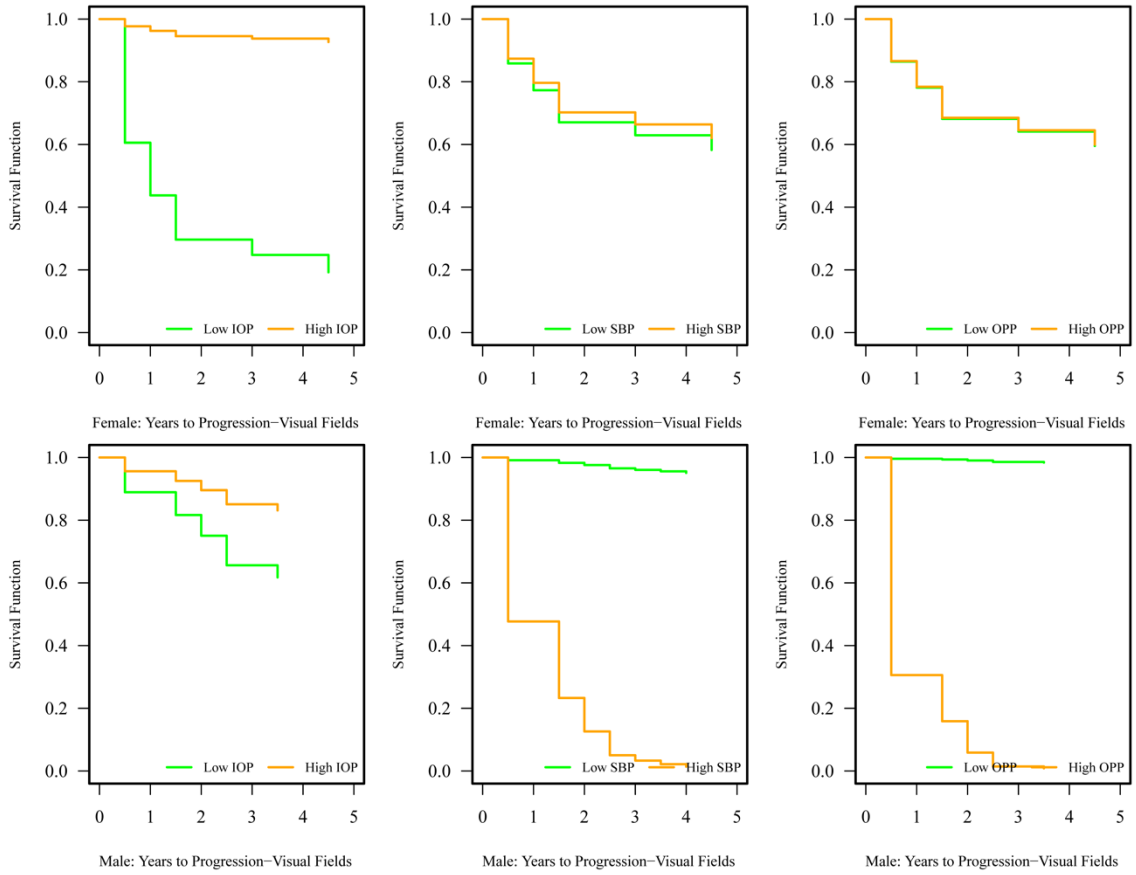

In female and male OAG patients, similar changes from baseline to 5 years were found in the retrobulbar blood flow parameters assessed by color Doppler imaging (except for OA PSV, which decreased in female with a mean change of -2.66, 95% CI: -5.67, 0.03, p=0.0530, while it increased in male with a mean change of 0.30, 95% CI: -2.91, 3.11, p=0.843), as showed in Table 1 and Figure 3: OA EDV decreased significantly (in female with a statistically significant mean change of -3.15, 95% CI: -4.27, -2.15, p<0.0001; in male with a statistically significant mean change of -1.43, 95% CI: -2.65, -0.38, p=0.0059); OA RI increased significantly (in female with a statistically significant mean change of 0.092, 95% CI: 0.130, 0.058, p<0.0001; in male with a statistically significant mean change of 0.066, 95% CI: 0.106, 0.030, p=0.0002), Table 1 and Figure 3.

Figure 3. Retrobulbar blood flow parameters in the ophthalmic artery (OA) assessed by color Doppler imaging (mean with 95% confidence interval) in female and male open-angle glaucoma patients. EDV: end diastolic velocity; PSV: peak systolic velocity; RI: resistivity index.

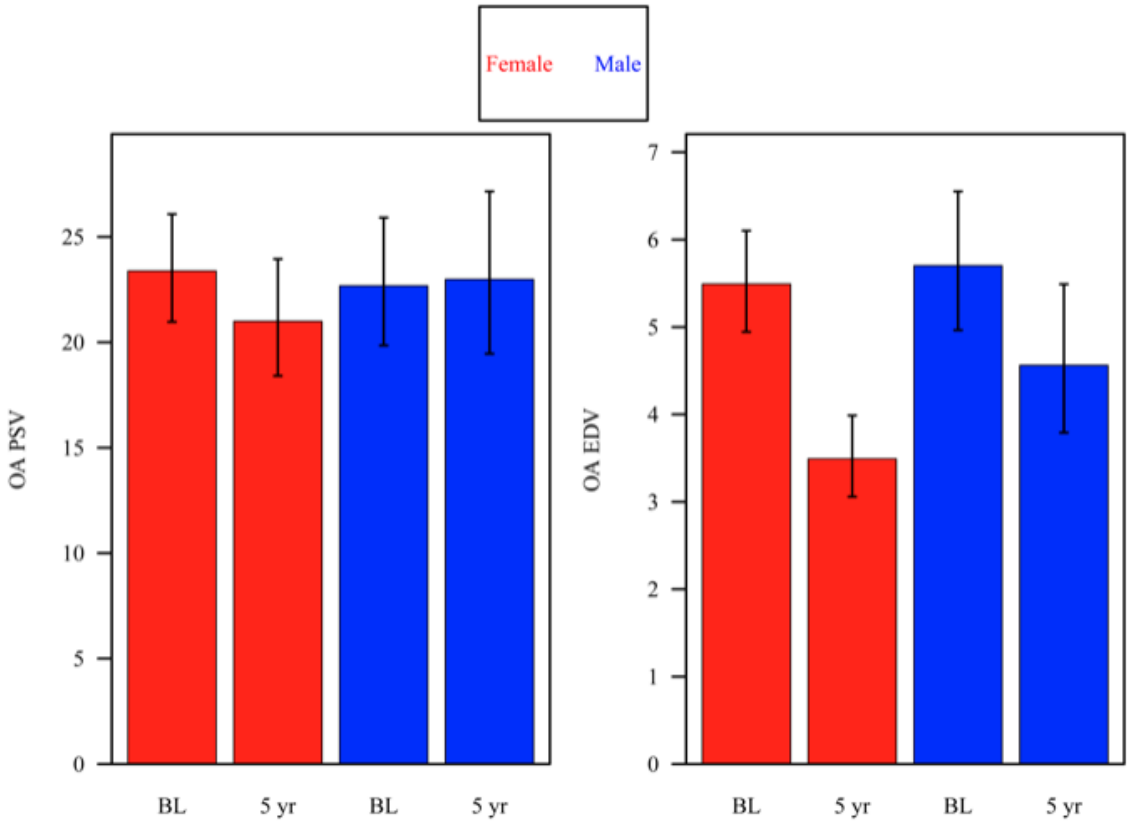

CRA PSV decreased (in female with a statistically significant mean change of -0.96, 95% CI: -1.51, -0.40, p=0.0008; in male, with a mean change of -0.13, -0.87, 0.60, p=0.7233); CRA EDV decreased significantly (in female with a statistically significant mean change of -0.66 (95% CI: -1.00, -0.36, p<0.0001; in male with a statistically significant mean change of -0.98, 95% CI: -1.45, -0.57, p<0.0001); CRA RI increased significantly (in female with a statistically significant mean change of 0.048 (95% CI: 0.025, 0.071, p<0.0001; in male with a statistically significant mean change of 0.084 (95% CI: 0.057, 0.111), p<0.0001), Table 1 and Figure 4.

Figure 4. Retrobulbar blood flow parameters in the central retinal artery (CRA) assessed by color Doppler imaging (mean with 95% confidence interval) in female and male open-angle glaucoma patients. EDV: end diastolic velocity; PSV: peak systolic velocity; RI: resistivity index.

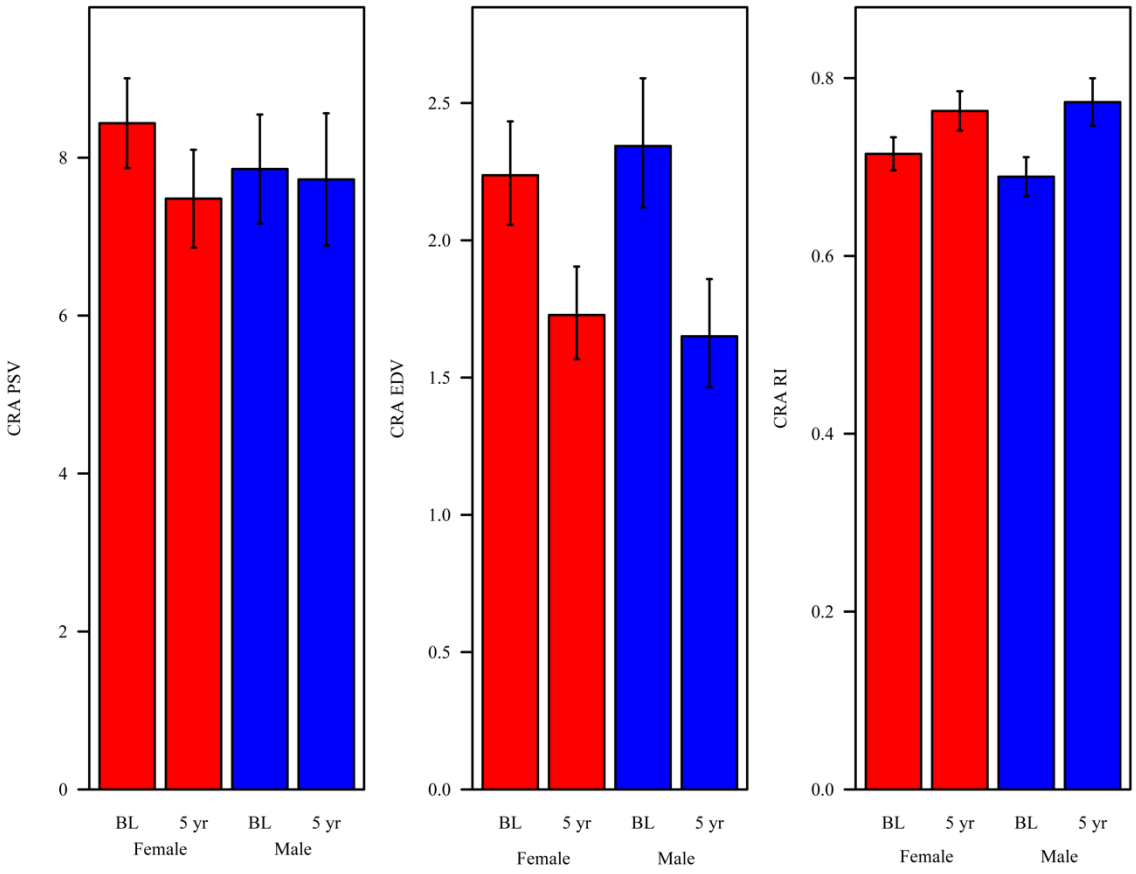

NPCA PSV decreased (in female with a mean change of -0.24, 95% CI: -0.90, 0.43, p=0.4856; in male with a mean change of 0.00, 95% CI: -0.66, 0.66, p=0.9966); NPCA EDV decreased significantly (in female with a statistically significant mean change of -0.64 (95% CI: -0.96, -0.35, p<0.0001; in male with a statistically significant mean change of -0.75 (95% CI: -1.13, -0.4, p<0.0001); NPCA RI increased significantly (in female with a statistically significant mean change of 0.064 (95% CI: 0.043, 0.085; p<0.0001; in male with a statistically significant mean change of 0.085; 95% CI: 0.056, 0.114; p<0.0001); TPCA PSV decreased (in female with a mean change of -0.01, 95% CI: -0.52, 0.51, p=0.9790; in male with a mean change of -

0.63, 95% CI: -1.32, 0.06, p=0.749); TPCA EDV decreased significantly (in female with a statistically significant mean change of -0.58 (95% CI: -0.87, -0.32; p<0.0001; in male with a statistically significant mean change of -1.04 (95% CI: -1.49, -0.64; p<0.0001); TPCA RI increased significantly (in female with a statistically significant mean change of 0.082, 95% CI: 0.114, 0.052; p<0.0001), in male with a statistically significant mean change of 0.108 (95% CI: 0.152, 0.068; p<0.0001).

Lower OA EDV was associated with shorter time to functional progression in OAG male patients (p=0.0027), but not in female patients(p=0.3809), leading to a significant difference between groups (p=0.0399), Figure 5.

Figure 5. Survival function for time to functional progression for male and female open-angle glaucoma patients for retrobulbar blood flow parameters in the ophthalmic artery (OA) assessed by color Doppler imaging. Lines represent survival curves for lowest and highest observed OA peak systolic velocity (PSV) and end diastolic velocity (EDV). Lower baseline OA EDV was associated with shorter time to functional progression in males but not in females.

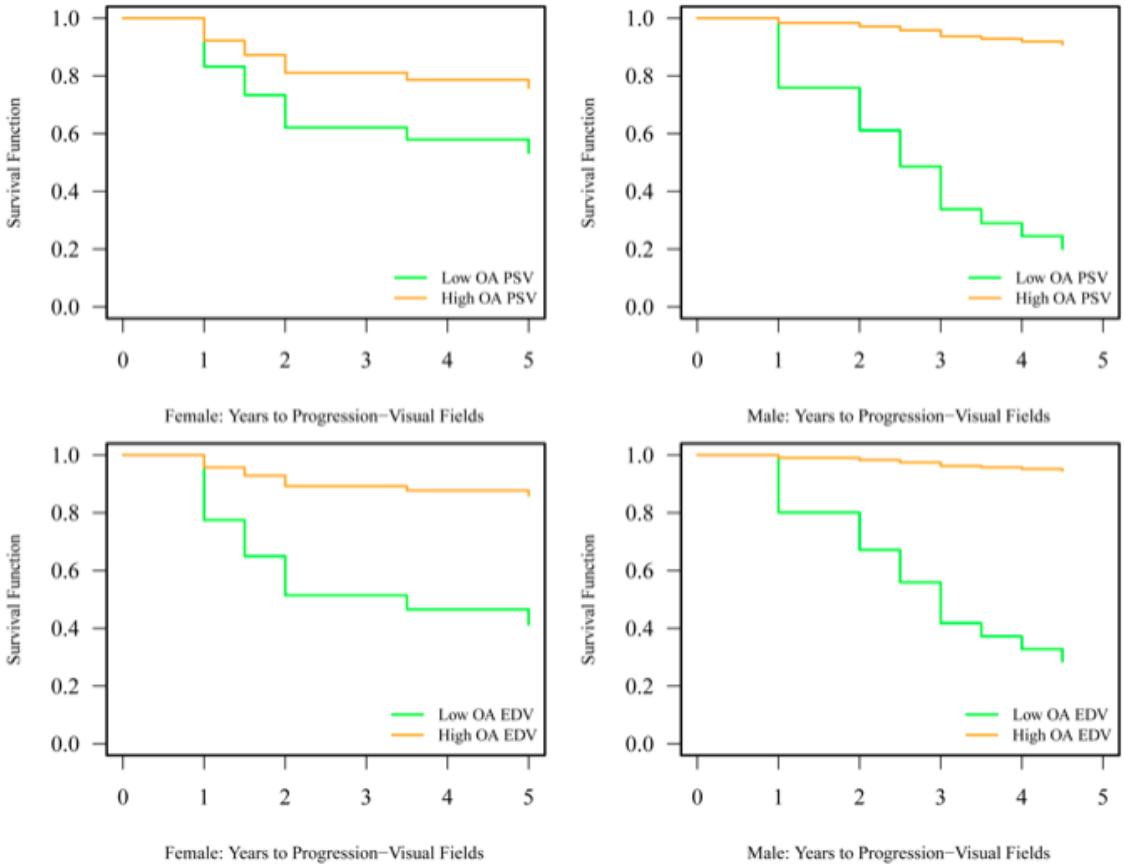

Lower baseline CRA PSV and EDV were associated with shorter time to structural progression in OAG male patients (PSV: p=0.0076; EDV: p=0.00131) but not in female patients (PSV: p=0.5459; EDV: p=0.0604), leading to a significant difference between groups (PSV: p=0.0113; EDV: p=0.0020), Figure 6.

Figure 6. Survival function for time to structural progression for male and female open-angle glaucoma patients for baseline retrobulbar blood flow parameters in the central retinal artery (CRA) assessed by color Doppler imaging. Lines represent survival curves for lowest and highest observed CRA peak systolic velocity (PSV) and end diastolic velocity (EDV). Lower CRA PSV and EDV were associated with shorter time to structural progression in males.

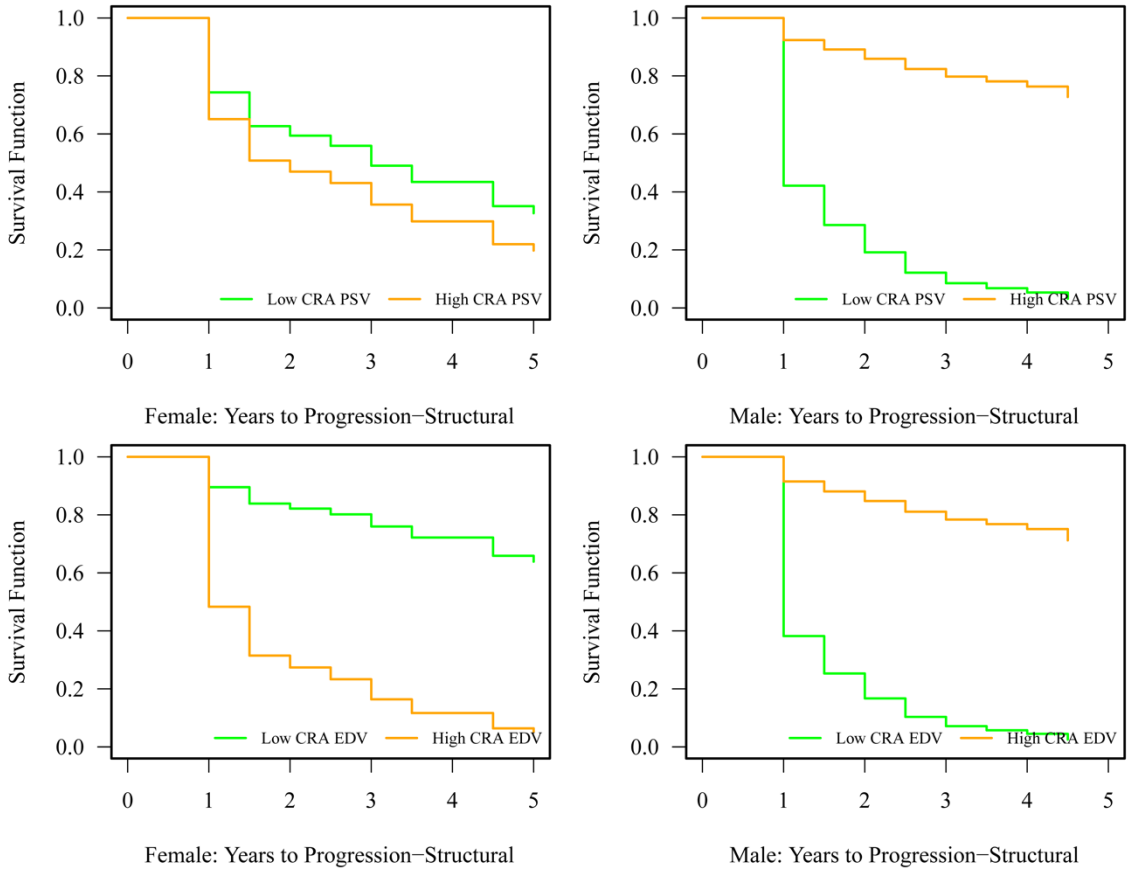

In an additional sub analysis was conducted on 42 patients with OAG (18 males, 24 females) at a single time point during the 5 year follow up to evaluate correlations between measurements. In male OAG patients, the percentage of avascular area in the superior retina assessed by confocal scanning laser Doppler flowmetry was positively and significantly correlated with IOP (r=0.52, p=0.02) and systolic blood pressure (SBP) (r=0.48, p=0.04). The percentage of avascular area in the inferior retina was positively correlated with IOP (r=0.34, p=0.16) and positively and significantly correlated with SBP (r=0.49, p=0.04). In addition, mean arterial pressure (MAP) (r=0.52, p=0.02) and diastolic blood pressure (DBP) (r=0.56, p=0.02) were positively and significantly correlated with IOP in male patients, Figure 7. In female OAG patients, these relationships were weakly and insignificantly correlated (all comparisons p>0.05), Figure 8.

Figure 7. Intraocular pressure (IOP) versus retinal capillary blood flow (superior % of avascular area, top; inferior % of avascular area, bottom) assessed by confocal scanning laser Doppler flowmetry in male with open-angle glaucoma.

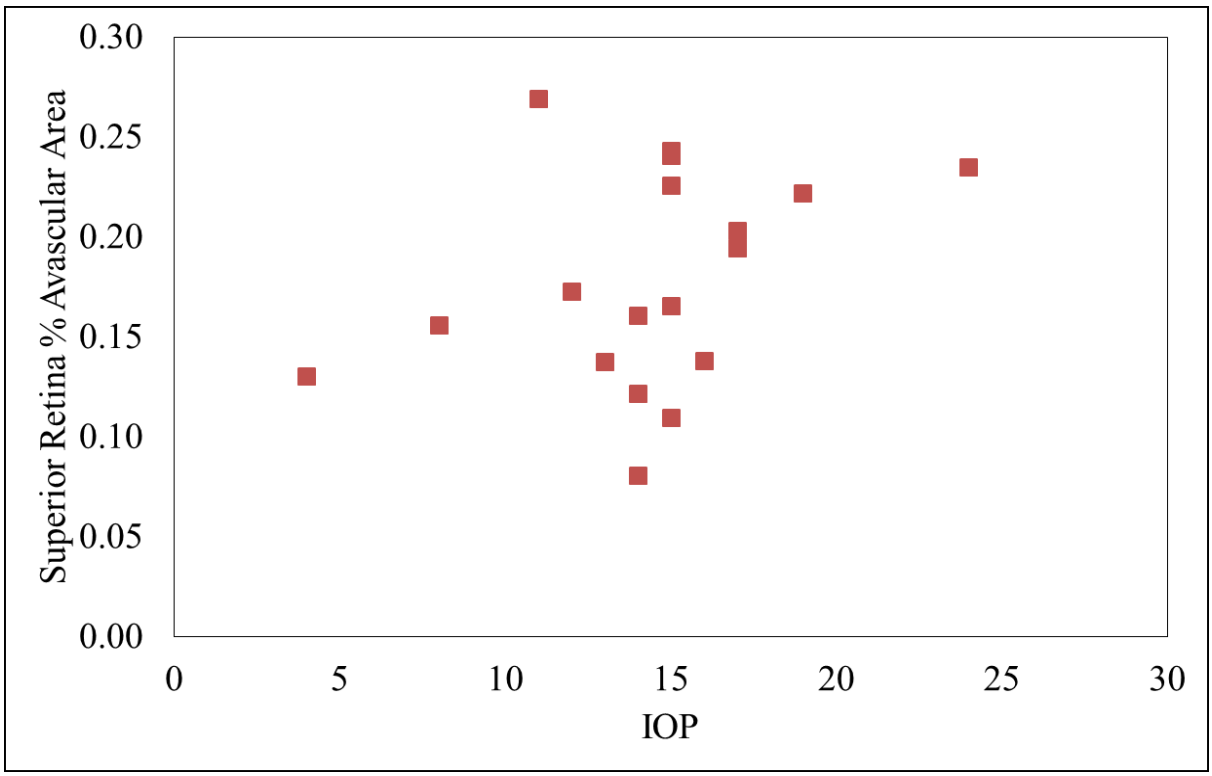

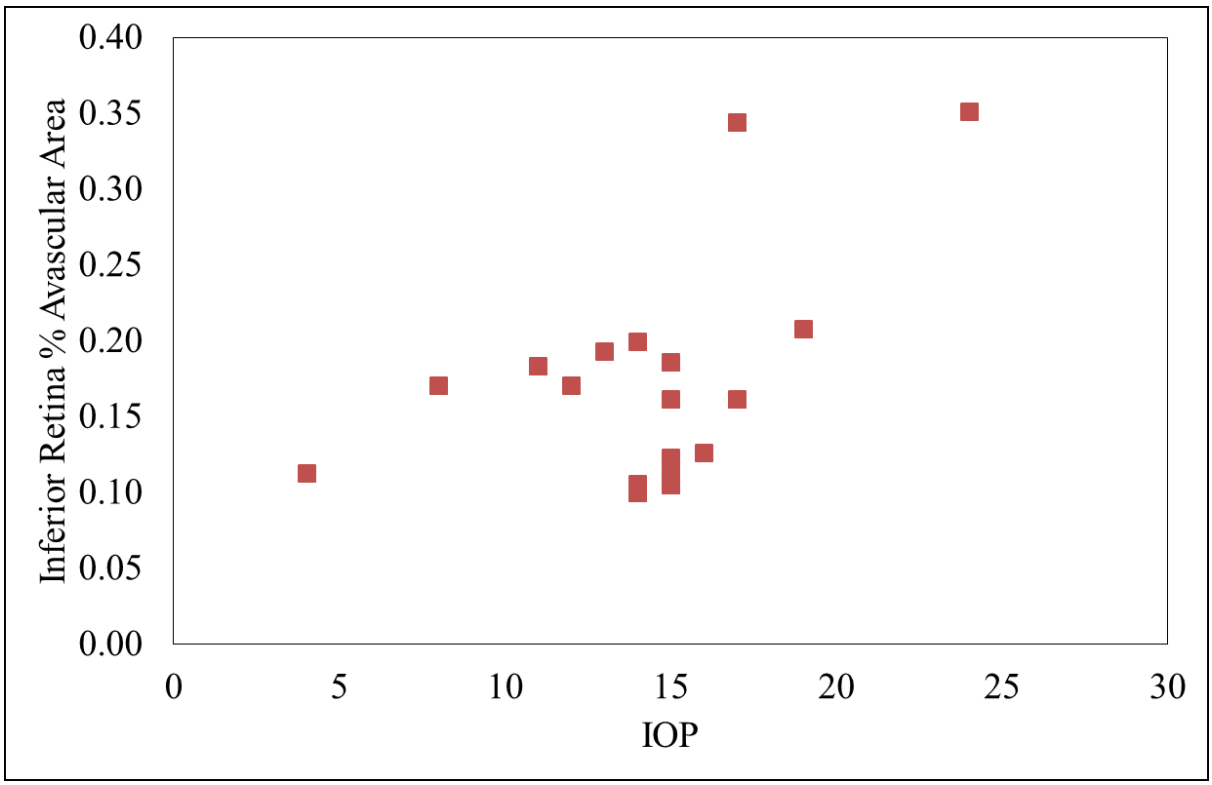

Figure 8. Intraocular pressure (IOP) versus retinal capillary blood flow (superior % of avascular area, top; inferior % of avascular area, bottom) assessed by confocal scanning laser Doppler flowmetry in female with open-angle glaucoma.

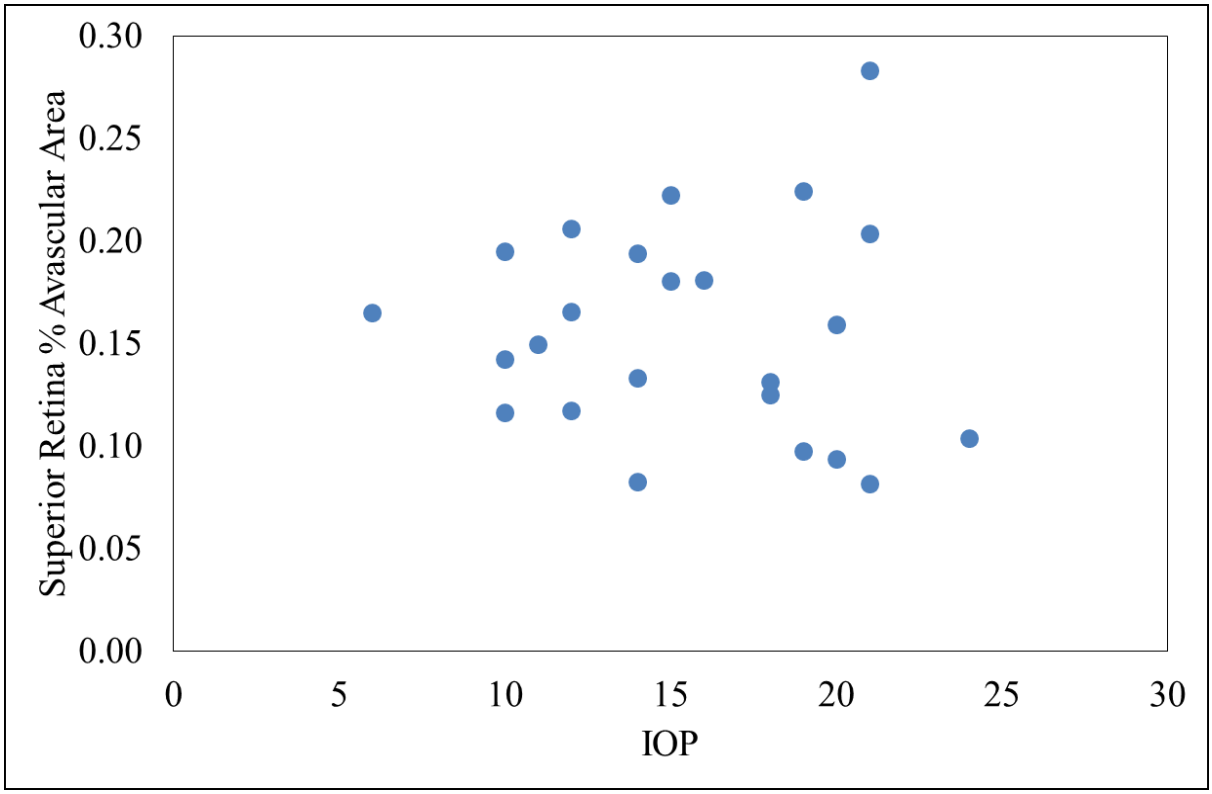

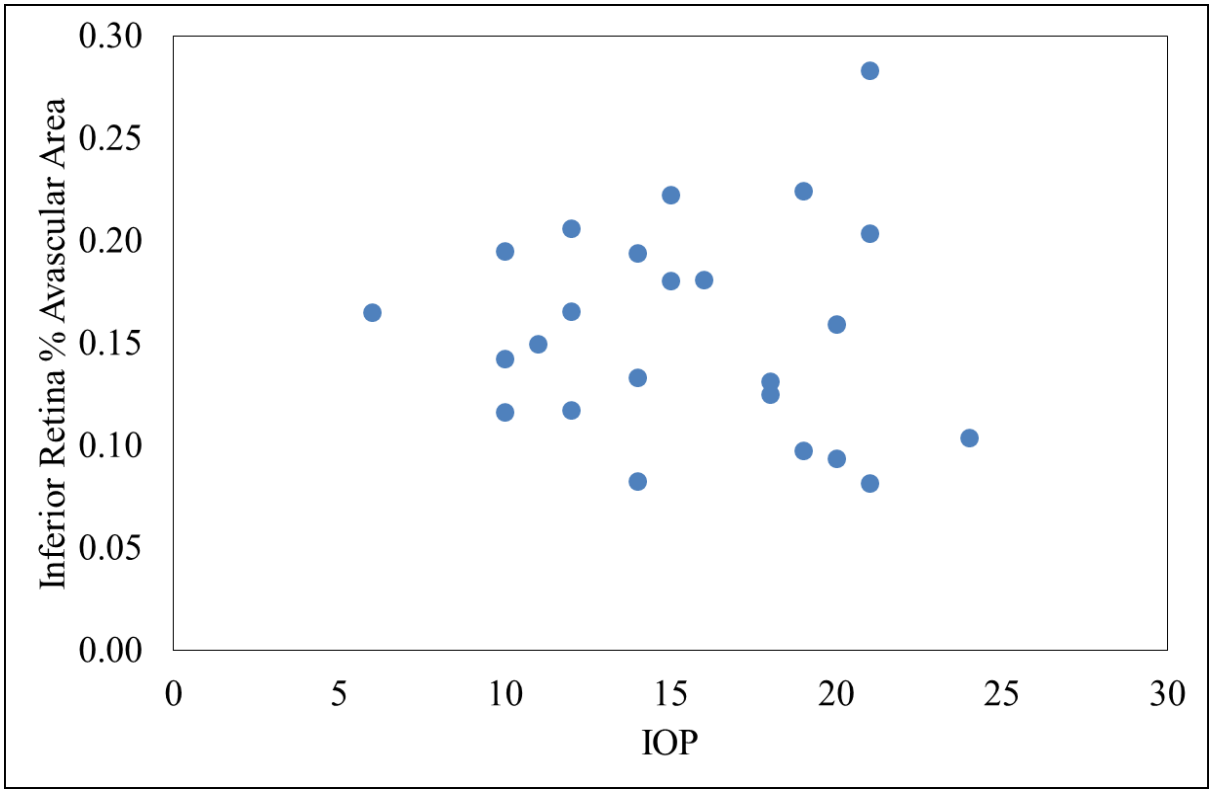

The summary of the other significant results of the Aim 4 of my PhD project are shown in Table 3.

Table 3. Summary of the significant changes over time and predictors of diseases progression from baseline to 5 years in open- angle glaucoma patients based on gender.

Changes from Baseline to 5 years by gender (male versus female)
OA EDV decreased more for females than males
CRA RI increased more for males than females
macular thickness outer temporal decreased, but decreased more in males than females
Baseline predictors of shorter time to progression by gender (male versus female)
FUNCTIONAL PROGRESSION
lower macular thickness outer temporal, for male
lower HRT3 Rim Area, for female
STRUCTURAL PROGRESSION
lower CRA PSV, for male
lower CRA EDV, for male

Predictors (multiple observations over time) of shorter time to progression by gender (male versus female)
FUNCTIONAL PROGRESSION
higher SBP, for male
higher MAP, for male
higher SPP, for male
higher DPP, for male
higher OPP, for male
higher MPP, for male
lower OA EDV, especially, for male
lower macular thickness outer superior, for male
lower macular thickness outer temporal, for male
STRUCTURAL PROGRESSION
N/A
Predictors (change from baseline measurements, multiple observations over time) of shorter time to progression by gender (male versus female)
FUNCTIONAL PROGRESSION
more increase in RNFL thickness nasal, for females
STRUCTURAL PROGRESSION
more decrease in CRA EDV, for females
more increase in NPCA RI, for females

4. Discussion – Aim 4:

The Aim 4 of my PhD project was to investigate the relationship between glaucoma progression, ocular hemodynamics, and *gender*.

In our study population, IOP, the major risk factor for glaucoma onset and progression, decreased over time both in male and female, with no significant different changes based on gender (Table 1 and 2, Figure 1). It is interesting to highlight however that previous studies showed how a possible protective mechanism for glaucoma progression in female, is represented by a decrease in IOP mediated by estrogens. In details, premenopausal women have been shown to present lower level of IOP, compared to postmenopausal women (Siesky et al., 2008). Also, multiple studies reported that in postmenopausal women undergoing postmenopausal hormone replacement therapy (HRT) present significantly lower levels of IOP compared with women who are not (Sator et al., 1997; Affinito et al., 2003; Altintas et al.,

2004; Uncu et al., 2006). Reductions in IOP also have been reported in pregnant women, with greater reductions in IOP in twin pregnancies compared to singleton pregnancies most likely due to their higher hormonal levels (Saylik et al., 2014). The reduction of IOP mediated by estrogens may occur via multiple mechanisms, including reduction of aqueous humor production and episcleral venous pressure or increase of aqueous humor outflow (Vajaranant et al., 2016). In our study however, we did not find significant difference between men and women with regards to IOP at baseline and over 5 years, thus supporting the notion that other factors, such as vascular biomarkers, both ocular and systemic, may represent separate risk factors for OAG differing between the sexes.

In analyzing the effect of gender systemic blood pressure and ocular perfusion pressures and disease progression, our study highlighted interesting results that differ between sexes (Table 1 and 2, Figure 1-2). In details, higher systolic blood pressure and OPP were predictive for glaucomatous functional progression in males but not in females (Figure 2). Also, male OAG patients had stronger positive correlations between superior and inferior retinal avascularity, IOP, and systemic blood pressure compared to female OAG patients (Figure 7 and 8). This data suggest that systemic and ocular vascular factors may play a different role in the disease progression of the disease according to gender, via different pathophysiologic mechanisms between male and female. Importantly, estrogens have been shown to have a protective effect on coronary artery disease, and female menopausal status is known to have systemic vascular effects, with studies showing vascular changes as early as 1-week postsurgical menopause in a group of women (Belchetz, 1994; Siesky et al. 2008). Also, the associations shown in our analises can illustrate differences in autoregulatory mechanisms between male and female OAG patients: gender may affect vascular reactivity in response to changes in BP, leading to long-term discrepancies in disease progression.

In our study, we also found significant differences between male and female in the retrobulbar

circulation assessed by CDI, thus highlighting the importance of the ocular blood flow in explaining the differences in the disease pathogenesis and progression between male and female. In details, we found statistically significant differences between gender in the change from baseline to five-year follow-up in the OA EDV and CRA RI (Table 1 and 2, Figure 3 and 4). In addition, lower baseline blood flow velocities in the OA (Figure 5) and CRA (Figure 6) were found to be predictive factors of glaucoma progression in open-angle glaucoma patients after five years in males, but not females. The effect of gender on blood flow have been previously evaluated in several studies, with contrasting results. Ustymowicz and colleagues showed how male had higher peak systolic velocities (PSV), end diastolic velocities (EDV), resistive index (RI) and pulsatile index (PI) in the ophthalmic artery (OA) compared to women, while higher PSV, EDV, RI and PI were found in the short posterior ciliary arteries (SPCA) compared to men (Ustymowicz et al., 2005). However, other analyses failed to find statistically significant differences in the hemodynamic parameters of retrobulbar vessels between male and female (Marjanovic et al., 2014). Importantly, several studies have shown how vascular differences between male and female, may be explained by the effect of sex hormones, since estrogens specifically affects ocular blood flow. Harris-Yitzhak et al. showed how premenopausal and postmenopausal women receiving estrogen exhibited reduced RI when compared to postmenopausal women not receiving estrogen, with younger women showed greater peak systolic velocity and end diastolic velocity in the SPCA versus both postmenopausal groups (Harris-Yitzhak et al., 2000). Atalay et al. found that pulsatility indices in the CRA declined after treatment with HRT was initiated (Atalay et al., 2005). Similarly, a positive effect of estrogens on ocular blood flow was shown in a study from Altintas and colleagues, in which the RI in the CRA, TPCA, and NPCA were higher in postmenopausal women than premenopausal women, and decreased after 2 months of HRT (Altintas et al. 2004). Taken together, these findings support he importance of sex hormones as viable

candidates to explain retrobulbar blood flow differences among men and women that may lead to the differences in glaucoma predilection and pathogenesis between men and women.

It is important to acknowledge as major limitation of our study that hormonal status of the female patients was unknown, and thus our analysis only provides information on systemic vascular risk factors, ocular biomarkers and glaucoma progression differences between the sexes.

In conclusion, the Aim 4 of my PhD project highlighted how differences in ocular blood flow, and systemic and ocular risk factors may influence the disease progression differently between male and female. The possible pathophysiologic mechanisms underlying differences between gender may be mediated by sex hormones (estrogens in particular) and their effects on the ocular and systemic circulation. It is important that ophthalmologists take into account the gender and the hormonal status (pre-postmenopausal status and hormonal therapy) of their glaucoma patients.

CHAPTER 8

PhD Research Project – Aim 5: To investigate the relationship between glaucoma progression, ocular hemodynamics, and *body mass index (BMI)*

1. Introduction – Aim 5:

The prevalence of obesity has reached epidemic levels all over the word (Finkelstein et al., 2012), raising interest on the relationship between between body mass index (BMI) and open-angle glaucoma, a leading cause of blindness worldwide. OAG is a multifactorial optic neuropathy with characteristic progressive loss of retinal ganglion cells and visual field. Although increased intraocular pressure (IOP) is considered to be a major risk factor in the development and progression of glaucoma, systemic and ocular vascular elements, such as systemic arterial blood pressure (BP) and ocular perfusion pressure (OPP), have also been shown to contribute to the pathogenesis of the disease (Harris et al., 2020).

Importantly, BMI has been shown to influence factors involved in the glaucoma pathogenesis, and multiple studies have evaluated the relationship between OAG and BMI with contrasting results (Kim et al., 2014; Kyari et al., 2016; Lin et al., 2018; Pasquale et al., 2010; Springelkamp et al., 2017). In fact, some studies reported an increased risk for OAG in subjects with lower BMI (Kyari et al., 2016; Lin et al., 2018; Pasquale et al., 2010; Springelkamp et al., 2017), while other showed how a higher BMI represent a risk factor for progression to glaucoma (Kim et al., 2014). Recently, Liu and colleagues in a meta-analysis of 15 studies (2,445,980 subjects) found a positive correlation between abdominal and general adiposity and glaucoma (Liu et al., 2017).

Indeed, the relationship between BMI in patients with OAG is not fully delineated, nor the underlying pathophysiologic mechanisms. Systemic changes associated with metabolic syndrome and obesity, such systemic arterial hypertension and insulin resistance, have been

shown to be positively correlated with IOP elevation, which is the major risk factor for glaucoma development possibly via increased ultrafiltration of the aqueous humor mediated by the high systemic BP (Sw et al., 2009). However, there is a lack of studies evaluating specifically the effect of BMI on ocular vascular biomarkers, including the retrobulbar and retinal circulations, that have been shown to contribute to the disease progression (Harris et al, 2020). In the Indianapolis Glaucoma Progression Study multiple hemodynamic imaging technologies have been used to assess the ocular and systemic hemodynamics in a large sample of OAG patients with different BMI, in which disease progression, both functionally and structurally, has been monitored over a 5 year period. The aim 5 of my PhD project has been to investigate the relationship between glaucoma progression, ocular hemodynamics, and *body mass index (BMI).*

2. Material and Methods - Aim 5:

The comprehensive discussion of the materials and methods is detailed in chapter 3.

In brief, a cohort of 112 OAG (38 normal weight, BMI <25, NW; 40 overweight, BMI 25-30, OW; 34 obese, BMI>30, OB) patients were enrolled at baseline, and prospectively examined at baseline and every 6 months over a period of five years at the Glaucoma and Diagnostic Center at Indiana University School of Medicine, Indianapolis, Indiana. The data were categorized into groups depending on BMI. Based on the measured weight and height of each patient, the following equation was used to calculate the BMI: BMI = weight (kg)/height (m^2). The BMI was categorized as follows: normal weight: BMI <25; overweight: BMI 25-30; obese, BMI>30. One qualified eye was randomly designated as the observational study eye in each subject. Measurements were made at baseline and every 6 months over a 5-year period.

To limit reproducibility bias with imaging, a single experienced operator with over ten years of experience performed all measurements in the same order and at the same time of the day for each patient.

Functional disease progression was monitored by visual field testing and defined as two consecutive visits with an Advanced Glaucoma Intervention Study (AGIS) score increase ≥2 from baseline, and/ or MD decrease ≥2 from baseline. Structural disease progression was monitored with optical coherence tomography and Heidelberg retinal tomography and defined as two consecutive visits with RNFL thickness decrease ≥8% and/or horizontal or vertical cup/disk ratio increase ≥0.2 compared to baseline.

The statistical analysis involved mixed-model analysis of covariance (ANCOVA) to test for significance of changes from baseline to 5-year follow-up separately by BMI category. Two-sample t tests and $\chi 2$ tests were used to analyze differences in baseline data between patients who progressed and those who did not progress. The models were then extended to test for whether the changes were different by BMI category. Time to functional progression and time to structural progression were analyzed using Cox proportional hazards survival analysis. Factors were analyzed as baseline measurements, as time-varying measurements, and as time-varying changes from baseline. Interactions were tested to determine if the effects of the factors on progression time differed by BMI category. Pearson correlation coefficients were calculated to evaluate linear associations. Correlations were adjusted for years of glaucoma, use of glaucoma or hypertension medications, gender, age, race, and diabetes status. Correlations were compared between groups using Fisher z tests. P values <0.05 were considered statistically significant.

3. Results – Aim 5:

A cohort of 112 OAG patients (38 normal weight, BMI <25, NW; 40 overweight, BMI 25-30,

OW; 34 obese, BMI>30, OB) were prospectively examined at baseline and every 6 months over a period of five years. After 5 years, 37 subjects (16 NW, 11 OW, 10 OB) progressed functionally, and 76 (31 NW, 25 OW, 20 OB) structurally. Table 1, 2 and 3 show the change in the study measurements (mean and 95% confidence interval, CI) from baseline to five years in OAG patients with BMI <25 (NW), BMI 25-30, (OW), and BMI>30 (OB), respectively. Table 4 summarizes all the significant results related to the changes between parameters from baseline to 5 years and to the associations between measurements and shorter time to functional and structural progression based on BMI.

Table 1. Change from baseline to five years in the study parameters in normal weight open-angle glaucoma patients (body mass index, BMI <25). * p-value statistically significant < 0.05.

	BMI <25 (Normal Weight, NW)							BMI NW vs OW		BMI NW vs OB	
	Baseline		5 year		Change			Change		Change	
	N	Mean (95% CI)	N	Mean (95% CI)	Mean (95% CI)	p-value		p-value		p-value	
IOP	38	16.53 (14.86, 18.21)	29	15.95 (14.22, 17.68)	-0.59 (-2.12, 0.95)	0.4537		0.1378		0.4569	
SBP	38	134.85 (127.66, 142.05)	29	125.08 (117.43, 132.72)	-9.78 (-16.88, -2.67)	0.0071	*	0.0914		0.8651	
DBP	38	83.17 (78.78, 87.55)	29	75.37 (70.95, 79.79)	-7.80 (-12.22, -3.37)	0.0006	*	0.1473		0.2566	
MAP	38	100.27 (95.33, 105.21)	29	91.87 (86.77, 96.98)	-8.39 (-13.31, -3.48)	0.0008	*	0.0908		0.4854	
HR	38	70.58 (66.32, 74.83)	30	70.88 (66.26, 75.50)	0.30 (-3.58, 4.18)	0.8785		0.7275		0.8523	
Visual Acuity	38	0.12 (0.07, 0.17)	29	0.24 (0.16, 0.31)	0.12 (0.06, 0.19)	0.0003	*	0.2874		0.8896	
OA PSV	38	21.57 (18.87, 24.65)	30	20.42 (17.50, 23.82)	-1.22 (-4.52, 1.67)	0.4260		0.9089		0.9730	
OA EDV	38	5.06 (4.41, 5.81)	30	3.44 (2.91, 4.06)	-2.40 (-3.63, -1.34)	0.0000	*	0.3560		0.7351	
OA RI	38	0.765 (0.786, 0.742)	30	0.827 (0.848, 0.804)	0.085 (0.131, 0.044)	0.0000	*	0.3572		0.6413	
CRA PSV	38	8.25 (7.54, 8.96)	30	7.24 (6.45, 8.03)	-1.01 (-1.74, -0.27)	0.0072	*	0.5720		0.1116	
CRA EDV	38	2.24 (2.01, 2.50)	30	1.68 (1.49, 1.89)	-0.75 (-1.20, -0.36)	0.0001	*	0.8697		0.8148	
CRA RI	38	0.714 (0.690, 0.737)	30	0.757 (0.733, 0.781)	0.043 (0.016, 0.070)	0.0017	*	0.6270		0.0656	
NPCA PSV	38	7.46 (6.79, 8.13)	30	7.20 (6.46, 7.95)	-0.26 (-0.96, 0.44)	0.4713		0.8091		0.2984	
NPCA EDV	38	2.43 (2.20, 2.68)	30	1.80 (1.60, 2.01)	-0.85 (-1.28, -0.47)	0.0000	*	0.2193		0.4790	
NPCA RI	38	0.660 (0.638, 0.683)	30	0.742 (0.720, 0.764)	0.082 (0.055, 0.108)	0.0000	*	0.0830		0.9249	
TPCA PSV	38	8.00 (7.38, 8.62)	30	7.20 (6.59, 7.81)	-0.80 (-1.40, -0.20)	0.0091	*	0.1544		0.0118	*
TPCA EDV	38	2.48 (2.25, 2.74)	30	1.88 (1.69, 2.08)	-0.80 (-1.21, -0.43)	0.0000	*	0.9892		0.5952	
TPCA RI	38	0.690 (0.711, 0.666)	30	0.742 (0.761, 0.720)	0.063 (0.098, 0.030)	0.0001	*	0.1509		0.1254	
Superior Zero Pixels	38	0.196 (0.179, 0.215)	9	0.222 (0.186, 0.264)	0.023 (-0.011, 0.052)	0.1728		0.9729		0.6712	
Inferior Zero Pixels	38	0.183 (0.166, 0.201)	9	0.203 (0.173, 0.238)	0.018 (-0.012, 0.044)	0.2207		0.8174		0.9827	
Inferior Mean Flow	38	412.67 (368.98, 461.55)	9	416.78 (337.17, 515.18)	4.06 (-88.76, 79.70)	0.9244		0.9103		0.1682	

Superior Mean Flow	38	422.47 (382.39, 466.75)	9	408.29 (325.11, 512.76)	-14.67 (-125.26, 73.59)	0.7663		0.6957		0.2646	
MD	38	-3.72 (-5.22, -2.23)	29	-5.76 (-7.73, -3.79)	-2.04 (-3.55, -0.53)	0.0083	*	0.7922		0.1712	
PSD	38	4.44 (3.05, 5.83)	29	5.54 (4.06, 7.02)	1.10 (0.47, 1.74)	0.0007	*	0.5573		0.1532	
AGIS score	38	1.59 (0.78, 2.77)	29	2.50 (1.30, 4.31)	0.67 (0.08, 1.13)	0.0297	*	0.9450		0.7474	
Disk area	38	2.197 (2.011, 2.383)	28	2.492 (2.280, 2.704)	0.295 (0.140, 0.450)	0.0002	*	0.4823		0.5516	
Cup area	38	1.111 (0.870, 1.352)	28	1.310 (1.039, 1.581)	0.199 (0.052, 0.345)	0.0081	*	0.1766		0.0370	*
Rim area	38	1.040 (0.869, 1.211)	28	1.140 (0.948, 1.331)	0.100 (-0.057, 0.257)	0.2130		0.5925		0.1977	
cup/disk area ratio	38	0.492 (0.409, 0.575)	28	0.516 (0.431, 0.601)	0.024 (-0.023, 0.070)	0.3156		0.3498		0.0591	
cup/disk horizontal ratio	38	0.69 (0.62, 0.75)	28	0.71 (0.64, 0.77)	0.02 (-0.02, 0.06)	0.2912		0.0443	*	0.0678	
cup/disk vert ratio	38	0.670 (0.608, 0.731)	28	0.663 (0.597, 0.729)	-0.007 (-0.044, 0.031)	0.7223		0.0922		0.0365	*
RNFL thickness superior	38	89.48 (79.70, 99.26)	27	80.44 (70.11, 90.78)	-9.04 (-16.70, -1.38)	0.0209	*	0.2915		0.3430	
RNFL thickness inferior	38	86.08 (74.69, 97.47)	27	82.69 (70.11, 95.27)	-3.39 (-11.20, 4.42)	0.3943		0.8188		0.6394	
RNFL thickness nasal	38	60.72 (53.99, 67.44)	27	67.01 (58.92, 75.09)	6.29 (-0.47, 13.06)	0.0682		0.5372		0.2562	
RNFL thickness temporal	38	53.36 (46.53, 60.19)	27	52.47 (45.00, 59.93)	-0.90 (-6.54, 4.75)	0.7554		0.7671		0.9075	
RNFL average	38	72.44 (65.71, 79.17)	27	71.10 (63.77, 78.42)	-1.34 (-6.33, 3.65)	0.5971		0.9856		0.6904	
macular thickness outer superior	38	217.13 (209.43, 224.84)	28	212.39 (204.24, 220.53)	-4.75 (-9.43, -0.06)	0.0471	*	0.3718		0.3392	
macular thickness inner superior	38	256.00 (247.50, 264.49)	28	248.44 (239.45, 257.44)	-7.55 (-12.00, -3.10)	0.0009	*	0.7868		0.0802	
macular thickness outer inferior	38	206.49 (198.70, 214.28)	28	200.86 (192.23, 209.49)	-5.63 (-10.92, -0.35)	0.0368	*	0.7779		0.4965	
macular thickness inner inferior	38	255.95 (247.16, 264.75)	28	248.77 (238.76, 258.78)	-7.18 (-13.30, -1.06)	0.0215	*	0.8866		0.2033	
macular thickness outer nasal	38	230.86 (223.18, 238.54)	28	227.65 (219.14, 236.16)	-3.21 (-7.89, 1.46)	0.1775		0.5205		0.1957	
macular thickness inner nasal	38	256.04 (247.64, 264.43)	28	248.28 (238.52, 258.04)	-7.75 (-14.51, -0.99)	0.0247	*	0.8335		0.3581	
macular thickness outer temporal	38	202.18 (195.20, 209.15)	28	193.42 (185.87, 200.98)	-8.75 (-13.58, -3.93)	0.0004	*	0.7735		0.6523	
macular thickness inner temporal	38	240.57 (231.80, 249.35)	28	238.43 (228.70, 248.16)	-2.14 (-9.07, 4.78)	0.5437		0.3810		0.0110	*
Macula center	38	199.79 (189.16, 210.42)	28	200.70 (189.16, 212.24)	0.91 (-7.74, 9.56)	0.8360		0.3390		0.1418	
macular volume	38	6.30 (6.11, 6.48)	28	6.14 (5.94, 6.34)	-0.16 (-0.26, -0.06)	0.0023	*	0.7383		0.1469	
HRT3 Cup Area	38	0.795 (0.615, 0.995)	29	0.881 (0.690, 1.093)	0.082 (0.024, 0.138)	0.0061	*	0.2483		0.0800	
HRT3 Rim Area	38	1.275 (1.122, 1.428)	29	1.181 (1.024, 1.338)	-0.094 (-0.163, -0.024)	0.0082	*	0.3325		0.0719	
HRT3 Cup Volume	38	0.287 (0.184, 0.389)	29	0.340 (0.237, 0.444)	0.054 (0.020, 0.088)	0.0021	*	0.1284		0.0083	*
HRT3 Rim Volume	38	0.308 (0.241, 0.375)	29	0.283 (0.214, 0.351)	-0.025 (-0.058, 0.008)	0.1334		0.2359		0.1328	
HRT3 Cup/Disk Area Ratio	38	0.388 (0.315, 0.460)	29	0.426 (0.352, 0.500)	0.038 (0.008, 0.069)	0.0129	*	0.4999		0.1154	
HRT3 Linear Cup/Disk Ratio	38	0.593 (0.529, 0.657)	29	0.624 (0.559, 0.690)	0.031 (0.007, 0.055)	0.0104	*	0.4315		0.1234	

HRT3 Mean Cup Depth	38	0.287 (0.243, 0.331)	29	0.301 (0.257, 0.346)	0.014 (0.000, 0.029)	0.0452	*	0.9028		0.1591	
HRT3 Max Cup Depth	38	0.724 (0.642, 0.806)	29	0.732 (0.650, 0.815)	0.009 (-0.027, 0.044)	0.6315		0.5453		0.4751	
HRT3 Cup Shape	38	-0.131 (-0.161, -0.102)	29	-0.122 (-0.154, -0.090)	0.009 (-0.010, 0.028)	0.3565		0.3972		0.9419	
HRT3 Height Variation Contour	38	0.335 (0.289, 0.389)	29	0.340 (0.288, 0.403)	0.005 (-0.036, 0.041)	0.7990		0.0709		0.7458	
HRT3 Mean RNFL Thickness	38	0.188 (0.158, 0.219)	29	0.161 (0.124, 0.197)	-0.028 (-0.055, -0.001)	0.0434	*	0.0798		0.0881	
HRT3 RNFL Cross-Sectional Area	38	0.993 (0.831, 1.156)	29	0.846 (0.651, 1.041)	-0.147 (-0.292, -0.002)	0.0468	*	0.0788		0.0632	

Table 2. Change from baseline to five years in the study parameters in overweigh open-angle glaucoma patients (body mass index, BMI 25-30). * p-value statistically significant < 0.05.

	BMI 25-30 (Overweight, OW)							**BMI NW v OW**		**BMI OW v OB**	
	Baseline		**5 yr**		**Change**			**Change**		**Change**	
	N	Mean (95% CI)	N	Mean (95% CI)	Mean (95% CI)	p-value		p-value		p-value	
IOP	40	16.93 (15.36, 18.49)	26	14.67 (12.93, 16.42)	-2.25 (-3.86, -0.65)	0.0060	*	0.1378		0.5241	
SBP	40	133.96 (127.99, 139.93)	27	133.37 (125.64, 141.11)	-0.59 (-8.65, 7.48)	0.8867		0.0914		0.1637	
DBP	40	83.56 (79.87, 87.25)	27	80.56 (76.23, 84.88)	-3.00 (-7.80, 1.79)	0.2192		0.1473		0.8013	
MAP	40	100.21 (96.12, 104.31)	27	98.11 (93.05, 103.17)	-2.10 (-7.56, 3.35)	0.4496		0.0908		0.3602	
HR	40	71.34 (67.58, 75.11)	27	72.64 (68.13, 77.15)	1.30 (-2.82, 5.41)	0.5360		0.7275		0.9215	
Visual Acuity	40	0.08 (0.04, 0.12)	26	0.26 (0.18, 0.34)	0.18 (0.10, 0.26)	0.0000	*	0.2874		0.4541	
OA PSV	40	23.59 (20.99, 26.51)	25	22.58 (19.38, 26.31)	-1.05 (-4.86, 2.25)	0.5529		0.9089		0.9486	
OA EDV	40	5.77 (5.10, 6.53)	25	4.36 (3.65, 5.20)	-1.87 (-3.30, -0.67)	0.0013	*	0.3560		0.6130	
OA RI	40	0.758 (0.779, 0.735)	25	0.806 (0.829, 0.779)	0.059 (0.102, 0.022)	0.0011	*	0.3572		0.7014	
CRA PSV	40	8.26 (7.64, 8.88)	25	7.57 (6.76, 8.37)	-0.70 (-1.50, 0.11)	0.0898		0.5720		0.3171	
CRA EDV	40	2.28 (2.06, 2.52)	25	1.74 (1.53, 1.98)	-0.71 (-1.19, -0.30)	0.0004	*	0.8697		0.7033	
CRA RI	40	0.705 (0.683, 0.727)	25	0.758 (0.730, 0.787)	0.053 (0.022, 0.085)	0.0008	*	0.6270		0.1991	
NPCA PSV	39	7.69 (7.04, 8.34)	25	7.30 (6.43, 8.16)	-0.39 (-1.23, 0.45)	0.3598		0.8091		0.2390	
NPCA EDV	39	2.38 (2.17, 2.62)	25	1.98 (1.76, 2.22)	-0.49 (-0.89, -0.14)	0.0047	*	0.2193		0.6033	
NPCA RI	39	0.668 (0.647, 0.689)	25	0.714 (0.689, 0.740)	0.046 (0.016, 0.076)	0.0025	*	0.0830		0.1132	
TPCA PSV	40	7.83 (7.27, 8.40)	25	7.71 (7.01, 8.41)	-0.12 (-0.85, 0.61)	0.7489		0.1544		0.3075	
TPCA EDV	40	2.43 (2.22, 2.67)	25	1.84 (1.64, 2.06)	-0.79 (-1.23, -0.40)	0.0000	*	0.9892		0.6010	
TPCA RI	40	0.681 (0.702, 0.658)	25	0.759 (0.780, 0.737)	0.105 (0.150, 0.064)	0.0000	*	0.1509		0.9115	
Superior Zero Pixels	40	0.212 (0.196, 0.231)	13	0.240 (0.206, 0.279)	0.024 (-0.009, 0.052)	0.1444		0.9729		0.6808	
Inferior Zero Pixels	39	0.186 (0.170, 0.203)	13	0.201 (0.175, 0.232)	0.014 (-0.015, 0.039)	0.3252		0.8174		0.8619	
Inferior Mean Flow	39	415.82 (375.76, 460.15)	13	426.67 (353.71, 514.68)	10.58 (-72.93, 79.82)	0.7872		0.9103		0.1261	
Superior Mean Flow	40	404.31 (371.90, 439.53)	13	414.29 (344.48, 498.25)	9.75 (-72.47, 77.79)	0.8002		0.6957		0.1248	
MD	40	-3.34 (-4.61, -2.06)	28	-5.08 (-7.06, -3.10)	-1.74 (-3.38, -0.10)	0.0376	*	0.7922		0.3343	
PSD	40	4.14 (2.98, 5.30)	28	4.91 (3.47, 6.35)	0.77 (-0.17, 1.70)	0.1075		0.5573		0.6223	
AGIS score	40	1.42 (0.77, 2.29)	27	2.22 (1.27, 3.57)	0.60 (0.12, 0.99)	0.0179	*	0.9450		0.7886	

Disk area	40	2.298 (2.139, 2.457)	25	2.674 (2.472, 2.875)	0.376 (0.211, 0.541)	0.0000	*	0.4823		0.9586	
Cup area	40	1.085 (0.882, 1.287)	25	1.453 (1.179, 1.727)	0.369 (0.168, 0.569)	0.0003	*	0.1766		0.6083	
Rim area	40	1.193 (1.030, 1.356)	25	1.233 (1.044, 1.422)	0.040 (-0.115, 0.195)	0.6131		0.5925		0.4067	
cup/disk area ratio	40	0.477 (0.400, 0.553)	25	0.540 (0.447, 0.632)	0.063 (-0.006, 0.132)	0.0724		0.3498		0.4846	
cup/disk horizontal ratio	40	0.66 (0.60, 0.72)	25	0.75 (0.67, 0.82)	0.09 (0.03, 0.14)	0.0019	*	0.0443	*	0.7518	
cup/disk vert ratio	40	0.647 (0.588, 0.706)	25	0.700 (0.622, 0.777)	0.053 (-0.006, 0.111)	0.0793		0.0922		0.9106	
RNFL thickness superior	40	86.33 (77.95, 94.70)	26	83.04 (73.82, 92.26)	-3.29 (-10.89, 4.31)	0.3959		0.2915		0.9462	
RNFL thickness inferior	40	92.95 (83.18, 102.72)	26	88.07 (75.13, 101.01)	-4.88 (-15.09, 5.32)	0.3477		0.8188		0.8482	
RNFL thickness nasal	40	63.47 (57.51, 69.43)	26	66.53 (57.95, 75.10)	3.06 (-4.79, 10.91)	0.4444		0.5372		0.6016	
RNFL thickness temporal	40	56.22 (50.19, 62.26)	26	56.56 (49.37, 63.75)	0.34 (-5.66, 6.33)	0.9121		0.7671		0.7169	
RNFL average	40	74.87 (69.16, 80.58)	26	73.59 (66.79, 80.40)	-1.28 (-6.59, 4.03)	0.6369		0.9856		0.6869	
macular thickness outer superior	40	220.95 (214.27, 227.63)	27	213.33 (206.29, 220.37)	-7.62 (-11.97, -3.26)	0.0006	*	0.3718		0.8857	
macular thickness inner superior	40	264.81 (257.66, 271.95)	27	256.17 (247.27, 265.08)	-8.64 (-15.23, -2.04)	0.0104	*	0.7868		0.2496	
macular thickness outer inferior	40	210.35 (204.25, 216.45)	27	205.69 (199.02, 212.35)	-4.66 (-8.96, -0.37)	0.0333	*	0.7779		0.2595	
macular thickness inner inferior	40	259.60 (252.61, 266.60)	27	251.81 (243.37, 260.26)	-7.79 (-13.68, -1.91)	0.0095	*	0.8866		0.2535	
macular thickness outer nasal	40	237.74 (231.89, 243.58)	27	236.37 (230.10, 242.63)	-1.37 (-4.69, 1.95)	0.4190		0.5205		0.0338	*
macular thickness inner nasal	40	266.88 (260.11, 273.65)	27	258.18 (250.37, 265.99)	-8.69 (-14.47, -2.91)	0.0033	*	0.8335		0.4403	
macular thickness outer temporal	40	205.41 (200.14, 210.68)	27	195.56 (188.78, 202.33)	-9.86 (-15.72, -3.99)	0.0010	*	0.7735		0.4984	
macular thickness inner temporal	40	251.79 (244.88, 258.70)	27	244.47 (234.26, 254.68)	-7.32 (-16.72, 2.08)	0.1269		0.3810		0.2362	
Macula center	40	206.59 (196.02, 217.16)	27	216.27 (198.85, 233.70)	9.68 (-6.18, 25.54)	0.2311		0.3390		0.0531	
macular volume	40	6.45 (6.30, 6.60)	27	6.27 (6.11, 6.43)	-0.18 (-0.28, -0.08)	0.0004	*	0.7383		0.2712	
HRT3 Cup Area	40	0.857 (0.702, 1.025)	28	0.890 (0.726, 1.068)	0.032 (-0.037, 0.099)	0.3577		0.2483		0.6692	
HRT3 Rim Area	40	1.295 (1.169, 1.420)	28	1.253 (1.117, 1.389)	-0.042 (-0.121, 0.036)	0.2925		0.3325		0.5333	
HRT3 Cup Volume	40	0.286 (0.205, 0.367)	28	0.302 (0.219, 0.385)	0.016 (-0.019, 0.051)	0.3641		0.1284		0.3449	
HRT3 Rim Volume	40	0.293 (0.235, 0.352)	28	0.296 (0.235, 0.357)	0.003 (-0.031, 0.037)	0.8638		0.2359		0.8459	
HRT3 Cup/Disk Area Ratio	40	0.402 (0.344, 0.460)	28	0.425 (0.362, 0.488)	0.023 (-0.012, 0.057)	0.2017		0.4999		0.4654	
HRT3 Linear Cup/Disk Ratio	40	0.606 (0.552, 0.660)	28	0.623 (0.565, 0.680)	0.016 (-0.012, 0.045)	0.2493		0.4315		0.5562	
HRT3 Mean Cup Depth	40	0.280 (0.243, 0.317)	28	0.296 (0.258, 0.333)	0.016 (0.001, 0.031)	0.0390	*	0.9028		0.1382	
HRT3 Max Cup Depth	40	0.680 (0.610, 0.751)	28	0.704 (0.634, 0.774)	0.024 (-0.012, 0.059)	0.1873		0.5453		0.1933	
HRT3 Cup Shape	40	-0.131 (-0.155, -0.107)	28	-0.112 (-0.138, -0.085)	0.020 (0.003, 0.036)	0.0231	*	0.3972		0.4383	
HRT3 Height Variation Contour	40	0.305 (0.268, 0.347)	28	0.356 (0.308, 0.412)	0.044 (0.016, 0.069)	0.0028	*	0.0709		0.0746	

HRT3 Mean RNFL Thickness	40	0.186 (0.159, 0.213)	28	0.187 (0.157, 0.218)	0.001 (-0.018, 0.020)	0.8832		0.0798		0.9343		
HRT3 RNFL Cross-Sectional Area	40	0.979 (0.837, 1.121)	28	0.987 (0.832, 1.143)	0.009 (-0.090, 0.108)	0.8628		0.0788		0.9096		

Table 3. Change from baseline to five years in the study parameters in obese open-angle glaucoma patients (body mass index, BMI >30). * p-value statistically significant < 0.05.

	BMI 30+ (Obese, OB)							**BMI NW v OB**		**BMI OW v OB**	
	Baseline		**5 year**		**Change**			**Change**		**Change**	
	N	Mean (95% CI)	N	Mean (95% CI)	Mean (95% CI)	p-value		p-value		p-value	
IOP	33	16.81 (15.40, 18.23)	20	15.34 (13.65, 17.03)	-1.47 (-3.27, 0.32)	0.1062		0.4569		0.5241	
SBP	33	141.14 (134.26, 148.03)	21	132.31 (123.99, 140.64)	-8.83 (-17.21, -0.45)	0.0389	*	0.8651		0.1637	
DBP	33	83.48 (79.34, 87.63)	21	79.58 (74.94, 84.22)	-3.90 (-9.01, 1.20)	0.1339		0.2566		0.8013	
MAP	33	102.66 (98.07, 107.25)	21	96.91 (91.66, 102.17)	-5.75 (-11.37, -0.13)	0.0450	*	0.4854		0.3602	
HR	33	74.94 (70.49, 79.39)	21	75.89 (69.66, 82.12)	0.95 (-4.69, 6.58)	0.7411		0.8523		0.9215	
Visual Acuity	33	0.09 (0.04, 0.13)	21	0.21 (0.12, 0.31)	0.13 (0.03, 0.22)	0.0081	*	0.8896		0.4541	
OA PSV	34	24.87 (21.60, 28.62)	21	23.63 (19.35, 28.86)	-1.30 (-6.48, 3.02)	0.5788		0.9730		0.9486	
OA EDV	34	6.17 (5.35, 7.10)	21	4.36 (3.56, 5.34)	-2.55 (-4.36, -1.05)	0.0003	*	0.7351		0.6130	
OA RI	34	0.750 (0.773, 0.724)	21	0.807 (0.834, 0.775)	0.074 (0.128, 0.028)	0.0010	*	0.6413		0.7014	
CRA PSV	34	7.99 (7.28, 8.70)	21	7.89 (6.99, 8.79)	-0.10 (-0.95, 0.75)	0.8162		0.1116		0.3171	
CRA EDV	34	2.28 (2.05, 2.55)	21	1.67 (1.46, 1.91)	-0.84 (-1.38, -0.38)	0.0001	*	0.8148		0.7033	
CRA RI	34	0.698 (0.673, 0.723)	21	0.781 (0.750, 0.812)	0.083 (0.050, 0.116)	0.0000	*	0.0656		0.1991	
NPCA PSV	34	7.43 (6.76, 8.10)	21	7.75 (6.87, 8.63)	0.32 (-0.52, 1.16)	0.4546		0.2984		0.2390	
NPCA EDV	34	2.32 (2.11, 2.55)	21	1.83 (1.64, 2.04)	-0.62 (-1.02, -0.27)	0.0003	*	0.4790		0.6033	
NPCA RI	34	0.672 (0.649, 0.695)	21	0.751 (0.728, 0.775)	0.080 (0.051, 0.108)	0.0000	*	0.9249		0.1132	
TPCA PSV	34	7.70 (7.07, 8.33)	21	8.12 (7.38, 8.86)	0.42 (-0.32, 1.16)	0.2653		0.0118	*	0.3075	
TPCA EDV	34	2.37 (2.14, 2.62)	21	1.88 (1.67, 2.11)	-0.62 (-1.04, -0.25)	0.0006	*	0.5952		0.6010	
TPCA RI	34	0.687 (0.710, 0.663)	21	0.766 (0.787, 0.744)	0.106 (0.151, 0.065)	0.0000	*	0.1254		0.9115	
Superior Zero Pixels	34	0.196 (0.179, 0.216)	8	0.209 (0.170, 0.258)	0.012 (-0.032, 0.048)	0.5576		0.6712		0.6808	
Inferior Zero Pixels	34	0.188 (0.170, 0.208)	8	0.209 (0.169, 0.258)	0.018 (-0.024, 0.052)	0.3628		0.9827		0.8619	
Inferior Mean Flow	34	403.28 (360.46, 451.18)	8	326.17 (255.52, 416.36)	-95.33 (-231.27, 11.48)	0.0844		0.1682		0.1261	
Superior Mean Flow	34	408.94 (370.63, 451.21)	8	323.21 (246.39, 423.99)	-108.47 (-270.73, 15.05)	0.0908		0.2646		0.1248	
MD	34	-3.01 (-4.32, -1.69)	21	-3.84 (-5.33, -2.35)	-0.83 (-1.69, 0.03)	0.0585		0.1712		0.3343	
PSD	34	3.77 (2.66, 4.89)	21	4.27 (3.06, 5.48)	0.50 (-0.05, 1.04)	0.0744		0.1532		0.6223	
AGIS score	34	1.36 (0.66, 2.35)	21	2.01 (1.09, 3.33)	0.51 (0.12, 0.84)	0.0130	*	0.7474		0.7886	
Disk area	34	2.280 (2.094, 2.466)	20	2.649 (2.411, 2.887)	0.369 (0.181, 0.558)	0.0001	*	0.5516		0.9586	
Cup area	34	1.183 (0.971, 1.395)	20	1.620 (1.354, 1.886)	0.437 (0.266, 0.608)	0.0000	*	0.0370	*	0.6083	
Rim area	34	1.081 (0.912, 1.249)	20	1.013 (0.787, 1.240)	-0.067 (-0.268, 0.134)	0.5124		0.1977		0.4067	
cup/disk area ratio	34	0.509 (0.435, 0.583)	20	0.604 (0.521, 0.687)	0.095 (0.037, 0.153)	0.0014	*	0.0591		0.4846	
cup/disk horizontal ratio	34	0.70 (0.64, 0.76)	20	0.78 (0.71, 0.84)	0.08 (0.03, 0.13)	0.0019	*	0.0678		0.7518	
cup/disk vert ratio	34	0.697 (0.642, 0.752)	20	0.754 (0.687, 0.821)	0.057 (0.010, 0.104)	0.0181	*	0.0365	*	0.9106	

RNFL thickness superior	34	89.53 (81.08, 97.98)	18	85.86 (76.38, 95.33)	-3.67 (-11.79, 4.44)	0.3747		0.3430		0.9462	
RNFL thickness inferior	34	91.98 (81.52, 102.44)	18	85.78 (73.20, 98.36)	-6.20 (-15.04, 2.65)	0.1694		0.6394		0.8482	
RNFL thickness nasal	34	64.78 (58.55, 71.00)	18	64.73 (55.26, 74.19)	-0.05 (-8.74, 8.64)	0.9908		0.2562		0.6016	
RNFL thickness temporal	34	56.46 (50.08, 62.84)	18	55.00 (46.30, 63.70)	-1.46 (-9.11, 6.20)	0.7089		0.9075		0.7169	
RNFL average	34	75.98 (69.82, 82.13)	18	73.18 (66.12, 80.23)	-2.80 (-8.02, 2.42)	0.2921		0.6904		0.6869	
macular thickness outer superior	34	225.12 (219.20, 231.05)	20	217.01 (210.23, 223.80)	-8.11 (-13.25, -2.97)	0.0020	*	0.3392		0.8857	
macular thickness inner superior	34	265.34 (258.47, 272.20)	20	251.85 (244.06, 259.64)	-13.49 (-18.51, -8.47)	0.0000	*	0.0802		0.2496	
macular thickness outer inferior	34	210.28 (203.58, 216.98)	20	202.49 (195.75, 209.22)	-7.79 (-11.18, -4.41)	0.0000	*	0.4965		0.2595	
macular thickness inner inferior	34	259.90 (251.82, 267.97)	20	247.66 (238.74, 256.57)	-12.24 (-17.15, -7.33)	0.0000	*	0.2033		0.2535	
macular thickness outer nasal	34	236.87 (230.70, 243.04)	20	229.33 (222.00, 236.67)	-7.54 (-12.20, -2.88)	0.0016	*	0.1957		0.0338	*
macular thickness inner nasal	34	266.02 (258.63, 273.41)	20	254.10 (245.59, 262.61)	-11.92 (-17.80, -6.04)	0.0001	*	0.3581		0.4403	
macular thickness outer temporal	34	209.02 (203.51, 214.53)	20	201.95 (195.15, 208.75)	-7.07 (-12.66, -1.47)	0.0133	*	0.6523		0.4984	
macular thickness inner temporal	34	252.02 (244.85, 259.18)	20	237.93 (230.19, 245.68)	-14.08 (-20.21, -7.95)	0.0000	*	0.0110	*	0.2362	
Macula center	34	203.65 (194.28, 213.01)	20	196.01 (186.37, 205.64)	-7.64 (-15.23, -0.05)	0.0485	*	0.1418		0.0531	
macular volume	34	6.49 (6.34, 6.64)	20	6.23 (6.07, 6.39)	-0.26 (-0.35, -0.17)	0.0000	*	0.1469		0.2712	
HRT3 Cup Area	33	0.820 (0.654, 1.003)	20	0.833 (0.665, 1.019)	0.013 (-0.041, 0.066)	0.6343		0.0800		0.6692	
HRT3 Rim Area	33	1.308 (1.183, 1.433)	20	1.297 (1.172, 1.422)	-0.011 (-0.069, 0.046)	0.7008		0.0719		0.5333	
HRT3 Cup Volume	33	0.265 (0.165, 0.365)	20	0.259 (0.160, 0.359)	-0.005 (-0.033, 0.023)	0.7105		0.0083	*	0.3449	
HRT3 Rim Volume	33	0.319 (0.253, 0.384)	20	0.326 (0.262, 0.390)	0.007 (-0.020, 0.035)	0.6008		0.1328		0.8459	
HRT3 Cup/Disk Area Ratio	33	0.387 (0.322, 0.451)	20	0.393 (0.328, 0.458)	0.006 (-0.020, 0.033)	0.6273		0.1154		0.4654	
HRT3 Linear Cup/Disk Ratio	33	0.601 (0.540, 0.661)	20	0.606 (0.545, 0.667)	0.006 (-0.016, 0.028)	0.6055		0.1234		0.5562	
HRT3 Mean Cup Depth	33	0.295 (0.250, 0.340)	20	0.295 (0.249, 0.340)	0.000 (-0.016, 0.015)	0.9559		0.1591		0.1382	
HRT3 Max Cup Depth	33	0.715 (0.628, 0.802)	20	0.705 (0.619, 0.791)	-0.010 (-0.045, 0.026)	0.6025		0.4751		0.1933	
HRT3 Cup Shape	33	-0.135 (-0.161, -0.110)	20	-0.126 (-0.154, -0.097)	0.010 (-0.008, 0.028)	0.2938		0.9419		0.4383	
HRT3 Height Variation Contour	33	0.336 (0.293, 0.384)	20	0.349 (0.304, 0.400)	0.013 (-0.014, 0.038)	0.3504		0.7458		0.0746	
HRT3 Mean RNFL Thickness	33	0.210 (0.178, 0.242)	20	0.211 (0.177, 0.245)	0.000 (-0.018, 0.018)	0.9718		0.0881		0.9343	
HRT3 RNFL Cross-Sectional Area	33	1.107 (0.930, 1.285)	20	1.124 (0.938, 1.310)	0.017 (-0.079, 0.112)	0.7325		0.0632		0.9096	

Similar changes were assessed in OAG patients of different BMI in the retrobulbar blood flow parameters assessed by color Doppler imaging in the ophthalmic artery (OA) from baseline over a five-year period: in NW, OA peak systolic velocity (PSV) decreased with changes of -1.22 (95%CI: -4.52, 1.67; p=0.4260), OA End Diastolic Velocity (EDV) decreased significantly with changes of -2.40 (-3.63, -1.34; p<0.0001); OA resistivity index (RI) increased significantly with statistically significant changes of 0.085 (95%CI: 0.131, 0.044; p<0.0001); in OW, OA PSV decreased with changes of -1.05 (95%CI: -4.86, 2.25; p=0.5529), OA EDV decreased significantly with statistically significant changes of -1.87 (95%CI: -3.30, -0.67; p=0.0013), OA RI increased significantly with statistically significant changes of 0.059 (95%CI : 0.102, 0.022; p=0.0011); in OB, OA PSV decreased with changes of -1.30 (95%CI: -6.48, 3.02; p=0.5788), OA EDV decreased significantly with statistically significant s changes of -2.55 (95%CI: -4.36, -1.05; p=0.0003), OA RI increased significantly with statistically significant changes of 0.043 (95%CI: 0.016, 0.070; p=0.0010), Table 1 and Figure 1.

Figure 1. Retrobulbar blood flow parameters in the ophthalmic artery (OA) assessed by color Doppler imaging (mean with 95% confidence interval) in open-angle glaucoma patients with different body mass index at baseline (BL) and 5 years (5 yr). EDV: end diastolic velocity; OA: ophthalmic artery; PSV: peak systolic velocity; RI: resistivity index.

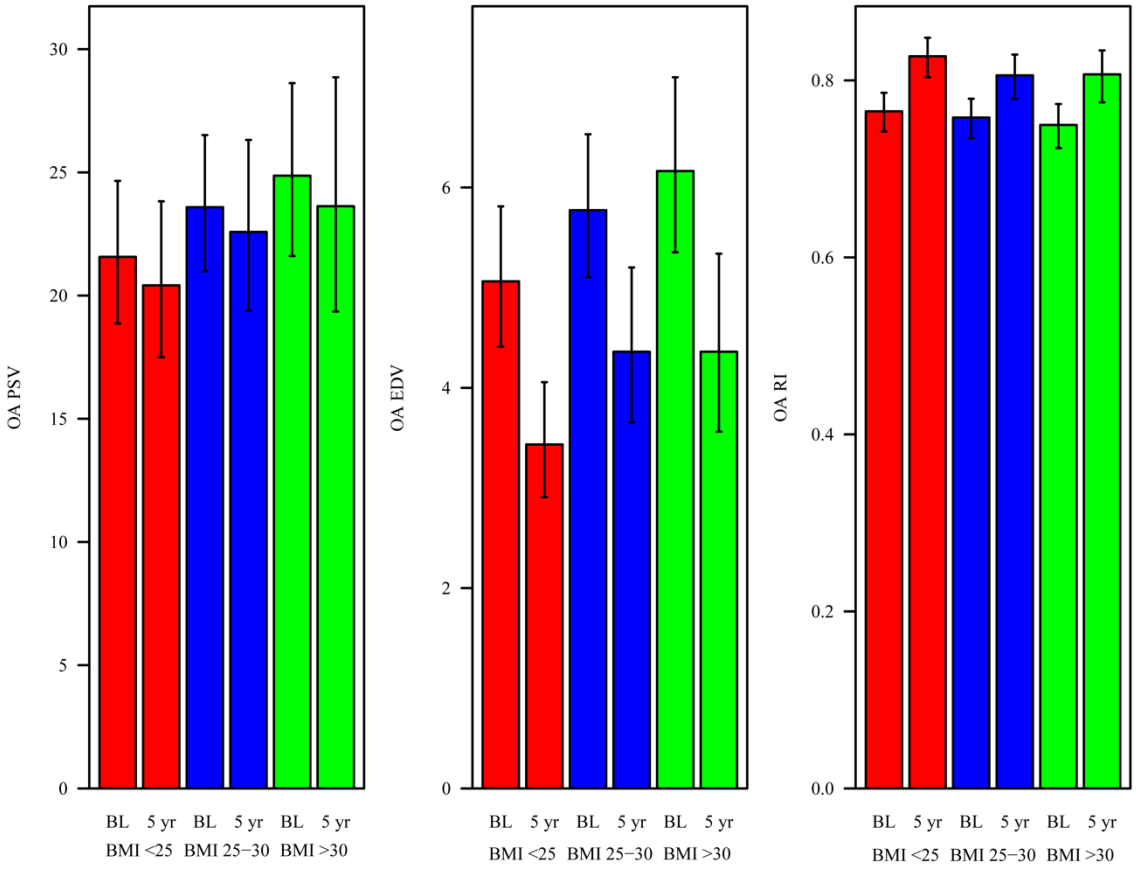

For the central retinal artery (CRA), in all the three groups the resistivity index (RI) increased significantly with statistically significant changes of 0.085 (95%CI: 0.131, 0.044; p=0.0017) in NW, of 0.053 (95%CI: 0.022, 0.085; p=0.0008) in OW, and of -0.84 (95%CI: -1.38, -0.38; p=0.0001) in OB, Table 1 and Figure 2.

Figure 2. Retrobulbar blood flow parameters in the central retinal artery (CRA) assessed by color Doppler imaging (mean with 95% confidence interval) in open-angle glaucoma patients with different body mass index at baseline (BL) and 5 years (5 yr). RI: resistivity index.

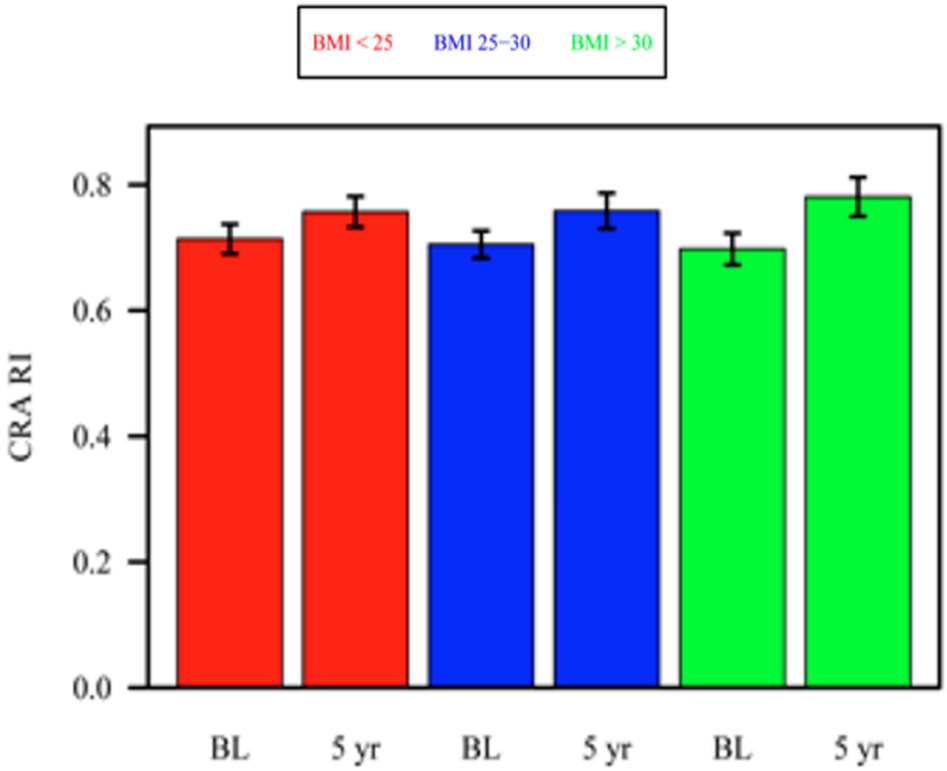

In the nasal posterior ciliary arteries (NPCA) the PSV did not change significantly within any weight group (NW, p=0.4713; OW, p=0.3598; OB, p=0.4546), while the EDV decreased significantly in all the three groups, with statistically significant changes of -0.85 (95%CI: -1.28, -0.47; p<0.0001) in NW, of -0.49 (95%CI: -0.89, -0.14; p=0.0047) in OW, and of -0.62 (95%CI: -1.02, -0.27; p<0.0003) in OB, Table 1 and Figure 3.

Figure 3. Retrobulbar blood flow parameters in the nasal posterior ciliary artery (NPCA) assessed by color Doppler imaging (mean with 95% confidence interval) in open-angle glaucoma patients with different body mass index at baseline (BL) and 5 years (5 yr). EDV: end diastolic velocity; PSV: peak systolic velocity.

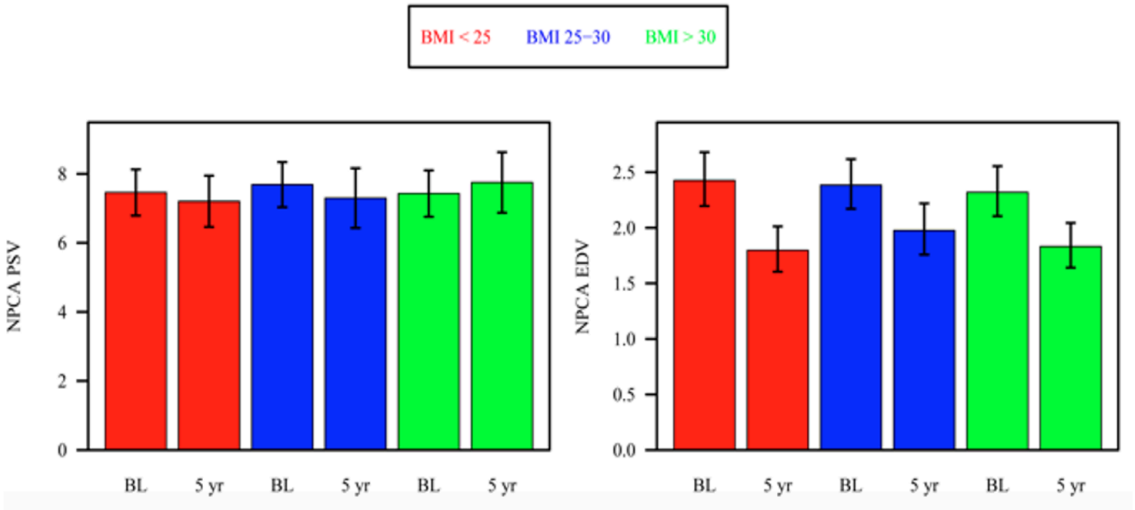

Lower baseline OA EDV was associated with shorter time to structural progression in OB (p=0.0097) but neither in NW (p=0.2776) nor OW (p=0.3328) patients, leading to a significant difference between groups (p=0.0289), Figure 4.

Figure 4. Survival function for time to structural progression for baseline retrobulbar blood flow parameters (ophthalmic artery end diastolic velocity, OA EDV) assessed by color Doppler imaging (mean with 95% confidence interval) in open-angle glaucoma patients with different body mass index. Lines represent survival curves for lowest and highest observed OA EDV. Lower baseline OA EDV was associated with shorter time to structural progression in obese patients (BMI >30).

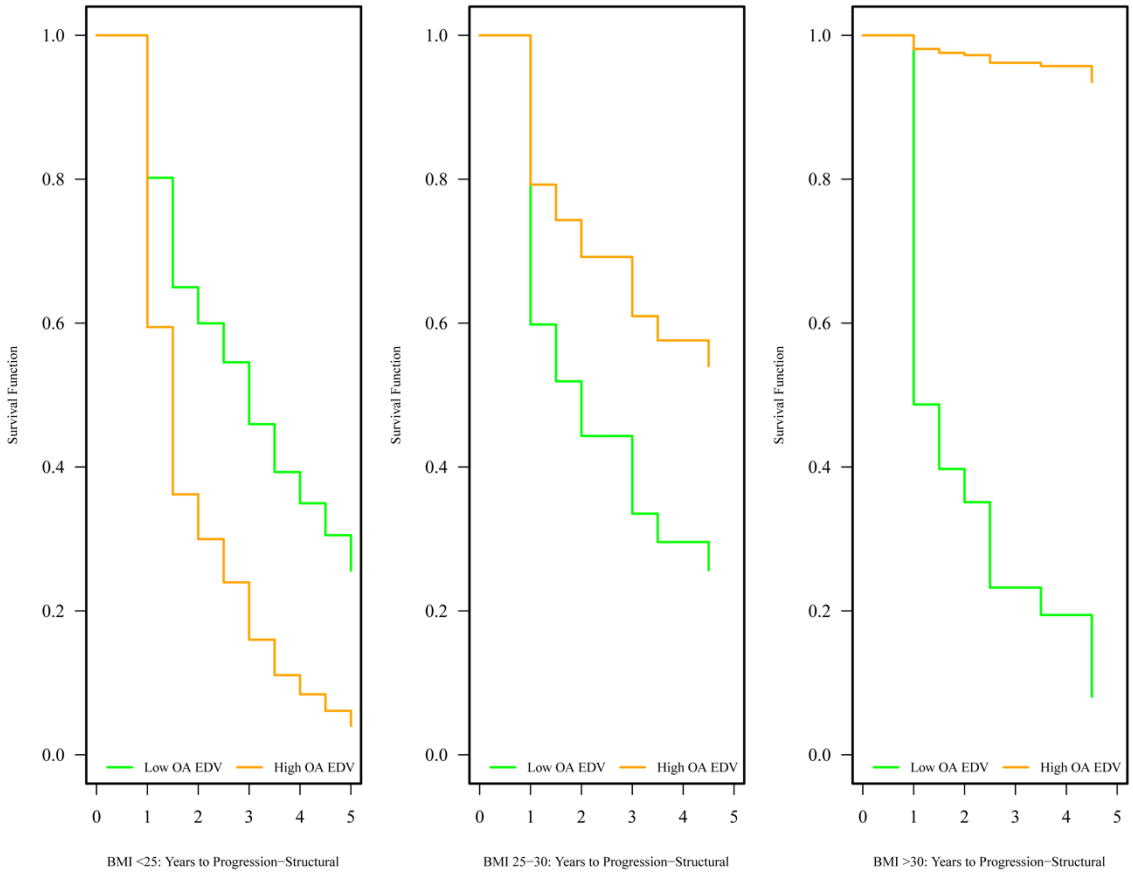

In OW OAG patients, higher OA RI and CRA RI were predictive of functional progression (OA RI: p=0.280, CRA RI: p=0.462). In OB OAG patients, lower CRA RI was predictive of functional progression (0.0439), and lower NPCA PSV was predictive of structural progression (p=0.125), Figure 5.

Figure 5. Survival function for time to functional and structural progression for retrobulbar blood flow parameters (ophthalmic artery (OA) and central retinal artery (CRI) resistivity index (RI) and nasal posterior ciliary artery (NPCA) end diastolic velocity (NPCA EDV) assessed by color Doppler imaging (mean with 95% confidence interval) in open-angle glaucoma patients with different body mass index. Lines represent survival curves for lowest and highest observed measurements. Higher OA RI and CRA RI were predictive of functional progression in overweight patients. Lower CRA RI was predictive of functional progression in obese patients. Lower NPCA PSV was predictive of structural progression in obese patients.

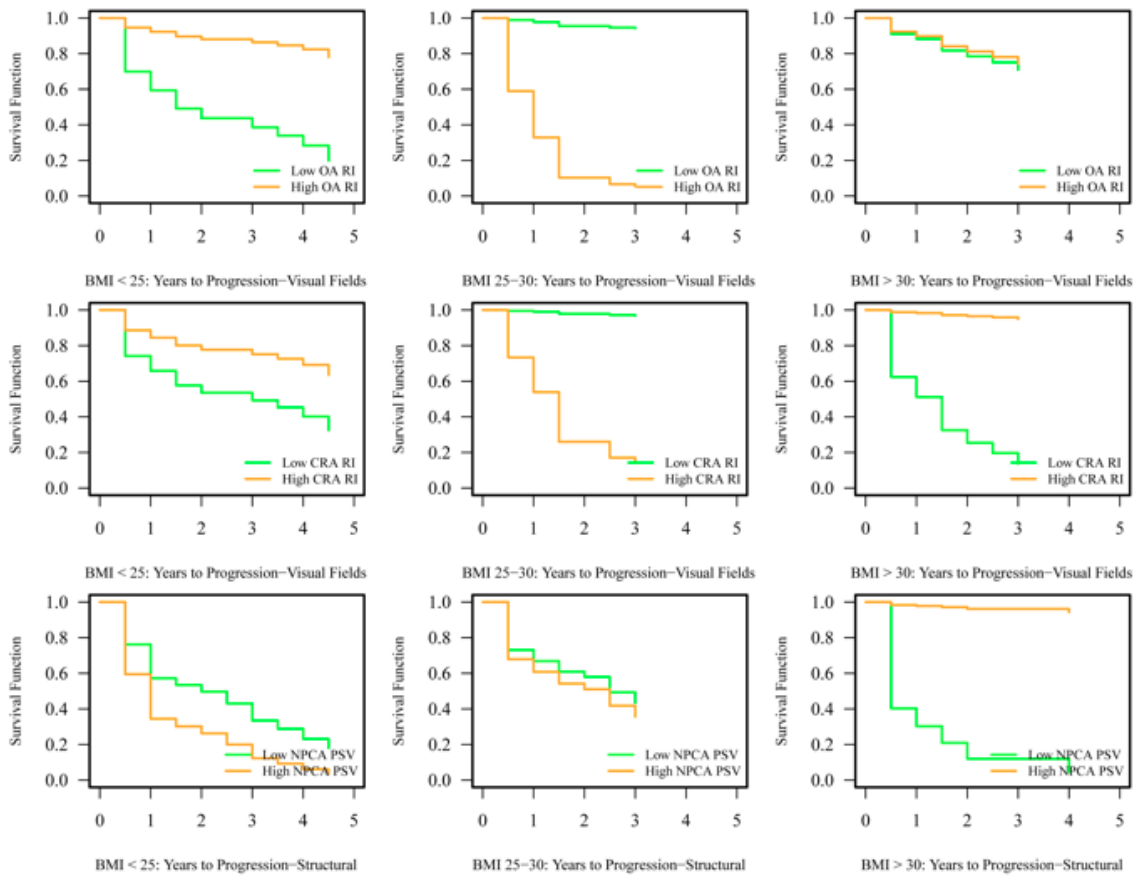

The retinal capillary blood flow measurements assessed by Heidelberg retinal flowmeter (HRF) did not changed significantly from baseline to 5 years in NW (p- value from 0.1728 to 0.9244), OW (p-value from 0.0844 to 0.9244), nor obese (p-value from 0.144 to 0.8002) OAG patients. The baseline parameters were as follows: the inferior mean flow at baseline was 412.67 (95% CI; 368.98, 461.55) for NW, 415.82 (95% CI: 375.76, 460.15) for OW and 403.28 (95% CI: 360.46, 451.18) for OB; the superior mean flow at baseline was 422.47 (95% CI: 382.39, 466.75) for NW, 404.31 (95% CI: 371.90, 439.53) for OW and 408.94 (95% CI: 370.63, 451.21) for OB, Table 1 and Figure 6.

Figure 6. Retinal capillary blood flow parameters (inferior and superior mean flow) assessed by Heidelberg retinal flowmeter (mean with 95% confidence interval) in open-

angle glaucoma patients with different body mass index at baseline (BL) and 5 years (5 yr).

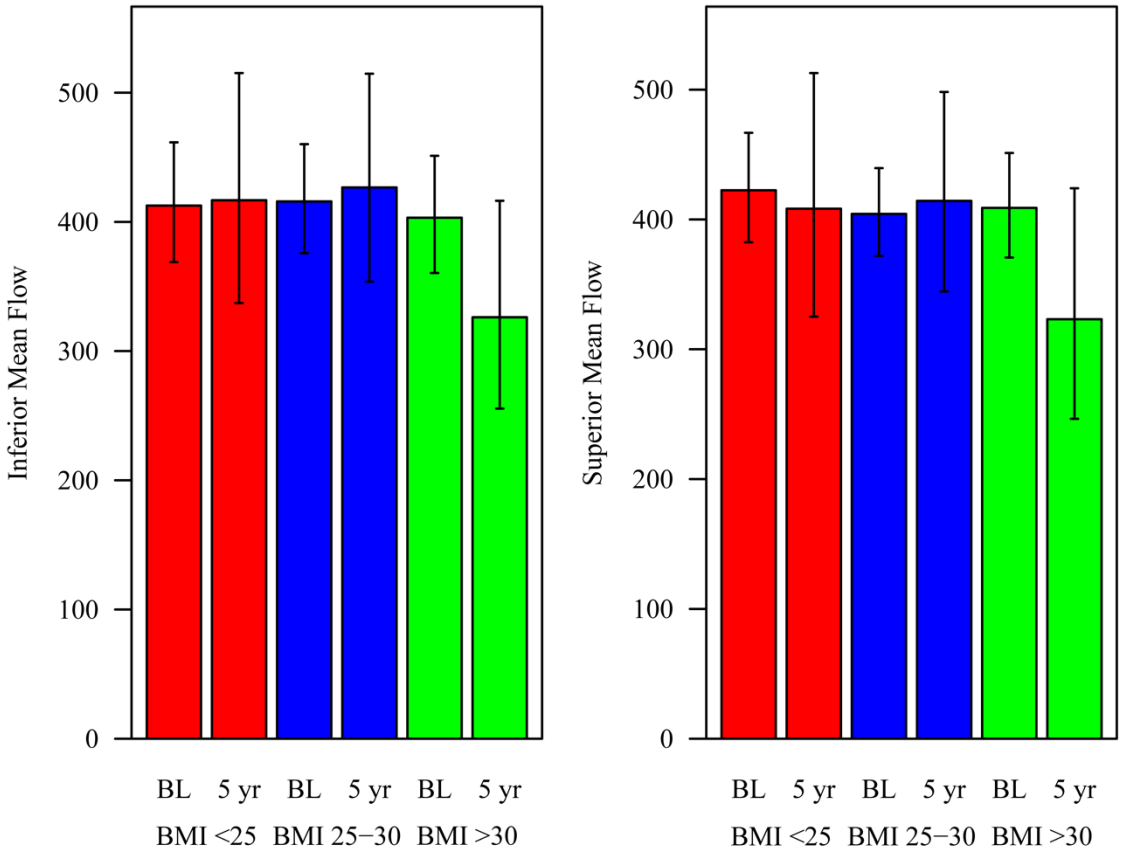

Lower baseline inferior mean flow was associated with shorter time to functional progression in OB patients (p=0.01440) but neither in NW (p=0.2475) nor OW patients (p=0.7323), leading to a significant difference between groups (p=0.0317), Figure 7.

Figure 7. Survival function for time to functional progression for retinal capillary blood flow parameter (inferior mean flow) in open-angle glaucoma patients with different body mass index. Lines represent survival curves for lowest and highest observed Superior Mean Flow. Lower baseline inferior mean flow was associated with shorter time to progression in obese patients (BMI >30).

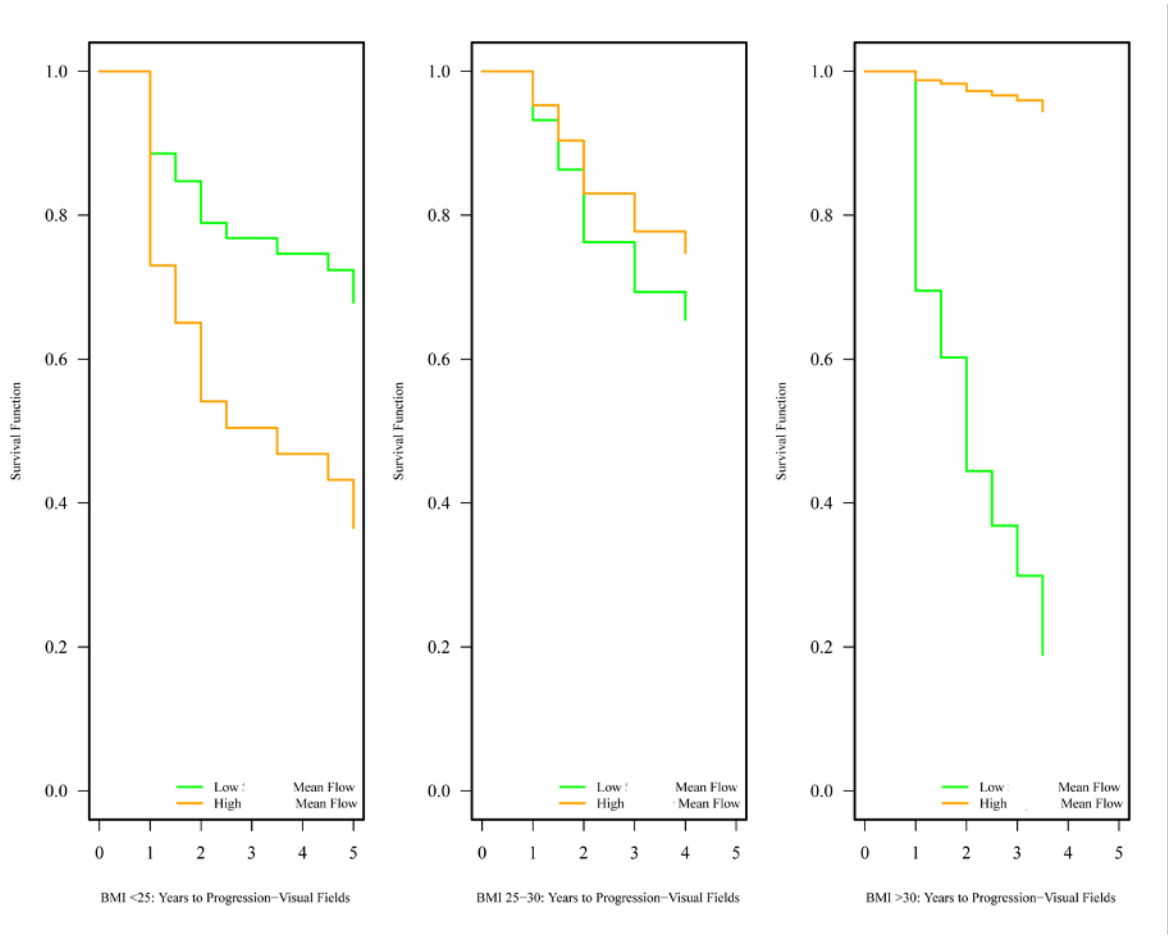

The optic nerve head parameters assessed by Heidelberg retinal tomograph 3 changed significantly from baseline to five years in NW (cup area increased with a statistically significant change of 0.082, 95% CI: 0.024, 0.138; p=0.0061; cup volume significantly increased with a statistically significant change of 0.054, 95% CI: 0.020, 0.088; p=0.0021; cup/disk area ratio significantly increased with a statistically significant change of 0.038, 95% CI: 0.008, 0.069; p=0.0129); the changes were not statistically significant for OW (cup area: p=0.3577; cup volume: p=0.364; cup/disk area ratio: p=0.2017) nor OB patients (cup area: p=0.6343; cup volume: p=0.6008; p=0.3641; cup/disk area ratio: p=0. 6055), Figure 8.

Figure 8. Optic nerve head structural parameters assessed by Heidelberg retinal tomograph 3 (mean with 95% confidence interval) in open-angle glaucoma patients with different body mass index at baseline (BL) and 5 years (5 yr).

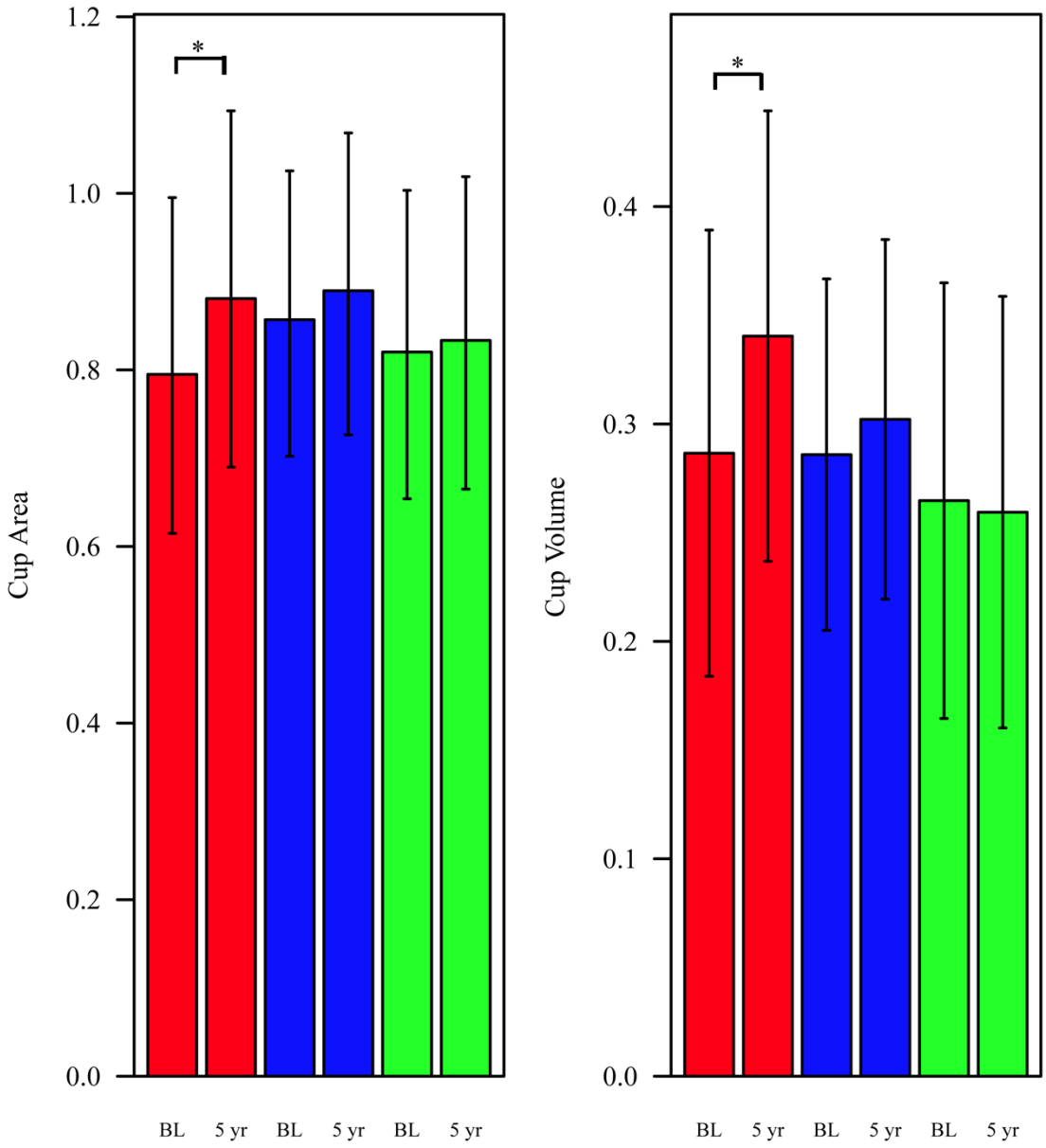

Smaller increases/larger decreases in cup area, cup volume and cup/disk area ratio were more predictive of functional progression in OW patients (p=0.0067, 0.0047, 0.0129, respectively), compared to NW or OB patients, with a significant difference between BMI groups (p=0.0064, 0.0024, 0.0085, respectively), Figure 9.

Figure 9. Survival function for time to functional progression for Optic nerve head structural parameters assessed by Heidelberg retinal tomograph 3 in open-angle

glaucoma patients with different body mass index (normal weight (BMI <25), top; overweight (BMI 25-30), center; and obese (BMI>30), bottom). Lines represent survival curves for lowest and highest values for changes in cup area and cup volume. Smaller increases/larger decreases in cup area, cup volume and cup/disk area ratio were more predictive of functional progression in OW patients

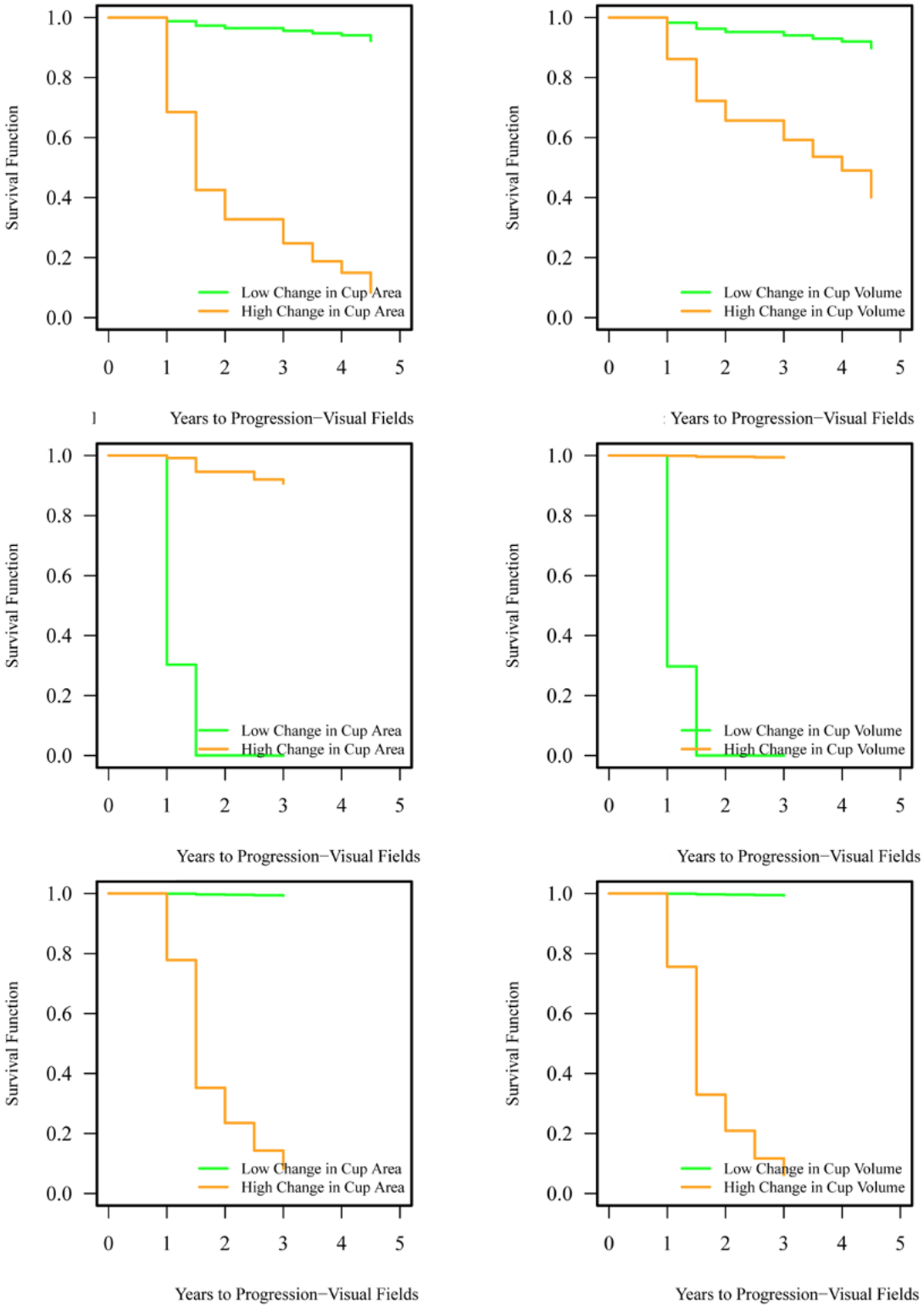

The summary of the other significant results of the Aim 5 of my PhD project are shown in Table 4.

Table 4. Summary of the significant changes over time and predictors of diseases progression from baseline to 5 years in open- angle glaucoma patients based on BMI.

Changes from Baseline to 5 years based on BMI
TPCA PSV decreased for normal BMI but did not change significantly (direction of TPCA PSV increase) in obese
Cup area increased more in obese than normal BMI
cup/disk vert ratio increased in obese but did not change in normal BMI
macular thickness inner temporal decreased in obese and did not change significantly in normal BMI
HRT3 Cup Volume increased in normal BMI but did not change in obese
Baseline predictors of shorter time to progression based on BMI
FUNCTIONAL PROGRESSION
lower Inferior Mean Flow, for obese
STRUCTURAL PROGRESSION
lower OA EDV, for obese
lower MD, for obese
lower RNFL thickness inferior, for obese
lower HRT3 Rim Area, for obese
Predictors (multiple observations over time) of shorter time to progression based on BMI
FUNCTIONAL PROGRESSION
Higher OA RI, for overweight
Higher CRA RI, for overweight
Lower CRA RI, for obese
STRUCTURAL PROGRESSION
lower NPCA PSV, for obese
Predictors (change from baseline measurements, multiple observations over time) of shorter time to progression based on BMI
FUNCTIONAL PROGRESSION
more decrease in CRA PSV, for normal BMI
Smaller increases/larger decreases in cup area, for OW
Smaller increases/larger decreases in cup volume for OW
Smaller increases/larger decreases in cup/disk area ratio, for OW
STRUCTURAL PROGRESSION
less increase in PSD, for obese

4. Discussion – Aim 5:

The aim 5 of my PhD project has been to investigate the relationship between glaucoma progression, ocular hemodynamics, and *body mass index (BMI).*

In our cohort of patients, we did not find significant differences at baseline and over 5 years in IOP, which represent the major risk factor for glaucoma, between normal weight, overweigh, and obese patients (Table 1-3), thus highlighting the importance of other risk factors. Interestingly, in 2013, Ngo et al. investigated the relationships between BP, OPP, IOP in OAG patients with normal weight, overweight and obesity, and the authors found a different correlation between the variables analyzed in OAG patients of different BMI categories (Ngo et al. 2013). Specifically, a significant positive correlation was demonstrated in NW patients between changes in systolic BP (SBP) and IOP ($r=0.36$, $p=0.0431$). In OW and OB OAG subjects, a negative correlation was shown between changes in IOP and OPP (OW: $r=-0.56$, $p=0.0002$; OB: $r=-0.38$, $p=0.0499$). The authors suggested that a possible explanation for the discrepancy reported in patients with different BMI was related to the fact that that normal-weight subjects are less likely to have elevated arterial BP, while overweight and obese individuals have a greater tendency toward systemic hypertension (Levine et al., 2011). A higher vulnerability to changes in OPP could therefore be explained in overweight and obese patients by pathologic changes in the ocular vessels induced by arterial hypertension specifically in these two populations, (De Ciuceis et al., 2011), while the ocular blood vessels of normal-weight patients could be more adaptable to changes in OPP. Also, it is important to highlight that several studies have previously shown the association of high arterial BP with increases in IOP, thus providing a possible explanation for the different prevalence of the glaucomatous disease in subjects with different BMI (Kawase et al., 2006; Xu et al., 2007; Jonas et al., 2011). Overall, these findings suggest that BMI may affect the interplay between

known risk factors for glaucoma onset and progression, such as IOP, OPP and BP, thus highlighting the complexity of the relationship between glaucoma and BMI.

In our study, significant differences in the predictive value of ocular hemodynamic biomarkers were found in OAG patients with different BMI. Importantly, retrobulbar and retinal capillary blood flow parameters were found to be indicative of glaucoma progression in particular in obese patients (Figure 4-5, 7). Also, our data showed that changes in optic nerve head parameters were more predictive of functional progression in overweight OAG patients than in normal weight (Figure 9). Taken together, this data suggests that OAG patients who are above normal weight may have compromising local vasculature leading to abnormal blood flow dynamics from the retrobulbar and retinal blood supply and subsequent glaucoma progression.

In conclusion, the Aim 5 of my PhD project highlighted how normal weight, overweight and obese glaucomatous patients may experience structural and functional disease progression differently depending on their BMI. Importantly, retinal capillary and retrobulbar blood flow biomarkers may be more involved in the progression based upon BMI. In the assessment of disease progression in glaucomatous patients, it is crucial to take into consideration the body mass index of the subjects.

CHAPTER 9

PhD Research Project – Aim 6: To investigate the relationship between glaucoma progression, ocular hemodynamics, and *age*

1. Introduction – Aim 6:

Increasing age has been suggested as a major risk factor for the development and progression of open angle glaucoma (OAG), the leading cause of blindness worldwide. OAG is characterized by a progressive loss of retinal ganglion cells and retinal nerve fiber layer (RNFL), with corresponding visual field loss. Elevated intraocular pressure (IOP) has been associated with the prevalence, incidence, and progression of the glaucoma; however, it is well known that glaucoma progression is observed in patients with IOP reduction, suggesting the multifactorial nature of OAG. Importantly, several studies with various imaging modalities, have revealed impairment of ocular blood flow in the retinal, choroidal, and retrobulbar circulations in OAG patients (Harris et al., 2020).

Importantly, a physiologic loss of retinal ganglion cells occurs with aging (Harwerth et al., 2008), and several studies have examined the association between age and the risk of development of glaucoma. In details, multiple longitudinal population-based studies have shown that age is a risk factor for the onset of OAG (Le et al., 2003; Müskens et al., 2007; Leske et al., 2008). In the Melbourne Visual Impairment Project, subjects with an age of 70-79 years old at baseline had a 12-fold higher five-year risk of developing OAG compared to subjects aged 40-49 years old at baseline (Le et al., 2003). Similarly, increased age was found to be a risk factor for OAG development by the Eye Disease Prevalence research group, who analyzed six population based studies and reported a prevalence of glaucoma of 0.68% in the age group 40-49, and of 7.74% in the age group of subjects over 80 years of age (Friedman et al. 2004). As shown in the Ocular Hypertension Treatment Study and in the European

Glaucoma Prevention Study, age is also a predictive factor associated with the development of OAG in patients with ocular hypertension (Kass et al., 2002; Miglior et al., 2005). Finally, older age at baseline has also be shown to be a predictive factor for OAG progression in the Early Manifest Glaucoma Trial (Heijl et al., 2002).

Even tough age has been widely recognized as a contributing factor for glaucoma onset and progression, the underlying pathophysiologic mechanisms are not fully understood. It has been suggested that vascular effects in the ocular circulation associated with structural changes that occur with aging may be contributing factors in the development and progression of OAG (Harris et al., 2000; Asejczyk-Widlicka et al., 2015). Notably, there is a lack of information regarding the effect of aging on ocular hemodynamics and its effect on glaucomatous progression. The Indianapolis Glaucoma Progression Study was designed to assess retrobulbar and retinal microcirculation and the relationship to structural and functional progression in patients with OAG. Aim 6 was to investigate the relationship between glaucoma progression, ocular hemodynamics, and *age.*

2. Material and Methods - Aim 6:

The comprehensive discussion of the materials and methods is detailed in chapter 3.

In brief, a cohort of 112 OAG patients (62 with age >=65years, 50 with age<65years) were enrolled at baseline, and prospectively examined at baseline and every 6 months over a period of five years at the Glaucoma and Diagnostic Center at Indiana University School of Medicine, Indianapolis, Indiana. The data were categorized into groups depending on age (age >=65year or age<65years) based on self-reported age. One qualified eye was randomly designated as the observational study eye in each subject. Measurements were made at baseline and every 6 months over a 5-year period.

To limit reproducibility bias with imaging, a single experienced operator with over ten years of experience performed all measurements in the same order and at the same time of the day for each patient.

Functional disease progression was monitored by visual field testing and defined as two consecutive visits with an Advanced Glaucoma Intervention Study (AGIS) score increase ≥2 from baseline, and/ or MD decrease ≥2 from baseline. Structural disease progression was monitored with optical coherence tomography and Heidelberg retinal tomography and defined as two consecutive visits with RNFL thickness decrease ≥8% and/or horizontal or vertical cup/disk ratio increase ≥0.2 compared to baseline.

The statistical analysis involved mixed-model analysis of covariance (ANCOVA) to test for significance of changes from baseline to 5-year follow-up separately by age (age >=65years, age<65years). Two-sample t tests and $\chi 2$ tests were used to analyze differences in baseline data between patients who progressed and those who did not progress. The models were then extended to test for whether the changes were different by age (age >=65years, age<65years). Time to functional progression and time to structural progression were analyzed using Cox proportional hazards survival analysis. Factors were analyzed as baseline measurements, as time-varying measurements, and as time-varying changes from baseline. Interactions were tested to determine if the effects of the factors on progression time differed by age (age >=65years, age<65years). Pearson correlation coefficients were calculated to evaluate linear associations. Correlations were adjusted for years of glaucoma, use of glaucoma or hypertension medications, gender, body mass index category, race, and diabetes status. Correlations were compared between groups using Fisher z tests. P values <0.05 were considered statistically significant.

3. Results – Aim 6:

A cohort of 112 OAG patients (62 with age >=65years, 50 with age<65years) were prospectively examined at baseline and every 6 months over a period of five years. After 5 years, 37 subjects (31 age >= 65yo, 6 age < 65yo) progressed functionally, and 76 (50 age >= 65yo, 26 age < 65yo) structurally. Table 1 and 2 show the change in the study measurements (mean and 95% confidence interval, CI) from baseline to five years in OAG patients with age >=65years, and with age <65years, respectively. Table 3 summarizes all the significant results related to the changes between parameters from baseline to 5 years and to the associations between measurements and shorter time to functional and structural progression based on age.

Table 1. Change from baseline to five years in the study parameters in open-angle glaucoma patients with age with age <65years. *p-value statistically significant <0.05.

	Age<65 years-old							Age >= vs < 65	
	Baseline		5 yr		Change			Change	
	N	Mean (95% CI)	N	Mean (95% CI)	Mean (95% CI)	p-value		p-value	
IOP	49	17.02 (15.46, 18.59)	27	15.93 (14.25, 17.61)	-1.10 (-2.44, 0.25)	0.1103		0.6754	
SBP	49	134.43 (128.26, 140.59)	27	129.96 (122.60, 137.33)	-4.47 (-11.58, 2.64)	0.2179		0.5302	
DBP	49	84.19 (80.41, 87.97)	27	80.51 (76.22, 84.81)	-3.68 (-8.02, 0.67)	0.0971		0.2790	
MAP	49	100.91 (96.66, 105.16)	27	96.94 (92.06, 101.83)	-3.97 (-8.80, 0.86)	0.1074		0.3460	
HR	49	72.48 (68.51, 76.45)	27	72.75 (67.83, 77.68)	0.28 (-3.80, 4.35)	0.8944		0.9724	
Visual Acuity	49	0.03 (-0.02, 0.07)	27	0.22 (0.14, 0.31)	0.20 (0.12, 0.28)	0.0000	*	0.0917	
OA PSV	50	23.72 (20.79, 27.07)	25	20.86 (17.56, 24.76)	-3.26 (-7.32, 0.27)	0.0717		0.2098	
OA EDV	50	6.32 (5.52, 7.23)	25	4.37 (3.61, 5.29)	-2.81 (-4.46, -1.42)	0.0000	*	0.9788	
OA RI	50	0.737 (0.759, 0.714)	25	0.783 (0.810, 0.753)	0.056 (0.100, 0.017)	0.0041	*	0.0582	
CRA PSV	50	8.08 (7.43, 8.72)	25	7.26 (6.44, 8.08)	-0.82 (-1.57, -0.06)	0.0341	*	0.4741	
CRA EDV	50	2.31 (2.10, 2.53)	25	1.74 (1.52, 1.99)	-0.74 (-1.23, -0.33)	0.0002	*	0.6472	
CRA RI	50	0.697 (0.676, 0.718)	25	0.755 (0.726, 0.783)	0.058 (0.029, 0.087)	0.0001	*	0.4827	
NPCA PSV	49	7.83 (7.16, 8.50)	25	7.16 (6.21, 8.10)	-0.67 (-1.51, 0.17)	0.1157		0.1256	
NPCA EDV	49	2.50 (2.28, 2.74)	25	1.84 (1.62, 2.07)	-0.91 (-1.36, -0.51)	0.0000	*	0.3353	
NPCA RI	49	0.661 (0.641, 0.680)	25	0.733 (0.706, 0.759)	0.072 (0.043, 0.101)	0.0000	*	0.7898	
TPCA PSV	50	7.76 (7.20, 8.32)	25	7.78 (7.08, 8.48)	0.02 (-0.62, 0.66)	0.9450		0.2918	
TPCA EDV	50	2.44 (2.24, 2.66)	25	1.92 (1.72, 2.14)	-0.66 (-1.05, -0.32)	0.0001	*	0.3843	
TPCA RI	50	0.680 (0.700, 0.659)	25	0.754 (0.774, 0.732)	0.096 (0.138, 0.058)	0.0000	*	0.9726	
Superior Zero Pixels	50	0.189 (0.175, 0.205)	11	0.219 (0.187, 0.257)	0.026 (-0.003, 0.051)	0.0812		0.7312	
Inferior Zero Pixels	49	0.171 (0.157, 0.186)	11	0.195 (0.166, 0.229)	0.021 (-0.006, 0.044)	0.1257		0.5536	
Inferior Mean Flow	49	421.36 (378.53, 469.05)	11	390.82 (320.21, 476.99)	-32.93 (-127.86, 45.59)	0.4363		0.6867	
Superior Mean Flow	50	424.12 (387.92, 463.70)	11	393.17 (320.01, 483.06)	-33.38 (-136.15, 50.54)	0.4630		0.7971	

MD	50	-2.94 (-4.30, -1.59)	28	-3.95 (-5.56, -2.33)	-1.00 (-2.01, 0.01)	0.0515		0.2559	
PSD	50	3.97 (2.64, 5.30)	28	4.64 (3.20, 6.09)	0.67 (0.03, 1.31)	0.0395	*	0.4659	
AGIS score	50	1.22 (0.58, 2.12)	27	1.81 (0.92, 3.11)	0.46 (0.03, 0.81)	0.0364	*	0.6076	
Disk area	50	2.260 (2.079, 2.441)	25	2.671 (2.457, 2.884)	0.411 (0.259, 0.564)	0.0000	*	0.2909	
Cup area	50	1.063 (0.835, 1.291)	25	1.484 (1.203, 1.766)	0.421 (0.247, 0.595)	0.0000	*	0.1880	
Rim area	50	1.156 (0.986, 1.327)	25	1.163 (0.952, 1.373)	0.006 (-0.160, 0.173)	0.9393		0.8452	
cup/disk area ratio	50	0.483 (0.403, 0.563)	25	0.567 (0.468, 0.667)	0.084 (0.015, 0.154)	0.0173	*	0.3742	
cup/disk horizontal ratio	50	0.66 (0.59, 0.72)	25	0.75 (0.67, 0.83)	0.09 (0.04, 0.14)	0.0004	*	0.0842	
cup/disk vert ratio	50	0.651 (0.588, 0.714)	25	0.718 (0.633, 0.802)	0.067 (0.005, 0.128)	0.0335	*	0.1583	
RNFL thickness superior	50	97.54 (88.39, 106.68)	25	89.13 (78.93, 99.34)	-8.40 (-15.69, -1.11)	0.0239	*	0.4191	
RNFL thickness inferior	50	99.70 (88.97, 110.42)	25	94.71 (81.54, 107.87)	-4.99 (-13.94, 3.96)	0.2740		0.8552	
RNFL thickness nasal	50	69.15 (62.77, 75.52)	25	64.69 (55.67, 73.71)	-4.46 (-12.11, 3.19)	0.2529		0.0195	*
RNFL thickness temporal	50	60.21 (53.81, 66.60)	25	60.86 (53.18, 68.53)	0.65 (-5.16, 6.46)	0.8267		0.5762	
RNFL average	50	81.86 (75.68, 88.03)	25	77.30 (69.90, 84.70)	-4.56 (-9.81, 0.69)	0.0886		0.2416	
macular thickness outer superior	50	224.38 (217.17, 231.60)	28	218.01 (210.38, 225.65)	-6.37 (-10.53, -2.21)	0.0027	*	0.7604	
macular thickness inner superior	50	266.04 (258.63, 273.46)	28	256.25 (248.61, 263.89)	-9.79 (-13.15, -6.43)	0.0000	*	0.5268	
macular thickness outer inferior	50	211.66 (205.15, 218.16)	28	205.18 (197.76, 212.60)	-6.48 (-10.99, -1.96)	0.0050	*	0.9116	
macular thickness inner inferior	50	260.35 (253.17, 267.52)	28	249.99 (242.23, 257.76)	-10.36 (-14.29, -6.42)	0.0000	*	0.5151	
macular thickness outer nasal	50	239.95 (233.11, 246.80)	28	236.98 (229.66, 244.31)	-2.97 (-6.38, 0.44)	0.0877		0.2122	
macular thickness inner nasal	50	265.87 (258.43, 273.31)	28	255.26 (247.42, 263.09)	-10.62 (-14.90, -6.33)	0.0000	*	0.9767	
macular thickness outer temporal	50	204.70 (198.82, 210.58)	28	194.55 (187.65, 201.46)	-10.15 (-15.25, -5.05)	0.0001	*	0.3982	
macular thickness inner temporal	50	249.33 (242.43, 256.22)	28	238.30 (231.04, 245.56)	-11.03 (-16.57, -5.49)	0.0001	*	0.4210	
Macula center	50	199.73 (189.50, 209.95)	28	196.07 (184.79, 207.34)	-3.66 (-11.27, 3.95)	0.3455		0.3778	
macular volume	50	6.48 (6.33, 6.64)	28	6.28 (6.11, 6.44)	-0.21 (-0.29, -0.13)	0.0000	*	0.9716	
HRT3 Cup Area	50	0.868 (0.693, 1.061)	28	0.921 (0.737, 1.125)	0.052 (-0.008, 0.109)	0.0884		0.5402	
HRT3 Rim Area	50	1.279 (1.141, 1.418)	28	1.228 (1.082, 1.375)	-0.051 (-0.120, 0.017)	0.1432		0.7410	
HRT3 Cup Volume	50	0.322 (0.217, 0.427)	28	0.340 (0.234, 0.446)	0.018 (-0.010, 0.046)	0.2017		0.7450	
HRT3 Rim Volume	50	0.314 (0.248, 0.379)	28	0.300 (0.233, 0.366)	-0.014 (-0.042, 0.014)	0.3203		0.3610	
HRT3 Cup/Disk Area Ratio	50	0.409 (0.343, 0.474)	28	0.438 (0.369, 0.506)	0.029 (-0.001, 0.059)	0.0572		0.4137	
HRT3 Linear Cup/Disk Ratio	50	0.614 (0.555, 0.674)	28	0.635 (0.572, 0.698)	0.021 (-0.006, 0.048)	0.1223		0.4567	
HRT3 Mean Cup Depth	50	0.316 (0.269, 0.363)	28	0.320 (0.273, 0.367)	0.004 (-0.010, 0.017)	0.5900		0.2938	

HRT3 Max Cup Depth	50	0.752 (0.663, 0.841)	28	0.744 (0.655, 0.833)	-0.008 (-0.040, 0.024)	0.6082		0.2740	
HRT3 Cup Shape	50	-0.136 (-0.163, -0.108)	28	-0.120 (-0.150, -0.090)	0.016 (0.000, 0.032)	0.0491	*	0.7159	
HRT3 Height Variation Contour	50	0.346 (0.299, 0.399)	28	0.361 (0.311, 0.418)	0.014 (-0.010, 0.037)	0.2351		0.4211	
HRT3 Mean RNFL Thickness	50	0.213 (0.181, 0.244)	28	0.200 (0.166, 0.235)	-0.012 (-0.031, 0.007)	0.2026		0.8975	
HRT3 RNFL Cross-Sectional Area	50	1.123 (0.956, 1.290)	28	1.063 (0.884, 1.241)	-0.060 (-0.155, 0.035)	0.2147		0.8760	

Table 2 Change from baseline to five years in the study parameters in open-angle glaucoma patients with age with age >=65years. *p-value statistically significant <0.05.

	Age>=65 year-old							**Age >= vs < 65**	
	Baseline		**5 yr**		**Change**			**Change**	
	N	**Mean (95% CI)**	**N**	**Mean (95% CI)**	**Mean (95% CI)**	**p-value**		**p-value**	
IOP	62	16.31 (15.01, 17.61)	48	14.83 (13.40, 16.26)	-1.48 (-2.71, -0.25)	0.0180	*	0.6754	
SBP	62	137.55 (131.93, 143.18)	50	130.24 (124.40, 136.07)	-7.32 (-12.77, -1.87)	0.0086	*	0.5302	
DBP	62	82.15 (78.84, 85.47)	50	75.43 (72.12, 78.75)	-6.72 (-10.14, -3.29)	0.0001	*	0.2790	
MAP	62	100.58 (96.82, 104.35)	50	93.67 (89.83, 97.51)	-6.91 (-10.73, -3.10)	0.0004	*	0.3460	
HR	62	71.25 (68.06, 74.44)	51	71.44 (67.71, 75.16)	0.18 (-3.01, 3.38)	0.9095		0.9724	
Visual Acuity	62	0.15 (0.11, 0.18)	49	0.26 (0.21, 0.32)	0.12 (0.06, 0.17)	0.0000	*	0.0917	
OA PSV	62	23.42 (21.13, 25.95)	51	23.05 (20.30, 26.17)	-0.38 (-3.11, 2.07)	0.7739		0.2098	
OA EDV	62	5.49 (4.97, 6.07)	51	3.81 (3.32, 4.37)	-2.42 (-3.50, -1.47)	0.0000	*	0.9788	
OA RI	62	0.767 (0.784, 0.748)	51	0.836 (0.851, 0.819)	0.098 (0.132, 0.067)	0.0000	*	0.0582	
CRA PSV	62	8.09 (7.52, 8.66)	51	7.62 (6.98, 8.26)	-0.47 (-1.06, 0.12)	0.1168		0.4741	
CRA EDV	62	2.25 (2.07, 2.45)	51	1.63 (1.49, 1.79)	-0.85 (-1.21, -0.54)	0.0000	*	0.6472	
CRA RI	62	0.704 (0.686, 0.722)	51	0.775 (0.754, 0.796)	0.071 (0.048, 0.093)	0.0000	*	0.4827	
NPCA PSV	62	7.43 (6.92, 7.94)	51	7.55 (6.93, 8.16)	0.11 (-0.45, 0.68)	0.6913		0.1256	
NPCA EDV	62	2.27 (2.11, 2.45)	51	1.80 (1.65, 1.96)	-0.60 (-0.88, -0.34)	0.0000	*	0.3353	
NPCA RI	62	0.674 (0.657, 0.692)	51	0.752 (0.732, 0.771)	0.077 (0.055, 0.099)	0.0000	*	0.7898	
TPCA PSV	62	7.89 (7.39, 8.40)	51	7.46 (6.86, 8.06)	-0.43 (-0.98, 0.12)	0.1257		0.2918	
TPCA EDV	62	2.38 (2.21, 2.58)	51	1.75 (1.61, 1.91)	-0.86 (-1.19, -0.56)	0.0000	*	0.3843	
TPCA RI	62	0.688 (0.706, 0.669)	51	0.760 (0.777, 0.743)	0.095 (0.128, 0.064)	0.0000	*	0.9726	
Superior Zero Pixels	62	0.210 (0.196, 0.225)	19	0.234 (0.204, 0.268)	0.022 (-0.007, 0.047)	0.1360		0.7312	
Inferior Zero Pixels	62	0.197 (0.183, 0.212)	19	0.211 (0.188, 0.236)	0.013 (-0.011, 0.034)	0.2747		0.5536	
Inferior Mean Flow	62	432.75 (398.32, 470.16)	19	422.47 (358.36, 498.05)	-10.53 (-88.53, 55.80)	0.7709		0.6867	
Superior Mean Flow	62	422.10 (393.61, 452.66)	19	404.80 (344.88, 475.13)	-18.04 (-95.25, 47.65)	0.6112		0.7971	
MD	62	-3.74 (-4.82, -2.65)	50	-5.66 (-7.22, -4.09)	-1.92 (-3.15, -0.69)	0.0023	*	0.2559	
PSD	62	3.91 (2.97, 4.86)	50	4.90 (3.84, 5.96)	0.99 (0.43, 1.55)	0.0006	*	0.4659	
AGIS score	62	1.73 (1.07, 2.59)	50	2.70 (1.74, 4.01)	0.72 (0.34, 1.04)	0.0005	*	0.6076	
Disk area	62	2.298 (2.160, 2.435)	48	2.603 (2.442, 2.765)	0.306 (0.181, 0.430)	0.0000	*	0.2909	
Cup area	62	1.215 (1.041, 1.390)	48	1.499 (1.298, 1.700)	0.284 (0.173, 0.394)	0.0000	*	0.1880	
Rim area	62	1.063 (0.925, 1.202)	48	1.090 (0.940, 1.240)	0.027 (-0.089, 0.142)	0.6512		0.8452	

cup/disk area ratio	62	0.519 (0.458, 0.580)	48	0.569 (0.506, 0.631)	0.049 (0.015, 0.084)	0.0049	*	0.3742	
cup/disk horizontal ratio	62	0.70 (0.66, 0.75)	48	0.75 (0.70, 0.79)	0.04 (0.01, 0.07)	0.0033	*	0.0842	
cup/disk vert ratio	62	0.694 (0.648, 0.739)	48	0.712 (0.664, 0.761)	0.019 (-0.009, 0.046)	0.1813		0.1583	
RNFL thickness superior	62	82.52 (75.07, 89.98)	46	77.98 (69.96, 86.00)	-4.55 (-10.51, 1.42)	0.1351		0.4191	
RNFL thickness inferior	62	89.19 (80.52, 97.86)	46	85.23 (75.16, 95.30)	-3.96 (-10.59, 2.67)	0.2414		0.8552	
RNFL thickness nasal	62	59.30 (54.25, 64.35)	46	65.82 (59.66, 71.99)	6.52 (1.34, 11.71)	0.0138	*	0.0195	*
RNFL thickness temporal	62	53.03 (47.78, 58.28)	46	51.64 (45.92, 57.36)	-1.39 (-5.61, 2.83)	0.5185		0.5762	
RNFL average	62	71.37 (66.24, 76.51)	46	70.63 (65.05, 76.21)	-0.74 (-4.44, 2.97)	0.6960		0.2416	
macular thickness outer superior	62	221.36 (215.29, 227.43)	47	214.16 (207.90, 220.43)	-7.19 (-10.55, -3.83)	0.0000	*	0.7604	
macular thickness inner superior	62	262.70 (256.15, 269.25)	47	251.12 (243.62, 258.62)	-11.58 (-16.09, -7.08)	0.0000	*	0.5268	
macular thickness outer inferior	62	208.46 (202.52, 214.41)	47	202.30 (196.07, 208.53)	-6.17 (-9.31, -3.03)	0.0001	*	0.9116	
macular thickness inner inferior	62	256.19 (249.42, 262.95)	47	247.92 (239.87, 255.97)	-8.27 (-13.27, -3.27)	0.0012	*	0.5151	
macular thickness outer nasal	62	232.44 (226.72, 238.15)	47	226.39 (219.99, 232.79)	-6.05 (-9.57, -2.53)	0.0008	*	0.2122	
macular thickness inner nasal	62	262.19 (256.04, 268.35)	47	251.48 (244.13, 258.82)	-10.72 (-15.88, -5.55)	0.0001	*	0.9767	
macular thickness outer temporal	62	206.32 (201.00, 211.65)	47	198.94 (193.14, 204.74)	-7.39 (-11.37, -3.41)	0.0003	*	0.3982	
macular thickness inner temporal	62	249.14 (242.24, 256.04)	47	241.58 (233.35, 249.81)	-7.56 (-14.05, -1.07)	0.0224	*	0.4210	
Macula center	62	203.57 (194.99, 212.16)	47	205.73 (193.31, 218.15)	2.15 (-8.40, 12.71)	0.6886		0.3778	
macular volume	62	6.40 (6.25, 6.55)	47	6.19 (6.04, 6.34)	-0.21 (-0.29, -0.13)	0.0000	*	0.9716	
HRT3 Cup Area	61	0.871 (0.727, 1.028)	49	0.899 (0.749, 1.062)	0.028 (-0.023, 0.077)	0.2834		0.5402	
HRT3 Rim Area	61	1.243 (1.127, 1.358)	49	1.206 (1.087, 1.325)	-0.037 (-0.091, 0.017)	0.1843		0.7410	
HRT3 Cup Volume	61	0.279 (0.201, 0.357)	49	0.303 (0.224, 0.382)	0.024 (-0.002, 0.050)	0.0649		0.7450	
HRT3 Rim Volume	61	0.283 (0.234, 0.332)	49	0.286 (0.236, 0.336)	0.003 (-0.022, 0.028)	0.8048		0.3610	
HRT3 Cup/Disk Area Ratio	61	0.416 (0.361, 0.472)	49	0.430 (0.372, 0.487)	0.013 (-0.011, 0.037)	0.2796		0.4137	
HRT3 Linear Cup/Disk Ratio	61	0.624 (0.575, 0.672)	49	0.632 (0.582, 0.683)	0.009 (-0.011, 0.028)	0.3854		0.4567	
HRT3 Mean Cup Depth	61	0.287 (0.252, 0.322)	49	0.300 (0.265, 0.335)	0.013 (0.002, 0.024)	0.0209	*	0.2938	
HRT3 Max Cup Depth	61	0.690 (0.625, 0.756)	49	0.706 (0.640, 0.773)	0.016 (-0.014, 0.046)	0.3005		0.2740	
HRT3 Cup Shape	61	-0.123 (-0.146, -0.101)	49	-0.111 (-0.135, -0.087)	0.012 (0.000, 0.025)	0.0577		0.7159	
HRT3 Height Variation Contour	61	0.324 (0.291, 0.360)	49	0.353 (0.313, 0.398)	0.027 (0.002, 0.050)	0.0382	*	0.4211	
HRT3 Mean RNFL Thickness	61	0.186 (0.164, 0.209)	49	0.176 (0.148, 0.203)	-0.011 (-0.030, 0.009)	0.2841		0.8975	
HRT3 RNFL Cross-	61	0.967 (0.850, 1.084)	49	0.918 (0.777, 1.059)	-0.049 (-0.151, 0.052)	0.3419		0.8760	

Sectional Area									

The retrobulbar blood flow parameters assessed by color Doppler imaging changed as follows from baseline to 5 years: in patients <65 years old, OA PSV did not significantly change from baseline to five years (p=0.072), while OA EDV decreased significantly with a statistically significant mean change of -2.81 (95% CI: -4.46, -1.42; p<0.0001), and OA RI increased significantly with a statistically significant mean change of 0.056, 95% CI: 0.100, 0.017; p=0.0041); TPCA PSV did not significantly change from baseline to five years (p=0.9450), while TPCA EDV also significantly decreased with a statistically significant mean change of -0.66 (95% CI: -1.05, -0.32; p=0.0001), and TPCA RI increased significantly with a statistically significant mean change of 0.096 (95% CI: 0.138, 0.058; p<0.0001), Figure 1 and Table 1. Similarly, in patients >65 years old, OA PSV did not significantly change (0.7739), OA EDV decreased significantly with a statistical significant mean change of -2.42 (95% CI: -3.50, -1.47; p<0.0001), TPCA EDV decreased significantly with a statistical significant mean change -0.86 (95% CI: -1.19, -0.56; p<0.0001), Figure 1 and Table 1.

Figure 1. Retrobulbar blood flow parameters assessed by color Doppler imaging (mean with 95% confidence interval) in open-angle glaucoma patients with age >=65 or < 65 at baseline (BL) and 5 years (5 yr). EDV: end diastolic velocity; OA: ophthalmic artery; PSV: peak systolic velocity; TPCA: nasal posterior ciliary artery.

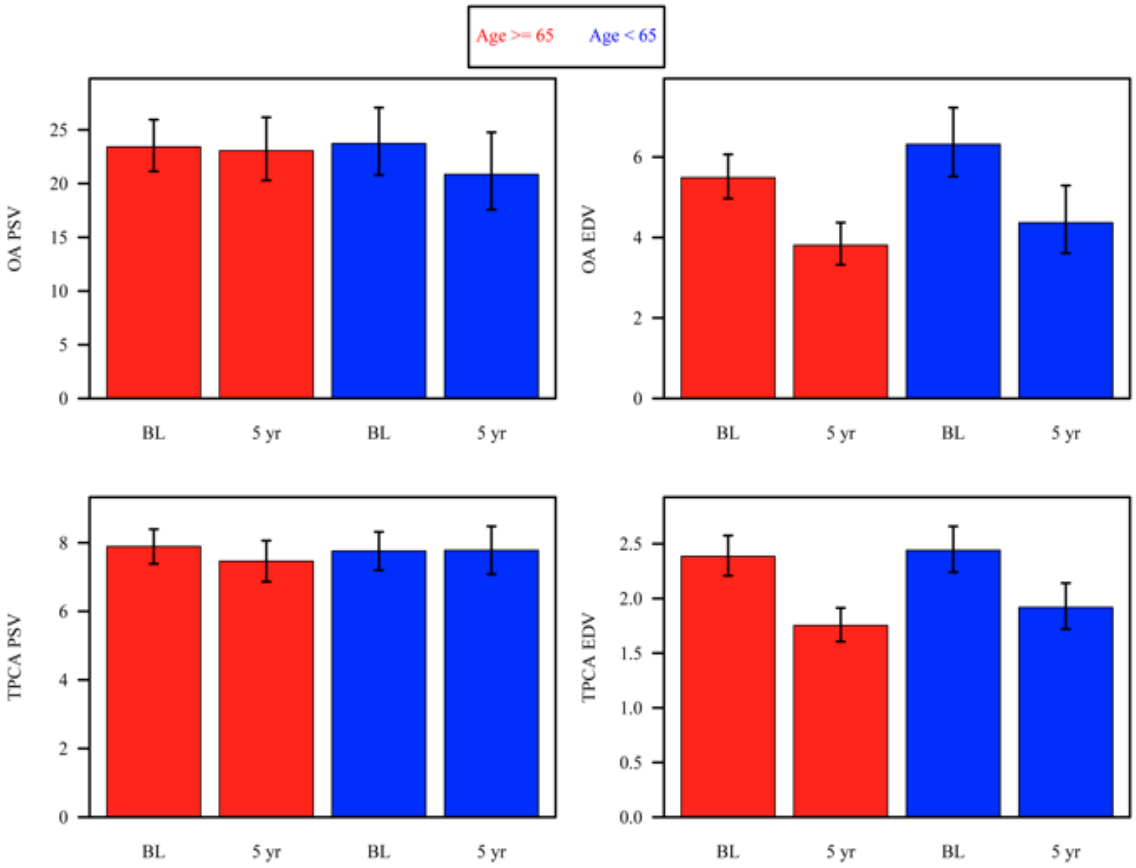

Lower OA PSV, lower OA EDV, and higher TPCA EDV were predictive of functional progression in OAG patients aged <65 (OA PSV: p=0.0017; OA EDV: p=0.0041; TPCA EDV; p=0.0358) resulting in a significant difference between age groups 65 (OA PSV: p=0.0140; OA EDV: p=0.0373; TPCA EDV; p=0.0086), Figure 2.

Figure 2. Survival function for time to functional progression for open-angle glaucoma patients with age >=65 or < 65 for retrobulbar blood flow parameters assessed by color Doppler imaging (ophthalmic artery (OA) and temporal posterior ciliary artery (TPCA) peak systolic velocity (PSV) and end diastolic velocity (EDV). Lines represent survival curves for lowest and highest observed measurements. Lower OA PSV and EDV and higher TPCA EDV were predictive of functional progression in OAG patients aged <65 years only.

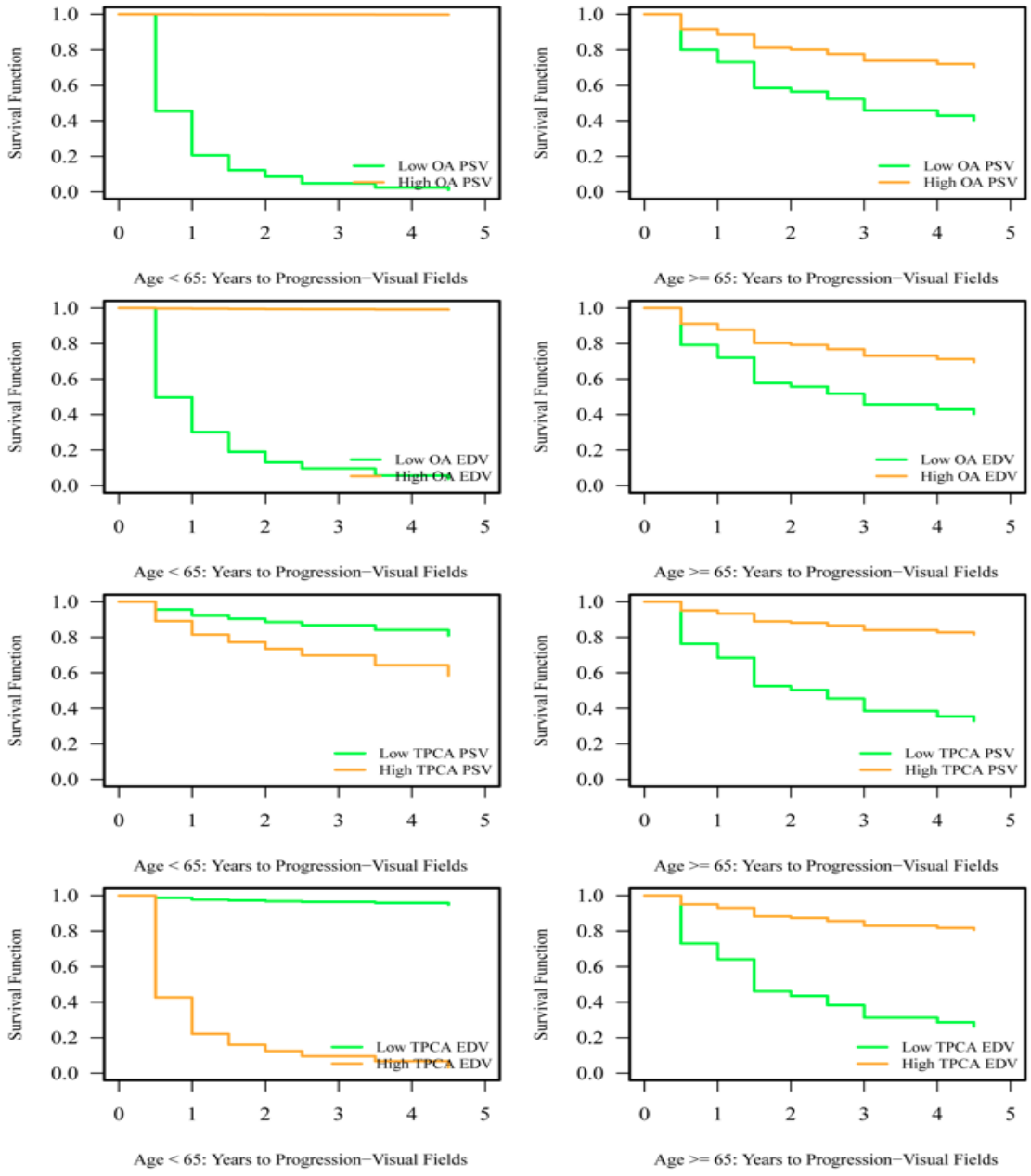

Table 3 summarizes all the significant results of the Aim 6 of my PhD project.

Table 3. Summary of the significant changes over time and predictors of diseases progression from baseline to 5 years in open- angle glaucoma patients based on age.

Changes from Baseline to 5 years based on age
RNFL thickness nasal increased in age>=65 but did not change significantly in age<65
Baseline predictors of shorter time to progression based on age

FUNCTIONAL PROGRESSION
lower BMI, for age<65
STRUCTURAL PROGRESSION
N/A
Predictors (multiple observations over time) of shorter time to progression in the overall population
FUNCTIONAL PROGRESSION
lower OA PSV, especially, for age<65
lower OA EDV, especially, for age<65
higher TPCA EDV, for age<65
lower HRT3 Height Variation Contour, for age<65
lower BMI, for age<65
STRUCTURAL PROGRESSION
lower BMI, for age<65
Predictors (change from baseline measurements, multiple observations over time) of shorter time to progression in the overall population
FUNCTIONAL PROGRESSION
more increase in CRA RI, for age>=65
less increase in HRT3 Cup Area, for age<65
STRUCTURAL PROGRESSION
less decrease in Inferior Mean Flow, for age<65

4. Discussion – Aim 6:

The aim 6 of my PhD project has been to investigate the relationship between glaucoma progression, ocular hemodynamics, and *age.*

While aging has been shown to be a significant risk factor for disease onset and progression, the relationship between ocular blood flow and the aging process is still unclear. Recently, a study from Jammal et al. showed how older patients are at increased risk of glaucoma progression compared to younger subjects even with the same level of IOP, thus highlighting how age represent an important modifier of the relationship between IOP and glaucomatous damage to the RNFL layer over time (Jammal et al., 2020). Also, it is important to note that OAG risk alleles have been shown to be associated with an earlier age at glaucoma diagnosis,

thus highlighting an interaction between individual genetic susceptibility and age-related changes (Fan et al., 2019). In our study, we found that in OAG patients of different age groups, lower OA PSV, lower OA EDV, and higher TPCA EDV were significantly more predictive of functional progression in OAG patients aged <65 years after five years as compared to patients with OAG aged >65 years old (Figure 1 and 2). Furthermore, we found that baseline age was a predictive factor of functional glaucoma progression after five years ($p=0.0098$). This data suggests that retrobulbar blood flow may influence functional progression of OAG differently according to the age of the subject. Previously, Harris et al. analyzed the effects of age on retrobulbar blood vessels and found a decrease in the OA EDV and an increase in the Pourcelot resistance indices with advanced age. Conversely, OA and CRA PSV velocities were not affected by age (Harris et al., 2000). Asejczyk-Widlicka and colleagues, analyzing age-related vascular changes in OAG patients and suspects for glaucoma and age-matched healthy controls found significant interaction between age and group for five out of nine retrobulbar blood vessel parameters evaluated. Specifically, the authors concluded that while age may play a role in changes in the retrobulbar blood supply and glaucoma risk, it was not a significant determining risk factor (Asejczyk-Widlicka et al., 2015). While aging may be an independent risk factor for OAG, there is also evidence to show that the vascular effects of aging may contribute to the progression of the disease. As aging of the vasculature occurs over a lifespan, vascular risk may increase overall risk of OAG.

CHAPTER 10

PhD Research Project – Conclusions

1. General conclusions

In conclusion my PhD project highlights the importance of vascular risk factors, assessed by multiple imaging modalities, in the progression of OAG. Currently OAG is a leading cause of blindness worldwide, and the disease has significant disparities in certain populations alongside limited therapy options. Reduction of IOP remains the only currently approved treatment option, yet many patients continue to develop OAG and/or experience disease progression despite medically lowered IOP. Vascular risk factors, both systemic and localized to ocular tissues have been identified in glaucoma patient for decades, however, the exact nature of hemodynamic alterations prior to and during glaucoma progression are poorly understood. My PhD contributes specific evidence of vascular involvement in the OAG disease process, especially in certain groups of patients. Our 5 years data analysis reveals that specific patients who might be at elevated risk for vascular involvement in OAG include persons of AD, individuals with high BMI and/or diabetes. Our findings adds to other reported systemic risk factors, such as low diastolic blood pressure, the use of systemic antihypertensive medications, obstructive sleep apnea, and migraine. One difficulty in realizing individualized medical approaches to glaucoma care is the integration of all risk factors, demographics, and clinical variables into a useable model of patient care.

One approach to improve future OAG disease management would be the creation of a clinician-friendly model that integrates all variables of risk for a given individual. Specifically, an OAG disease management plan that is inclusive of vascular risk factors, in combination with clinical and demographic considerations, has the potential to improve diagnostic and therapeutic specificity and individual patient outcomes. This modeling has the potential to provide clinicians a user-friendly tool to evaluate their patients as individuals in consideration of all of

their unique variability versus a static norm of isolated IOP assessments. In the field of ophthalmology, multi-input modeling algorithms have been recently employed to characterize glaucoma progression based on biomechanical changes of the eye and its ocular hemodynamics (Harris et al., 2020). However, the use of artificial intelligence is still underdeveloped, and a comprehensive modeling of glaucoma development and progression and the role of vascular and demographic risk factors is still missing. Future research should be focused on the development and use of combined clinical, mathematical, and statistical modeling approaches to elucidate the specific relationships between ocular structural, functional and hemodynamic parameters in disease onset and progression. Comprehensively modeling for all risk variables represents an important improvement in identifying patients at highest risk for developing glaucoma and experiencing disease progression, and provides a path forward to individualize and improve disease management for each glaucoma patient.

REFERENCES

Abe RY, Diniz-Filho A, Zangwill LM, Gracitelli CPB, Marvasti AH, Weinreb RN, Baig S, Medeiros FA. The Relative Odds of Progressing by Structural and Functional Tests in Glaucoma. *Investigative ophthalmology & visual science.* 2016;57:OCT421-OCT428.

Affinito P, Sardo AS, Di Carlo C, et al. Effects of hormone replacement therapy on ocular function in postmenopause. *Menopause.* 2003;10:482–487.

Alencar LM, Medeiros FA. The role of standard automated perimetry and newer functional methods for glaucoma diagnosis and follow-up. *Indian J Ophthalmol*. 2001;59,Suppl S1:53-8.

Altintas O, Caglar Y, Yuksel N, Demirci A, Karabas L. The effects of menopause and hormone replacement therapy on quality and quantity of tear, intraocular pressure and ocular blood flow. *Ophthalmologica.* 2004;218:120–9.

American Academy of Ophthalmology Glaucoma Preferred Practice Pattern Panel. Primary Open-Angle Glaucoma Preferred Practice Pattern. 2020; American Academy of Ophthalmology.

Asejczyk-Widlicka M, Krzyzanowska-Berkowska P, Sander BP, Iskander DR. Age-Related Changes in Ocular Blood Velocity in Suspects with Glaucomatous Optic Disc Appearance. Comparison with Healthy Subjects and Glaucoma Patients. *PLoS One*. 2015;10(7):e0134357.

Atalay E, Karaali K, Akar M, et al. Early impact of hormone replacement therapy on vascular hemodynamics detected via ocular colour Doppler analysis. *Maturitas.* 2005;50:282–8.

Beck RW, Messner DK, Musch DC, Martonyi CL, Lichter PR. Is there a racial difference in physiologic cup size? *Ophthalmology*. 1985;92:873–876.

Belchetz FK. Hormonal treatment of postmenopausal women. *N Engl J Med.* 1994;330:1062–71.

Bonomi L, Marchini G, Marrafa M, et al. Vascular risk factors for primary open angle glaucoma: the Egna-Neumarkt Study. *Ophthalmology.* 2000;107:1287–93.

Bonovas S, Peponis V, Filioussi K. Diabetes mellitus as a risk factor for primary open-angle glaucoma: a meta-analysis. *Diabet Med.* 2004;21:609-14.

Brandt JD, Beiser JA, Kass MA, Gordon MO. Central corneal thickness in the Ocular Hypertension Treatment Study (OHTS). *Ophthalmology*. 2001 Oct;108(10):1779-88.

Burgansky-Eliash Z, Nelson DA, Bar-Tal OP, Lowenstein A, Grinvald A, Barak A. Reduced retinal blood flow velocity in diabetic retinopathy. *Retina*. 2010;30:765-73.

Burgansky-Eliash Z, Barak A, Barash H, et al. Increased retinal blood flow velocity in patients with early diabetes mellitus. *Retina*. 2012;32:112-9.

Bursell SE, Clermont AC, Kinsley BT, et al. Retinal blood flow changes in patients with insulin-dependent diabetes mellitus and no diabetic retinopathy. *Invest Ophthalmol Vis Sci*. 1996;37:886–897.

Butt Z, McKillop G, O'Brien C, Allan P, Aspinall P. Measurement of ocular blood flow velocity using colour Doppler imaging in low tension glaucoma. *Eye.* 1995;9:29-33..

Calvo P, Ferreras A, Polo V, et al. Predictive value of retrobulbar blood flow parameters in glaucoma suspects. *Invest Ophthalmol Vis Sci.* 2012;53:3875–84.

Chait A, Bornfeldt KE. Diabetes and atherosclerosis: is there a role for hyperglycemia? *J Lipid Res*. 2009;50(suppl):S335–S339.

Cheung N, Mitchell P, Wong TY. Diabetic retinopathy. *Lancet.* 2010;376(9735):124–36.

Chi T, Ritch R, Stickler D, Pitman B, Tsai C, Hsieh FY. Racial differences in optic nerve head parameters. *Arch Ophthalmol*. 1989;107:836–839.

Chopra V, Varma R, Francis BA, Wu J, Torres M, Azen SP. Type 2 diabetes mellitus and the risk of open-angle glaucoma the Los Angeles Latino Eye Study. *Ophthalmology.* 2008;115:227–232.

Chung HS, Harris A, Kagemann L, et al. Peripapillary retinal blood flow in normal tension glaucoma. *Br J Ophthalmol.* 1999;83:466–9.

Coleman AL, Caprioli J. The logic behind target intraocular pressure. *Am J Ophthalmol.* 2009;147(3):379-80

Coleman AL, Lum FC, Velentgas P. Su Z. Gliklich RE. Impact of treatment strategies for open angle glaucoma on intraocular pressure: the RiGOR study. *Journal of comparative effectiveness research.* 2016;5:87-98.

Coleman AL, Miglior S. Risk factors for glaucoma onset and progression. *Surv Ophthalmol.* 2008;53(suppl 1):S3–S10.

Congdon N, O'Colman B, Klaver CC, et al. Causes and prevalence of visual impairment among adults in the United States. *Arch Ophthalmol*. 2004;122:477–485.

Costa VP, Harris A, Anderson D, Stodtmeister R, Cremasco F, Kergoat H, Lovasik J, Stalmans I, Zeitz O, Lanzl I, Gugleta K, Schmetterer L. Ocular perfusion pressure in glaucoma. *Acta Ophthalmol*. 2014 Jun;92(4):e252-66.

Creager MA, Luscher TF, Cosentino F, et al. Diabetes and vascular disease: pathophysiology, clinical consequences, and medical therapy: part I. *Circulation.* 2003;108:1527–1532.

DeLeón Ortega JE, Sakata LM, Kakati B, McGwin Jr G, Monheit BE, Arthur SN, et al. Effect of glaucomatous damage on repeatability of confocal scanning laser ophthalmoscope, scanning laser polarimetry, and optical coherence tomography. *Invest Ophthalmol Vis Sci.* 2007;48:1156-63.

De Ciuceis C, Porteri E, Rizzoni D, et al. Effects of weight loss on structural and functional alterations of subcutaneous small arteries in obese patients. *Hypertension*. 2011;58:29-36.

de Voogd S, Ikram MK, Wolfs RC, et al. Is diabetes mellitus a risk factor for open-angle glaucoma? The Rotterdam Study. *Ophthalmology.* 2006;113:1827–1831

de Voogd S, Wolfs RC, Jansonius NM, et al. Estrogen receptors alpha and beta and the risk of open-angle glaucoma: the Rotterdam Study. *Arch Ophthalmol.* 2008;126:110–4.

Dielemans I, de Jong PT, Stolk R, Vingerling JR, Grobbee DE, Hofman A. Primary open-angle glaucoma, intraocular pressure, and diabetes mellitus in the general elderly population. The Rotterdam Study. *Ophthalmology.* 1996;103:1271-1275.

Dimitrova G, Kato S, Yamashita H, et al. Relation between retrobulbar circulation and progression of diabetic retinopathy. *Br J Ophthalmol.* 2003;87:622-5.

Drance S, Anderson DR, Schulzer M. Risk factors for progression of visual field abnormalities in normal-tension glaucoma. *Am J Ophthalmol.* 2001;131:699–708.

Eid TM, el-Hawary I, el-Menawy W. Prevalence of glaucoma types and legal blindness from glaucoma in the western region of Saudi Arabia: a hospital-based study. *Int Ophthalmol.* 2009;29:477-483.

Evans DW, Harris A, Danis RP, et al. Altered retrobulbar vascular reactivity in early diabetic retinopathy. *Br J Ophthalmol*. 1997;81:279–282.

Heidelberg Engineering. Examinations of the optic nerve head [Internet]. 2021. Available from: https://www.spectralis-eyehealthcheck.co.uk/examinations/examinations-of-the-optic-nerve-head/

Fan BJ, Bailey JC, Igo RP Jr, et al. Association of a Primary Open-Angle Glaucoma Genetic Risk Score With Earlier Age at Diagnosis. *JAMA Ophthalmol*. 2019;137(10):1190-1194.

Fayers T, Strouthidis NG, Garway-Heath DF. Monitoring Glaucomatous Progression Using a Novel Heidelberg Retina Tomograph Event Analysis. *Ophthalmology*. 2007 Jul 25; [Epub ahead of print].

Fechtner RD, Weinreb RN. Mechanisms of optic nerve damage in primary open angle glaucoma. *Surv Ophthalmol.* 1994;39:23–42.

Feke GT, Pasquale LR. Retinal blood flow response to posture change in glaucoma patients compared with healthy subjects. *Ophthalmology*. 2008;115:246-52.

Ferdinand KC. Cardiovascular disease in blacks: can we stop the clock? *J Clin Hypertens (Greenwich)*. 2008;10(5):382–389.

Finkelstein EA, Khavjou OA, Thompson H, et al. Obesity and severe obesity forecasts through 2030. *Am J Prev Med*. 2012;42(6):563-570.

Flammer J. The vascular concept of glaucoma. *Surv Ophthalmol*. 1994;38 Suppl:S3-S6.

Flammer J, Orgül S, Costa VP, et al. The impact of ocular blood flow in glaucoma. *Prog Retin Eye Res.* 2002;21:359–93.

Friedman DS, Wolfs RC, O'Colman BJ, et al. Prevalence of open-angle glaucoma among adults in the United States. *Arch Ophthalmol*. 2004;122:532–538.

Galassi F, Sodi A., Ucci F, Harris A, Chung HS. Ocular haemodynamics in glaucoma associated with high myopia. *Int Ophthalmol.* 1998;22: 299-305.

Galassi F, Sodi A, Ucci F, et al. Ocular hemodynamics and glaucoma prognosis: a color Doppler imaging study. *Arch Ophthalmol.* 2003;121:1711–15.

Garway-Heath DF, Poinoosawmy D, Fitzke FW, Hitchings RA, (a). Mapping the visual field to the optic disc in normal tension glaucoma eyes. *Ophthalmology.* 2000;107(10):1809–15.

Garway-Heath DF, Caprioli J, Fitzke FW, Hitchings RA, (b). Scaling the hill of vision: the physiological relationship between light sensitivity and ganglion cell numbers. *Invest Ophthalmol Vis Sci.* 2000;41(7):1774–82.

Geisert E. Glaucoma and Corneal Thickness [Internet]. BrightFocus Foundation. 2020 [cited 2021Jan11]. Available from: https://www.brightfocus.org/glaucoma/article/glaucoma-and-corneal-thickness

Gerber AL, Harris A, Siesky B, et al. Vascular Dysfunction in Diabetes and Glaucoma: A Complex Relationship Reviewed. *J Glaucoma*. 2015;24(6):474-479.

Girkin CA, McGwin G Jr, McNeal SF, DeLeon-Ortega J. Racial differences in the association between optic disc topography and early glaucoma. *Invest Ophthalmol Vis Sci.* 2003;44:3382–3387.

Girkin CA, McGwin G Jr, Xie A, DeLeon-Ortega J. Differences in optic disc topography between black and white normal subjects. *Ophthalmology*. 2005;112:33–39.

Girkin CA, Sample PA, Liebmann JM, et al. African Descent and Glaucoma Evaluation Study (ADAGES): II. Ancestry differences in optic disc, retinal nerve fiber layer, and macular structure in healthy subjects. *Arch Ophthalmol.* 2010;128(5):541–550.

Girkin CA, Nievergelt CM, Kuo JZ, et al. Biogeographic Ancestry in the African Descent and Glaucoma Evaluation Study (ADAGES): Association With Corneal and Optic Nerve Structure. *Invest Ophthalmol Vis Sci.* 2015;56(3):2043–2049.

Goebel W, Lieb WE, Ho A, et al. Color Doppler imaging: a new technique to assess orbital blood flow in patients with diabetic retinopathy. *Invest Ophthalmol Vis Sci*. 1995;36: 864–870.

Gordon MO, Beiser JA, Brandt JD, et al. The Ocular Hypertension Treatment Study: baseline factors that predict the onset of primary open-angle glaucoma. *Arch Ophthalmol.* 2002;120:714–720.

Gordon MO, Beiser JA, Kass MA. Is a history of diabetes mellitus protective against developing primary open-angle glaucoma? *Arch Ophthalmol.* 2008;126: 280–281.

Gramer G, Weber BH, Gramer E. Migraine and Vasospasm in Glaucoma: Age-Related Evaluation of 2027 Patients With Glaucoma or Ocular Hypertension. *Invest Ophthalmol Vis Sci*. 2015;56(13):20157999-8007.

Gugleta K, Orgül S, Hasler PW, Picornell T, Gherghel D, Flammer J. Choroidal vascular reaction to hand-grip stress in subjects with vasospasm and its relevance in glaucoma. *Invest Ophthalmol Vis Sci.* 2003;44:1573-80.

Harper R, Reeves B. The sensitivity and specificity of direct ophthalmoscopic optic disc assessment in screening for glaucoma: a multivariate analysis. *Graefes Arch Clin Exp Ophthalmol*. 2000 Dec;238(12):949-55.

Harris A, Sergott RC, Spaeth GL, et al. Color doppler analysis of ocular vessel blood velocity in normal-tension glaucoma. *Am J Ophthalmol.* 1994;118:642–9.

Harris A, Harris M, Biller J, et al. Aging affects the retrobulbar circulation differently in women and men. *Arch Ophthalmol.* 2000;118:1076–80.

Harris A, Kagemann L, Ehrlich R, et al. Measuring and interpreting ocular blood flow and metabolism in glaucoma. *Can J Ophthalmol*. 2008;43:328–336.

Harris A, Jonescu C, Kagemann L, Ciulla T, Krieglstein GK. Atlas of Ocular Blood Flow. 2010; Philadelphia: Butterworth-Heinemann, Elsevier.

Harris A, Guidoboni G, Siesky B, et al. Ocular blood flow as a clinical observation: Value, limitations and data analysis. *Prog Retin Eye Res*. 2020;100841.

Harris A, Williamson T, Martin B, Shoemaker J, Sergott R, Spaeth G, et al. Test/Retest Reproducibility of Color Doppler Imaging Assessment of Blood Flow Velocity in Orbital Vessels. *J Glaucoma.* 1995;4:281-286.

Harris-Yitzhak M, Harris A, Ben-Refael Z, et al. Estrogen-replacement therapy: effects on retrobulbar hemodynamics. Am J Ophthalmol. 2000;129(5):623-628.

Harwerth RS, Wheat JL, Rangaswamy NV. Age-related losses of retinal ganglion cells and axons. Invest Ophthalmol Vis Sci. 2008;49:4437–4443.

Haseltine SJ, Pae J, Ehlrich JR, Shammas M, Radcliffe NM. Variation in corneal hysteresis and central corneal thickness among black, hispanic and white subjects. Acta Ophthalmol. 2012;90:e626–631.

Haymes SA, Leblanc RP, Nicolela MT, Chiasson LA, Chauhan BC. Risk of falls and motor vehicle collisions in glaucoma. *Invest Ophthalmol Vis Sci*. 2007 Mar;48(3):1149-55.

Hayreh SS, Revie IH, Edwards J. Vasogenic origin of visual field defects and optic nerve changes in glaucoma. *Br J Ophthalmol.* 1970;54:461-72.

Hayreh SS, Zimmerman MB, Podhajsky P, et al. Nocturnal arterial hypotension and its role in optic nerve head and ocular ischemic disorders. *Am J Ophthalmol.* 1994;117:603–24.

Heijl A, Leske MC, Bengtsson B, Bengtsson B, Hussein M, EMGT Group. Measuring visual field progression in the Early Manifest Glaucoma Trial. *Acta Ophthalmologica Scandinavica.* 2003;81:286–293.

Heijl A, Leske MC, Bengtsson B, et al. Reduction of intraocular pressure and glaucoma progression: results from the Early Manifest Glaucoma Trial. *Arch Ophthalmol.* 2002;120:1268–79.

Hennis A, Wu SY, Nemesure B, Leske MC. Hypertension, diabetes and longitudinal changes in intraocular pressure. *Ophthalmology*. 2003;110:908–914.

Herndon LW, Weizer JS, Stinnett SS. Central corneal thickness as a risk factor for advanced glaucoma damage. Arch Ophthalmol. 2004 Jan;122(1):17-21.

Hesse RJ. The relationship between progression of visual field defects and retrobulbar circulation in patients with glaucoma.[comment]. *Am J Ophthalmol.* 1998;125:566-7.

Higginbotham EJ, Gordon MO, Beiser JA, et al. The Ocular Hypertension Treatment Study: topical medication delays or prevents primary open-angle glaucoma in African American individuals. *Arch Ophthalmol*. 2004;122(6):813–820.

Higgenbotham EJ. Does sex matter in glaucoma? *Arch Ophthalmol*. 2004;122:374–375.

Hood DC, Kardon RH. A framework for comparing structural and functional measures of glaucomatous damage. *Prog Retin Eye Res.* 2007;26(6):688–710.

Hollows RC, Graham PA. Intra-ocular pressure, glaucoma, and glaucoma suspects in a defined population. *Br J Ophthalmol.* 1966;50:570–86.

Huck A, Harris A, Siesky B, et al. Vascular considerations in glaucoma patients of African and European descent. *Acta Ophthalmol*. 2014;92(5):e336-e340.

Hulsman CA, Westendorp ICD, Ramrattan RS, et al. Is open-angle glaucoma associated with early menopause? The Rotterdam Study. *Am J Epidemiol.* 2001;154:138–44.

Hyman L, Wu SY, Connell AM, et al. Prevalence and causes of visual impairment in The Barbados Eye Study. *Ophthalmology.* 2001;108:1751–1756.

Hwang YH, Jeong YC, Kim HK, et al. Macular ganglion cell analysis for early detection of glaucoma. Ophthalmology. 2014;121:1508–1515.

Jammal AA, Berchuck SI, Thompson AC, Costa VP, Medeiros FA. The Effect of Age on Increasing Susceptibility to Retinal Nerve Fiber Layer Loss in Glaucoma. *Invest Ophthalmol Vis Sci*. 2020;61(13):8.

Jimenez-Aragon F, Garcia-Martin E, Larrosa-Lopez R, et al. Role of color Doppler imaging in early diagnosis and prediction of progression in glaucoma. *BioMed Res Int.* 2013;2013:871689.

Johnson LN, Baloh FG. The accuracy of confrontation visual field test in comparison with automated perimetry. *J Natl Med Assoc*. 1991 Oct;83(10):895-8.

Jonas JB, Nangia V, Matin A, et al. Intraocular pressure and associated factors: the central India eye and medical study. *J Glaucoma.* 2011;20:405-9.

Jonas JB, Stroux A, Velten I, Juenemann A, Martus P, Budde WM. Central Corneal Thickness Correlated with Glaucoma Damage and Rate of Progression. *Invest. Ophthalmol. Vis. Sci.* 2005;46(4):1269-1274.

Jonescu-Cuypers CP, Harris A, Bartz-Schmidt KU, Kagemann L, Boros AS, Heimann UE, et al. Reproducibility of Circadian Retinal and Optic Nerve Head Blood Flow Measurements by Heidelberg Retinal Flowmetry. *Br J Ophthalmol*. 2004;88:348-53.

Jonescu-Cuypers CP, Harris A, Wilson R, Kagemann L, Mavroudis LV, Topouzis F, et al. Reproducibility of the Heidelberg Retinal Flowmeter in determining Low Perfusion Areas in Peripapillary Retina. *Br J Ophthalmol.* 2004;88:1266-9.

Kagemann L, Harris A, Chung HS, Evans D, Buck S, Martin BJ. Heidelberg Retinal Flowmetry: Factors affecting blood flow measurement. *Br J Ophthalmol.* 1998;82:131-6.

Kahook MY, Noecker RJ. How Do You Interpret a 24-2 Humphrey Visual Field Printout? [Internet]. Glaucoma Today. Bryn Mawr Communications; 2007 [cited 2021Jan11]. Available from: https://glaucomatoday.com/articles/2007-nov-dec/GT1107_10-php

Kanakamedala P, Harris A, Siesky B, et al. Optic nerve head morphology in glaucoma patients of African descent is strongly correlated to retinal blood flow. *Br J Ophthalmol*. 2014;98(11):1551-1554.

Kass MA, Heuer DK, Higginbotham EJ, et al. The Ocular Hypertension Treatment Study: a randomized trial determines that topical ocular hypotensive medication delays or prevents the onset of primary open-angle glaucoma. *Arch Ophthalmol.* 2002;120(6):701- 713.

Kawase K, Tomidokoro A, Araie M, et al. Ocular and systemic factors related to intraocular pressure in Japanese adults: the Tajimi study. *Br J Ophthalmol.* 2006;92:1175-9.

Kim J, Dally LG, Ederer F, Gaasterland DE, VanVeldhuisen PC, Blackwell B, Sullivan EK, Prum B, Shafranov G, Beck A, et al. The Advanced Glaucoma Intervention Study (AGIS): 14. Distinguishing progression of glaucoma from visual field fluctuations. *Ophthalmology.* 2004,*111*,2109-2116.

Kim YK, Choi HJ, Jeoung JW, Park KH, Kim DM. Five-year incidence of primary open-angle glaucoma and rate of progression in health center-based Korean population: the Gangnam Eye Study. *PLoS One*. 2014;9(12):e114058.

Klein BE, Klein R, Sponsel WE, et al. Prevalence of glaucoma. The Beaver Dam Eye Study. *Ophthalmology*. 1992;99:1499–504.

Klein BE, Klein R, Jensen SC. Open-angle glaucoma and older-onset diabetes. The Beaver Dam Eye Study. *Ophthalmology*. 1994;101:1173-1177.

Kyari F, Abdull MM, Wormald R, et al. Risk factors for open-angle glaucoma in Nigeria: results from the Nigeria National Blindness and Visual Impairment Survey. *BMC Ophthalmol*. 2016;16:78.

Lalezary M, Medeiros FA, Weinreb RN, et al. Baseline optical coherence tomography predicts the development of glaucomatous change in glaucoma suspects. *Am J Ophthalmol.* 2006;142:576–82.

Le A, Mukesh BN, McCarty CA, Taylor HR. Risk factors associated with the incidence of open-angle glaucoma: the visual impairment project. *Invest Ophthalmol Vis Sci.* 2003;44(9):3783-3789.

Lee E, Harris A, Siesky B, et al. The influence of retinal blood flow on open-angle glaucoma in patients with and without diabetes. *Eur J Ophthalmol*. 2014;24(4):542-549.

Leighton DA, Phillips CI. Systemic blood pressure in open-angle glaucoma, low tension glaucoma, and the normal eye. *Br J Ophthalmol.* 1972;56:447–53.

Leske MC. The epidemiology of open-angle glaucoma: a review. *Am J Epidemiol*. 1983 Aug;118(2):166-91.

Leske MC, Wu SY, Nemesure B, et al. Incident open-angle glaucoma and blood pressure. *Arch Ophthalmol.* 2002;120:954–9.

Leske MC. Open-angle glaucoma: an epidemiologic overview. *Ophthalmic Epidemiol.* 2007;14:166-72.

Leske MC, Heijl A, Hyman L, et al. Predictors of long-term progression in the early manifest glaucoma trial. *Ophthalmology.* 2007;114:1965–72.

Leske MC, Wu SY, Hennis A et al. Risk factors for incident open-angle glaucoma: The Barbados Eye Studies. *Ophthalmology*. 2008;115(1):85-93.

Levine DA, Calhoun DA, Prineas RJ, Cushman M, Howard VJ, Howard G. Moderate waist circumference and hyper- tension prevalence: the REGARDS Study. *Am J Hypertens.* 2011;24:482-8.

Lin SC, Pasquale LR, Singh K, Lin SC. The Association Between Body Mass Index and Open-angle Glaucoma in a South Korean Population-based Sample. *J Glaucoma*. 2018;27(3):239-245.

Liu W, Ling J, Chen Y, Wu Y, Lu P. The Association between Adiposity and the Risk of Glaucoma: A Meta-Analysis. *J Ophthalmol*. 2017;2017:9787450.

Logan JF, Rankin SJ, Jackson AJ. Retinal blood flow measurements and neuroretinal rim damage in glaucoma. *Br J Ophthalmol.* 2004;88:1049–1054.

Ludovico J, Bernardes R, Pires I, Figueira J, Lobo C, Cunha-Vaz J. Alterations of retinal capillary blood flow in preclinical retinopathy in subjects with type 2 diabetes. *Graefes Arch Clin Exp Ophthalmol.* 2003;241:181-6.

Marcus MW, de Vries MM, Junoy Montolio FG, Jansonius NM. Myopia as a risk factor for open-angle glaucoma: a systematic review and meta-analysis. *Ophthalmology*. 2011 Oct;118(10):1989-1994.e2.

Mark HH. Gender differences in glaucoma and ocular hypertension. *Arch Ophthalmol.* 2005;123:284.

Marjanovic I, Marjanovic M, Gvozdenovic R, et al. Retrobulbar heodynamic parameters in men and women with open angle glaucoma. *Voinosanit Pregl.* 2014;71(12):1128-31.

Martin MJ, Sommer A, Gold EB, Diamond EL. Race and primary open-angle glaucoma. *Am J Ophthalmol.* 1985;99:383–387.

Martínez A, Sánchez M. Predictive value of colour Doppler imaging in a prospective study of visual field progression in primary open-angle glaucoma. *Acta Ophthalmol Scand.* 2005;83:716–22.

Miglior S, Torri V, Zeyen T, Pfeiffer N, Vaz JC, Adamsons I. Intercurrent Factors Associated with the Development of Open-Angle Glaucoma in the European Glaucoma Prevention Study. *Am J Ophthalmol*. 2007;144:266-275.e1. Epub 2007 Jun 4.

Miglior S, Zeyen T, Pfeiffer N, Cunha-Vaz J, Torri V, Adamsons I. Results of the European Glaucoma Prevention Study. *Ophthalmology*. 2005;112(3):366-375.

Miglior S, Pfeiffer N, Torri V, Zeyen T, Cunha-Vaz J, Adamsons I. Predictive factors for open angle glaucoma among patients with ocular hypertension in the European Glaucoma Prevention Study. *Ophthalmology*. 2007;114:3–9.

Mihailovic A, Varadaraj V, Ramulu PY, Friedman DS. Evaluating Goldmann Applanation Tonometry Intraocular Pressure Measurement Agreement Between Ophthalmic Technicians and Physicians. *Am J Ophthalmol*. 2020 Nov;219:170-176.

Mikelberg FS, Parfitt CM, Swindale NV, Graham SL, Drance SM, Gosine R. Ability of the heidelberg retina tomograph to detect early glaucomatous visual field loss. *J Glaucoma*. 1995;4:242–247.

Mitchell P, Smith W, Attebo K, et al. Prevalence of open-angle glaucoma in Australia. *Ophthalmology*. 1996;103:1661–9

Mitchell P, Smith W, Chey T, Healey PR. Open angle glaucoma and diabetes: the Blue Mountains eye study, Australia. *Ophthalmology*. 1997;104:712–718.

Moore D, Harris A, Wudunn D, et al. Dysfunctional regulation of ocular blood flow: a risk factor for glaucoma? *Clin Ophthalmol.* 2008;2:849–61.

Moore GH, Bowd C, Medeiros FA, et al. African descent and glaucoma evaluation study: asymmetry of structural measures in normal participants. *J Glaucoma*. 2013;22(2):65–72.

Mukesh BN, McCarty CA, Rait JL, et al. Five-year incidence of open-angle glaucoma: the visual impairment project. *Ophthalmology.* 2002;109:1047–1051.

Moore NA, Harris A, Wentz S, Verticchio Vercellin AC, Parekh P, Gross J, Hussain RM, Thieme C, Siesky B. Baseline retrobulbar blood flow is associated with both functional and structural glaucomatous progression after 4 years. *The British journal of ophthalmology.* 2017,*101*,305-308.

Moyer VA. U.S. Preventive Services Task Force. Screening for glaucoma: U.S. Preventive Services Task Force Recommendation Statement. *Ann Intern Med*. 2013 Oct 1;159(7):484-9.

Musch DC, Gillespie BW, Niziol LM, Janz NK, Wren PA, Rockwood EJ, Lichter PR. Collaborative Initial Glaucoma Treatment Study Group. Cataract extraction in the collaborative initial glaucoma treatment study: incidence, risk factors, and the effect of cataract progression and extraction on clinical and quality-of-life outcomes. *Arch Ophthalmol*. 2006 Dec;124(12):1694-700.

Müskens RPHM, de Voogd S, Wolfs RCW, Witteman JCM, Hofman A, de Jong PTVM, et al. Systemic antihypertensive medication and incident open-angle glaucoma. *Ophthalmology.* 2007;114(12):2221- 2226.

Newman-Casey PA, Talwar N, Nan B, Musch DC, Stein JD. The relationship between components of metabolic syndrome and open-angle glaucoma. *Ophthalmology.* 2011;118: 1318-26.

Ngo S, Harris A, Siesky BA, Schroeder A, Eckert G, Holland S. Blood pressure, ocular perfusion pressure, and body mass index in glaucoma patients. *Eur J Ophthalmol*. 2013;23(5):664-669.

Nouri-Mahdavi K, Hoffman D, Coleman AL, Liu G, Li G, Gaasterland D, Caprioli J. Predictive factors for glaucomatous visual field progression in the Advanced Glaucoma Intervention Study. *Ophthalmology.* 2004;111:1627-1635.

O'Brien JM, Salowe RJ, Fertig R, et al. Family History in the Primary Open-Angle African American Glaucoma Genetics Study Cohort. *Am J Ophthalmol*. 2018;192:239-247.

Park HY, Hong KE, Park CK. Impact of Age and Myopia on the Rate of Visual Field Progression in Glaucoma Patients. *Medicine.* 2016;95,e3500.

Pasquale LR, Willett WC, Rosner BA, Kang JH. Anthropometric measures and their relation to incident primary open-angle glaucoma. *Ophthalmology*. 2010;117(8):1521-1529.

Phillps CI, Gore SM. Ocular hypotensive effect of late pregnancy with and without high blood pressure. *Br J Ophthalmol.* 1985;69:117–9.

Prada D, Sacco R, Cockburn B, Bociu L, Webster J, Siesky BA, Harris A, Guidoboni G. Influence of tissue viscoelasticity on the optic nerve head perfusion: a mathematical model. *Investigative ophthalmology & visual science.* 2016;57:3558-3558.

Prum BE Jr, Rosenberg LF, Gedde SJ, Mansberger SL, Stein JD, Moroi SE, Herndon LW Jr, Lim MC, Williams RD. Primary Open-Angle Glaucoma Preferred Practice Pattern(®) Guidelines. *Ophthalmology*. 2016 Jan;123(1):P41-P111.

Quaranta L, Harris A, Donato F, Cassamali M, Semeraro F, Nascimbeni G, et al. Color Doppler imaging of ophthalmic artery blood flow velocity: a study of repeatability and agreement. *Ophthalmology.* 1997;104:653-8.

Quigley HA, Broman AT. The number of people with glaucoma worldwide in 2010 and 2020. *Br J Ophthalmol*. 2006;90: 262–267.

Quigley HA, West SK, Rodriguez J, Munoz B, Klein R, Snyder R. The prevalence of glaucoma in a population-based study of Hispanic subjects: Proyecto VER. *Arch Ophthalmol.* 2001;119:1819-1826.

Racette L, Wilson MR, Zangwill LM, Weinreb RN, Sample PA. Primary open-angle glaucoma in blacks: a review. *Surv Ophthalmol.* 2003;48(3):295–313.

Racette L, Boden C, Kleinhandler SL, et al. Differences in visual function and optic nerve structure between healthy eyes of blacks and whites. *Arch Ophthalmol.* 2005;123:1547–1553.

Racette L, Liebmann JM, Girkin CA, et al. ADAGES Group. African Descent and Glaucoma Evaluation Study (ADAGES): III. Ancestry differences in visual function in healthy eyes. *Arch Ophthalmol.* 2010;128:551–559.

Ren R, Jonas JB, Tian G, et al. Cerebrospinal fluid pressure in glaucoma: a prospective study. Ophthalmology. 2010;117(2):259-266.

Resch H, Schmidl D, Hommer A, et al. Correlation of optic disc morphology and ocular perfusion parameters in patients with primary open angle glaucoma. *Acta Ophthalmol.* 2011;89(7):e544–e549.

Rojanapongpun P, Drance SM, Morrison BJ. Ophthalmic artery flow velocity in glaucomatous and normal subjects. *Br J Ophthalmol.* 1993;77: 25-9.

Sample PA, Girkin CA, Zangwill LM, et al. The African Descent and Glaucoma Evaluation Study (ADAGES): design and baseline data. *Arch Ophthalmol* 2009;127(9):1136–1145.

Sample PA, Medeiros FA, Racette L, Pascual JP, Boden C, Zangwill LM, et al. Identifying glaucomatous vision loss with visual-function-specific perimetry in the diagnostic innovations in glaucoma study. *Invest Ophthalmol Vis Sci.* 2006;47:3381-9.

Satilmis M, Orgul S, Doubler B, et al. Rate of progression of glaucoma correlates with retrobulbar circulation and intra-ocular pressure. *Am J Ophthalmol*. 2003;135:664–669.

Schumann J, Orgül S, Gugleta K, Dubler B, Flammer J. Interocular difference in progression of glaucoma correlates with interocular differences in retrobulbar circulation. *Am J Ophthalmol 2000;l.*129:728-33.

Schuman JS, Kostanyan T, Bussel I. Review of Longitudinal Glaucoma Progression: 5 Years after the Shaffer Lecture. *Ophthalmology. Glaucoma.* 2020;3:158-166.

Stevens S, Gilbert C, Astbury N. How to measure intraocular pressure: applanation tonometry. *Community Eye Health.* 2007 Dec;20(64):74-5.

Sator MO, Joura EA, Frigo P, et al. Hormone replacement therapy and intraocular pressure. *Maturitas.* 1997;28:55–58.

Saylik M, Saylik SA. Not only pregnancy but also the number of fetuses in the uterus affects intraocular pressure. *Indian J Ophthalmol*. 2014;62:680–682.

Schalkwijk CG, Stehouwer CD. Vascular complications in diabetes mellitus: the role of endothelial dysfunction. *Clin Sci* (Lond). 2005;109:143–159.

Sehi M, Iverson SM. Glaucoma Diagnosis and Monitoring Using Advanced Imaging Technologies. *US Ophthalmic Rev.* 2013;6:15–25.

Shoshani Y, Harris A, Shoja MM, et al. Impaired ocular blood flow regulation in patients with open-angle glaucoma and diabetes. *Clin Experiment Ophthalmol.* 2012;40:697-705.

Siesky B, Harris A, Racette L, et al. Differences in ocular blood flow in glaucoma between patients of African and European descent. *J Glaucoma*. 2015;24(2):117-121.

Siesky B, Harris A, Carr J, et al. Reductions in Retrobulbar and Retinal Capillary Blood Flow Strongly Correlate With Changes in Optic Nerve Head and Retinal Morphology Over 4 Years in Open-angle Glaucoma Patients of African Descent Compared With Patients of European Descent. *J Glaucoma*. 2016;25(9):750-757.

Siesky BA, Harris A, Patel C, et al. Comparison of visual function and ocular hemodynamics between pre- and post-menopausal women. *Eur J Ophthalmol.* 2008;18:320–3.

Sigal IA, Ethier CR. Biomechanics of the optic nerve head. *Exp Eye Res.* 2009;88:799–807.

Silver DM, Farrell RA, Langham ME, O'Brien V, Schilder P. Estimation of pulsatile ocular blood flow from intraocular pressure. *Acta Ophthalmol Suppl.* 1989;191:25-9.

Sommer A, Tielsch JM, Katz J, Quigley HA, Gottsch JD, Javitt JC, Martone JF, Royall RM, Witt KA, Ezrine S. Racial differences in the cause-specific prevalence of blindness in east Baltimore. *N Engl J Med.* 1991;325:1412–1417.

Springelkamp H, Wolfs RC, Ramdas WD, et al. Incidence of glaucomatous visual field loss after two decades of follow-up: the Rotterdam Study. *Eur J Epidemiol*. 2017;32(8):691-699.

Suzuki Y, Shirato S, Adachi M, et al. Risk factors for the progression of treated primary open-angle glaucoma: a multivariate life-table analysis. *Graefes Arch Clin Exp Ophthalmol.* 1999;237:463–7.

Sw OH, Lee S, Park C, et al. Elevated intraocular pressure is associated with insulin resistance and metabolic syndrome. *Diabetes Metab Res Rev.* 2005;21(5):434-40.

Tan GS, Wong TY, Fong CW, Aung T; Singapore Malay Eye Study. Diabetes, metabolic abnormalities, and glaucoma. *Arch Ophthalmol.* 2009;127:1354-61.

Tham YC, Li X, Wong TY, Quigley HA, Aung T, Cheng CY. Global prevalence of glaucoma and projections of glaucoma burden through 2040: a systematic review and meta-analysis. *Ophthalmology*. 2014;121(11):2081-2090.

Tielsch JM, Sommer A, Katz J, Royall RM, Quigley HA, Javitt J. Racial variations in the prevalence of primary open-angle glaucoma. The Baltimore Eye Survey. *JAMA.* 1991;266:369–374.

Tielsch JM, Katz J, Sommer A, et al. Hypertension, perfusion pressure, and primary open-angle glaucoma. A population-based assessment. *Arch Ophthalmol.* 1995;113:216–21.

Tobe LA, Harris A, Trinidad J, et al. Should men and women be managed differently in glaucoma? *Ophthalmol Ther.* 2012;1:1.

Tobe LA, Harris A, Hussain RM, et al. The role of retrobulbar and retinal circulation on optic nerve head and retinal nerve fibre layer structure in patients with open-angle glaucoma over an 18-month period. *Br J Ophthalmol.* 2015;99:609–12.

Topouzis F, Coleman AL, Harris A, et al. Association of blood pressure status with the optic disk structure in non-glaucoma subjects: the Thessaloniki eye study. *Am J Ophthalmol.* 2006;142:60–7.

Triggle CR, Ding H. A review of endothelial dysfunction in diabetes: a focus on the contribution of a dysfunctional eNOS. *J Am Soc Hypertens*. 2010;4:102–115.

Toh TY, Liew SHM, MacKinnon JR, Hewitt AW, Poulsen JL, Spector TD, Gilbert CE, Craig JE, Hammond CJ, Mackey DA. Central Corneal Thickness Is Highly Heritable: The Twin Eye Studies. *Invest. Ophthalmol. Vis. Sci.* 2005;46(10):3718-3722

Uncu G, Avci R, Uncu Y, et al. The effects of different hormone replacement therapy regimens on tear function, intraocular pressure and lens opacity. *Gynecol Endocrincol.* 2006;22:501–505.

Ustymowicz A, Mariak Z, Weigele J, Lyson T, Kochanowicz J, Krejza J. Normal reference intervals and ranges of side-to-side and day-to-day variability of ocular blood flow Doppler parameters. *Ultrasound Med Biol.* 2005;31(7):895-903.

Vajaranant TS, Maki PM, Pasquale LR, et al. Effects of hormone therapy on intraocular pressure: the Women's Health Initiative- Sight Exam Study. *Am J Ophthalmol.* 2016;165:115–124.

Varma R, Ying-Lai M, Francis BA, Los Angeles Latino Eye Study Group, et al. Prevalence of open- angle glaucoma and ocular hypertension in Latinos: the Los Angeles Latino Eye Study. *Ophthalmology*. 2004;111:1439–48.

Wang N, Xie X, Yang D, Xian J, Li Y, Ren R, Peng X, Jonas JB, Weinreb RN. Orbital cerebrospinal fluid space in glaucoma: the Beijing intracranial and intraocular pressure (iCOP) study. *Ophthalmology.* 2012;119:2065-2073.e2061.

Wang Y, Fawzi AA, Varma R, et al. Pilot study of optical coherence tomography measurement of retinal blood flow in retinal and optic nerve diseases. *Invest Ophthalmol Vis Sci*. 2011;52:840–845.

Weinreb RN, Harris A. World Glaucoma Association Consensus Series – 6. Ocular blood flow in glaucoma. 2009; Kugler Publications, Amsterdam, the Netherlands.

Weinreb RN, Aung T, Medeiros FA. The pathophysiology and treatment of glaucoma: a review. *JAMA*. 2014;311(18):1901-1911.

Wensor MD, McCarty CA, Stanislavsky YL, Livingston PM, Taylor HR. The prevalence of glaucoma in the Melbourne Visual Impairment Project. *Ophthalmology*. 1998;105:733–9.

Word Health Organization. Blindness and Vision Impairment. Internet; 2020. Accessed January 2021.

Wilensky JT, Gandhi N, Pan T. Racial influences in open-angle glaucoma. *Ann Ophthalmol.* 1978;10:1398–1402.

Williamson TH and Harris A: Color Doppler Ultrasound Imaging of the Eye and Orbit. *Surv Ophthalmol.* 1996;40:255-67.

Wilson MR, Hertzmark E, Walker AM, Childs-Shaw K, Epstein DL. A case-control study of risk factors in open angle glaucoma. *Arch Ophthalmol.* 1987;105:1066–1071.

Xu G, Zhu H, Wang Z, Wei H, Shi Y, Hao J. [Analysis of blood flow in ophthalmic arteries in patients with middle and late stages of glaucoma with Doppler sonography]. [Chinese] Chung-Hua Yen Ko Tsa Chih [*Chinese Journal of Ophthalmology*]. 1998;34:37-8.

Xu L, Wang H, Wang Y, et al. Intraocular pressure correlated with arterial blood pressure: the Beijing Eye Study. *Am J Ophthalmol.* 2007;144:461-2.

Xu L, Xie XW, Wang YX, Jonas JB. Ocular and systemic factors associated with diabetes mellitus in the adult population in rural and urban China. The Beijing Eye Study. *Eye*. 2009;23:676-82.

Yamazaki Y, Drance SM. The relationship between progression of visual field defects and retrobulbar circulation in patients with glaucoma.[see comment]. Comment in: *Am J Ophthalmol.* 1998;125:566-7.

Yin ZQ, Vaegan, Millar TJ, Beaumont P, Sarks S. Widespread choroidal insufficiency in primary open-angle glaucoma. *J Glaucoma.* 1997;6:23–32.

Youngblood H, Hauser MA, Liu Y. Update on the genetics of primary open-angle glaucoma. *Exp Eye Res.* 2019;188:107795.

Yu DY, Townsend R, Cringle SJ, Balwantray CC, Morgan WH. Improved interpretation of flow maps obtained by scanning laser Doppler flowmetry using a rat model of retinal artery occlusion. *Investigative Ophthalmology & Visual Science.* 2005;46:166-74.

Zangwill LM, Bowd C, Berry CC, et al. Discriminating between normal and glaucomatous eyes using the Heidelberg Retina Tomograph, GDx Nerve Fiber Analyzer, and Optical Coherence Tomograph. *Arch Ophthalmol.* 2001;119(7):985-993.

Zangwill LM, Van Horn S, De Souza M, Sample PA, Weinreb RN. Optic nerve head topography in ocular hypertensive eyes using confocal scanning laser ophthalmoscopy. *Am J Ophthalmol.* 1996:122:520-5.

Zangwill LM, Weinreb RN, Beiser JA, Berry CC, Cioffi GA, Coleman AL, et al. Baseline topographic optic disc measurements are associated with the development of primary open-angle glaucoma: the Confocal Scanning Laser Ophthalmoscopy Ancillary Study to the Ocular Hypertension Treatment Study. *Arch Ophthalmol.* 2005;123:1188-97.

Zangwill LM, Weinreb RN, Berry CC, Smith AR, Dirkes KA, Liebmann JM, et al. The confocal scanning laser ophthalmoscopy ancillary study to the ocular hypertension treatment study: study design and baseline factors. *Am J Ophthalmol.* 2004;137:219-27.

Zeitz O, Galambos P, Wagenfeld L, et al. Glaucoma progression is associated with decreased blood flow velocities in the short posterior ciliary artery. *Br J Ophthalmol.* 2006;90:1245–8.

Zetterberg M. Age-related eye disease and gender. *Maturitas.* 2016;83:19–26.

Zhang H, Jia H, Duan X, Li L, Wang H, Wu J, Hu J, Cao K, Zhao A, Liang J, et al. The Chinese Glaucoma Study Consortium for Patients With Glaucoma: Design, Rationale and Baseline Patient Characteristics. *J Glaucoma.* 2019;28:974-978.

Zhao D, Cho J, Kim MH, Guallar E. The association of blood pressure and primary open-angle glaucoma: a meta-analysis. *Am J Ophthalmol*. 2014 Sep;158(3):615-27.e9.

Zhao D, Cho J, Kim MH, Friedman DS, Guallar E. Diabetes, fasting glucose, and the risk of glaucoma: a meta-analysis. *Ophthalmology*. 2015 Jan;122(1):72-8.

Zukerman R, Harris A, Verticchio Vercellin A, Siesky B, Pasquale LR, Ciulla TA. Molecular Genetics of Glaucoma: Subtype and Ethnicity Considerations. *Genes*. 2021;12(1):55.